

In presenting the dissertation as a partial fulfillment of the requirements for an advanced degree from the Georgia Institute of Technology, I agree that the Library of the Institution shall make it available for inspection and circulation in accordance with its regulations governing materials of this type. I agree that permission to copy from, or to publish from, this dissertation may be granted by the professor under whose direction it was written, or, in his absence, by the Dean of the Graduate Division when such copying or publication is solely for scholarly purposes and does not involve potential financial gain. It is understood that any copying from, or publication of, this dissertation which involves potential financial gain will not be allowed without written permission.

NONISOTHERMAL LAMINAR FLOW AND HEAT TRANSFER
WITH TEMPERATURE DEPENDENT PHYSICAL PROPERTIES

A THESIS

Presented to

The Faculty of the Graduate Division

by

Bert Wilkins, Jr.

In Partial Fulfillment

of the Requirements for the Degree

Doctor of Philosophy

in the School of Chemical Engineering

Georgia Institute of Technology

April, 1965

NONISOTHERMAL LAMINAR FLOW AND HEAT TRANSFER
WITH TEMPERATURE DEPENDENT PHYSICAL PROPERTIES

Approved:

Date Approved by Chairman: April 26, 1965

"We dance around in a ring and suppose,
But the Secret sits in the middle and knows."
— Robert Frost

ACKNOWLEDGMENTS

The author expresses his appreciation to his thesis advisor, Dr. Henderson C. Ward, for his interest and helpful suggestions during this study. The constructive criticisms of Dr. William B. Harrison and Dr. Charles W. Gorton, who served on the reading committee, are gratefully acknowledged.

The large amount of computer time required by this study was made available by the Rich Electronic Computer Center through the cooperation of Mr. William A. Bezair.

The author is grateful for the financial assistance provided by two Humble Oil Company Graduate Fellowships. Thanks are also due Dr. Homer V. Grubb for providing several teaching assistantships which were valuable for the teaching experience they provided as well as the financial remuneration.

Many long hours were spent by the author's wife, Anne G. Wilkins, in helping to organize and type the numerous preliminary drafts. Her sincere interest and encouragement in no small measure contributed to the completion of this work.

TABLE OF CONTENTS

	Page
ACKNOWLEDGMENTS	iii
LIST OF TABLES	vi
LIST OF ILLUSTRATIONS	xv
NOMENCLATURE	xxiii
SUMMARY	xxvii
CHAPTER	
I. INTRODUCTION	1
II. MATHEMATICAL DESCRIPTION OF THE PROBLEM	4
III. CONSTANT PROPERTY SOLUTIONS	13
IV. VARIABLE PROPERTY SOLUTIONS	36
V. CONCLUSIONS AND RECOMMENDATIONS	76
APPENDICES	
A. DEVELOPMENT OF FINITE DIFFERENCE APPROXIMATIONS	79
B. DIGITAL COMPUTER APPLICATION OF CALCULATION SCHEME	118
C. EMPIRICAL PROPERTY EQUATIONS	135
D. CALCULATED CONSTANT PROPERTY FLUID FLOW AND HEAT TRANSFER RESULTS	138
E. COMPARISON CONDITIONS AND COMPARISON RESULTS	147
F. FRICTION FACTOR CORRELATIONS	173
G. HEAT TRANSFER CORRELATIONS	182
H. TEMPERATURE AND VELOCITY PROFILE CORRELATIONS	212
I. SAMPLE CALCULATIONS	274

TABLE OF CONTENTS (Continued)

	Page
LITERATURE CITED	279
VITA	283

LIST OF TABLES

Table	Page
1. Comparison of Constant Property Calculated Entry Length and Kinetic Energy Correction Factor with the Results of Other Investigations Entrance Profile: Uniform	20
2. Comparison of Constant Property Heat Transfer Calculations with Results Calculated from the Analytical Solutions of Graetz Entrance Profile: Parabolic	25
3. Comparison of Variable Property Heat Transfer Calculations with the Results of Experimental Measurements Entrance Profile: Parabolic	37
4. Constant Property Axial Velocity Calculations Entrance Profile: Uniform	139
5. Constant Property Heat Transfer Calculations Entrance Profile: Parabolic	140
6. Constant Property Heat Transfer Calculations Entrance Profile: Uniform Prandtl Number: 0.1	141
7. Constant Property Heat Transfer Calculations Entrance Profile: Uniform Prandtl Number: 0.7	142
8. Constant Property Heat Transfer Calculations Entrance Profile: Uniform Prandtl Number 1.0	143
9. Constant Property Heat Transfer Calculations Entrance Profile: Uniform Prandtl Number: 5	144
10. Constant Property Heat Transfer Calculations Entrance Profile: Uniform Prandtl Number: 10	145
11. Constant Property Heat Transfer Calculations Entrance Profile: Uniform Prandtl Number: 100	146

LIST OF TABLES (Continued)

Table	Page
12. Conditions for Variable Property Comparison Calculations for Water	148
13. Conditions for Variable Property Comparison Calculations for Air, Helium, n-Octane	149
14. Conditions for Variable Property Comparison Calculations for Oil A	150
15. Variable Property Mean Temperature and Local Nusselt Number Calculations for Liquids Entrance Profile: Parabolic Viscosity Ratio: 0.1	183
16. Variable Property Mean Temperature and Local Nusselt Number Calculations for Liquids Entrance Profile: Parabolic Viscosity Ratio: 0.5	184
17. Variable Property Mean Temperature and Local Nusselt Number Calculations for Liquids Entrance Profile: Parabolic Viscosity Ratio: 1	185
18. Variable Property Mean Temperature and Local Nusselt Number Calculations for Liquids Entrance Profile: Parabolic Viscosity Ratio: 2	186
19. Variable Property Mean Temperature and Local Nusselt Number Calculations for Liquids Entrance Profile: Parabolic Viscosity Ratio: 5	187
20. Variable Property Mean Temperature and Local Nusselt Number Calculations for Liquids Entrance Profile: Parabolic Viscosity Ratio: 10	188
21. Variable Property Mean Temperature and Local Nusselt Number Calculations for Liquids Entrance Profile: Parabolic Viscosity Ratio: 20	189
22. Variable Property Mean Temperature and Local Nusselt Number Calculations for Gases Entrance Profile: Parabolic Viscosity Ratio: 0.5	190

LIST OF TABLES (Continued)

Table	Page
23. Variable Property Mean Temperature and Local Nusselt Number Calculations for Gases Entrance Profile: Parabolic Viscosity Ratio: 0.75	191
24. Variable Property Mean Temperature and Local Nusselt Number Calculations for Gases Entrance Profile: Parabolic Viscosity Ratio: 1	192
25. Variable Property Mean Temperature and Local Nusselt Number Calculations for Gases Entrance Profile: Parabolic Viscosity Ratio: 1.5	193
26. Variable Property Mean Temperature and Local Nusselt Number Calculations for Gases Entrance Profile: Parabolic Viscosity Ratio: 2	194
27. Variable Property Mean Temperature and Local Nusselt Number Calculations for Liquids Entrance Profile: Uniform Viscosity Ratio: 0.1 Prandtl Number: 1	195
28. Variable Property Mean Temperature and Local Nusselt Number Calculations for Liquids Entrance Profile: Uniform Viscosity Ratio: 0.5 Prandtl Number: 1	196
29. Variable Property Mean Temperature and Local Nusselt Number Calculations for Liquids Entrance Profile: Uniform Viscosity Ratio: 1 Prandtl Number: 1	197
30. Variable Property Mean Temperature and Local Nusselt Number Calculations for Liquids Entrance Profile: Uniform Viscosity Ratio: 5 Prandtl Number: 1	198

LIST OF TABLES (Continued)

Table	Page
31. Variable Property Mean Temperature and Local Nusselt Number Calculations for Liquids Entrance Profile: Uniform Viscosity Ratio: 10 Prandtl Number: 1	199
32. Variable Property Mean Temperature and Local Nusselt Number Calculations for Liquids Entrance Profile: Uniform Viscosity Ratio: 20 Prandtl Number: 1	200
33. Variable Property Mean Temperature and Local Nusselt Number Calculations for Liquids Entrance Profile: Uniform Viscosity Ratio: 0.1 Prandtl Number: 10	201
34. Variable Property Mean Temperature and Local Nusselt Number Calculations for Liquids Entrance Profile: Uniform Viscosity Ratio: 0.5 Prandtl Number: 10	202
35. Variable Property Mean Temperature and Local Nusselt Number Calculations for Liquids Entrance Profile: Uniform Viscosity Ratio: 1 Prandtl Number: 10	203
36. Variable Property Mean Temperature and Local Nusselt Number Calculations for Liquids Entrance Profile: Uniform Viscosity Ratio: 5 Prandtl Number: 10	204
37. Variable Property Mean Temperature and Local Nusselt Number Calculations for Liquids Entrance Profile: Uniform Viscosity Ratio: 10 Prandtl Number: 10	205
38. Variable Property Mean Temperature and Local Nusselt Number Calculations for Liquids Entrance Profile: Uniform Viscosity Ratio: 20 Prandtl Number: 10	206

LIST OF TABLES (Continued)

Table	Page
39. Variable Property Mean Temperature and Local Nusselt Number Calculations for Gases Entrance Profile: Uniform Viscosity Ratio: 0.5 Prandtl Number 0.7	207
40. Variable Property Mean Temperature and Local Nusselt Number Calculations for Gases Entrance Profile: Uniform Viscosity Ratio: 0.75 Prandtl Number: 0.7	208
41. Variable Property Mean Temperature and Local Nusselt Number Calculations for Gases Entrance Profile: Uniform Viscosity Ratio: 1 Prandtl Number: 0.7	209
42. Variable Property Mean Temperature and Local Nusselt Number Calculations for Gases Entrance Profile: Uniform Viscosity Ratio: 1.5 Prandtl Number: 0.7	210
43. Variable Property Mean Temperature and Local Nusselt Number Calculations for Gases Entrance Profile: Uniform Viscosity Ratio: 2 Prandtl Number: 0.7	211
44. Variable Property Velocity and Temperature Profile Calculations for Liquids Entrance Profile: Parabolic Viscosity Ratio: 0.1	213
45. Variable Property Velocity and Temperature Profile Calculations for Liquids Entrance Profile: Parabolic Viscosity Ratio: 0.5	216
46. Variable Property Velocity and Temperature Profile Calculations for Liquids Entrance Profile: Parabolic Viscosity Ratio: 1	219

LIST OF TABLES (Continued)

Table	Page
47. Variable Property Velocity and Temperature Profile Calculations for Liquids Entrance Profile: Parabolic Viscosity Ratio: 2	222
48. Variable Property Velocity and Temperature Profile Calculations for Liquids Entrance Profile: Parabolic Viscosity Ratio: 5	224
49. Variable Property Velocity and Temperature Profile Calculations for Liquids Entrance Profile: Parabolic Viscosity Ratio: 10	226
50. Variable Property Velocity and Temperature Profile Calculations for Liquids Entrance Profile: Parabolic Viscosity Ratio: 20	228
51. Variable Property Velocity and Temperature Profile Calculations for Gases Entrance Profile: Parabolic Viscosity Ratio: 0.5	230
52. Variable Property Velocity and Temperature Profile Calculations for Gases Entrance Profile: Parabolic Viscosity Ratio: 0.75	232
53. Variable Property Velocity and Temperature Profile Calculations for Gases Entrance Profile: Parabolic Viscosity Ratio: 1.0	234
54. Variable Property Velocity and Temperature Profile Calculations for Gases Entrance Profile: Parabolic Viscosity Ratio: 1.5	236
55. Variable Property Velocity and Temperature Profile Calculations for Gases Entrance Profile: Parabolic Viscosity Ratio: 2	238

LIST OF TABLES (Continued)

Table	Page
56. Variable Property Velocity and Temperature Profile Calculations for Liquids Entrance Profile: Uniform Viscosity Ratio: 0.1 Prandtl Number: 1	240
57. Variable Property Velocity and Temperature Profile Calculations for Liquids Entrance Profile: Uniform Viscosity Ratio: 0.5 Prandtl Number: 1	242
58. Variable Property Velocity and Temperature Profile Calculations for Liquids Entrance Profile: Uniform Viscosity Ratio: 1 Prandtl Number: 1	244
59. Variable Property Velocity and Temperature Profile Calculations for Liquids Entrance Profile: Uniform Viscosity Ratio: 5 Prandtl Number: 1	246
60. Variable Property Velocity and Temperature Profile Calculations for Liquids Entrance Profile: Uniform Viscosity Ratio: 10 Prandtl Number: 1	248
61. Variable Property Velocity and Temperature Profile Calculations for Liquids Entrance Profile: Uniform Viscosity Ratio: 20 Prandtl Number: 1	250
62. Variable Property Velocity and Temperature Profile Calculations for Liquids Entrance Profile: Uniform Viscosity Ratio: 0.1 Prandtl Number: 10	252
63. Variable Property Velocity and Temperature Profile Calculations for Liquids Entrance Profile: Uniform Viscosity Ratio: 0.5 Prandtl Number: 10	254

LIST OF TABLES (Continued)

Table	Page
64. Variable Property Velocity and Temperature Profile Calculations for Liquids Entrance Profile: Uniform Viscosity Ratio: 1 Prandtl Number: 10	256
65. Variable Property Velocity and Temperature Profile Calculations for Liquids Entrance Profile: Uniform Viscosity Ratio: 5 Prandtl Number: 10	258
66. Variable Property Velocity and Temperature Profile Calculations for Liquids Entrance Profile: Uniform Viscosity Ratio: 10 Prandtl Number: 10	260
67. Variable Property Velocity and Temperature Profile Calculations for Liquids Entrance Profile: Uniform Viscosity Ratio: 20 Prandtl Number: 10	262
68. Variable Property Velocity and Temperature Profile Calculations for Gases Entrance Profile: Uniform Viscosity Ratio: 0.5 Prandtl Number: 0.7	264
69. Variable Property Velocity and Temperature Profile Calculations for Gases Entrance Profile: Uniform Viscosity Ratio: 0.75 Prandtl Number: 0.7	266
70. Variable Property Velocity and Temperature Profile Calculations for Gases Entrance Profile: Uniform Viscosity Ratio: 1 Prandtl Number: 0.7	268

LIST OF TABLES (Continued)

Table	Page
71. Variable Property Velocity and Temperature Profile Calculations for Gases Entrance Profile: Uniform Viscosity Ratio: 1.5 Prandtl Number: 0.7	270
72. Variable Property Velocity and Temperature Profile Calculations for Gases Entrance Profile: Uniform Viscosity Ratio: 2 Prandtl Number: 0.7	272

LIST OF ILLUSTRATIONS

Figure	Page
1. Diagram of Problem	5
2. Constant Property Axial Velocity Calculations Entrance Profile: Uniform	16
3. Comparison of Constant Property Axial Velocity Calculations with the Results of Other Investigations Entrance Profile: Uniform	17
4. Constant Property Radial Velocity Profile Calculations Entrance Profile: Uniform	18
5. Constant Property Radial Velocity Profile Calculations Entrance Profile: Uniform	19
6. Constant Property Pressure Drop Calculations Entrance Profile: Uniform	21
7. Comparison of Constant Property Pressure Drop Calculations with the Results of Experimental Measurements Entrance Profile: Uniform	22
8. Constant Property Logarithmic Mean Nusselt Number Calculations Entrance Profile: Uniform	27
9. Constant Property Mean Temperature Calculations Entrance Profile: Uniform	28
10. Constant Property Local Nusselt Number Calculations Entrance Profile: Uniform	29
11. Comparison of Constant Property Heat Transfer with Results of Experimental Measurements Entrance Profile: Uniform	30
12. Effect of Radial Velocity Term on Calculated Constant Property Local Nusselt Numbers Entrance Profile: Uniform	31

LIST OF ILLUSTRATIONS (Continued)

Figure	Page
13. Effect of Radial Velocity Term on Calculated Mean Temperature Entrance Profile: Uniform	32
14. Comparison of Variable Property Pressure Drop Calculations with the Results of Experimental Measurements Entrance Profile: Uniform	39
15. Comparison of Variable Property Mean Temperature Calculations with the Results of Experimental Measurement Entrance Profile: Uniform	41
16. Comparison of Variable Property Mean Temperature Calculations for Oil A and Water Entrance Profile: Parabolic Viscosity Ratio: 0.5	47
17. Comparison of Variable Property Local Nusselt Number Calculations for Oil A and Water Entrance Profile: Parabolic Viscosity Ratio: 2	48
18. Comparison of Variable Property Velocity Profile Calculations for Oil A and Water Entrance Profile: Parabolic Viscosity Ratio: 2 Free Convection Parameter: 200	49
19. Comparison of Variable Property Friction Factor Calculations for Oil A and Water Entrance Profile: Parabolic Viscosity Ratio: 2 Prandtl Number: 100	50
20. Comparison of Variable Property Friction Factor Calculations for Oil A and Water Entrance Profile: Parabolic Viscosity Ratio: 2 Prandtl Number: 10	51
21. Comparison of Variable Property Temperature Profile Calculations for Oil A and Water Entrance Profile: Parabolic Viscosity Ratio: 2 Free Convection Parameter: 200	52

LIST OF ILLUSTRATIONS (Continued)

Figure		Page
22.	Comparison of Variable Property Mean Temperature Calculations for Air and Helium Entrance Profile: Parabolic Viscosity Ratio: 1.5	54
23.	Comparison of Variable Property Local Nusselt Number Calculations for Air and Helium Entrance Profile: Parabolic Viscosity Ratio: 1.5	55
24.	Comparison of Variable Property Velocity Profile Calculations for Air and Helium Entrance Profile: Parabolic Viscosity Ratio: 1.5 Free Convection Parameter: 800	56
25.	Comparison of Variable Properties Friction Factor Calculations for Air and Helium Entrance Profile: Parabolic Viscosity Ratio: 0.667	57
26.	Comparison of Variable Property Temperature Profile Calculations for Air and Helium Entrance Profile: Parabolic Viscosity Ratio: 0.667 Free Convection Parameter: 800	58
27.	Comparison of Variable Property Local Nusselt Number Calculations for Oil A, n-Octane, and Water Entrance Profile: Uniform Viscosity Ratio: 2 Prandtl Number: 10	60
28.	Comparison of Variable Property Mean Temperature Calculations for n-Octane and Water Entrance Profile: Uniform Viscosity Ratio: 0.5 Prandtl Number: 5	61
29.	Comparison of Variable Property Velocity Profile Calculations for Oil A and Water Entrance Profile: Uniform Viscosity Ratio: 2 Free Convection Parameter: 800 Prandtl Number: 1	62

LIST OF ILLUSTRATIONS (Continued)

Figure	Page
30. Comparison of Variable Property Friction Factor Calculations for Oil A and Water Entrance Profile: Uniform Viscosity Ratio: 0.5 Prandtl Number: 10	63
31. Comparison of Variable Property Temperature Calculations for Oil A and Water Entrance Profile: Uniform Viscosity Ratio: 2 Free Convection Parameter: 0.1 Prandtl Number: 10	64
32. Comparison of Variable Property Local Nusselt Number Calculations for Air and Helium Entrance Profile: Uniform Viscosity Ratio: 1.5	65
33. Comparison of Variable Property Mean Temperature Calculations for Air and Helium Entrance Profile: Uniform Viscosity Ratio: 0.667	66
34. Comparison of Variable Property Velocity Profile Calculations for Air and Helium Entrance Profile: Uniform Viscosity Ratio: 0.667 Free Convection Parameter: 0.1	67
35. Comparison of Variable Property Friction Factor Calculations for Air and Helium Entrance Profile: Uniform Viscosity Ratio: 0.667	68
36. Comparison of Variable Property Temperature Profile Calculations for Air and Helium Entrance Profile: Uniform Viscosity Ratio: 1.5 Free Convection Parameter: 800	69
37. Comparison of Variable Property Mean Temperature Calculations for Air with Results of Previous Work Entrance Profile: Parabolic Viscosity Ratio: 0.667	73

LIST OF ILLUSTRATIONS (Continued)

Figure	Page
38. Comparison of Variable Property Mean Temperature Calculations for Oil A with Results of Previous Work Entrance Profile: Parabolic Viscosity Ratio: 2	74
39. Comparison of Variable Property Friction Factor Calculations for Air with Results of Previous Work Entrance Profile: Parabolic Viscosity Ratio: 0.667	75
40. Comparison of Variable Property Local Nusselt Number Calculations for Oil A and Water Entrance Profile: Parabolic Viscosity Ratio: 0.5	151
41. Comparison of Variable Property Mean Temperature Calculations for Oil A and Water Entrance Profile: Parabolic Viscosity Ratio: 3.4	152
42. Comparison of Variable Property Mean Temperature Calculations for Oil A Entrance Profile: Parabolic Viscosity Ratio: 5 Free Convection Parameter: 0.1	153
43. Comparison of Variable Property Mean Temperature Calculations for Water Entrance Profile: Parabolic Viscosity Ratio: 2.5 Free Convection Parameter: 200	154
44. Comparison of Variable Property Mean Temperature Calculations for Oil A and n-Octane Entrance Profile: Parabolic Viscosity Ratio: 0.1	155
45. Comparison of Variable Property Mean Temperature Calculations for Oil A and n-Octane Entrance Profile: Parabolic Viscosity Ratio: 10	156
46. Comparison of Variable Property Mean Temperature Calculations for Oil A and Water Entrance Profile: Parabolic Viscosity Ratio: 2	157

LIST OF ILLUSTRATIONS (Continued)

Figure		Page
47.	Comparison of Variable Property Mean Temperature Calculations for Air and Helium Entrance Profile: Parabolic Viscosity Ratio: 0.667	158
48.	Comparison of Variable Property Velocity Profile Calculations for Oil A and Water Entrance Profile: Parabolic Viscosity Ratio: 2 Free Convection Parameter: 0.1	159
49.	Comparison of Variable Property Velocity Profile Calculations for Oil A and Water Entrance Profile: Parabolic Viscosity Ratio: 0.5 Free Convection Parameter: 200	160
50.	Comparison of Variable Property Friction Factor Calculations for Air and Helium Entrance Profile: Parabolic Viscosity Ratio: 1.5	161
51.	Comparison of Variable Property Friction Factor Calculations for Oil A and Water Entrance Profile: Parabolic Viscosity Ratio: 2 Prandtl Number: 100	162
52.	Comparison of Variable Property Friction Factor Calculations for Oil A and n-Octane Entrance Profile: Parabolic Viscosity Ratio: 0.1 Prandtl Number: 100.	163
53.	Comparison of Variable Property Mean Temperature Calculations for Water and n-Octane Entrance Profile: Uniform Viscosity Ratio: 2 Prandtl Number: 10	164
54.	Comparison of Variable Property Mean Temperature Calculations for Water and n-Octane Entrance Profile: Uniform Viscosity Ratio: 2 Prandtl Number: 10	165

LIST OF ILLUSTRATIONS (Continued)

Figure	Page
55. Comparison of Variable Property Mean Temperature Calculations for Oil A and Water Entrance Profile: Uniform Viscosity Ratio: 2 Prandtl Number: 1	166
56. Comparison of Variable Property Mean Temperature Calculations for Oil A and Water Entrance Profile: Uniform Viscosity Ratio: 2 Prandtl Number: 10	167
57. Comparison of Variable Property Mean Temperature Calculations for Air and Helium Entrance Profile: Uniform Viscosity Ratio: 1.5	168
58. Comparison of Variable Property Velocity Profile Calculations for Water and n-Octane Entrance Profile: Uniform Viscosity Ratio: 0.5 Free Convection Parameter: 0.1 Prandtl Number: 5	169
59. Comparison of Variable Property Friction Factor Calculations for Air and Helium Entrance Profile: Uniform Viscosity Ratio: 1.5	170
60. Comparison of Variable Property Friction Factor Calculations for Oil A and Water Entrance Profile: Uniform Viscosity Ratio: 2 Prandtl Number: 10	171
61. Comparison of Variable Property Friction Factor Calculations for Oil A and Water Entrance Profile: Uniform Viscosity Ratio: 2 Prandtl Number: 1	172
62. Variable Property Friction Factor Calculations for Gases Entrance Profile: Parabolic.	174

Figure		Page
63.	Variable Property Friction Factor Calculations for Gases Entrance Profile: Uniform	175
64.	Variable Property Friction Factor Calculations for Liquids Entrance Profile: Parabolic Prandtl Number: 10	176
65.	Variable Property Friction Factor Calculations for Liquids Entrance Profile: Parabolic Prandtl Number: 100	177
66.	Variable Property Friction Factor Calculations for Liquids Entrance Profile: Parabolic Prandtl Number: 500	178
67.	Variable Property Friction Factor Calculations for Liquids Entrance Profile: Uniform Prandtl Number: 1	179
68.	Variable Property Friction Factor Calculations for Liquids Entrance Profile: Uniform Prandtl Number: 10	180
69.	Variable Property Friction Factor Calculations for Liquids Entrance Profile: Uniform Prandtl Number: 100	181

NOMENCLATURE

This table contains symbols which are used frequently throughout this work. It does not include common mathematical symbols or symbols which are defined and used only locally within the body of the work. Dimensional variables are primed to distinguish them from the dimensionless variables. Vector quantities are denoted by an arrow.

Symbol	Definition
\underline{A}	matrix defined by equation (9)
\underline{B}	matrix defined by equation (10)
\underline{C}	matrix defined by equation (11)
c_1	constant in heat capacity equation (133)
c_p	dimensionless heat capacity at constant pressure, c'_p/c'_{p_0}
D'	tube diameter
E_t	difference equation truncation error defined by equation (195)
E_q	energy balance error term defined by equation (172)
f	friction factor
f_{APP}	apparent friction factor
f_{APPW}	apparent friction factor for fluid at wall conditions
Fc	free convection parameter defined by equation (26)
Fr	Froude number, $\bar{u}'^2/g'_z D'$

Symbol	Definition
g'_z	acceleration due to gravity in z direction
Gr	Grashof number, $D_o^3 \rho_o'^2 g'_z \beta' (T'_w - T'_o) / \mu_o'^2$
Gr_w	Grashof number defined with μ'_w
h'	local heat transfer coefficient defined by equation (138)
h'_{AM}	arithmetic average heat transfer coefficient defined by equation (141)
h'_{LN}	logarithmic mean heat transfer coefficient defined by equation (144)
H	dimensionless enthalpy, $\frac{H'}{c'_{p_o} (T'_w - T'_o)}$
\mathcal{I}_q	heat energy integral defined by equation (136)
\mathcal{I}_u	material balance integral defined by equation (8)
k	dimensionless thermal conductivity, $\frac{k'}{k'_o}$
N	number of radial grid divisions
Nu	local Nusselt number defined by equation (138)
Nu_{AM}	arithmetic mean Nusselt number defined by equation (143)
Nu_{LN}	logarithmic mean Nusselt number defined by equation (145)
$O()$	order of magnitude function, a function whose value is proportional to its argument
p	dimensionless pressure, $\frac{p'}{\rho_o' \bar{u}'^2}$
Pe	Peclet number, $\frac{D' \bar{u}' \rho_o' c'_{p_o}}{k'_o} = \frac{Pr Re}{z^*}$
Pe_L	Peclet number defined with c'_{p_L} and k'_L

Symbol	Definition
Pe_M	Peclet number defined with c'_{p_M} and k'_M
Pe_w	Peclet number defined with c'_{p_w} and k'_w
Pr	Prandtl number, $c'_{p_o} \mu'_o / k'_o$
Pr^*	pseudo Prandtl number
Q	dimensionless rate of heat transfer defined by equation (129)
r	dimensionless radial coordinate, r'/D'
Δr	radial mesh spacing
R'	tube radius
Re	Reynolds number, $D' \bar{u}' \rho'_o / \mu'_o$
Re_w	Reynolds number defined with μ'_w
T	dimensionless temperature, $\frac{T' - T'_o}{T'_w - T'_o}$
$\Delta T'_{wo}$	temperature difference ($T'_w - T'_o$)
T'_M	dimensionless mean temperature defined by equation (132)
u	dimensionless axial velocity, u'/\bar{u}'
\bar{u}'	average axial velocity at entrance of the tube
v	dimensionless radial velocity, $\frac{D' v' \rho'_o}{\mu'_o}$
\vec{V}'	net vector velocity
W'	mass flow rate
z	dimensionless axial coordinate, $\frac{z'}{D' Re}$
z^*	dimensionless axial coordinate, z'/D'
Δz	axial grid spacing
$(\Delta z)_o$	initial axial grid spacing

Greek Symbol

Definition

$\bar{\beta}'$	coefficient of thermal expansion
ρ	dimensionless density, ρ'/ρ'_0
μ	dimensionless viscosity, μ'/μ'_0
μ_r	viscosity ratio, μ'_0/μ'_w
θ	ratio of Reynolds number and Froude number, Re/Fr

Subscripts

Definition

AM	arithmetic mean or evaluated at $\frac{T'_0 + T'_M}{2}$
ℓ	axial grid coordinate
L	local or evaluated at $T'(r', z')$
LN	log mean or evaluated at $\frac{T'_M - T'_0}{\ln(\frac{T'_M}{T'_0})}$
m	radial grid coordinate
M	mean or evaluated at T'_M
o	entrance conditions or evaluated at T'_0
w	wall condition or evaluated at T'_w

SUMMARY

Analytical studies involving the laminar flow of fluids in tubes are numerous; however, few analyses have been made in which the physical properties of the fluid were considered variable. In particular, the variation of physical properties with temperature in laminar flow heat transfer can have a profound effect on the fluid-flow and heat-transfer characteristics as compared to the isothermal case. The mathematical difficulties involved in treating such a case analytically by conventional methods of analysis are overwhelming; however, the advent of high speed computing machines has made the application of numerical techniques to this problem practicable. This investigation was primarily concerned with the solution by numerical methods of a system of partial differential equations which describe nonisothermal, laminar flow in tubes.

The specific objective of this work was to solve numerically the equations of continuity, motion, and energy for a Newtonian fluid with temperature-dependent fluid properties flowing laminarly in a vertical tube with a constant wall temperature. The properties ρ , μ , c_p , and k were to be considered functions of temperature in a realistic manner. The velocity profile entering the heated section of the tube was considered to be either parabolic or uniform. A further objective was to establish a correlation scheme for the fluid-flow and heat-transfer variables calculated from the solution.

Boundary-layer analysis reduces the general equations of continuity, motion, and energy in cylindrical coordinates to a system of three non-

linear partial differential equations sometimes known as the Prandtl boundary layer equations. These equations, along with an overall material balance and appropriate boundary conditions, were transformed by finite difference approximations into systems of linear algebraic equations. While the order of the systems of equations involved was large, a special technique was developed for advancing the pressure term step by step along the tube which allowed the systems describing the axial velocities and the temperatures to be solved by a direct and rapid (with respect to computer time) technique. This was important due to the large number of calculations involved when variable properties are considered. Calculation of the velocity and temperature profiles allowed the calculation of pertinent fluid-flow and heat-transfer variables. A valuable step-by-step heat balance used in assessing the accuracy of the numerical scheme was developed. The calculations were programmed for a Burroughs B-5000 Data Processing System.

By setting the properties constant in the program it was possible also to solve a number of interesting constant property problems. Those which were studied include the description of flow in the entrance of a tube, the classic Graetz heat-transfer problem, and the case of heat transfer in the entrance length of a tube. An interesting facet of these studies was the establishment of the importance of the radial velocity term in the equation of energy for heat transfer in the entrance of a tube. Comparison between the numerical solution of the Graetz problem and its analytical counterpart were excellent, but it was further shown that due to the constancy of the axial velocities for this case, it is not a severe test of the numerical solution.

A more stringent test of the numerical solution, and hence of the mathematical model, was a comparison of calculated values with experimentally determined values for fluid flow and heat transfer in which considerable property variation occurred. Agreement was excellent except in those cases where the numerical solution and experimental evidence indicated unstable flow. In those cases the experimental results were higher than the calculated heat transfer rates, implying turbulence.

An examination of the results for variable properties indicates that viscosity variations and free convection forces due to density variation can profoundly affect the fluid-flow and heat-transfer properties of the system as compared to the constant property case. It was also concluded that the inertia and radial velocity terms in the equations of motion and energy, which have been neglected in past analyses of this problem, are very important where free convection effects are significant and where density variations are great.

Using calculated results from the numerical solution for actual fluids, a correlation scheme based on the Prandtl number,

$$Pr = \frac{c_p' \mu_o'}{k_o'}$$

a viscosity ratio,

$$\mu_r = \frac{\mu_o'}{\mu_w'}$$

a free convection parameter,

$$Fc = 2\left(\frac{Re}{Fr}\right) \frac{\rho_w' - \rho_o'}{\rho_w' + \rho_o'}$$

and a length parameter,

$$\frac{Pe}{z^*} = \frac{PrRe}{z'/D'}$$

was established. The effect of c_p and k was taken into account by evaluating Pe/z^* with respect to these quantities at a suitable correlation temperature. Based on the above correlation scheme, values of the local Nusselt number, the mean temperature, a relative friction factor, the velocity profiles, and the temperature profiles were tabulated for ranges of μ_r from 0.1 to 20 and F_c from -200 to 800 for a number of values of Pr .

CHAPTER I

INTRODUCTION

Many of the classical problems in momentum and energy transport have been concerned with the study of laminar flow of Newtonian fluids in tubes. However, the majority of the analytical work in this area has been restricted to constant physical property solutions of the equations of continuity, motion, and energy. Although the effect of the variation of physical properties, especially density and viscosity, in many laminar flow heat-transfer situations is significant, the mathematical difficulties are great. Hence the value of the results of previous laminar flow heat-transfer studies for flow in tubes which considered the temperature dependence of fluid properties has been limited by simplifying assumptions designed to make the equations involved tractable. Only with the advent of modern high speed computing machines have massive assaults on the partial differential equations of laminar nonisothermal flow in tubes become practicable.

Thus, numerical methods utilizing high speed digital computers have marked the most successful papers in which the effect of the variation of fluid properties was investigated. This technique is highly versatile and in theory seems to have few limitations, but in practice many problems arise which prevent unlimited application. Excessive computation time, intolerable growth of error inherent in the numerical approximations, and nonconvergence of the approximate equations to the actual equations in the

mathematical sense of the limit can singly or in concert negate the value of numerical calculations. With respect to these problems a prior analysis of numerical schemes for the solution of a partial differential equation is impossible, at present, for all but the simplest of cases. This is unfortunate, but for this reason some indulgence in "experimental" mathematics must be condoned. This is not to imply a neglect of sound mathematical principles but is meant to point out that often suitably chosen trial tests can decisively rule out poor approaches which cannot be analyzed theoretically. Hence, numerical approaches put a premium on a thorough understanding of the physical principles of the problem being solved. The work described in this study is of this nature.

Lee⁽¹⁾ has reviewed most of the previous work in laminar nonisothermal flow in tubes.^(2,3,4,5,6,7,8,9,10) Additional experimental data have been presented by Kays and Nicoll⁽¹¹⁾ and Davenport and Leppert.⁽¹²⁾ Numerical studies by Lee⁽¹⁾ and Lemmon⁽¹³⁾ have also appeared. A solution by Bodia⁽¹⁴⁾ for natural convection between parallel plates is also significant in its application of boundary-layer type equations to internal flows. The most comprehensive of these studies has been that by Lee⁽¹⁾ who considered realistic fluids and took into account the variation in viscosity, density, thermal conductivity, and heat capacity. His solution is limited, however, in neglecting radial velocity effects in the energy equation and inertia terms in the equation of motion. These terms are necessary when considering development from a uniform velocity profile and in general are necessary when natural convection effects are pronounced.

This study presents a numerical solution of the equations of continuity, motion, and energy for laminar flow heat transfer in a vertical

tube with a constant wall temperature. All physical properties are considered functions of temperature in a realistic manner. Contributions from inertia terms and radial velocities are included in the equations solved. Heat-transfer and fluid-flow parameters are correlated for design convenience, and data are presented on the general nature of nonisothermal laminar flow. In addition, results for constant property heat transfer and flow in the entrance of a tube are presented.

CHAPTER II

MATHEMATICAL DESCRIPTION OF THE PROBLEM

The physical description of the problem which concerns this work is described in detail in the following discussion. A mathematical model in terms of a system of partial differential equations is proposed, and a numerical calculation scheme for the solution of the system based on finite difference approximations of the derivatives is outlined.

Description of the Problem

Consider the steady laminar flow of a Newtonian fluid in a vertical tube under the following conditions. The wall temperature of the tube is maintained constant. The fluid enters the tube with a uniform temperature and either a uniform or a parabolic velocity profile. The flow direction may be either in the direction of the gravity force or opposite it. The fluid properties are considered functions of temperature only. The Mach number is much less than unity, and the bulk viscosity is zero. The flow is axially symmetric with respect to the tube center line. Heat generation due to viscous dissipation is negligible. This description is diagrammatically represented in Figure 1. A definition of terms and symbols used in this work is presented in the Nomenclature.

Mathematical Model

The general equations of continuity, motion, and energy in various

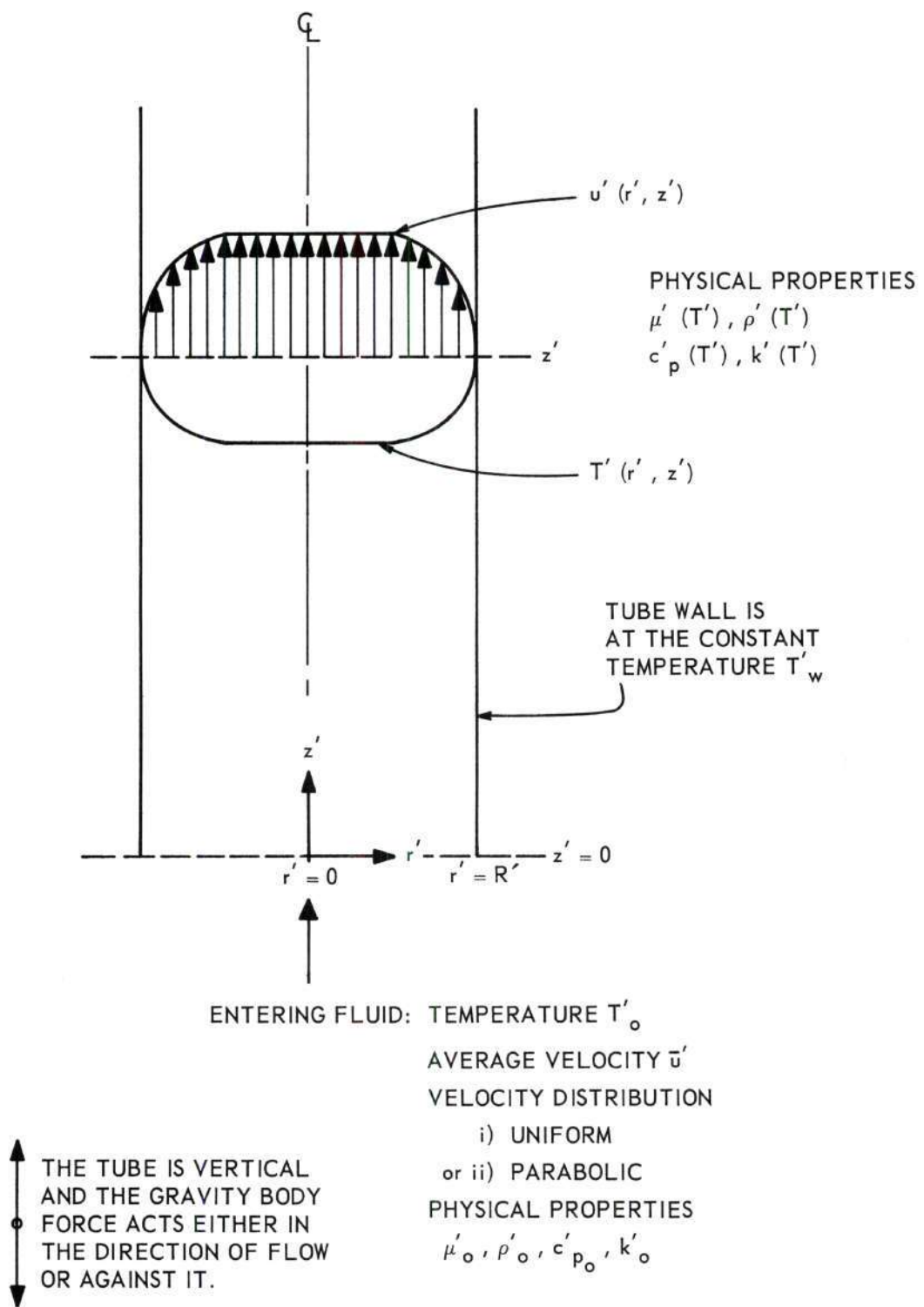


Figure 1. Diagram of Problem.

coordinate systems for laminar flow can be found in Bird.⁽¹⁵⁾ The equations which apply to the present case are

(Continuity)

$$\frac{1}{r'} \frac{\partial}{\partial r'} (\rho' r' v') + \frac{\partial}{\partial z'} (\rho' u') = 0 \quad (1)$$

(Motion)

$$\begin{aligned} \rho' (v' \frac{\partial v'}{\partial r'} + u' \frac{\partial v'}{\partial z'}) &= - \frac{\partial p'}{\partial r'} - \left[\frac{1}{r'} \frac{\partial}{\partial r'} (-2\mu' r' \frac{\partial v'}{\partial r'}) \right. \\ &+ \frac{2}{3} \mu' \frac{\partial}{\partial r'} (r' v') + \frac{2}{3} \mu' r' \frac{\partial u'}{\partial z'} + \frac{2\mu' v'}{r'^2} + \frac{2}{3} \frac{\mu'}{r'^2} \frac{\partial (r' v')}{\partial r'} \\ &\left. - \frac{2}{3} \frac{\mu'}{r'} \frac{\partial u'}{\partial z'} - \frac{\partial}{\partial z'} (\mu' \frac{\partial u'}{\partial r'} + \mu' \frac{\partial v'}{\partial z'}) \right] \end{aligned} \quad (2)$$

$$\begin{aligned} \rho' (v' \frac{\partial u'}{\partial r'} + u' \frac{\partial u'}{\partial z'}) &= \frac{\partial p'}{\partial z'} - \left[\frac{1}{r'} \frac{\partial}{\partial r'} (-\mu' r' (\frac{\partial u'}{\partial r'} + \frac{\partial v'}{\partial z'})) \right. \\ &\left. + \frac{\partial}{\partial z'} (-2\mu' \frac{\partial u'}{\partial z'} + \frac{2}{3} \mu' (\frac{1}{r'} \frac{\partial}{\partial r'} (r' v') + \frac{\partial u'}{\partial z'})) \right] \end{aligned} \quad (3)$$

(Energy)

$$\begin{aligned} \rho' c_p' (v' \frac{\partial T'}{\partial r'} + u' \frac{\partial T'}{\partial z'}) &= \frac{1}{r'} \frac{\partial}{\partial r'} (r' k' \frac{\partial T'}{\partial r'}) + \frac{\partial}{\partial z'} (k' \frac{\partial T'}{\partial z'}) \\ &+ \rho' T' \left(\frac{\partial (\frac{1}{\rho'})}{\partial T'} \right)_{p'} (v' \frac{\partial p'}{\partial r'} + u' \frac{\partial p'}{\partial z'}) - \left\{ \left[-2\mu' \frac{\partial v'}{\partial r'} \right. \right. \\ &+ \frac{2}{3} \mu' \left(\frac{1}{r'} \frac{\partial}{\partial r'} (r' v') + \frac{\partial u'}{\partial z'} \right) \frac{\partial v'}{\partial r'} + \left[-\frac{2\mu' v'}{r'} \right. \\ &+ \frac{2}{3} \mu' \left(\frac{1}{r'} \frac{\partial}{\partial r} (r' v') + \frac{\partial u'}{\partial z'} \right) \frac{v'}{r'} + \left[-2\mu' \frac{\partial u'}{\partial z'} + \frac{2}{3} \mu' \left(\frac{1}{r'} \frac{\partial}{\partial r'} (r' v') \right. \right. \\ &\left. \left. + \frac{\partial u'}{\partial z'} \right) \frac{\partial u'}{\partial z'} - \mu' \left(\frac{\partial u'}{\partial r'} + \frac{\partial v'}{\partial z'} \right) \left(\frac{\partial u'}{\partial r'} + \frac{\partial v'}{\partial z'} \right) \right] \right\} \end{aligned} \quad (4)$$

The usual boundary-layer order of magnitude analysis performed^(1,16) on equations (1), (2), (3), and (4) simplifies them to the Prandtl boundary-layer equations in cylindrical coordinates. These equations are listed below in terms of dimensionless variables. Among the assumptions inherent in the boundary-layer simplifications are the assumptions of negligible axial heat conduction and negligible radial pressure gradient.

$$\frac{1}{r} \frac{\partial(\rho r v)}{\partial r} + \frac{\partial(\rho u)}{\partial z} = 0 \quad (\text{Continuity}) \quad (5)$$

$$\rho \left(v \frac{\partial u}{\partial r} + u \frac{\partial u}{\partial z} \right) = - \frac{dp}{dz} + \frac{1}{r} \frac{\partial}{\partial r} \left(r \mu \frac{\partial u}{\partial r} \right) + \theta \rho \quad (\text{Motion}) \quad (6)$$

$$\rho c_p \left(v \frac{\partial T}{\partial r} + u \frac{\partial T}{\partial z} \right) = \frac{1}{r Pr} \frac{\partial}{\partial r} \left(r k \frac{\partial T}{\partial r} \right) \quad (\text{Energy}) \quad (7)$$

Equations (5), (6), and (7) resulting from the boundary-layer type analysis serve as a basis for the calculations found in the following pages. For the problem of interest, the associated boundary conditions in terms of dimensionless variables are

$$\text{I. } z = 0 \quad \dots \quad \mu = \rho = c_p = k = 1 \quad (0 \leq r \leq \frac{1}{2})$$

$$v = T = p = 0$$

$$\text{a. Parabolic Profile: } u = 2(1 - 4r^2)$$

$$\text{b. Uniform Profile: } u = 1$$

$$\text{II. } r = 0 \quad \dots \quad \frac{\partial u}{\partial r} = \frac{\partial T}{\partial r} = v = 0 \quad (z \geq 0)$$

$$\text{III. } r = \frac{1}{2} \quad \dots \quad v = u = 0 \quad (z > 0)$$

$$T = 1$$

The reference value of the pressure at $z = 0$ is arbitrary, and it is set equal to zero as a matter of convenience. The dimensionless variables are defined as:

$$\begin{aligned} z &= \frac{z'}{D' Re} , \quad r = \frac{r'}{D'} , \quad u = \frac{u'}{\bar{u}'} , \quad v = \frac{v' D' \rho_o'}{\mu_o'} \\ T &= \frac{T' - T_o'}{T_w' - T_o'} , \quad p = \frac{p'}{\rho_o' \bar{u}'^2} , \quad \mu = \frac{\mu'}{\mu_o'} , \quad \rho = \frac{\rho'}{\rho_o'} \\ k &= \frac{k'}{k_o'} , \quad c_p = \frac{c_p'}{c_{p_o}'} , \quad Re = \frac{\bar{u}' D' \rho_o'}{\mu_o'} , \quad Pr = \frac{c_{p_o}' \mu_o'}{k_o'} \\ Fr &= \frac{\bar{u}'^2}{g_z' D'} , \quad Pe = \frac{D' \bar{u}' \rho_o' c_{p_o}'}{k_o'} , \quad \theta = \frac{Re}{Fr} \end{aligned}$$

The prime indicates a dimensional quantity, the subscript o indicates entrance conditions, the subscript w indicates wall conditions, and the \bar{u}' represents the average entrance velocity.

An overall material balance results in the following useful relationship.

$$\mathcal{Q}_u = \int_0^{\frac{1}{2}} \rho u r dr = \frac{1}{8} \quad (8)$$

Notice that the inertia terms

$$\rho \left(v \frac{\partial u}{\partial r} + u \frac{\partial u}{\partial z} \right)$$

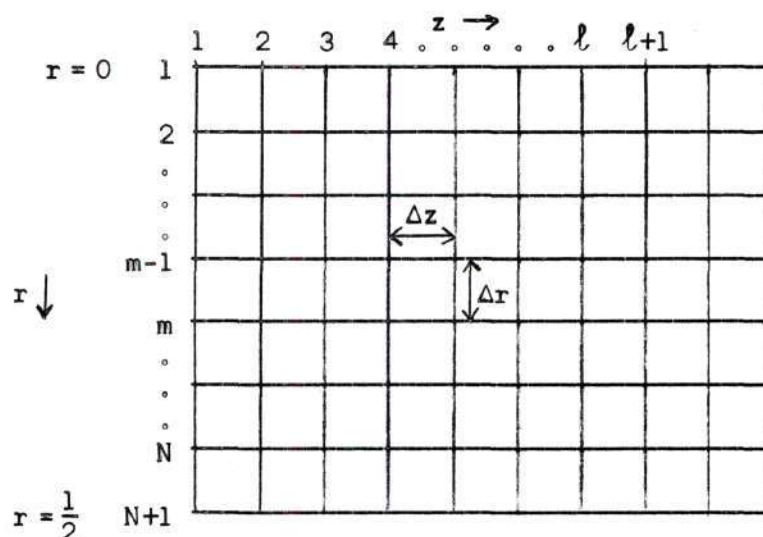
in the simplified equation of motion and the radial velocity term

$$v \frac{\partial T}{\partial r}$$

in the simplified energy equation are not neglected in this study as they have often been in previous studies.

Outline of Numerical Solution

Consider the following semi-infinite grid superimposed on half the flow field from $r = 0$ to $r = \frac{1}{2}$.



The grid is used to locate point functions defined in terms of functional notation as

$$f_{m,l} = f((m-1)\Delta r, (l-1)\Delta z)$$

The variables in equations (5), (6), (7), and (8) are considered point functions on this grid and the derivatives are replaced by finite difference approximations. These approximations lead to systems of linear algebraic equations. The resulting algebraic equations are summarized below in matrix-vector notation.

In matrix-vector notation the finite difference equations of motion and energy become

$$\underline{A} \vec{u}(p) = \vec{a} + \vec{b}p \quad (9)$$

$$\underline{B} \vec{t} = \vec{c} \quad (10)$$

and the equation of continuity and the overall material balance can be written as

$$\vec{v} = \underline{C} \vec{u}(p) + \vec{d} \quad (11)$$

$$\mathcal{Q}_u = (\vec{e}, \vec{u}(p)) \quad (12)$$

These equations apply at step $\ell + 1$ and all components of \underline{A} , \underline{B} , \underline{C} , \vec{a} , \vec{b} , \vec{c} , and \vec{d} are either constants or are values determined at steps up to and including $\ell + 1$. The matrices \underline{A} and \underline{B} are tridiagonal in form and equations (9) and (10) must be solved implicitly for \vec{u} and \vec{t} , which represent the point values of the axial velocity and the temperature respectively. The vector representing the point values of the radial velocity, \vec{v} , is given explicitly as a function of the matrices \underline{C} and the vectors \vec{d} and \vec{u} . The scalar product of \vec{e} and \vec{u} is formed by a numerical integration of equation (8). Note that \vec{u} is written in equations (9), (10), (11), and (12) as a function of the scalar representing pressure. This is done to emphasize the method of attack which makes use of this functional relationship and which will be described now.

Since a fundamental requirement is that

$$\mathcal{Q}_u = \frac{1}{8}$$

we can form the function

$$F(p) = \frac{1}{8} - \mathcal{Q}_u$$

and a correct solution to equation (9) requires that

$$F(p) = 0$$

Hence, we apply the Newton-Raphson iterative technique to find the zero of $F(p)$ which is the correct value of the pressure. The Newton-Raphson iteration for this solution is

$$p_{l+1}^{i+1} = p_{l+1}^i + \frac{\frac{1}{8} - (\vec{e}, \vec{u}(p_{l+1}^i))}{(\vec{e}, \vec{u}'(p_{l+1}^i))} \quad (14)$$

where

$$\vec{u}'(p) = D_p \vec{u}(p) \quad (15)$$

and

$$\underline{A} \vec{u}'(p) = \vec{b} \quad (16)$$

It is seen that at step $l+1$, $\vec{u}'(p)$ is independent of p , and $F(p)$ is linear with respect to p . Hence the first approximation p_{l+1}^0 should result in the correct value for p_{l+1} . In practice, p_l is used for p_{l+1}^0 . An approximate value of \vec{u} and the value of \vec{u}' are determined and used to get p_{l+1} . The correct value of \vec{u} is then calculated.

This procedure allows the use of a simple and accurate computational scheme for tridiagonal matrices of high order. Also this scheme is very efficient with respect to machine computation time.

The calculation scheme is initiated by evaluating \underline{B} and \underline{C} at step l and then \vec{t} at $l+1$. Then \underline{A} , \underline{C} , \vec{a} , \vec{b} , and \vec{d} are evaluated

and used to solve for \vec{u} and \vec{v} . With the velocity and temperature fields known, numerical differentiation and integration are applied to calculate various pertinent heat-transfer and fluid-flow parameters.

Descriptions of the components of the matrices and vectors in the equations above and a detailed description of the calculation scheme are given in Appendix A.

A description of the computer program for implementing the calculation scheme is given in Appendix B. Empirical property equations for the fluids studied are presented in Appendix C.

CHAPTER III

CONSTANT PROPERTY SOLUTIONS

Although the main purpose of this study was to obtain solutions to equations (5), (6), and (7) with the properties considered as functions of temperature, a number of constant property solutions were obtained. Comparison of these solutions with previous studies served not only to establish confidence in the accuracy of the numerical scheme but also gave more complete solutions in some cases. Insight was obtained as to the effect of radial velocities on heat transfer when the axial velocity profile is changing, and an accuracy criterion for the numerical scheme based on step-by-step energy balance was developed. These constant property solutions are described in this chapter.

Constant Property Forms of the Equations

Equations (5), (6), (7), and (8) for the case of constant properties become

$$\frac{\partial(rv)}{\partial r} + r \frac{\partial u}{\partial z} = 0 \quad \text{(Continuity)} \quad (17)$$

$$v \frac{\partial u}{\partial r} + u \frac{\partial u}{\partial z} = - \frac{dp}{dz} + \frac{1}{r} \frac{\partial}{\partial r} \left(r \frac{\partial u}{\partial r} \right) \quad \text{(Motion)} \quad (18)$$

$$v \frac{\partial T}{\partial r} + u \frac{\partial T}{\partial z} = \frac{1}{rPr} \frac{\partial}{\partial r} \left(r \frac{\partial T}{\partial r} \right) \quad \text{(Energy)} \quad (19)$$

and

$$\int_0^{\frac{1}{2}} u r dr = \frac{1}{8} \quad \text{(Overall Material Balance)} \quad (20)$$

For these equations the finite difference scheme described in Chapter II applies if the property values are set equal to unity. Although the variable property program can be used by inserting constants for the property equations, extensive use in this manner wastes computation time. Therefore, the program used in the constant property solutions was rewritten completely deleting the variable properties.

Laminar Entrance Flow

Laminar flow of a constant property Newtonian fluid in the entrance region of a tube has long been of interest. Analytical solutions have been obtained by a number of investigators, who further simplified equations (17), (18) and (20) by making various approximations which allowed a solution to be obtained. It is interesting that even with the variety of approaches that have been applied to this problem, the most comprehensive of these solutions are in reasonable agreement with each other and with what limited experimental data that are available. Due to the boundary-layer nature of the flow it is not surprising that boundary-layer techniques for external flows have been adapted to give satisfactory solutions very near the entrance of the tube. A brief review of previous work in this area is given by Campbell.⁽¹⁷⁾

Equations (17), (18) and (20) were solved numerically subject to the conditions

- I. $z = 0$ $u = 1, v = 0, p = 0$ ($0 \leq r < \frac{1}{2}$)
- II. $r = 0$ $\frac{\partial u}{\partial r} = v = 0$ ($z \geq 0$)
- III. $r = \frac{1}{2}$ $u = v = 0$ ($z > 0$)

The results are presented in Figures 2, 3, 4, 5, 6, and 7 and Table 1, along with the results of some previous studies for comparison. Table 4 in Appendix D contains numerical values from which Figure 2 was constructed. In the calculation of the pressure it was found by starting the solution at successively smaller z that a short interval was always required for the pressure values to converge to the solution. Since the radial velocities appear to have a discontinuity at $z = 0$, inaccuracies in them during the first few steps probably cause this pressure effect. However, a procedure for starting the solution was developed which takes into account the rapid change of radial velocities near the entrance and thereby minimizes the pressure effect. It is noted that the radial velocities at the tube entrance are zero, but at an infinitesimal distance^{*} down the tube they are large and directed toward the center of the tube. They decrease in magnitude very rapidly just inside the entrance. Hence, while the marching approximation

$$v_{m,l} = v_{m,l+1} + O(\Delta z)$$

is reasonable where the radial velocities are continuous functions of z ,

* Distance here is meant in the sense of the magnitude of the dimensionless variable $z'/D'Re$.

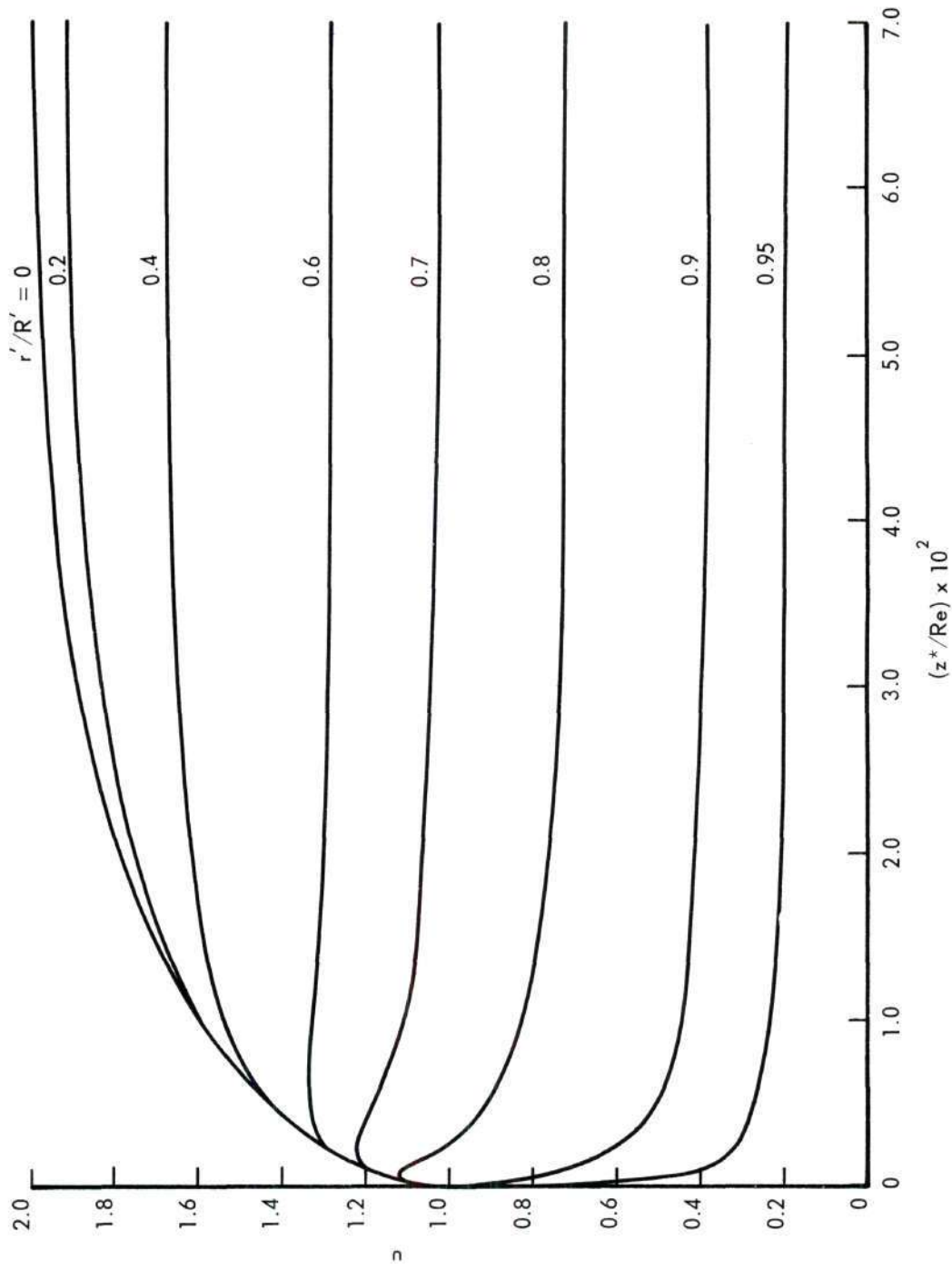


Figure 2. Constant Property Axial Velocity Calculations.
Entrance Profile: Uniform.

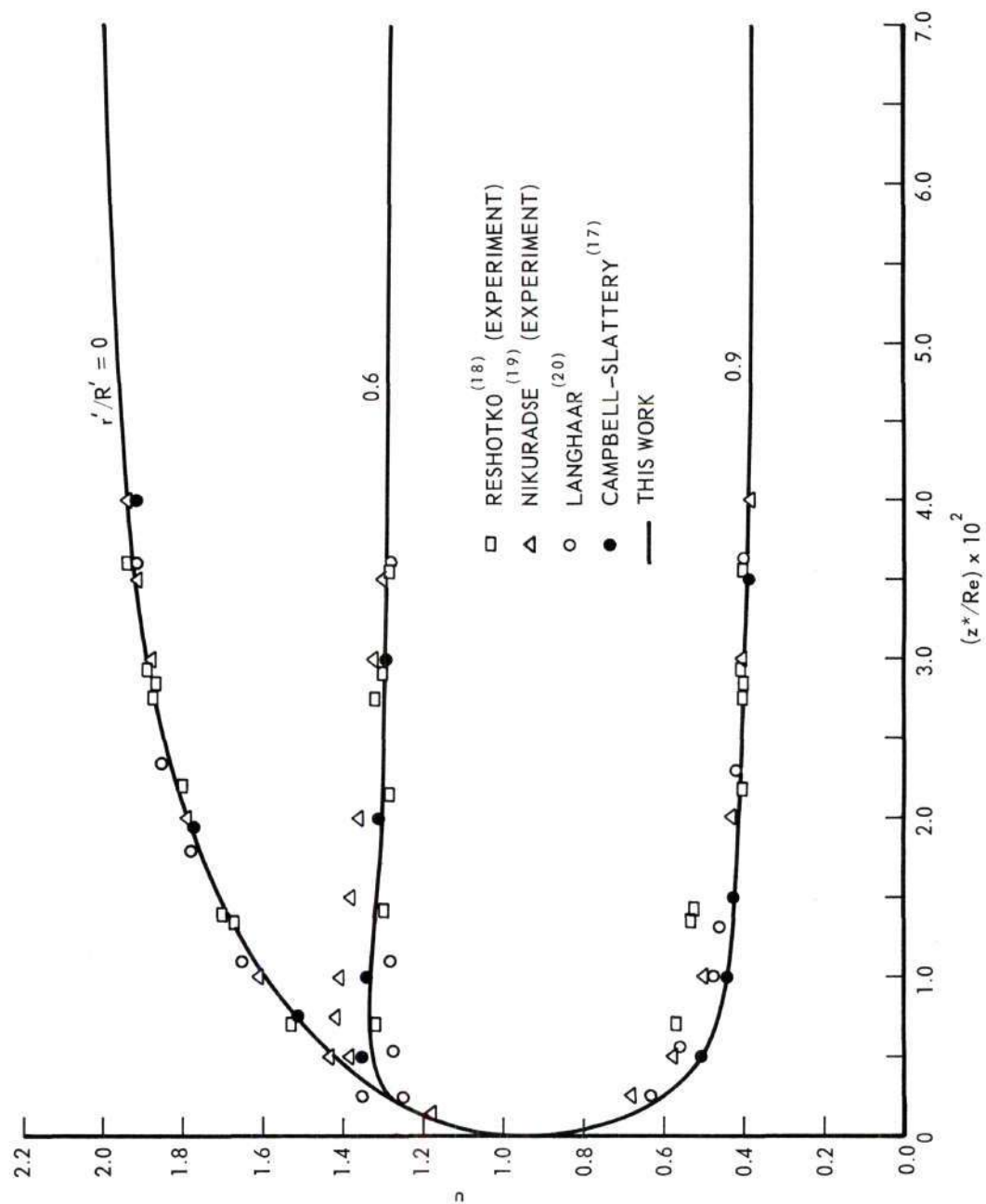


Figure 3. Comparison of Constant Property Axial Velocity Calculations with the Results of Other Investigations. Entrance Profile: Uniform.

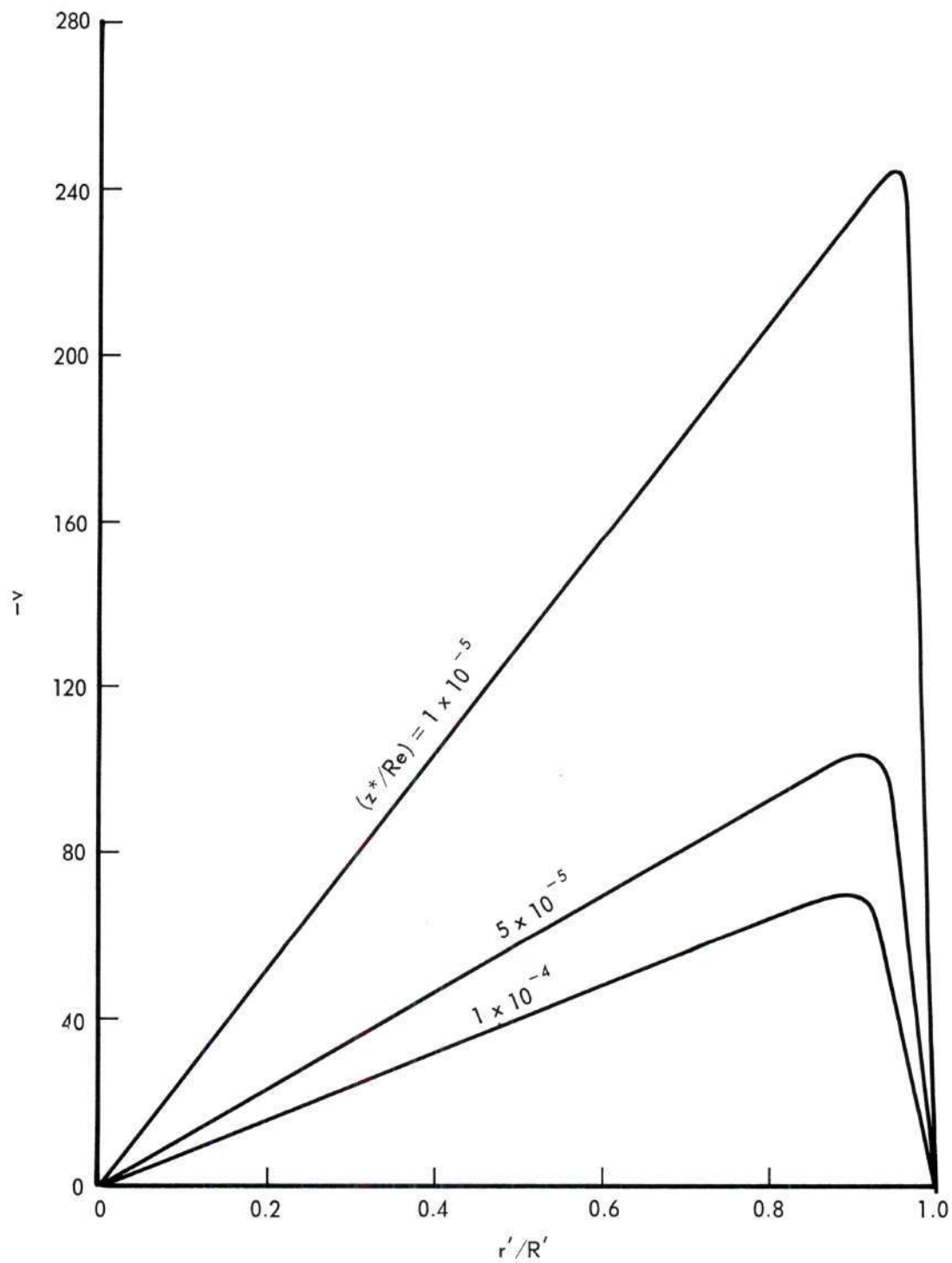


Figure 4. Constant Property Radial Velocity Profile Calculations.
Entrance Profile: Uniform.

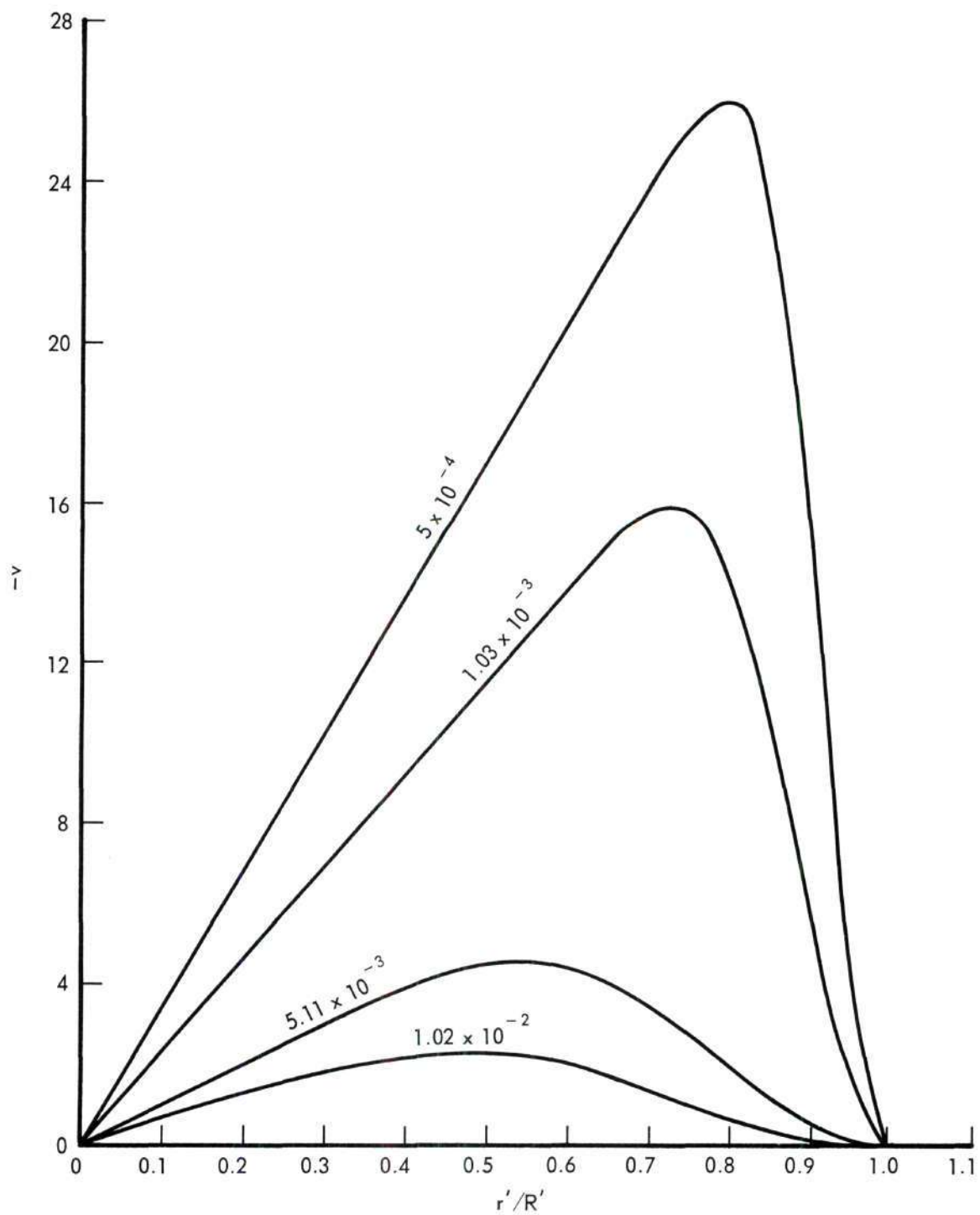


Figure 5. Constant Property Radial Velocity Profile Calculations.
Entrance Profile: Uniform.

Table 1. Comparison of Constant Property Calculated
Entry Length and Kinetic Energy
Correction Factor with the Results
of Other Investigations
Entrance Profile: Uniform

Investigation	Entry Length, z^*/Re (99 Per Cent Criterion)	ζ^*
This work	0.060	1.26
Collins ⁽²¹⁾	0.061	1.33
Bogue ⁽²²⁾	0.0287	1.16
Goldstein ⁽²³⁾	-	1.41
Langharr ⁽²⁰⁾	0.0575	1.28
Schiller ⁽²⁴⁾	0.0287	1.16
Tomita ⁽²⁵⁾	0.050	1.22
Campbell ⁽¹⁷⁾	-	1.18
Schiller ⁽²⁴⁾	-	1.159*
Reiman ⁽²⁶⁾	-	1.124*

^{*}Defined by $-2\Delta p = 64z + C$. It does not include energy required to accelerate the fluid from the reservoir.

* Experimental

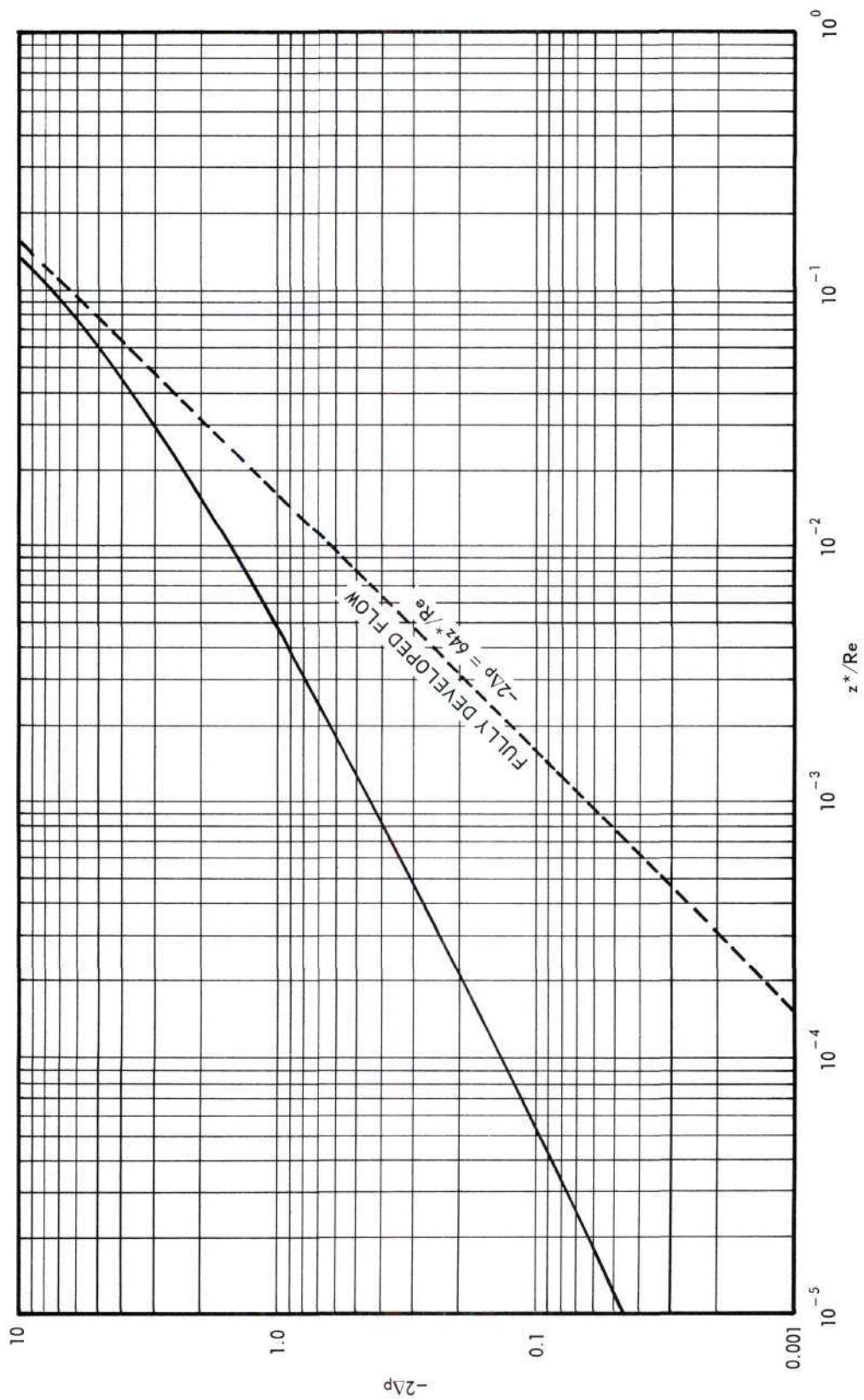


Figure 6. Constant Property Pressure Drop Calculations.
Entrance Profile: Uniform.

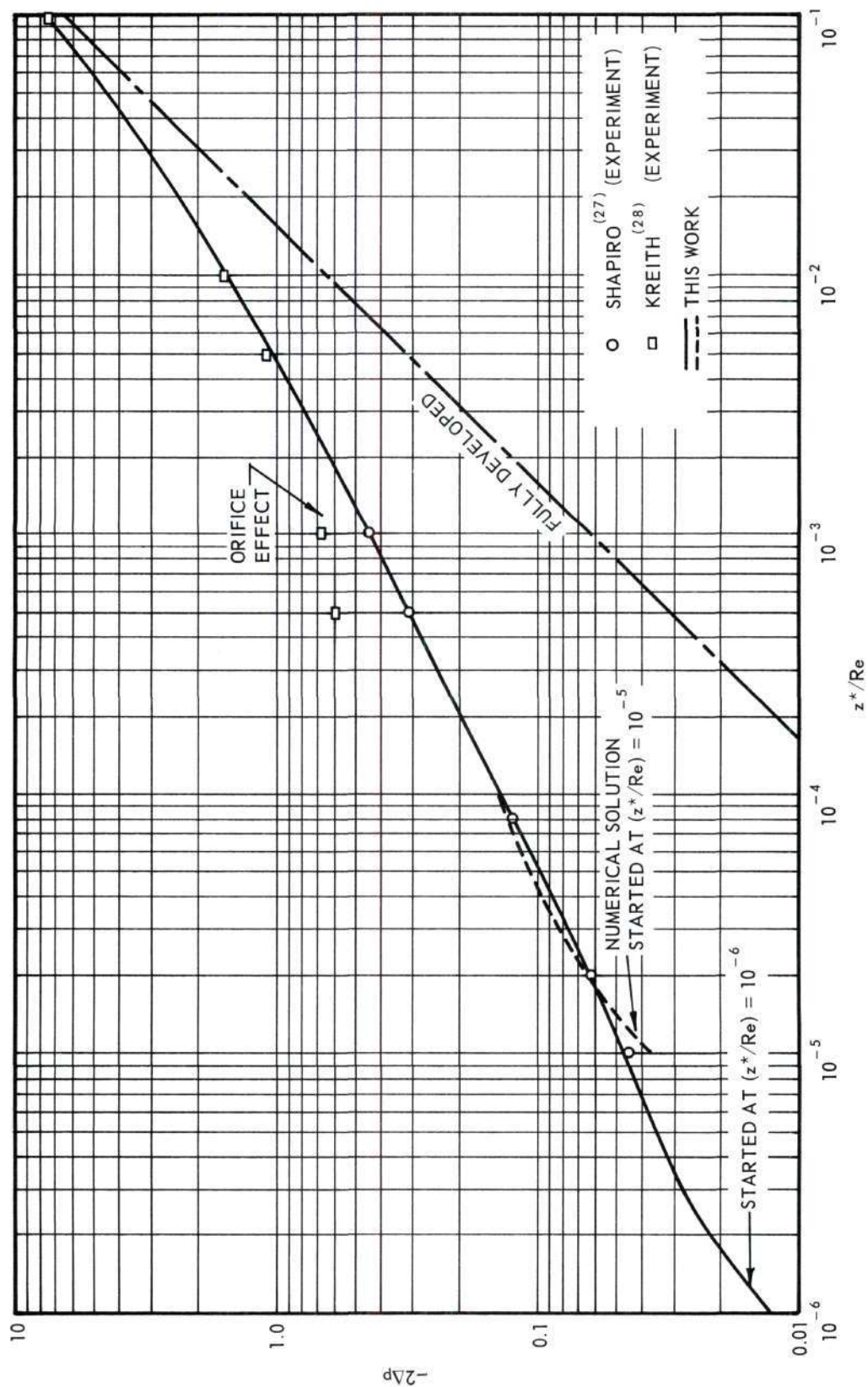


Figure 7. Comparison of Constant Property Pressure Drop Calculations with the Results of Experimental Measurements. Entrance Profile: Uniform.

it is unreasonable to make the approximation

$$v_{m,1} = v_{m,2} = 0$$

The starting procedure then is to approximate $v_{m,2}$ by $v_{m,1}$ as above, and then calculate a better value of $v_{m,2}$ from equation (11) and use this value as an improved starting value. Also, in order to anticipate the rapid decrease in the magnitude of the radial velocities, the approximation

$$\frac{v_{m,2}}{2} = v_{m,3}$$

is made at the next step. The procedure outlined in Chapter II is followed thereafter.

To give the dimensionless radial velocity values somewhat more meaning, it is noted that an easy way to compare the magnitudes of the radial velocities with the axial velocities is to recognize that

$$\frac{v}{uRe} = \frac{v'}{u'} \quad (21)$$

Constant Property Heat Transfer with Parabolic Velocity Profile

Consider a tube whose wall is maintained at the constant temperature T'_w . If a constant property fluid flows at temperature T'_0 through this tube such that it enters the tube with a fully developed parabolic velocity profile then the heat transfer is described by

$$u = 2(1 - 4r^2) \quad (22)$$

Table 2. Comparison of Constant Property Heat Transfer
Calculations with Results Calculated from
the Analytical Solutions of Graetz*
Entrance Profile: Parabolic

Pe/z*	<u>Mean Temperature</u>		<u>Local Nusselt Number</u>	
	<u>Numerical</u>	<u>Graetz</u>	<u>Numerical</u>	<u>Graetz</u>
980	0.0606	0.0605	10.1	10.0
746	0.0718	0.0719	9.23	9.17
435	0.101	0.101	7.71	7.68
220	0.152	0.154	6.22	6.18
97.1	0.253	0.253	4.91	4.88
64.9	0.318	0.321	4.44	4.41
43.3	0.402	0.403	4.09	4.06
20.5	0.595	0.597	3.72	3.72
18.6	0.623	0.626	3.71	3.70
10.0	0.805	0.810	3.66	3.66

* Graetz values calculated by Lee⁽¹⁾.

solution, which is an asymptotic solution of the Graetz problem, for large values of Pe/z^* as is seen below:

$\frac{Pe}{z^*}$	$T_{M\text{Calc}}$	$T_{M\text{Lévéque}}$	<u>Per Cent Deviation</u>
100	0.247	0.300	17.7
1000	0.0595	0.0646	7.9
10000	0.0134	0.0139	3.6

The Lévéque mean temperature equation is given by

$$T_M = 6.46 \left(\frac{Pe}{z^*} \right)^{-2/3} \quad (24)$$

Constant Property Heat Transfer with a Developing Velocity Profile

Now consider the case where the wall temperature of the tube is again held constant, but now the entering velocity profile is uniform across the tube. Again the equations (17), (18), (19), and (20) describe the problem and must be solved subject to the conditions

- I. $z = 0$ $u = 1, v = T = p = 0$ ($0 \leq r < \frac{1}{2}$)
- II. $r = 0$ $\frac{\partial u}{\partial r} = \frac{\partial T}{\partial r} = 0$ ($z \geq 0$)
- III. $r = \frac{1}{2}$ $u = v = 0, T = 1$ ($z > 0$)

Results of the numerical solution of these equations are summarized in Figures 8, 9, and 10. Numerical values are presented in Tables 6 through 11 of Appendix D.

Previous investigations of this problem have been undertaken by Businger⁽³¹⁾, Kays⁽³²⁾, Goldberg⁽³³⁾, Stephens⁽³⁴⁾, and Lemmon⁽¹³⁾.

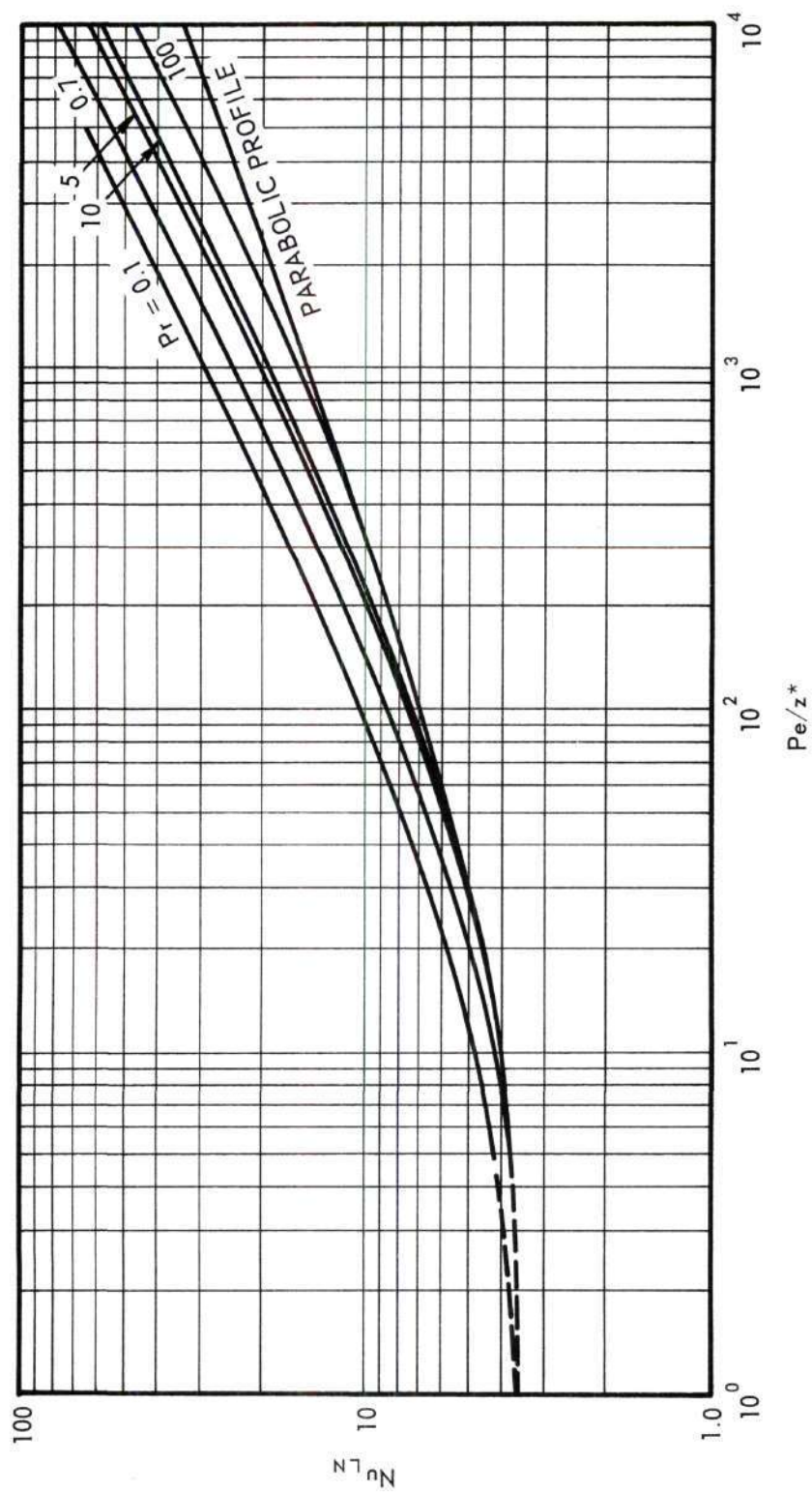


Figure 8. Constant Property Logarithmic Mean Nusselt Number Calculations.
Entrance Profile: Uniform.

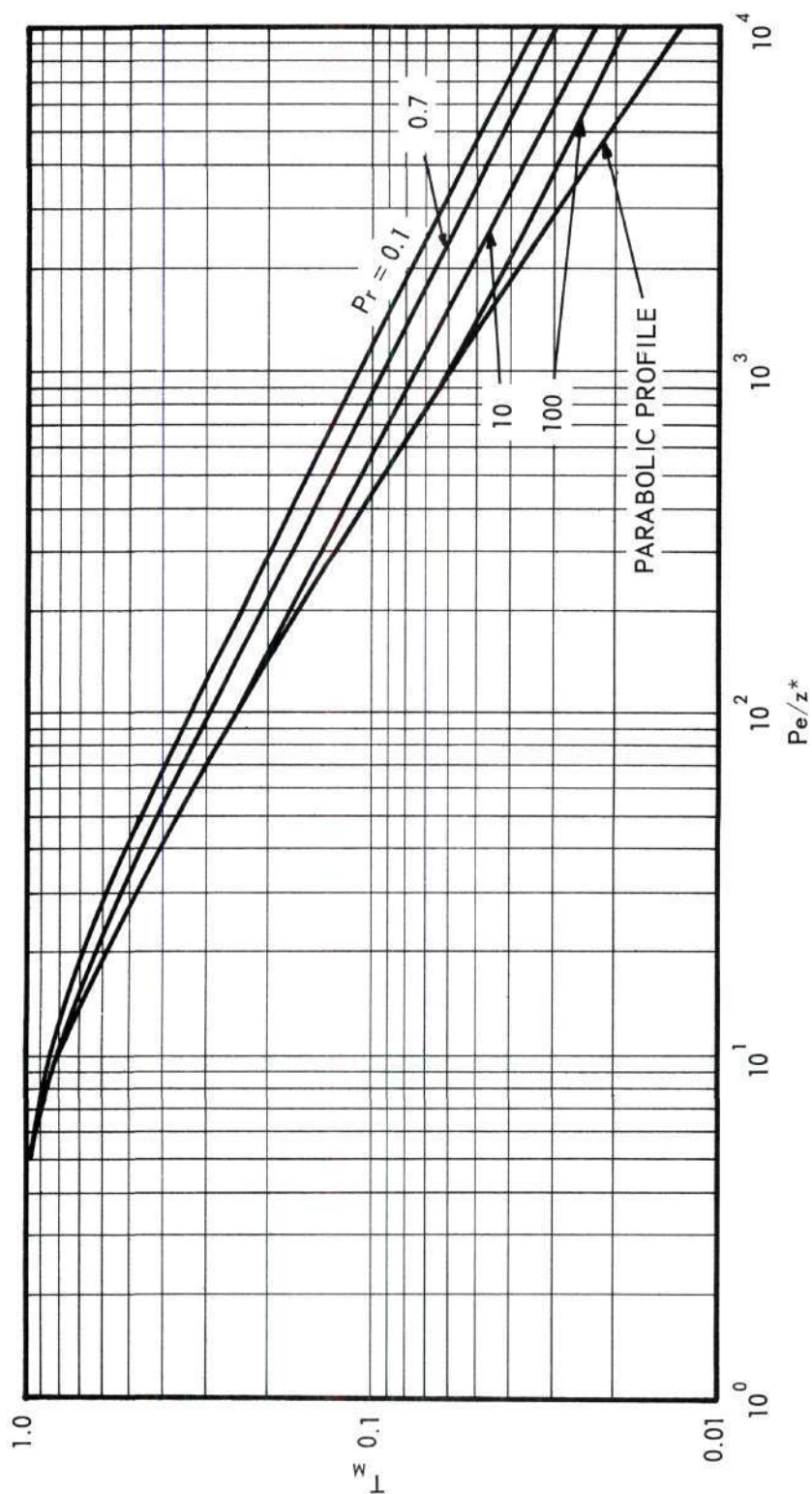


Figure 9. Constant Property Mean Temperature Calculations.
Entrance Profile: Uniform.

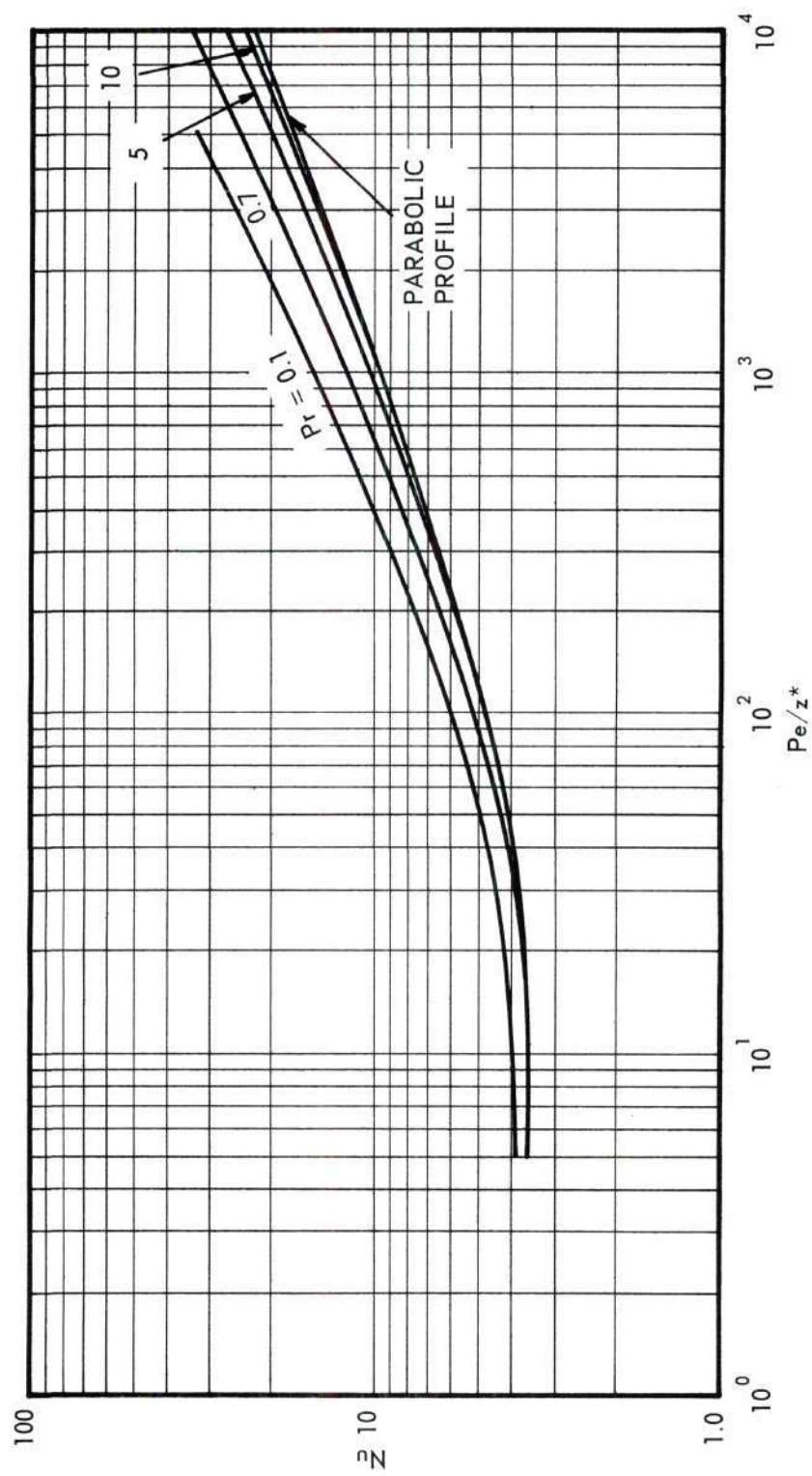


Figure 10. Constant Property Local Nusselt Number Calculations.
Entrance Profile: Uniform.

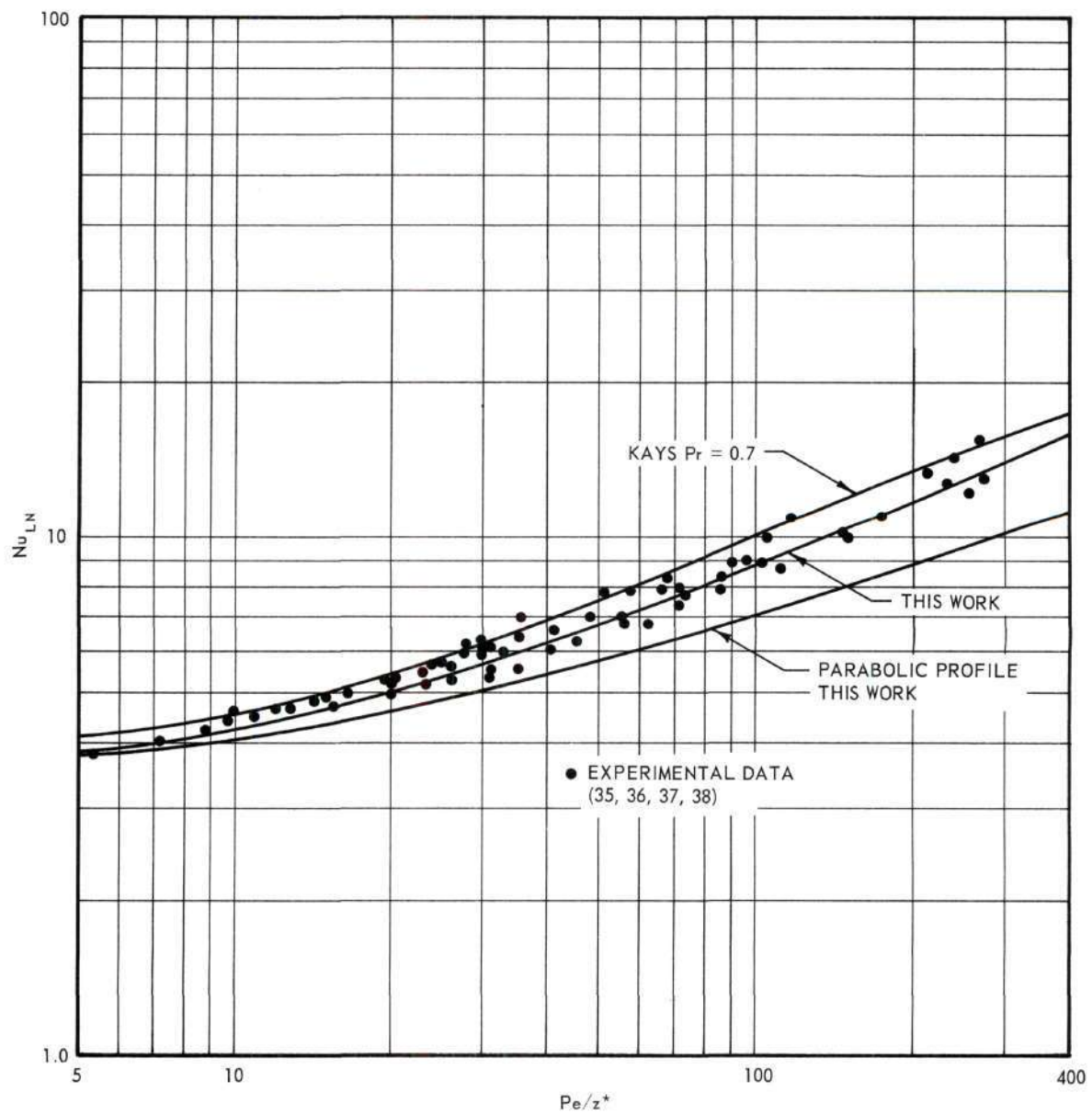


Figure 11. Comparison of Constant Property Heat Transfer with Results of Experimental Measurements.
Entrance Profile: Uniform.

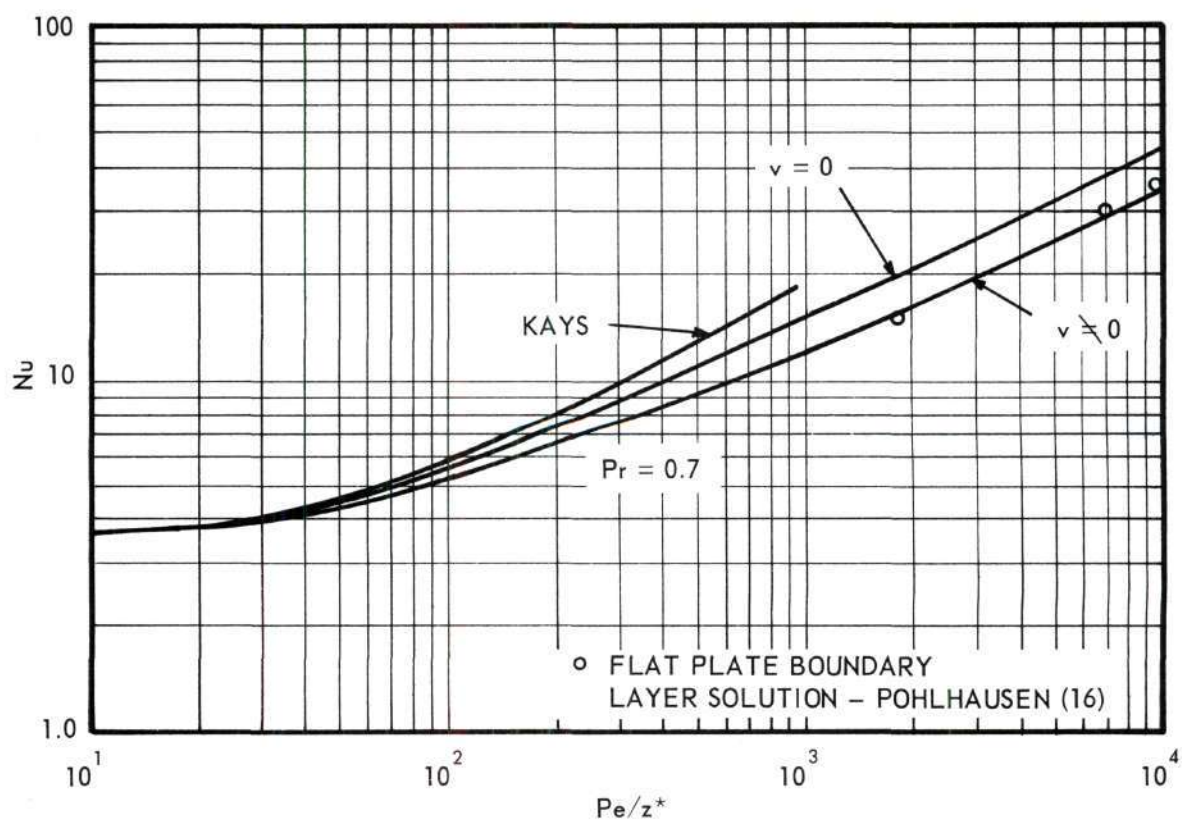


Figure 12. Effect of Radial Velocity Term on Calculated Constant Property Local Nusselt Numbers. Entrance Profile: Uniform.

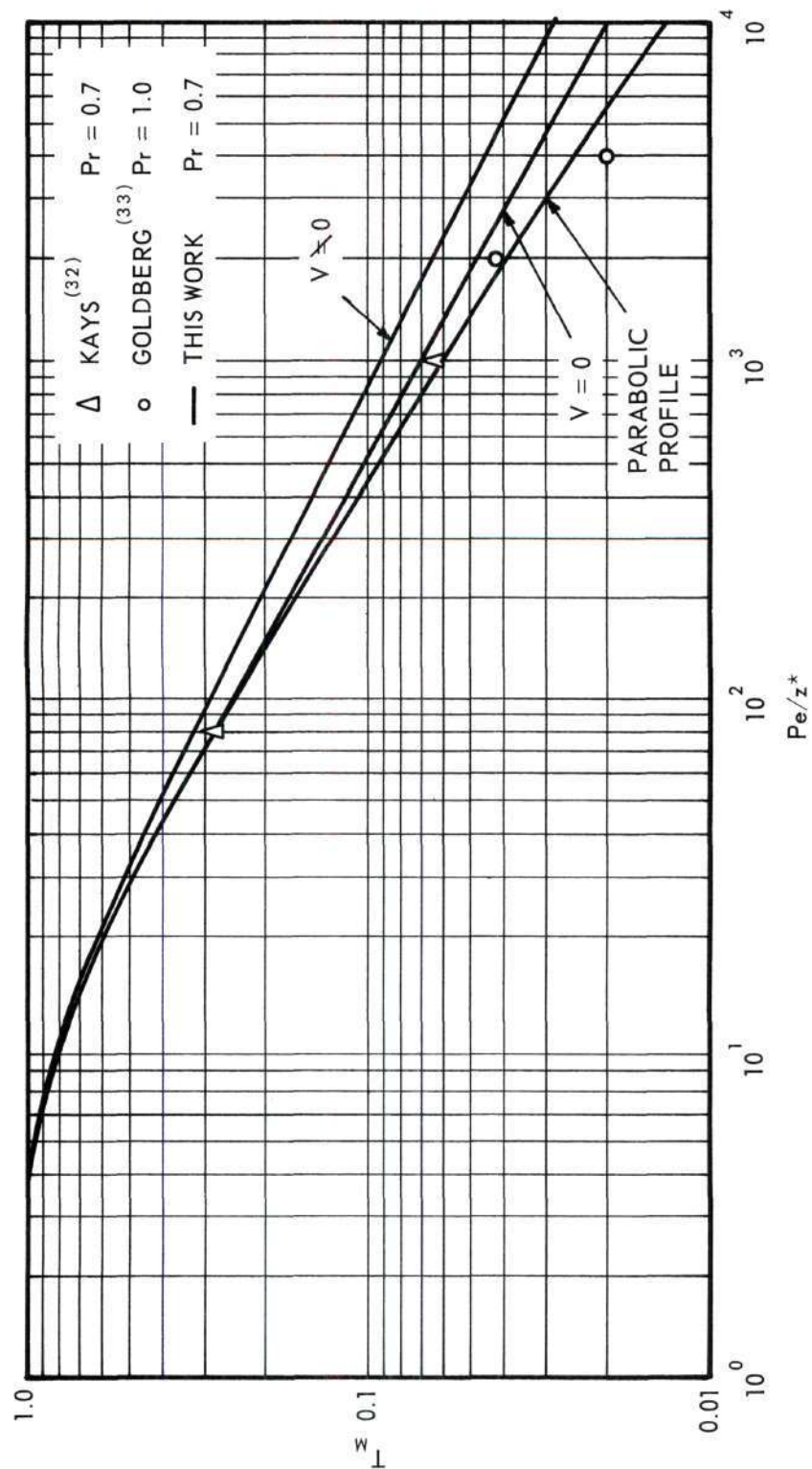


Figure 13. Effect of Radial Velocity Term on Calculated Mean Temperature.
Entrance Profile: Uniform.

Businger used an approximate form of Schiller's axial velocities, assumed the thermal and momentum boundary layer thicknesses equal ($Pr \approx 1$) and forced an asymptotic agreement with the Graetz solution. Kays employed Langhaar's axial velocity expression and numerically solved (apparently by hand calculation) equation (19) neglecting the radial velocity term. Goldberg programmed Kays' solution on a digital computer and extended the results to cover a range of Prandtl numbers. Stephens' mathematical approach is similar to that of Atkinson and Goldstein.⁽²³⁾ Near the entrance of the tube a similarity variable is used to reduce the equations from partial to ordinary differential equations, and a perturbation of the parabolic profile is used in the nearly developed region. The two solutions are interpolated to form one continuous solution. Lemmon has obtained a numerical solution to equations (17), (18), (19), and (20). Unfortunately the solution is somewhat inefficient and does not include any step-by-step energy balance. The importance of the energy balance will be discussed in the following section of this chapter. Comparison between the solution described in this work and previous theoretical and experimental work is found in Figures 11, 12, and 13. Also included in this comparison are results obtained with the numerical scheme in this work for the radial velocity term in equation (19) neglected. Kays mean temperature values in Figure 13 were calculated from temperature profile data presented in his paper.

Step-by-Step Energy Balance

It is possible to calculate the energy transferred to the fluid in the tube between any two cross sections from either the difference in the

mean temperatures from one cross section to the other or by an integration of the temperature gradient at the wall between the two sections.

Letting

QT = Energy in by Mean Temperature Calculation

QN = Energy in by Temperature Gradient Calculation

and error term may be defined as

$$E_q = \frac{QT - QN}{QT + QN} \quad (25)$$

This error gives the \pm deviation of QT or QN from their average.

Details for the calculation of this error term may be found in Appendix A.

In this work it was found that a step-by-step calculation of E_q was a good indication of the proper marching step size in the numerical scheme. It was found that E_q could be made as small as desired by simply reducing Δz enough. However, practical considerations of computation time and the finally desired accuracy indicated that a maximum E_q of approximately two per cent would be reasonable. The average error was usually much smaller than this.

On the other hand, numerical solutions for heat transfer with a developing velocity profile in which the radial velocity term in equation (19) was neglected exhibited very large E_q . Furthermore, the error could not be reduced below 10 to 20 per cent even by resorting to impracticably small values of Δz . A check of the numerical solutions of Kays,⁽³²⁾ Goldberg,⁽³³⁾ Bosworth,⁽³⁹⁾ and Lee⁽¹⁾ indicate similar behavior. This perhaps explains why Kays' results for the local Nusselt number appear to be too high and the mean temperature values too low. In recent work

by Ulrichson and Schmitz,⁽⁴⁰⁾ numerical mass transfer calculations for a wall catalyzed reaction seem to confirm this observation. It is interesting to note that when the axial velocity profile was not a function of the axial distance, such as in the Graetz problem, E_q could be made small by decreasing the marching step sufficiently. Thus, a comparison with the Graetz solution does not indicate the difficulty encountered in the numerical solution when the axial velocity is changing and the radial velocity is neglected in equation (19).

CHAPTER IV

VARIABLE PROPERTY SOLUTIONS

The main aim of this work was to develop a calculation procedure for equations (5), (6), and (7) for flow in a tube with constant wall temperature which considered the fluid properties to be realistic functions of temperature. The results of a numerical scheme which represent the accomplishment of this aim are presented in this chapter. The entrance velocity profile is considered either parabolic or uniform. The calculation procedure has been previously summarized in Chapter II, and details are in Appendix A.

Calculations are compared with experimental data and are used to establish a correlation scheme for heat-transfer and fluid-flow variables.

Comparison with Experiment

Parabolic Entrance Profile

Martinelli et al.⁽²⁾ have reported data on the heating of oil and water in vertical tubes such that the entering velocity profile was fully developed and the wall temperature constant. Kays and Nicoll⁽¹¹⁾ measured heat-transfer rates for the cooling of air under similar flow conditions with high bulk-to-wall temperature differences. In both cases, fluid properties varied considerably. A representative comparison of the numerical solution with these investigations is presented in Table 3.

Taking into account experimental accuracies, the agreement between experiment and calculation is good except in the case of the water experiments. It is to be noted, however, that about half of the water runs

Table 3. Comparison of Variable Property Heat Transfer Calculations with the Results of Experimental Measurements
Entrance Profile: Parabolic

Investigator	Exp. Run No.	Fluid	Re	Pr	z^*	μ_r	Fc	$T_{M\text{Exp.}}$	$T_{M\text{Calc.}}$	Per Cent Deviation From $T_{M\text{Exp.}}$
Alves and Southwell ⁽²⁾	4	Oil A*	516	680	602	17	1	0.116	0.120	+3.5
Alves and Southwell	15	Oil A	7.33	697	602	18	62	0.901	0.921	+2.2
Alves and Southwell	15a	Oil A	7.33	697	297	18	62	0.856	0.791	-7.0
Alves and Southwell	27	Oil A	2150	244	602	6	1	0.081	0.0808	-0.2
Weinberg ⁽²⁾	5a	Oil A	440	463	126	12	1	0.0610	0.0614	+0.7
Weinberg	47	Water	1769	6.3	126	3	310	0.558**	0.390	-30
Weinberg	48	Water	1567	6.2	126	3	365	0.633**	0.432	-30
Kays and Nicoll ⁽¹¹⁾	2	Air	1270	0.690	62.5	1.3	-6	0.662	0.659	-0.5
Kays and Nicoll	8	Air	1160	0.688	62.5	1.4	-6	0.697	0.676	-3.0
Kays and Nicoll	11	Air	1060	0.684	62.5	1.6	-5	0.713	0.688	-3.5
Kays and Nicoll	14	Air	980	0.683	62.5	1.8	-4	0.728	0.701	-3.7

*This oil was supplied to Martinelli et al.⁽²⁾ by the Standard Oil Company of California.

**Turbulence indicated in these runs.

reported were indicated by the investigators as having become turbulent; although it is not clear what criterion was used to judge which runs were turbulent. Apparently extremely high heat-transfer rates were the indication, but this of course forces some arbitrary range selection and does not provide an absolute method for judging unstable flow. The indicated "laminar" runs gave heat-transfer rates consistently greater than predicted by the investigators' semi-empirical correlation. Since the calculated velocity profiles exhibit the extreme distortion (center-line velocity nearly zero) which Scheele et al.⁽⁴¹⁾ have shown to be unstable, the high values of the experimental mean temperatures for the water runs are most certainly attributable to either transition or turbulent flow in the latter portions of the heating length of the tube. Pigford⁽⁴⁾ also came to this conclusion based on his analysis.

It is interesting to observe that the results of Kays and Nicoll⁽¹¹⁾ differ little from constant property solutions. This is probably due to the large wall directed, radial velocity component which offsets the increase in heat transfer for a flattened velocity profile. A more general illustration of such effects will follow in later sections of this chapter.

Martinelli⁽²⁾ also reported pressure drop data for the nonisothermal flow of oil. Unfortunately in many of the runs apparently the total pressure drop and the gravity pressure drop were of comparable magnitude making it difficult to get the apparent frictional pressure drop by difference. However, one of the runs where the pressure drop due to gravity and the apparent frictional pressure drop were about the same size is shown in Figure 14 along with the calculated values. Agreement is very

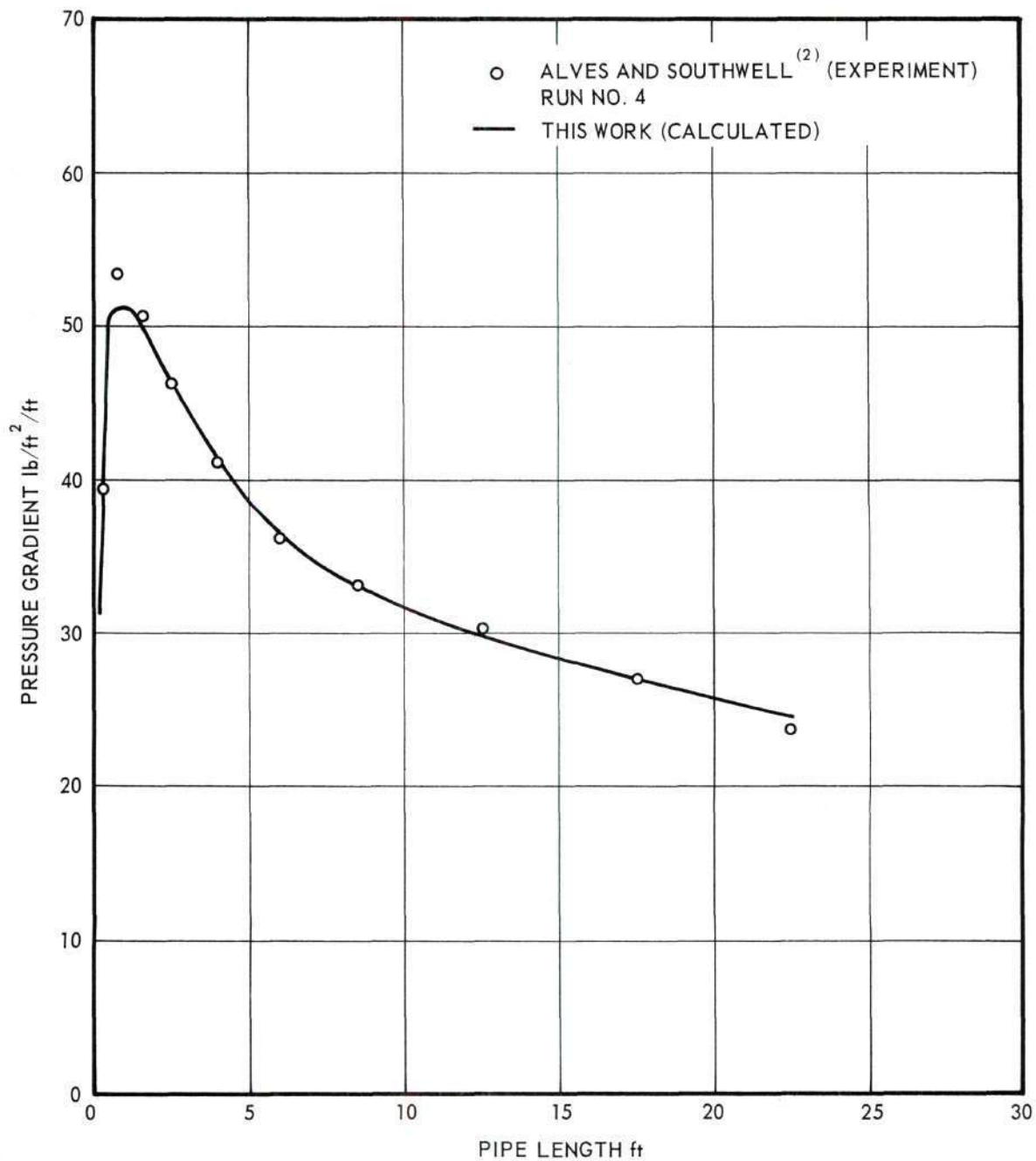


Figure 14. Comparison of Variable Property Pressure Drop Calculations with the Results of Experimental Measurement.
Entrance Profile: Parabolic.

good. It is especially significant to note that the calculated values verify the experimentally observed low pressure gradient near the entrance which was characteristic of nearly all of the experimental runs. The explanation is found in the recognition that the observed frictional pressure drop is due not only to fluid friction, but also to kinetic energy changes in the stream due to a rearrangement of the velocity profile. This effect will be illustrated more fully when correlated friction factor data are presented.

Uniform Entrance Profile

Very little experimental data are available to compare with the variable property solution for the case of a uniform velocity profile. Watzinger and Johnson⁽⁴²⁾ report heat-transfer data with large natural convection effects, but it is difficult to exactly characterize their experimental conditions. Their apparatus essentially consisted of a vertical countercurrent double-pipe heat exchanger. Water was cooled in downflow. However, the cooling water flow was not high enough to prevent a significant variation in the wall temperature. No estimate of this effect can be made from their data since they only reported a mean wall temperature.

However, using their measured mean wall temperature a number of their runs were calculated. In all cases the free convection effects were found to be extremely large ($Fc > 6000$), causing the center-line velocity to become zero well before the exit of their tube. Since the numerical scheme was not stable for negative axial velocities the calculations were always terminated for negative center-line velocities. As already stated, this condition physically is indicative of turbulence.

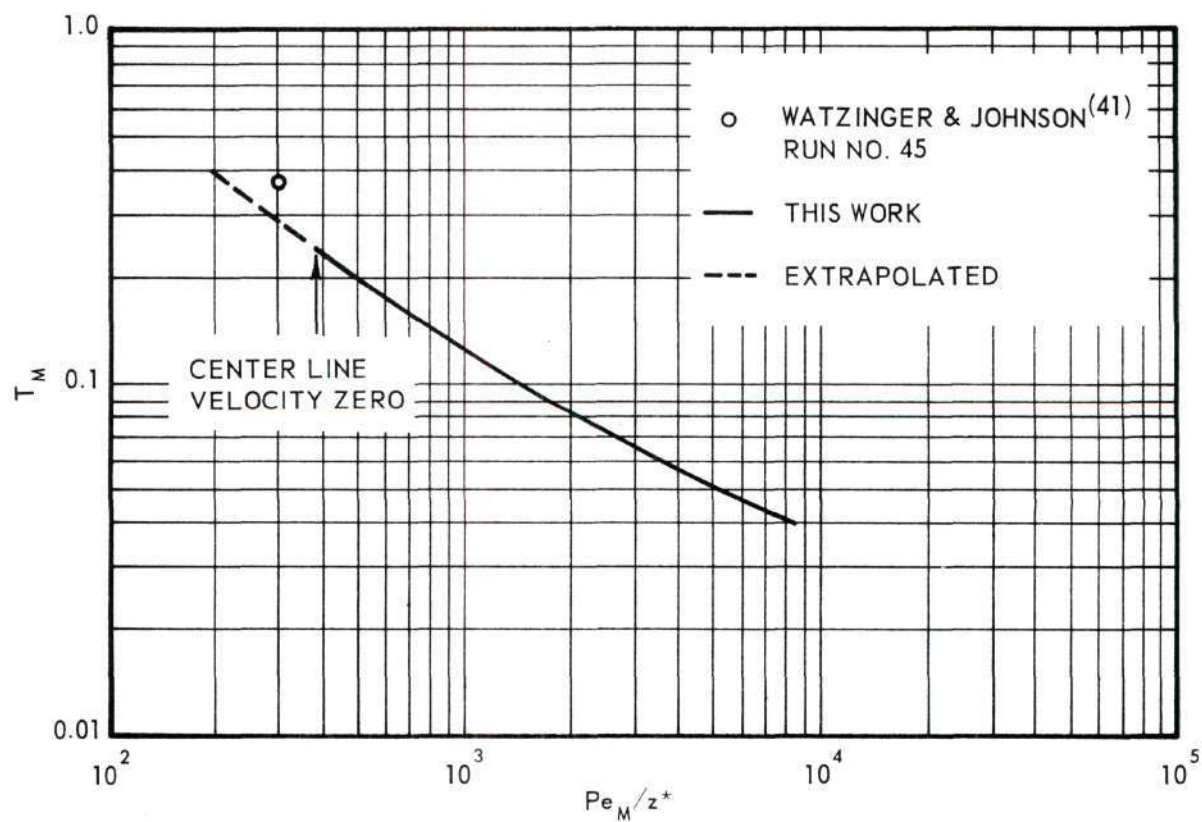


Figure 15. Comparison of Variable Property Mean Temperature Calculations with the Results of Experimental Measurements.
Entrance Profile: Uniform.

A typical run is shown in Figure 15. Extrapolation of the calculated mean temperature to the end of the tube indicates that the measured mean temperature was high, lending support to the supposition that turbulence was present in the latter portion of the tube.

The paucity of experimental data for this case is unfortunate. However, the excellent constant property results for the developing flow heat-transfer calculations imply accurate variable property results. Furthermore, a comparison of the velocity profiles for the parabolic and uniform entrance condition to be presented later would indicate little difference in the calculation difficulties after the initial few steps down the tube.

Correlation Scheme

The correlation scheme used for Nu , T_M , T , u , and f_{APP}/f_{APPW} is basically that of Lee⁽¹⁾ who used intuitive arguments to modify and combine the ideas of Pigford⁽⁴⁾ and Cherry⁽¹⁰⁾. Lee points out that the correlating parameters are not derivable directly from the equations of continuity, motion, and energy as solved in this work; they are based on a much simpler picture. The supposition is that they will hold for the more complicated situations here, if the correlated values are not rapidly varying functions of the correlating parameters.

The controlling parameters are the viscosity ratio

$$\mu_r = \mu_o'/\mu_w'$$

and a free convection number

$$Fc = 2 \left(\frac{Re}{Fr} \right) \left[\frac{\rho'_w - \rho'_o}{\rho'_w + \rho'_o} \right] \quad (26)$$

The free convection number is just a modification of

$$\left(\frac{Gr_w}{Re_w} \right) \mu_r^{-1} = \frac{Re}{Fr} \bar{\beta}' (T'_w - T'_o) \quad (27)$$

obtained by replacing $\bar{\beta}'(T'_w - T'_o)$ with $2 \frac{\rho'_w - \rho'_o}{\rho'_w + \rho'_o}$. For liquids this amounts to little change since

$$\bar{\beta}'(T'_w - T'_o) = \frac{\rho'_o - \rho'_w}{\rho'_o} \quad (28)$$

where $\bar{\beta}'$ = coefficient of volumetric expansion
and

$$\frac{\rho'_o + \rho'_w}{2} \approx \rho'_o$$

For gases where

$$\bar{\beta}' = \frac{1}{T'} \quad (29)$$

it amounts to evaluating $\bar{\beta}'$ at $\frac{T'_w + T'_o}{2}$. This modification compensates for the variation of $\bar{\beta}'$ with temperature.

The difference $(\rho'_w - \rho'_o)$ is chosen to impart a positive sign to cases where free convection aids forced convection. The sign convention is summarized below.

<u>Sign</u>	<u>Condition</u>
+	Heating - Upflow
+	Cooling - Downflow
-	Heating - Downflow
-	Cooling - Upflow

The dimensionless length for correlation purposes is

$$\frac{Pe}{z^*} = \frac{RePr}{z^*} = \frac{Pr}{z} \quad (30)$$

The numbers μ_r and F_c primarily account for viscosity and density effects. The variation in thermal conductivity and heat capacity is secondary in importance and can be accounted for by evaluating the length parameter, Pe/z^* at an appropriate temperature. The proper temperature, which depends on the quantity being studied, will be defined with each correlation in following sections of this chapter.

As is implied by constant property solutions, the uniform entrance profile solutions required that the additional correlation parameter Pr be included. This additional parameter was also required for the friction factor correlation in the case of the parabolic entrance profile.

Other necessary slight modifications such as the separate treatment of gases and liquids will be discussed with the correlation in which they are included.

Generation of Correlation Data

Having established confidence in the accuracy of the numerical scheme both by examining constant property solutions and by a comparison with experimental measurements, it can be used to generate data for actual

liquids and gases. The only requirement is that each property dependence on temperature be representable by some analytical expression which can be inserted in the computer program. The generation of correlation data then from the mathematical model is analogous to the generation of experimental data from a physical model. Obviously the computer generation of data allows for much more versatility in the selection of substances and conditions than could be possibly achieved in a single piece of experimental equipment. Also the speed with which the data can be generated is usually much greater. Perhaps even more important, the mathematical model is a permanent, established tool ready to be used over and over again.

From an examination of the equations of continuity (5), motion (6), and energy (7) in their dimensionless form, it is apparent that the physical properties are normalized to the initial condition. This means that the type of variation with temperature is more important than the absolute magnitudes of the properties. Hence, it is possible to tailor-make a material for study. For example, the effect of Prandtl number can be studied by choosing the properties of a real substance, water for instance, and arbitrarily specifying the Prandtl number in the numerical scheme. This of course could never be accomplished in a physical model.

The materials chosen for study in this work were selected not only because reasonably good property data were available but also because their variation in properties is so different. The liquids chosen were water, n-octane, and oil A. Water and oil A differ radically in chemical composition and as a result in their physical properties. Octane is somewhat intermediate between oil A and water. Its viscosity range is

greater than water, but the Prandtl number range is comparable to that of water. Octane also exhibits a much greater density variation than either oil A or water. The gases chosen were air and helium which appear to be representative of most common gases under conditions where the mathematical model holds.

The empirical equations which fit the property variation with temperature can be found in Appendix C. A list of conditions for which correlating data were generated can be found in Tables 12, 13, and 14 of Appendix E.

Verification of Correlation Scheme

Parabolic Entrance Profile

Due to the extreme difference in the way that properties of gases and liquids vary with temperature it was necessary to treat them separately.

For liquids, typical correlations employing the parameters μ_T and F_c are presented in Figures 16 through 21. The properties k and c_p are taken into account by evaluating Pe/z^* with respect to these variables at T_M for Nu and T_M , at T_w for f_{APP}/f_{APPW} , and at the local point temperature for the velocity and temperature profiles. It was necessary to include an additional correlating parameter, Pr , for the apparent friction factor correlation. This complication is due to the fact that the intense viscosity gradients which cause rearrangements in the velocity profile and affect the kinetic energy changes are a function of the thermal boundary-layer thickness, while the viscosity at the wall, which affects the frictional drag, is independent of the thermal boundary-

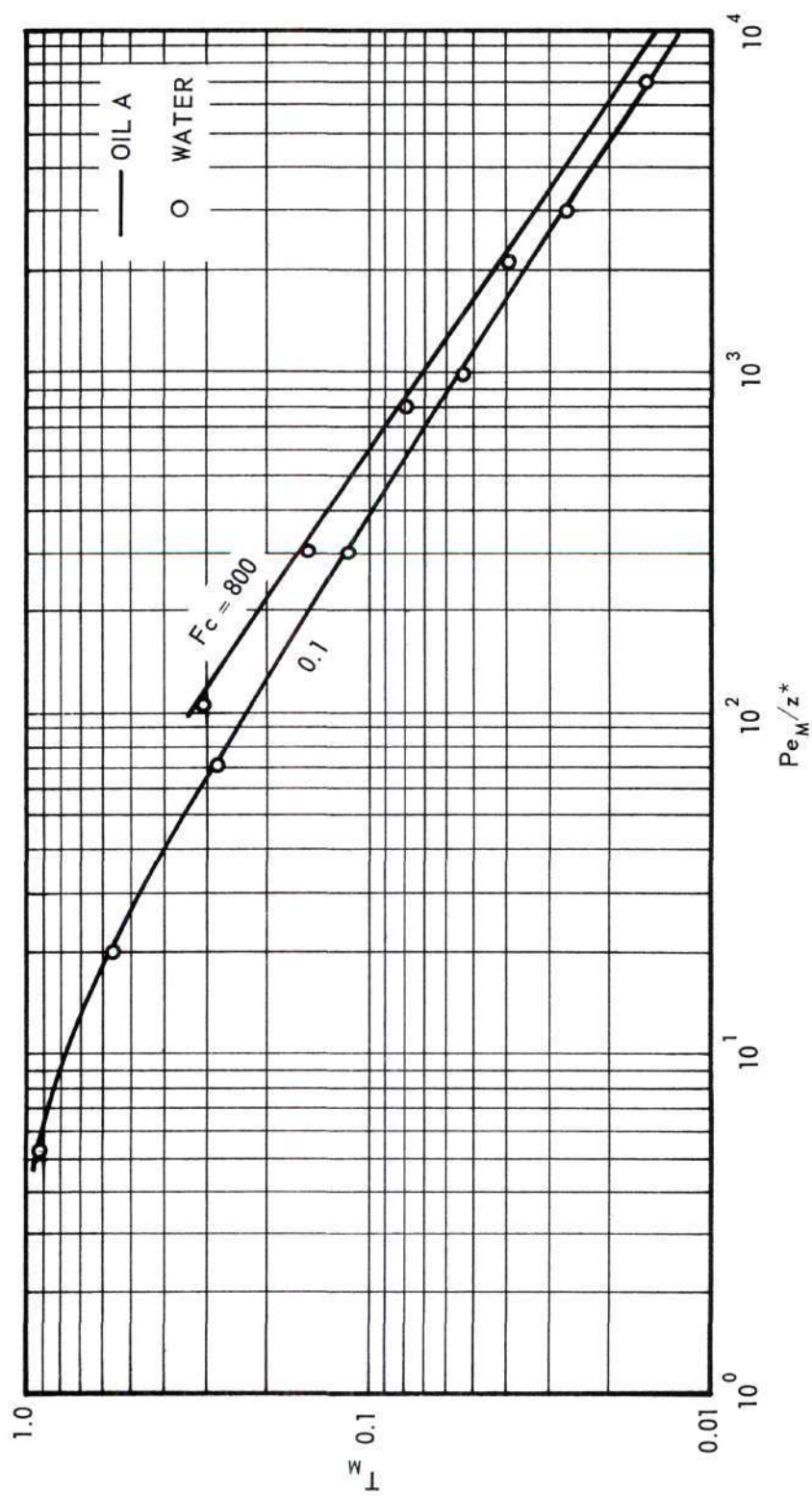


Figure 16. Comparison of Variable Property Mean Temperature Calculations for Oil A and Water.
Entrance Profile: Parabolic.
Viscosity Ratio: 0.5.

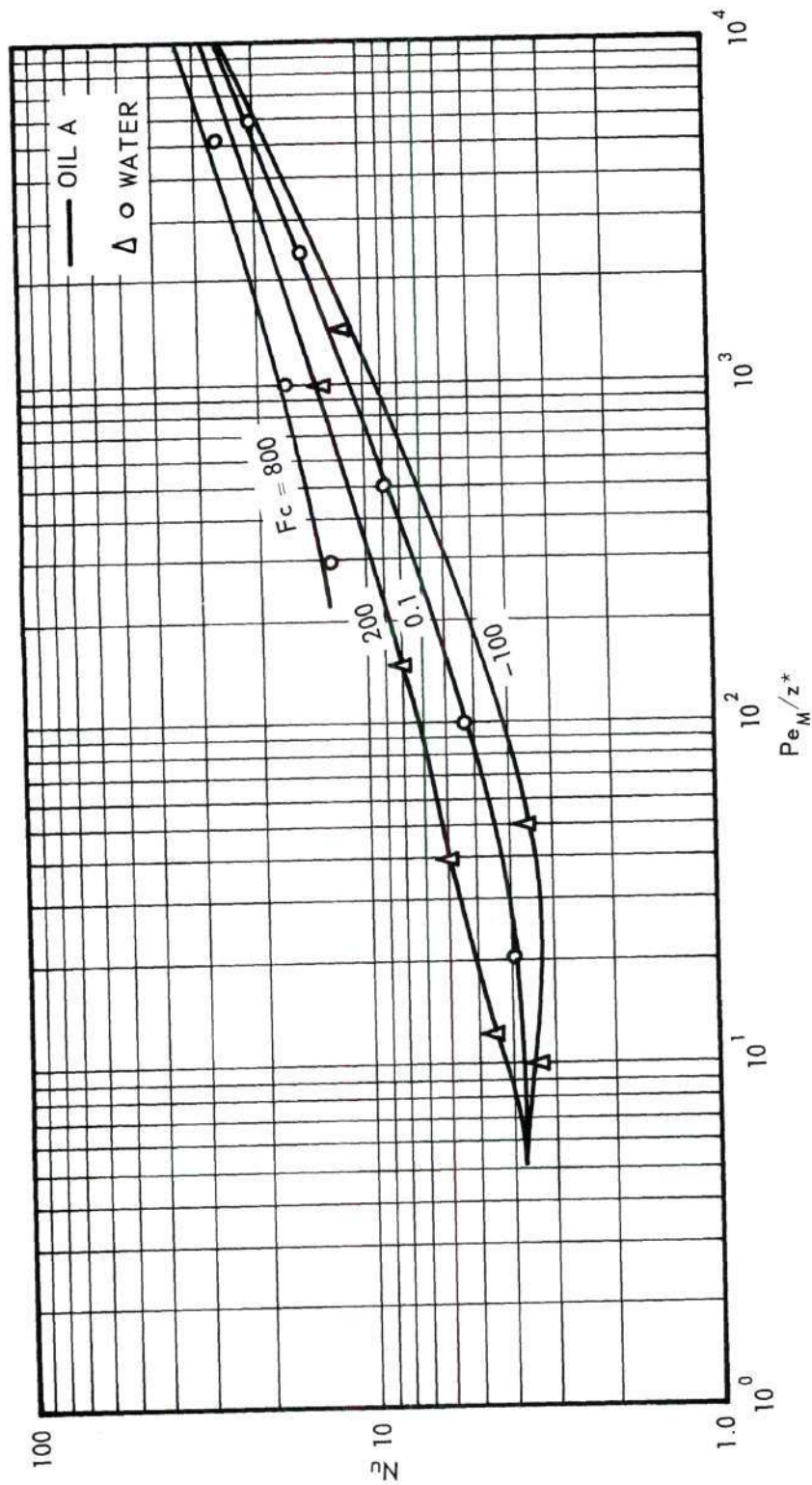


Figure 17. Comparison of Variable Property Local Nusselt Number Calculations for Oil A and Water.
Entrance Profile: Parabolic.
Viscosity Ratio: 2.

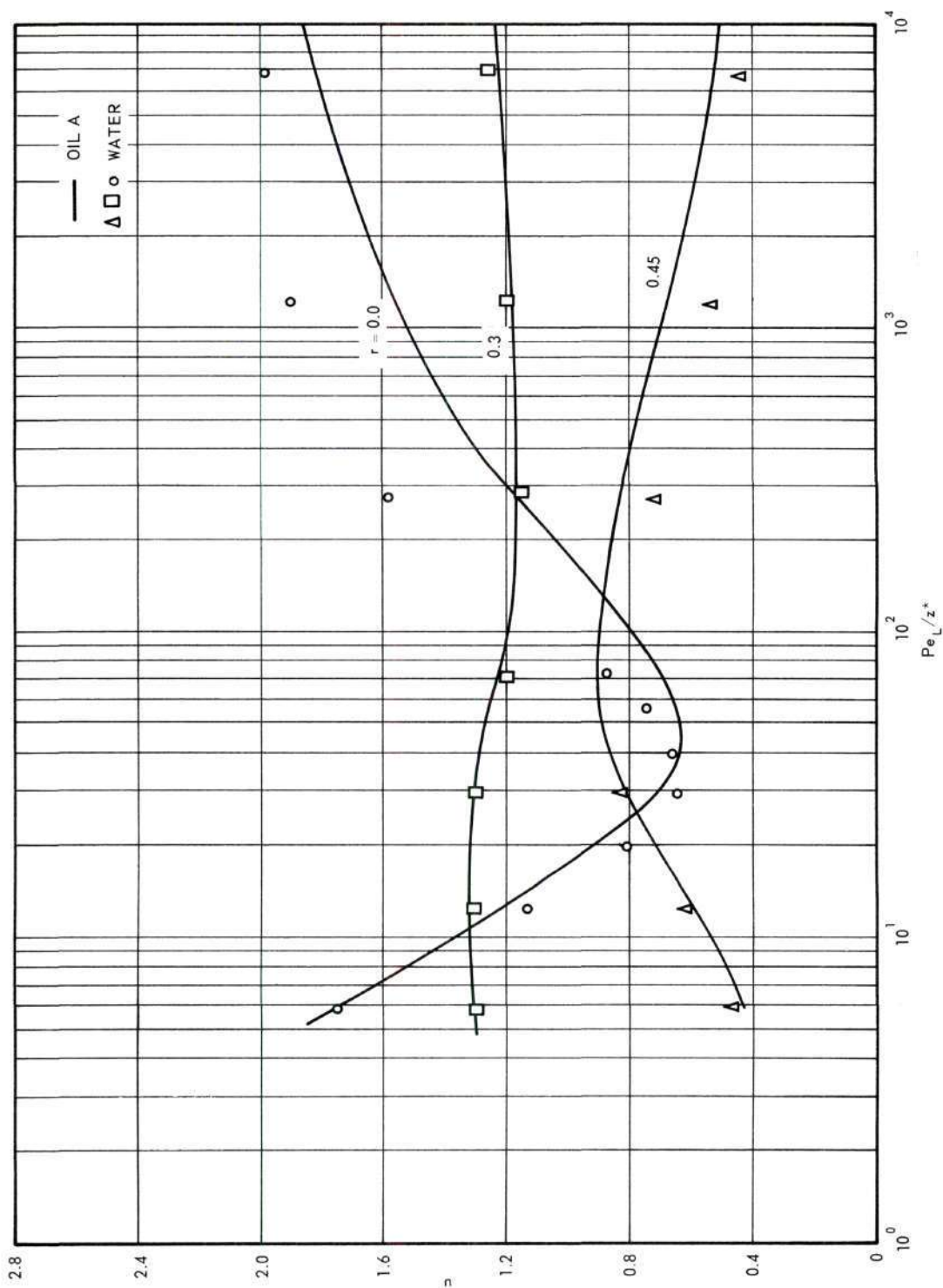


Figure 18. Comparison of Variable Property Velocity Profile Calculations for Oil A and Water. Entrance Profile: Parabolic. Viscosity Ratio: 2. Free Convection Parameter: 200.

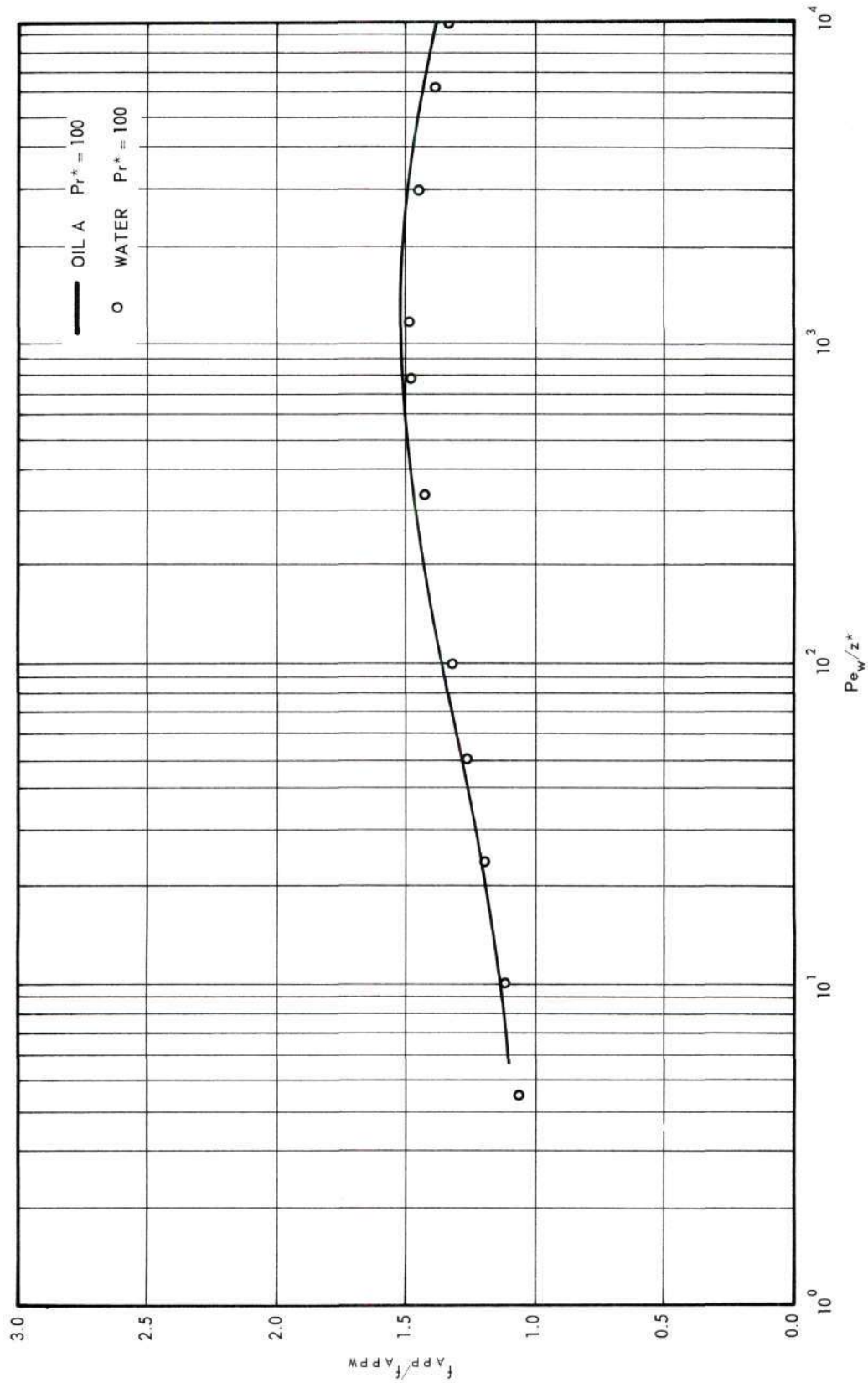


Figure 19. Comparison of Variable Property Friction Factor Calculations for Oil A and Water. Entrance Profile: Parabolic. Viscosity Ratio: 2. Prandtl Number: 100.

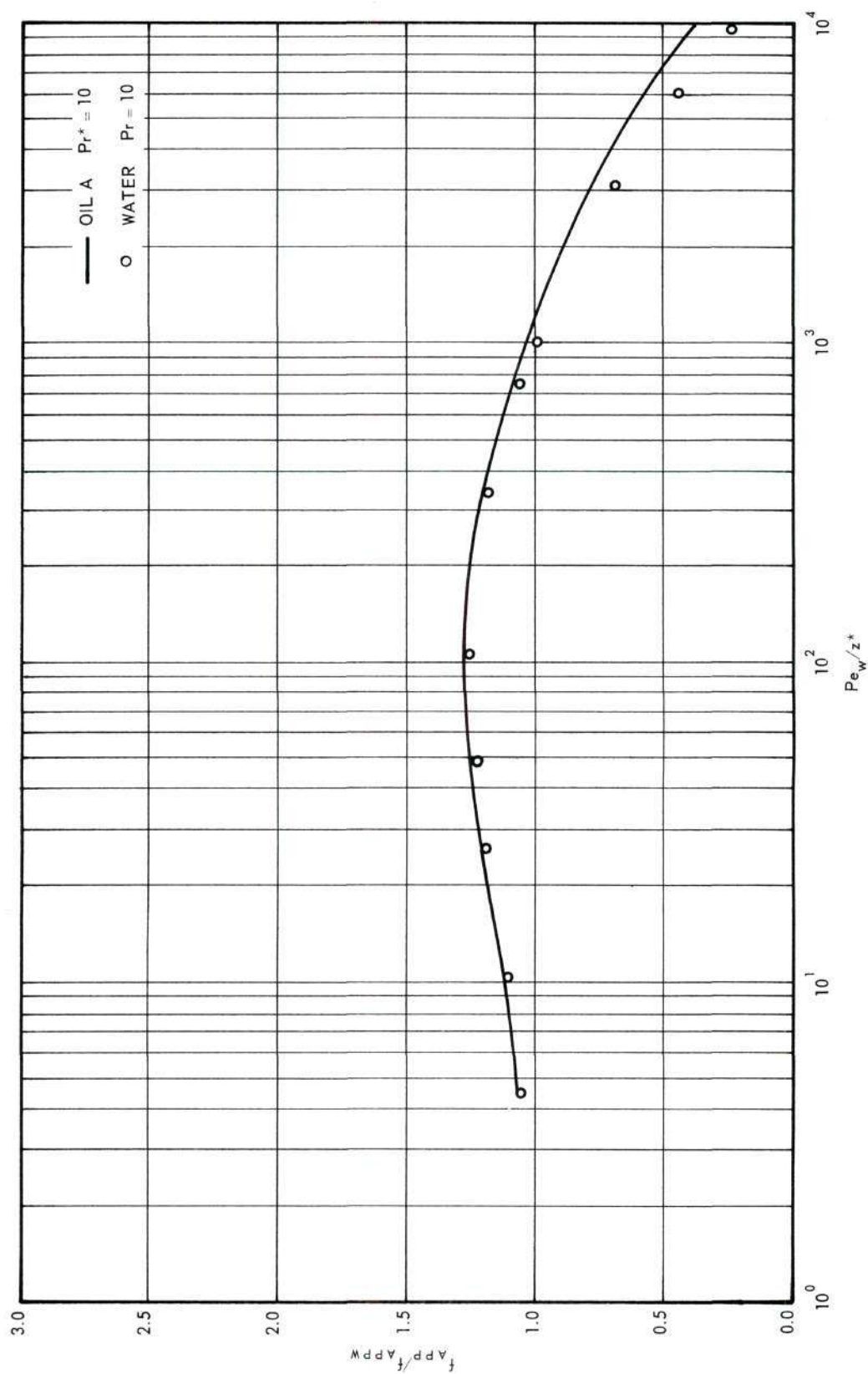


Figure 20. Comparison of Variable Property Friction Factor Calculations for Oil A and Water. Entrance Profile: Parabolic. Viscosity Ratio: 2. Prandtl Number: 10.

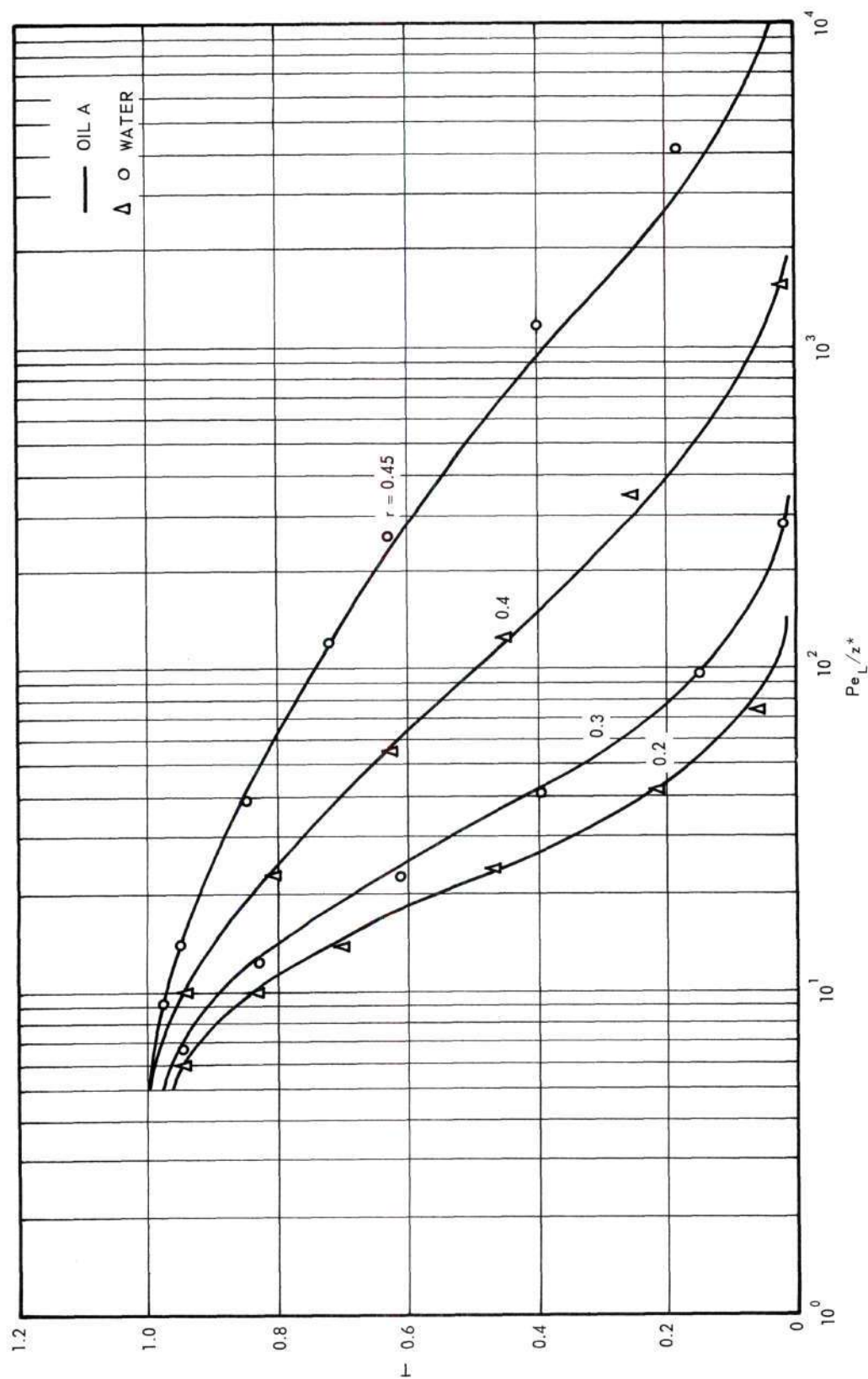


Figure 21. Comparison of Variable Property Temperature Profile Calculations for Oil A and Water. Entrance Profile: Parabolic. Viscosity Ratio: 2. Free Convection Parameter: 200.

layer thickness. Thus a comparison of a low Prandtl number material with a high Prandtl number material, when their thermal boundary-layer thicknesses are the same, means a comparison of an apparent friction factor due primarily to kinetic energy changes to one due primarily to frictional drag at the wall. The effect of the Prandtl number on the relative apparent friction factor was studied by specifying a value of the Prandtl number in the program. This pseudo Prandtl number is denoted by Pr^* .

Some improvement in the other correlations could probably be attained for large values of F_c by adding Pr as a correlating parameter. However, the added complication does not seem justified, except in the case of the velocity profiles, because the spread in the comparison calculations for Nu and T_M is ten per cent at worst, and this occurs only for extreme values of F_c . Most of the comparison calculations agree much better than this.

The velocity profiles correlate poorly below a value of Pr/z^* of approximately 200, especially the center-line velocity. However, critical values such as maxima and minima in the profiles and the general behavior are represented well. Only much more extensive sets of correlations would adequately describe the velocity profiles, but fortunately the velocity profiles are of secondary importance in design calculations. For accurate values of the velocity profile the numerical scheme must be employed for each particular case.

Typical correlations for gases are presented in Figures 22 through 26. They are similar to those for liquids except that $\left(\frac{\rho_M}{\rho_w}\right)\left(\frac{f_{APP}}{f_{APPW}}\right)$ and pu were correlated to take into account the extreme variations in density

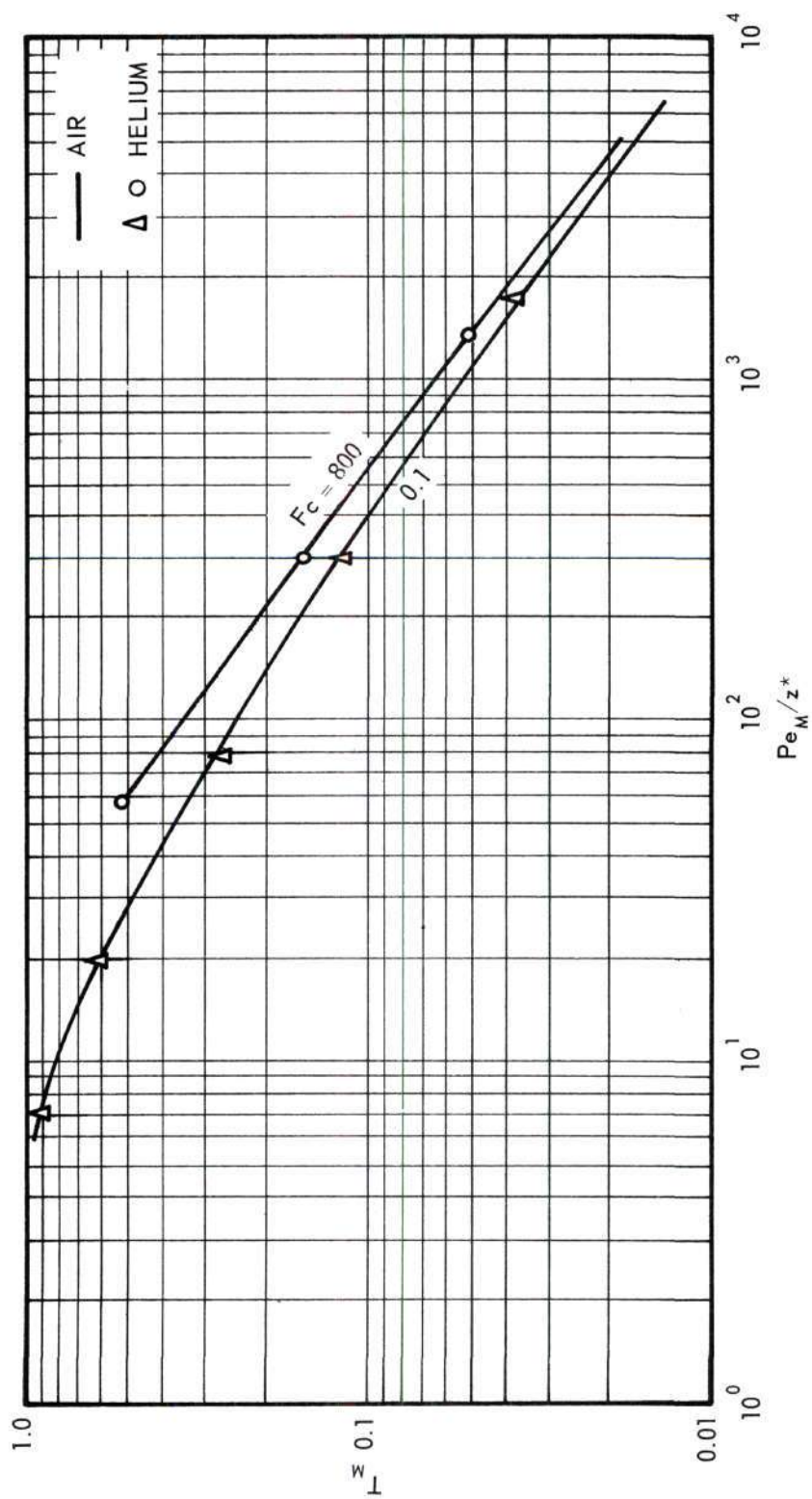


Figure 22. Comparison of Variable Property Mean Temperature Calculations for Air and Helium.
Entrance Profile: Parabolic.
Viscosity Ratio: 1.5.

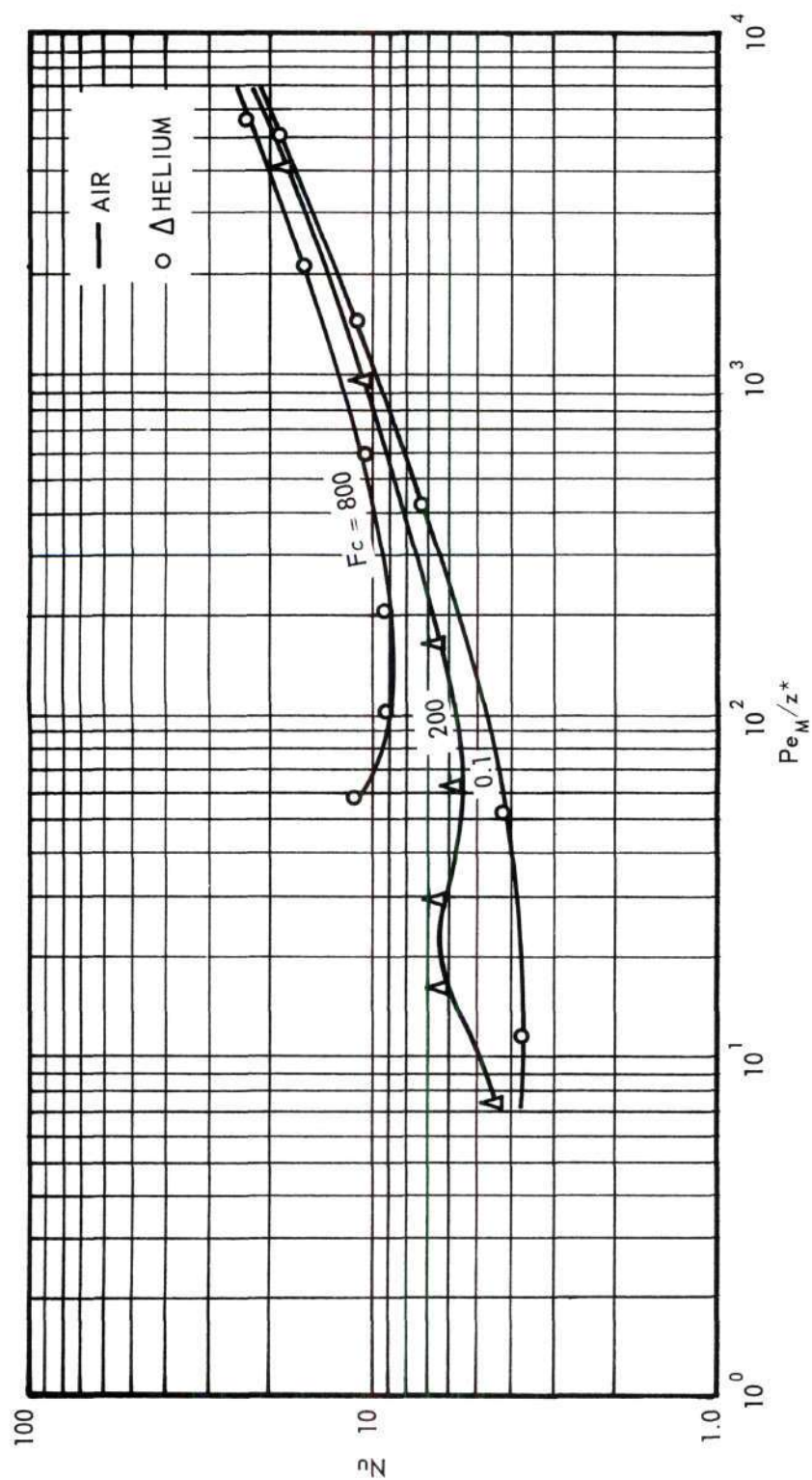


Figure 23. Comparison of Variable Property Local Nusselt Number Calculations for Air and Helium.
Entrance Profile: Parabolic.
Viscosity Ratio: 1.5.

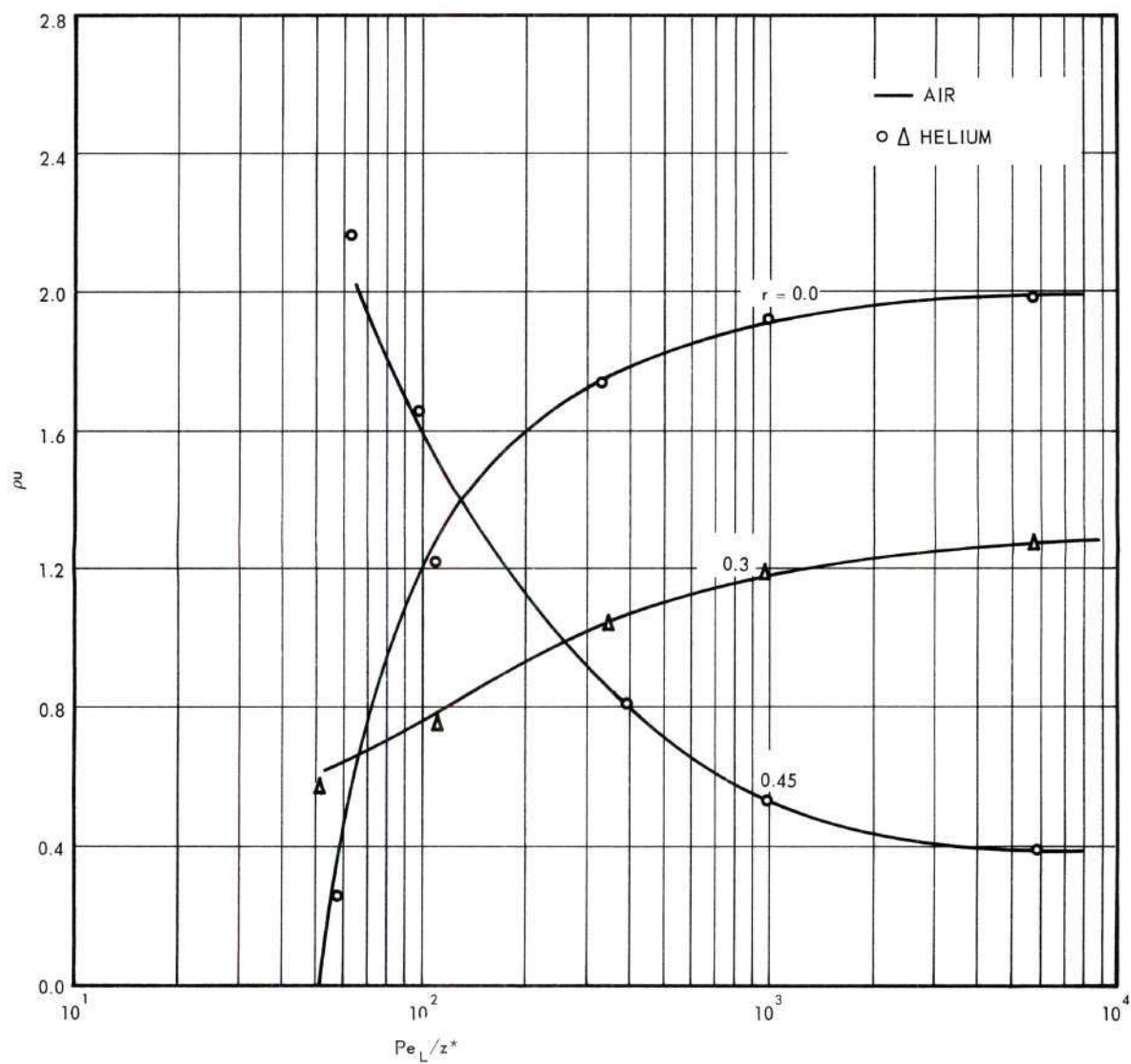


Figure 24. Comparison of Variable Property Velocity Profile Calculations for Air and Helium.
 Entrance Profile: Parabolic.
 Viscosity Ratio: 1.5.
 Free Convection Parameter: 800.

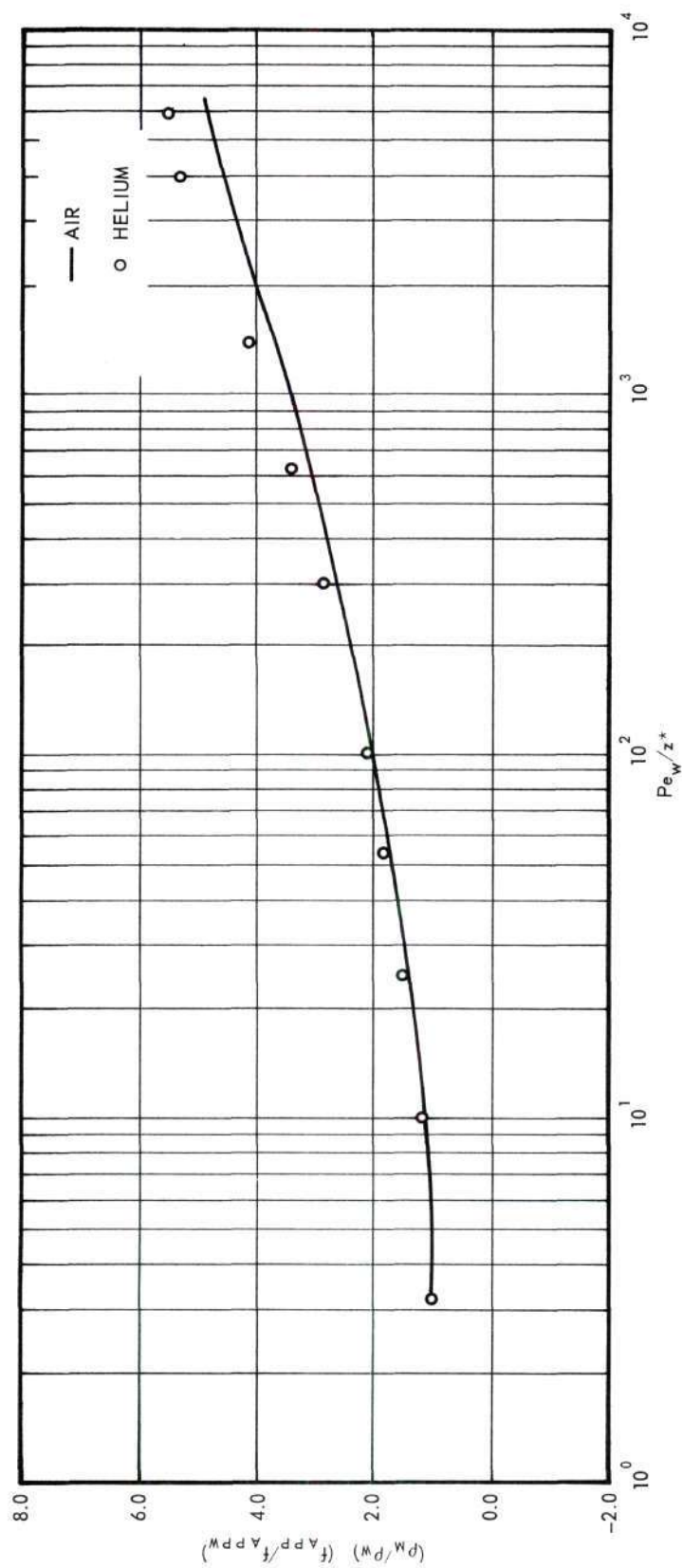


Figure 25. Comparison of Variable Properties Friction Factor Calculations for Air and Helium.
Entrance Profile: Parabolic.
Viscosity Ratio: 0.667.

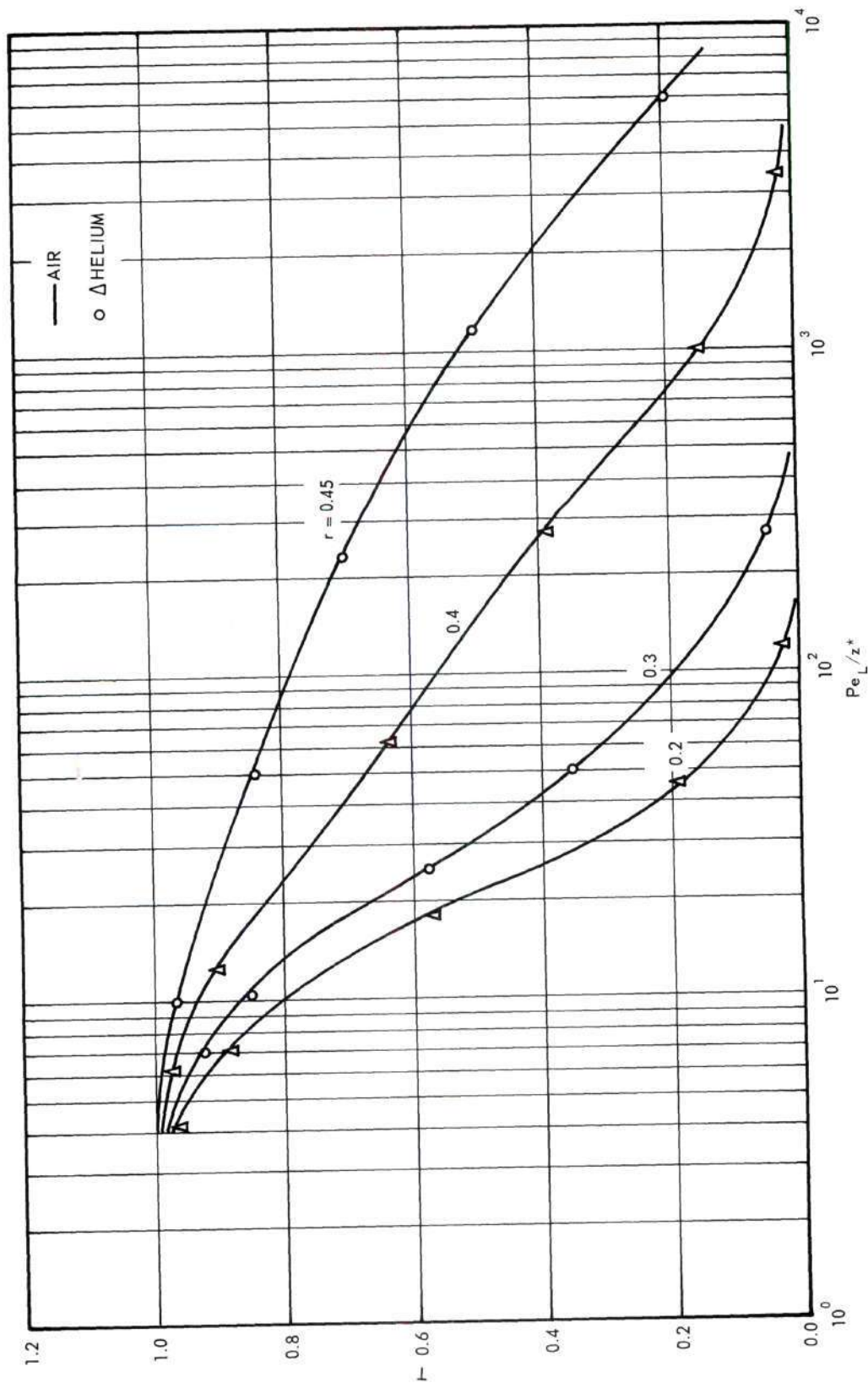


Figure 26. Comparison of Variable Property Temperature Profile Calculations for Air and Helium. Entrance Profile: Parabolic. Viscosity Ratio: 0.667. Free Convection Parameter: 800.

found in gases. There was no necessity to include Pr in the friction factor correlations for gases due to the fact that the Prandtl number for most common gases is close to 0.7. It is interesting to note that the large increase in friction factors for the heating of gases has been qualitatively verified by the experiments of Davenport.⁽¹²⁾

Additional comparison examples for liquids and gases are given in Figures 40 through 51 of Appendix E.

The relative apparent friction factor correlations are presented only for negligible free convection effects for both gases and liquids even though a definite dependence on Fc was noticed. However in those cases where Fc was significant, the pressure drop due to gravity was so large that this dependence was insignificant. Typical values of

$\left| \frac{P_{KE} + P_F}{P_G} \right|$ are shown below:

<u>Material</u>	<u>Fc</u>	<u>$\left \frac{P_{KE} + P_F}{P_G} \right$</u>
Oil A, $\mu_r = 5$	0.1	7
Oil A, $\mu_r = 5$	400	0.004
Air, $\mu_r = 0.75$	0.1	500
Air, $\mu_r = 0.75$	400	0.15

Uniform Velocity Profile

Typical correlation examples for liquids and gases can be found in Figures 27 through 36. The correlation procedure differed from the parabolic entrance profile case only in the inclusion of the parameter Pr for all correlated variables. This is expected in analogy with the constant property uniform profile calculations. Again, use was made of Pr^* .

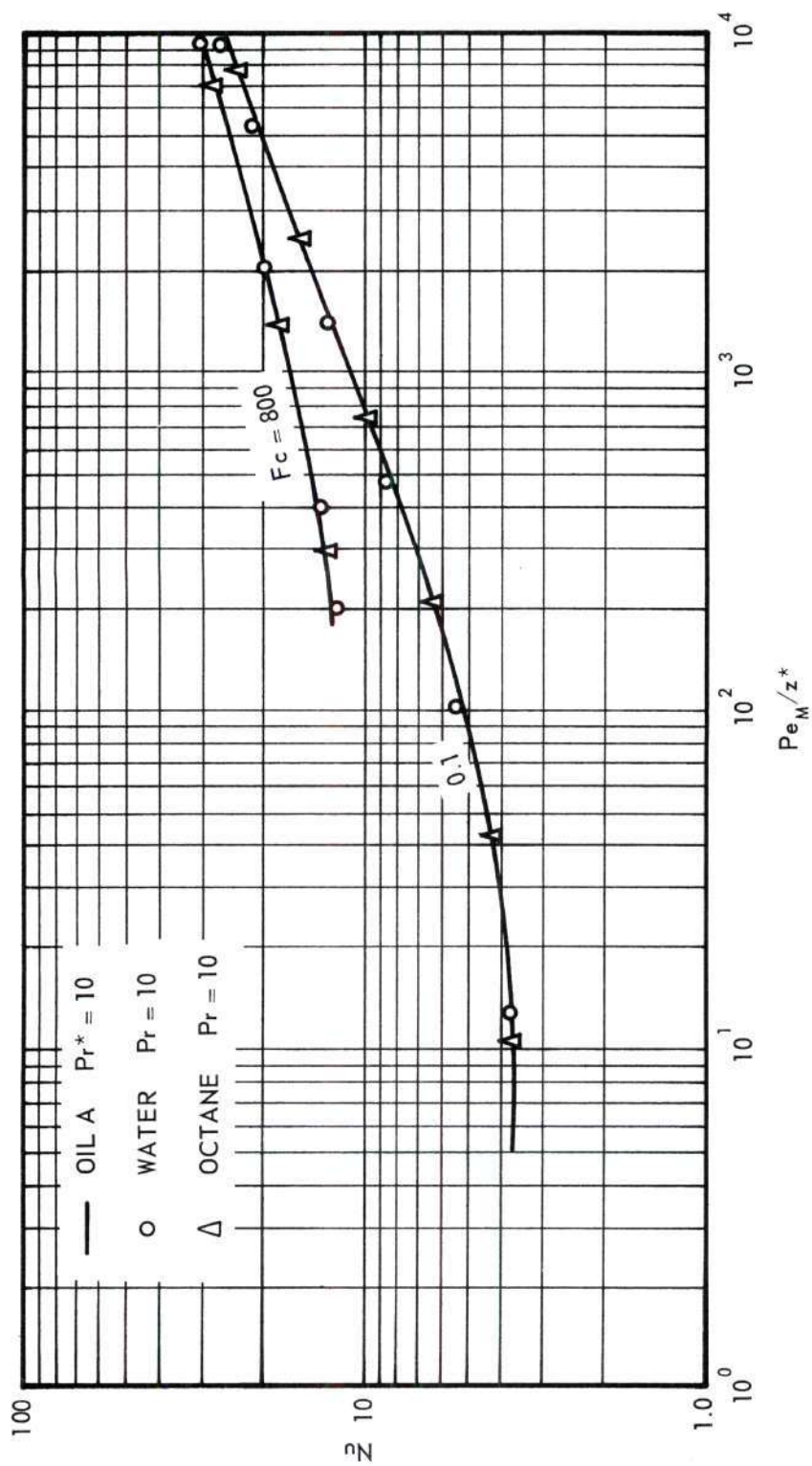


Figure 27. Comparison of Variable Property Local Nusselt Number Calculations for Oil A, n-Octane, and Water.
 Entrance Profile: Uniform.
 Viscosity Ratio: 2.
 Prandtl Number: 10.

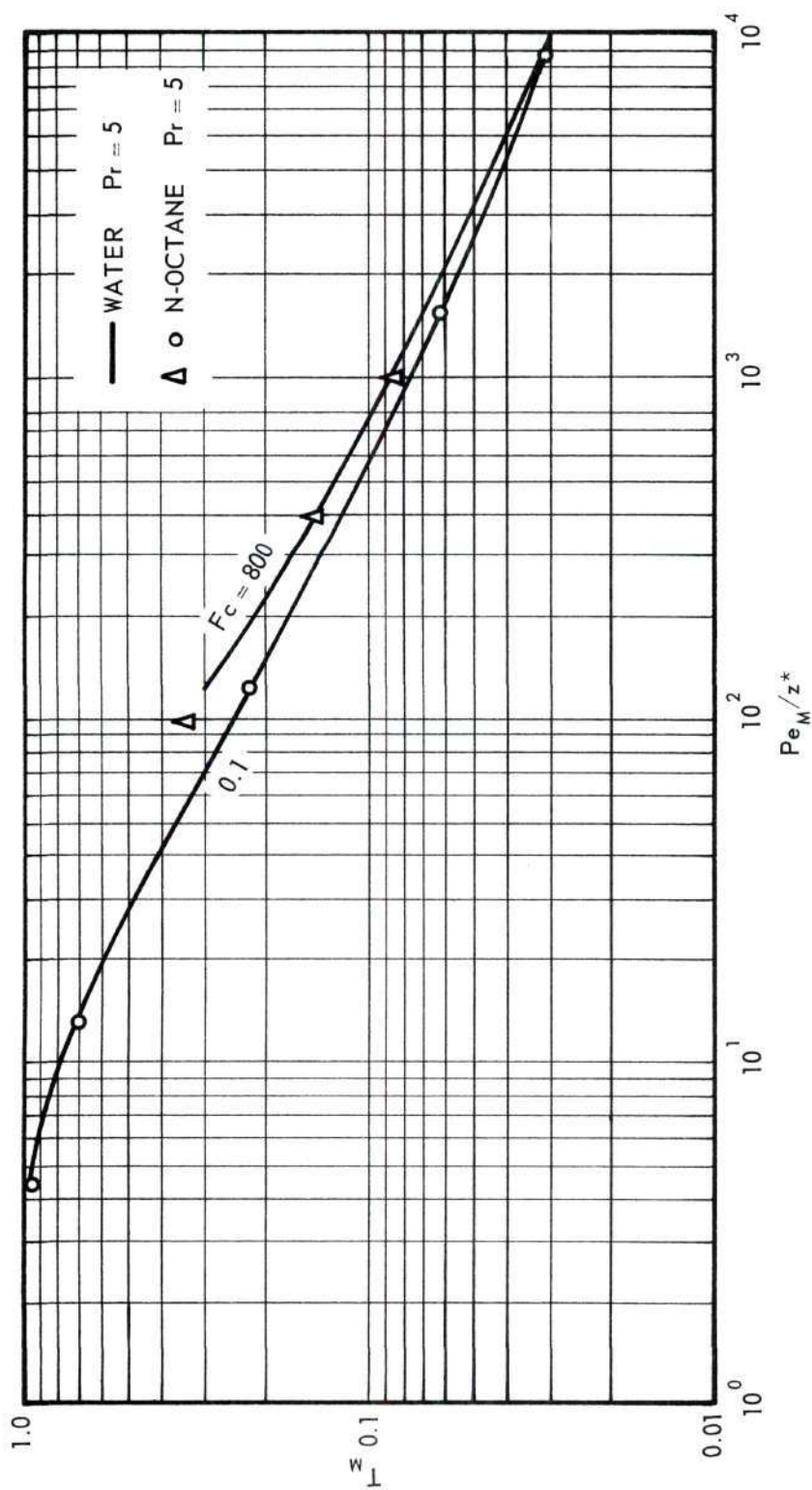


Figure 28. Comparison of Variable Property Mean Temperature Calculations for n-Octane and Water.
 Entrance Profile: Uniform.
 Viscosity Ratio: 0.5.
 Prandtl Number: 5.

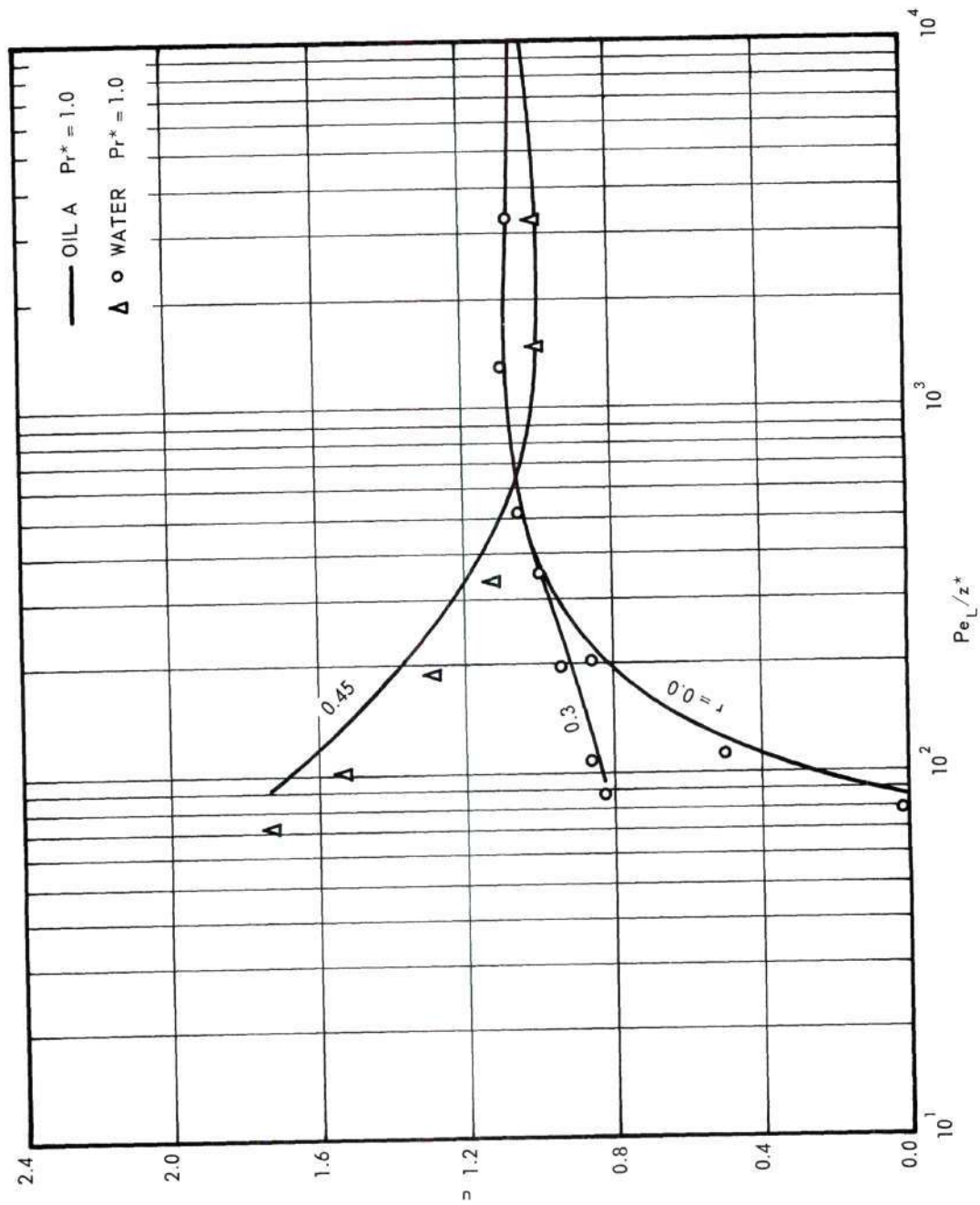


Figure 29. Comparison of Variable Property Velocity Profile Calculations for Oil A and Water. Entrance Profile: Uniform. Viscosity Ratio: 2. Free Convection Parameter: 800. Prandtl Number: 1.

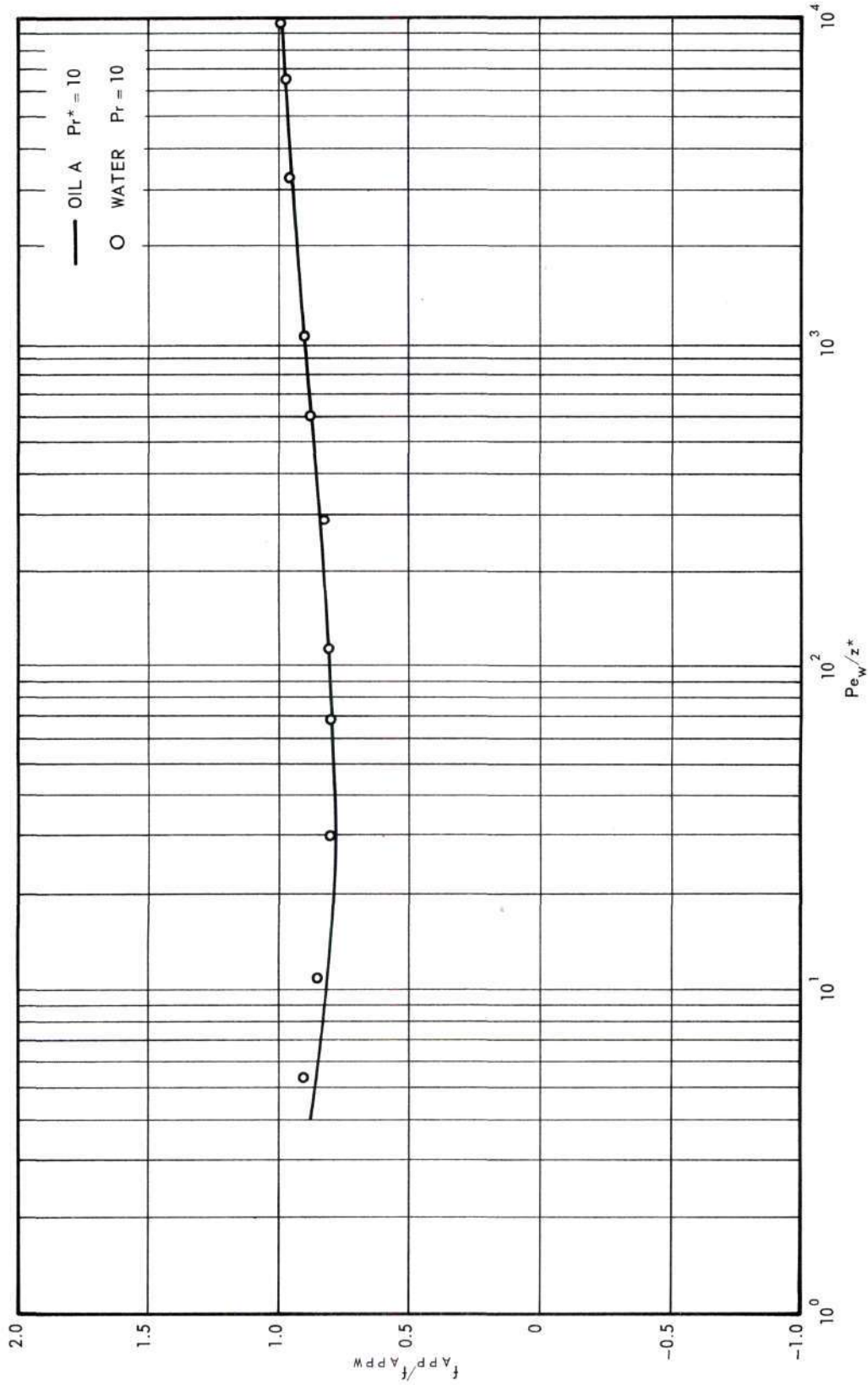


Figure 30. Comparison of Variable Property Friction Factor Calculations for Oil A and Water. Entrance Profile: Uniform. Viscosity Ratio: 0.5. Prandtl Number: 10.

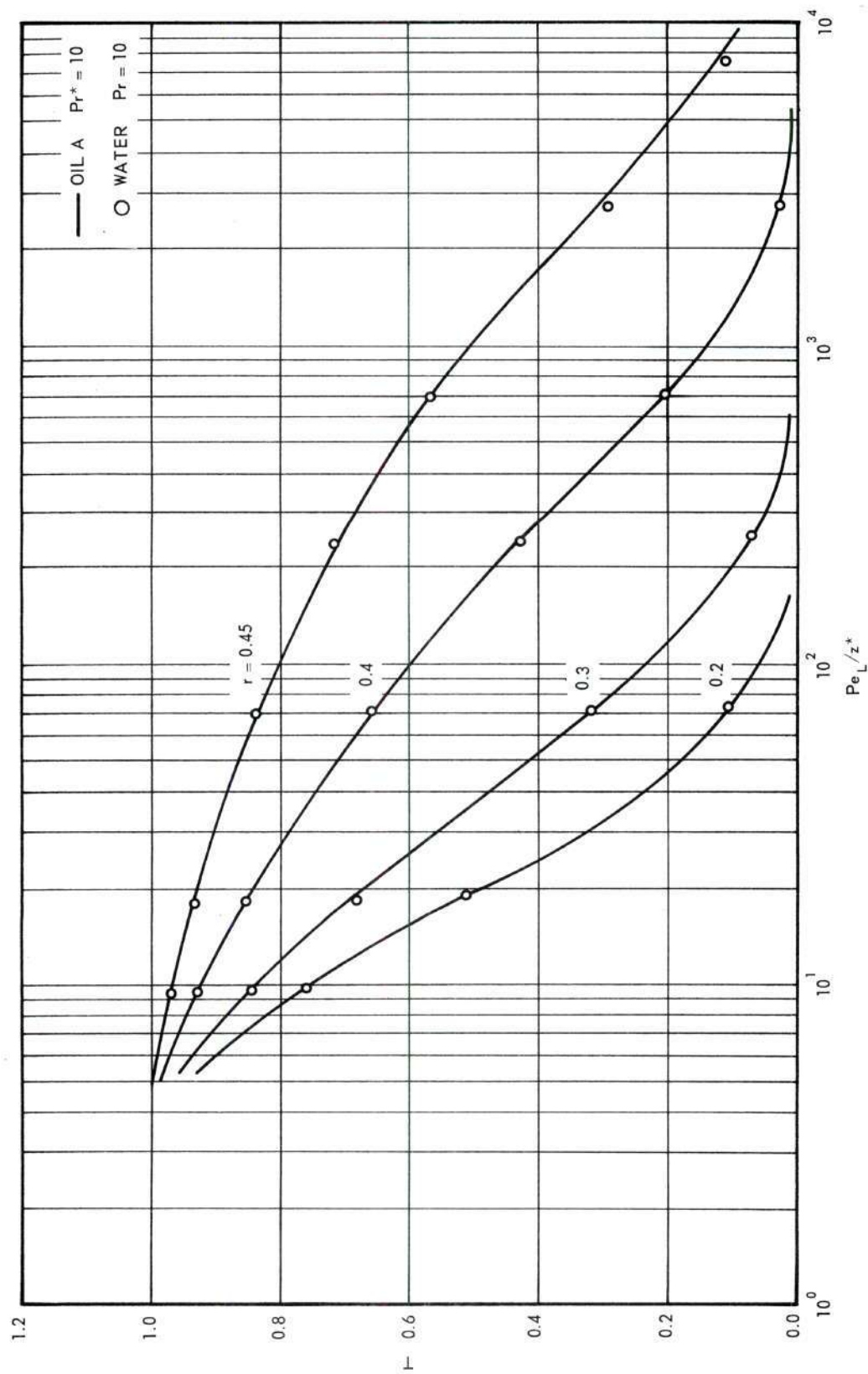


Figure 31. Comparison of Variable Property Temperature Calculations for Oil A and Water. Entrance Profile: Uniform. Viscosity Ratio: 2. Free Convection Parameter: 0.1. Prandtl Number: 10.

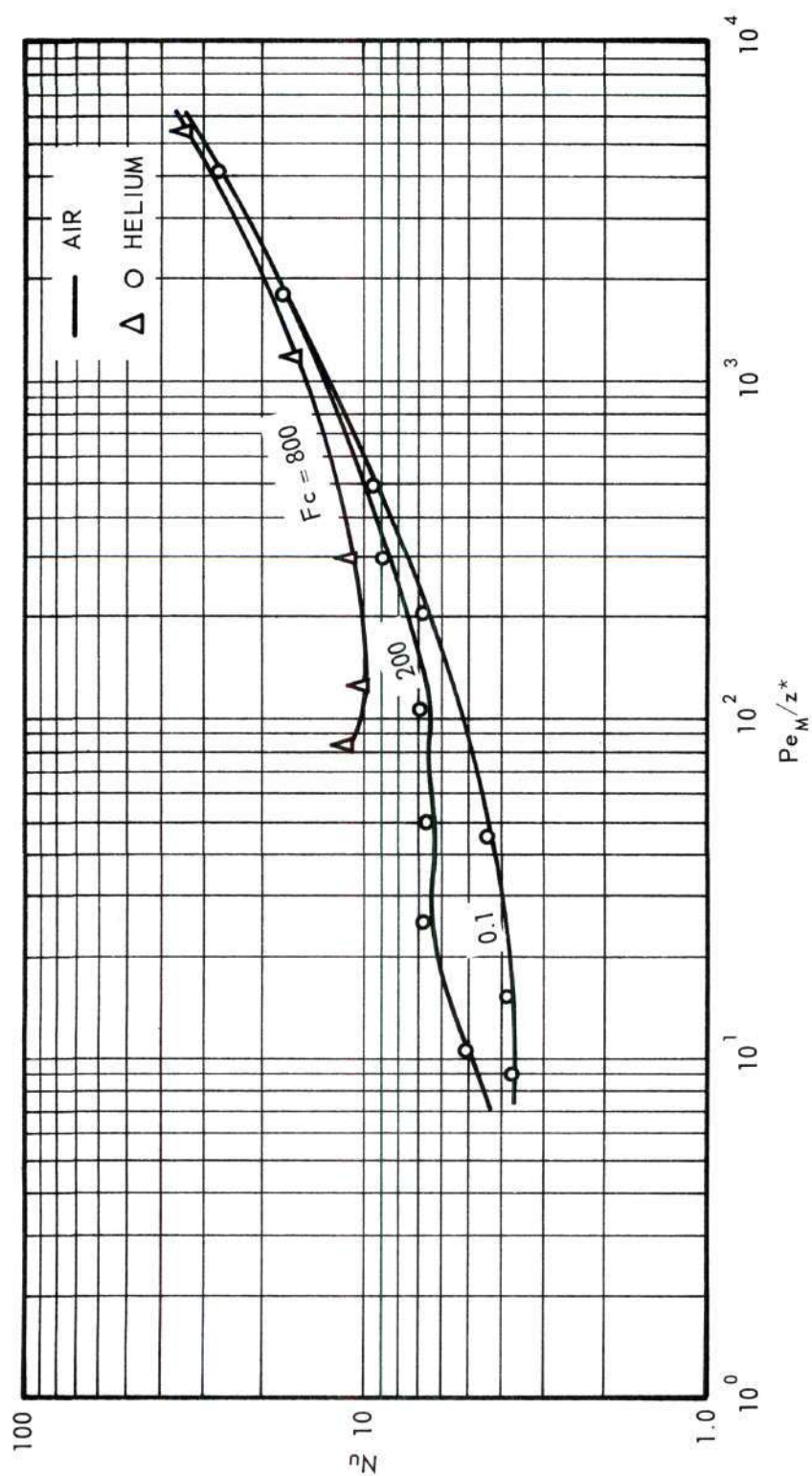


Figure 32. Comparison of Variable Property Local Nusselt Number Calculations for Air and Helium.
Entrance Profile: Uniform.
Viscosity Ratio: 1.5.

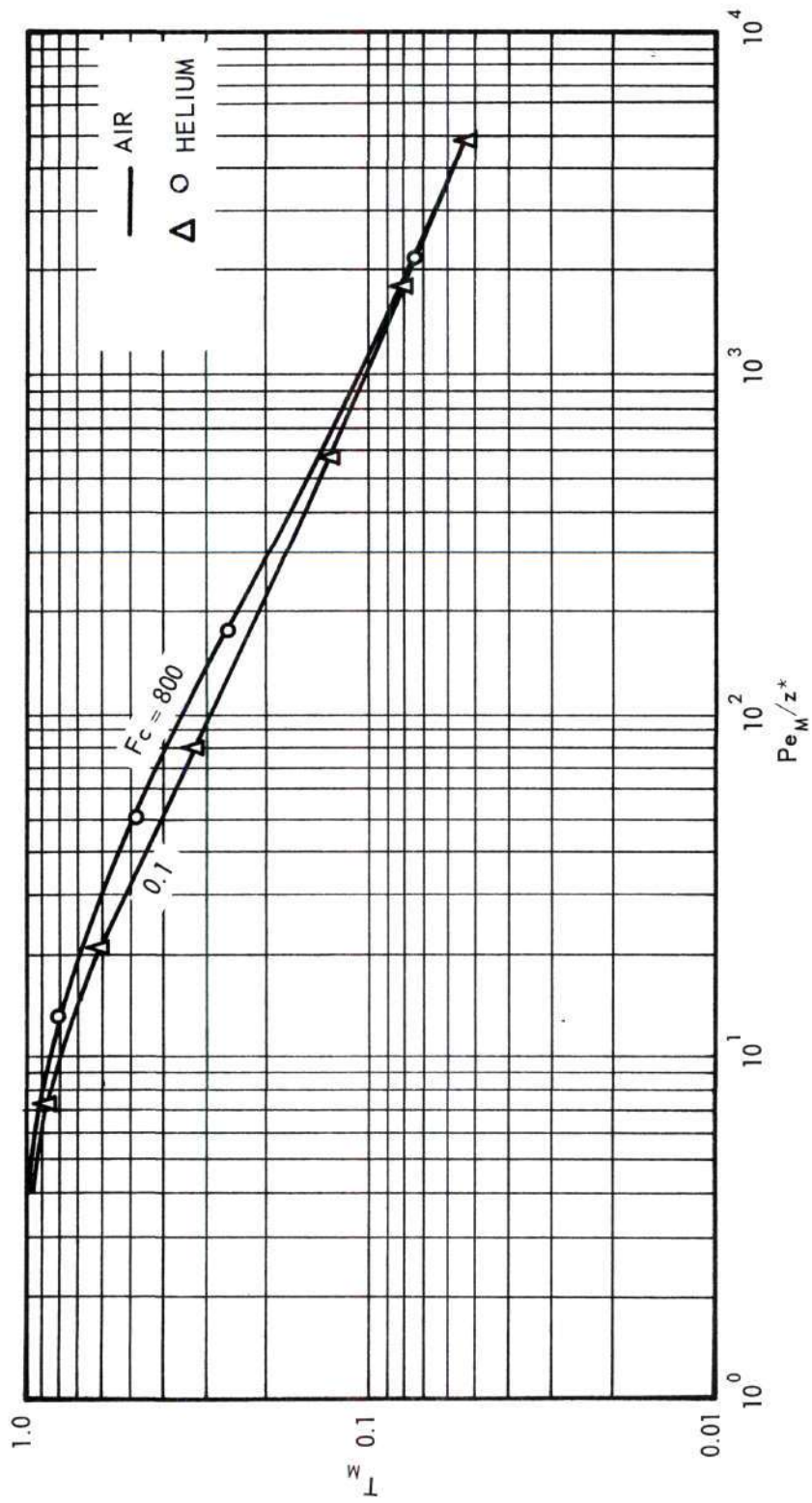


Figure 33. Comparison of Variable Property Mean Temperature Calculations for Air and Helium.
Entrance Profile: Uniform.
Viscosity Ratio: 0.667.

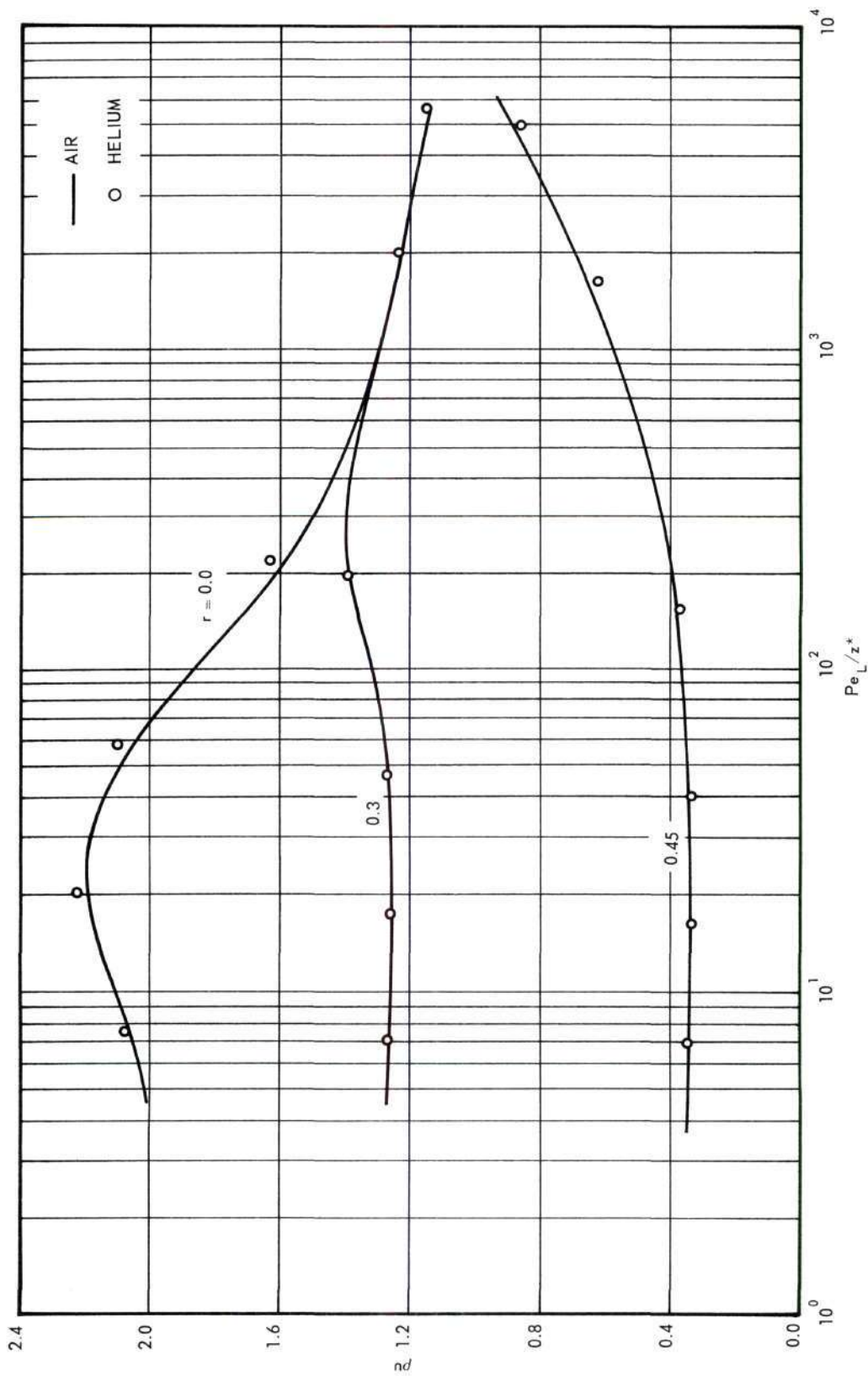


Figure 34. Comparison of Variable Property Velocity Profile Calculations for Air and Helium. Entrance Profile: Uniform. Viscosity Ratio: 0.667. Free Convection Parameter: 0.1.

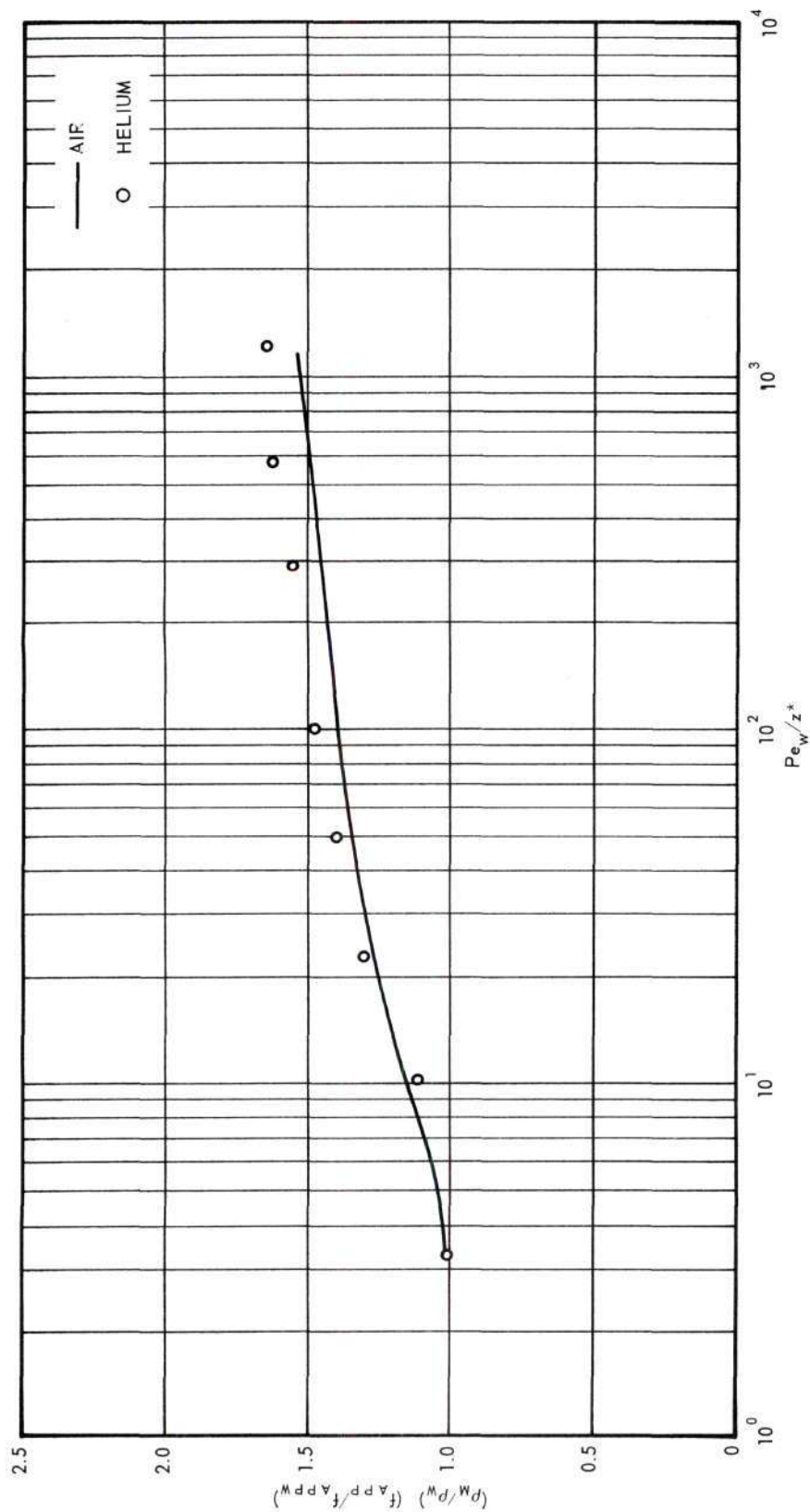


Figure 35. Comparison of Variable Property Friction Factor Calculations for Air and Helium.
Entrance Profile: Uniform.
Viscosity Ratio: 0.667.

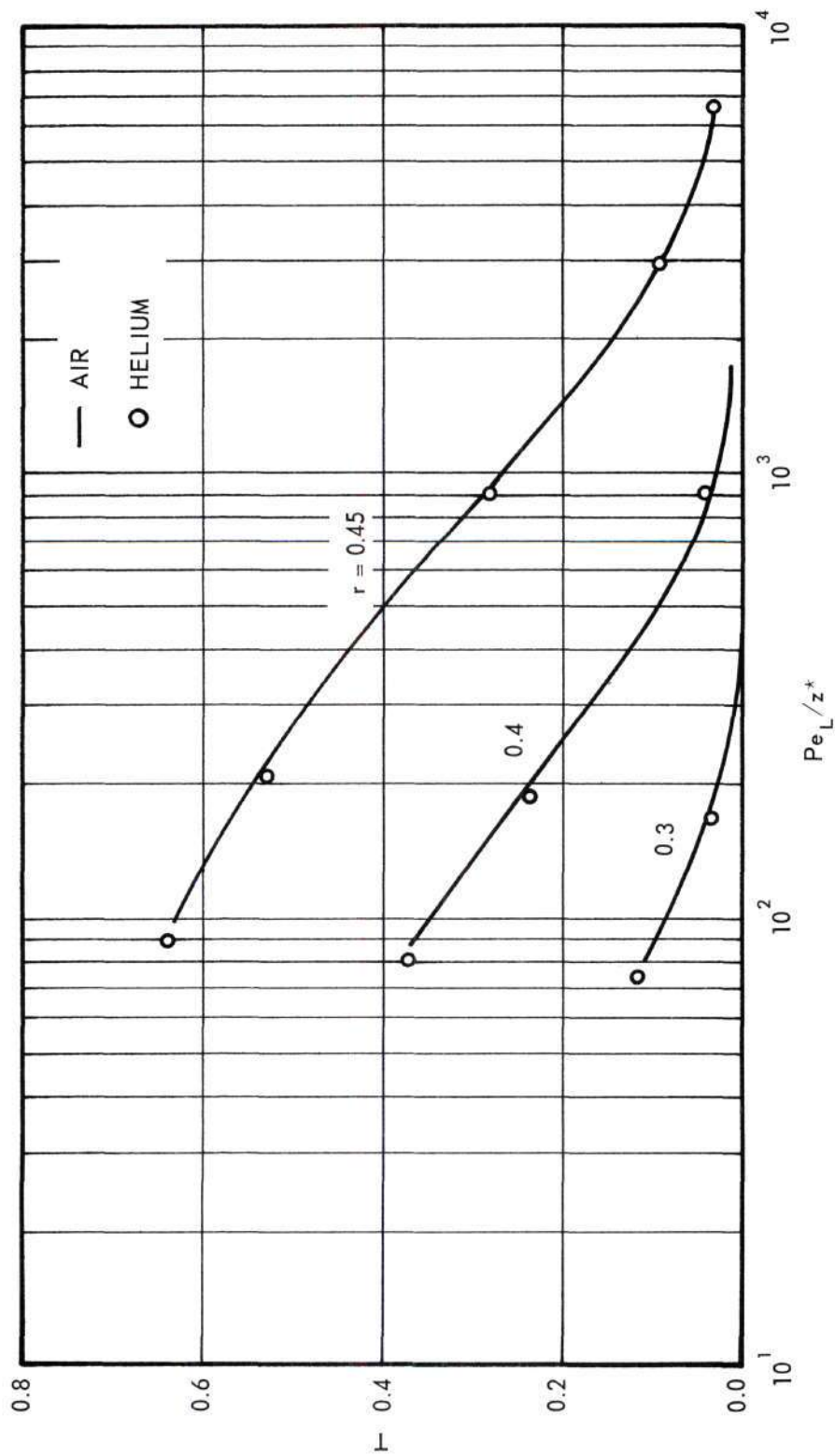


Figure 36. Comparison of Variable Property Temperature Profile Calculations for Air and Helium.
 Entrance Profile: Uniform.
 Viscosity Ratio: 1.5.
 Free Convection Parameter: 800.

For a Pr of 10 it was observed that at values of Pr/z^* less than about 90, the results converged to the parabolic entrance profile results. Another interesting observation was that for values of μ_r greater than about five in the relative friction factor correlation this parameter was unimportant. Additional comparison examples for liquids and gases are presented in Figures 53 through 61 of Appendix E.

Tabulated Results

Using oil A as a model for liquids and air as a model for gases, calculated tabulations of heat-transfer and fluid-flow variables for both the parabolic entrance profile and the uniform entrance profile are contained in the appendices. The relative apparent friction factors are presented in graphical form in Figures 62 through 69 of Appendix F. Values of the local Nusselt number and mean temperature are presented in Tables 15 through 43 of Appendix G. Values of the velocity and temperature profiles are presented in Tables 44 through 72 of Appendix H.

For the uniform entrance profile case Prandtl numbers of one and ten were considered because this covers the most significant range for heat transfer. Using the constant property solution as a guide, interpolation can be easily accomplished.

Sample calculations using these results are presented in Appendix I.

Discussion of Calculation Conditions

At this point something should be said about some of the practical calculation requirements made on the numerical scheme. The question of

the mesh size may be broken into a separate consideration of the size of Δr and Δz since the numerical scheme is unconditionally stable.

The selection of an optimum Δr value is difficult because of the extremely wide variation in velocities which can occur in the tube. For example, when free convection forces cause the axial velocities to decrease at the center line they also cause the axial velocities near the wall to increase. These regions require a small value of Δr . On the other hand, much larger Δr mesh lengths can be used where the velocity gradients near the wall are not so steep. The development of the thermal boundary layer is also a factor. In order to get accurate results in some situations it was found necessary to use 160 radial mesh points; this, of course, requires the solution of systems of linear equations of order 160.

In deciding on the axial step size, Δz , not only is it necessary to decide how to refine the value of Δz as the solution proceeds, but the starting value of Δz must also be decided. It was also found that an order of magnitude of Pe/z^* was required for initial errors to be "washed" out. Thus if accurate values are desired at $Pe/z^* = 10^4$, the solution should be started at $Pe/z^* = 10^5$. The optimum step size was easily tested by examining the error term, E_q . By keeping this error term less than a maximum of two per cent an accurate, fast computer solution was obtained.

The calculation was always stopped if u_1 or u_N became less than zero. These conditions occur when the center-line velocity is negative and when the velocity gradient is negative at the wall. The first condition usually results at some point along the tube when $F_c \gg 0$. The second

condition usually results at some point along the tube when $F_c < 0$. Aside from the fact that the numerical scheme was not developed to handle negative axial velocities, these conditions indicate unstable flow patterns which are not described by the mathematical model.

Effect of Inertia and Radial Velocity Terms

A comparison of the results of this work with those of Lee⁽¹⁾ illustrates the effect of including the inertia term in the equation of motion and the radial velocity in the energy equation. In general, it was found that predicted heat-transfer rates were in agreement for cases where free convection effects were small and large density gradients were not encountered, that is, where the inertia and radial velocities were not important in describing the velocity field. However, differences up to 50 per cent were observed in some extreme cases. Friction factor results were radically different due to the definite contribution of the inertia term through P_{KE} . Typical comparisons are shown in Figures 37, 38, and 39. The general shape of velocity profiles due to viscosity and free convection effects were found to be the same as calculated by Lee,⁽¹⁾ Hanratty,⁽⁹⁾ and Pigford.⁽⁴⁾

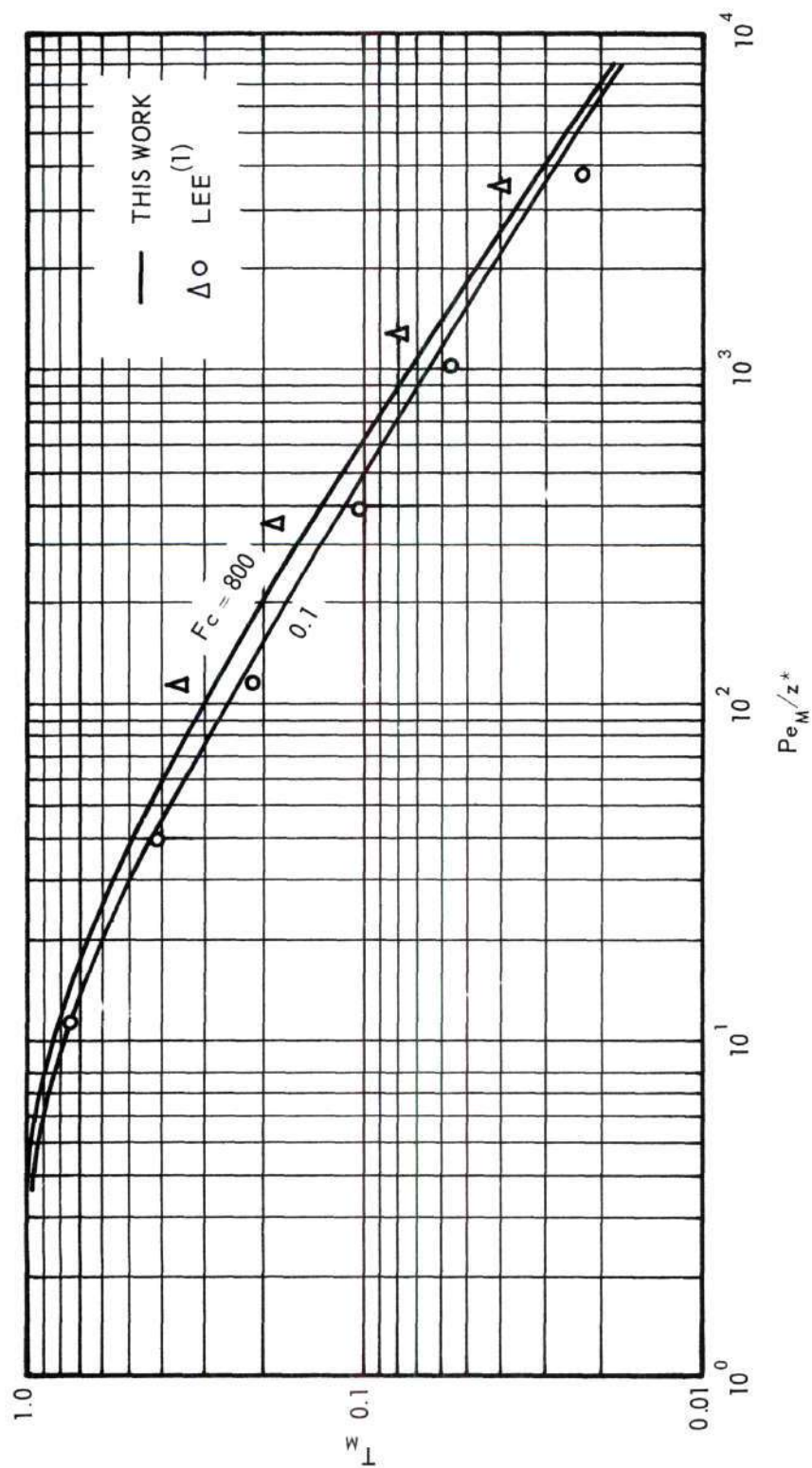


Figure 37. Comparison of Variable Property Mean Temperature Calculations for Air and Results of Previous Work.
Entrance Profile: Parabolic.
Viscosity Ratio: 0.667.

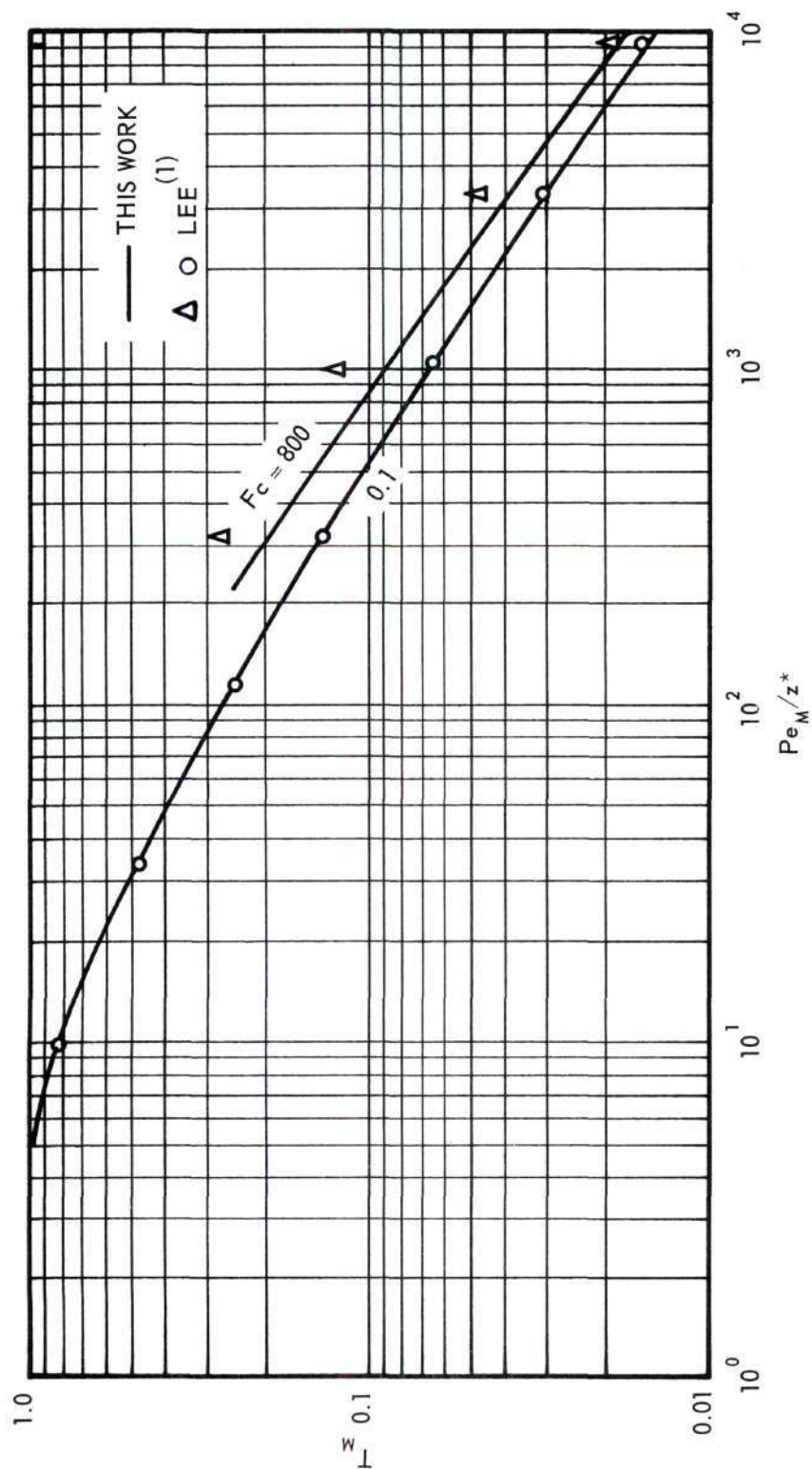


Figure 38. Comparison of Variable Property Mean Temperature Calculations for Oil A with Results of Previous Work.
Entrance Profile: Parabolic.
Viscosity Ratio: 2.

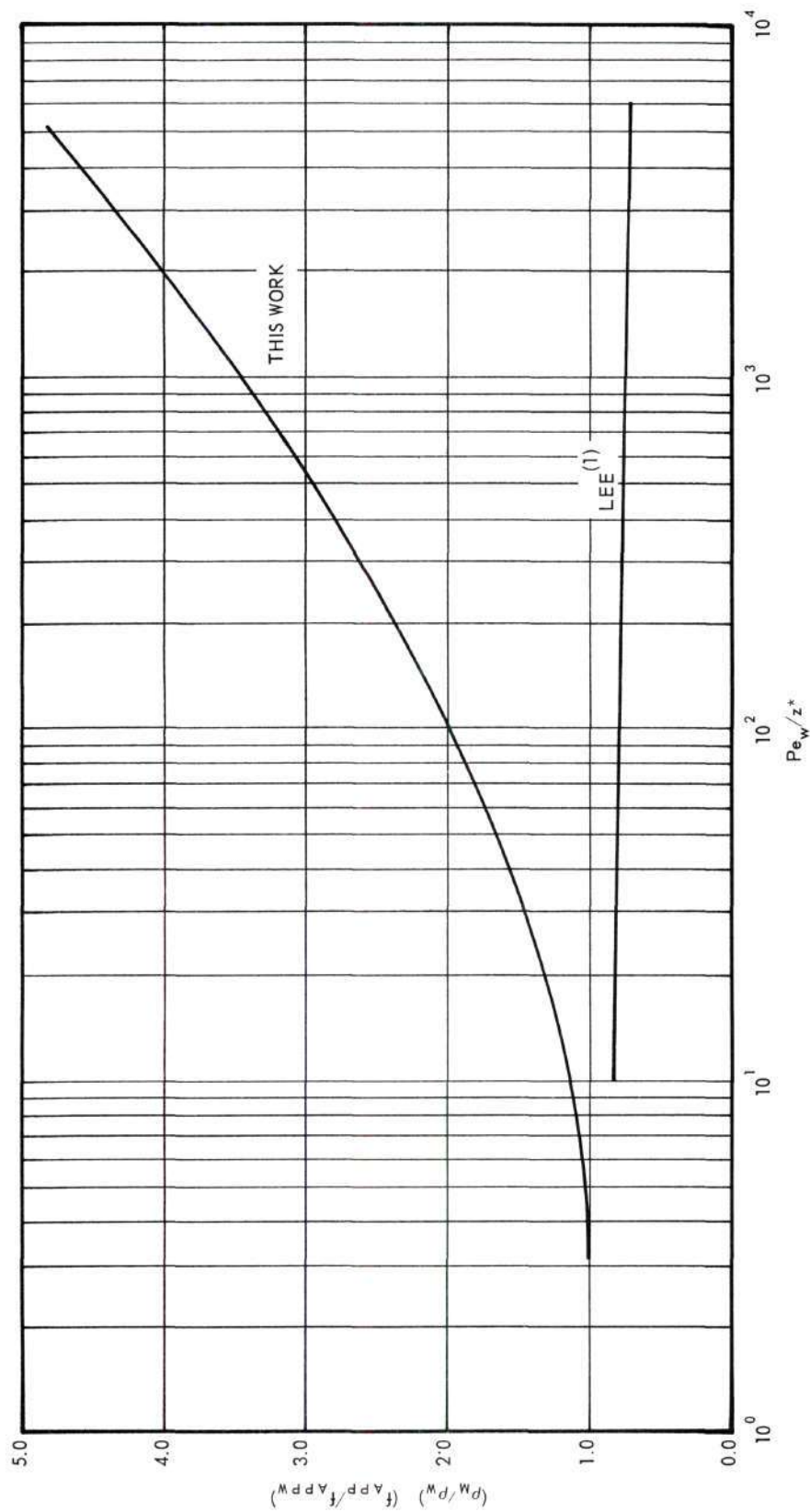


Figure 39. Comparison of Variable Property Friction Factor Calculations for Air with Results of Previous Work. Entrance Profile: Parabolic. Viscosity Ratio: 0.667.

CHAPTER V

CONCLUSIONS AND RECOMMENDATIONS

Based on this work the following conclusions are reached:

1. The numerical scheme described in this work gives an accurate, efficient computer solution for equations (5), (6), and (7) for a variable property fluid flowing in a constant wall temperature tube with either a parabolic or uniform entrance profile.
2. Neglecting the inertia term in equation (5) and the radial velocity term in equation (6) can result in significant errors in calculated results.
3. Calculations indicate that variation in viscosity and density are important in laminar flow heat transfer and can have pronounced effects on friction factors. Variation of thermal conductivity and heat capacity are much less important.
4. Based on the parameters μ_r and F_c it is possible to correlate heat-transfer and fluid-flow results with a reasonable degree of accuracy over a wide range of property variations.
5. For heat transfer, the initial profile is of no practical significance for Prandtl numbers greater than about ten. However, friction factors will depend on the initial profile even for large Prandtl numbers.
6. Extreme distortion of the parabolic velocity profile probably leads to turbulence even before negative axial velocities are encountered.

Recommendations for additional studies are suggested by this work.

They are

1. the modification of the numerical scheme described in this work to include other tube wall conditions such as constant heat flux,
2. an extension of these calculations to the interesting and important case of non-Newtonian fluids,
3. the measurement of more experimental data under the conditions of this study, particularly for cases where free convection effects are important, and
4. a study of the development of turbulence in nonisothermal flow based on velocity profile data that can be generated from this work.

APPENDICES

APPENDIX A

DEVELOPMENT OF CALCULATION SCHEME

Development of Finite Difference Approximations

Consider the function $f(r, z)$ defined on the semi-infinite strip of the (r, z) plane bounded by

$$0 \leq r \leq \frac{1}{2}$$

and

$$0 \leq z < \infty$$

Further, let a rectangular grid of mesh spacing $(\Delta r, \Delta z)$ be superimposed on this domain. Define

$$r_m = (m - 1)\Delta r \quad (31)$$

$$z_\ell = (\ell - 1)\Delta z \quad (32)$$

and

$$f_{m,\ell} = f((m - 1)\Delta r, (\ell - 1)\Delta z) \quad (33)$$

By a Taylor's series expansion about a

$$f(r, z) = f(a, z) + (r - a) \left(\frac{\partial f}{\partial r} \right)_{a, z} + \frac{(r - a)^2}{2!} \left(\frac{\partial^2 f}{\partial r^2} \right)_{a, z} + \dots +$$

$$\frac{(r - a)^{i-1}}{(i - 1)!} \left(\frac{\partial^{i-1} f}{\partial r^{i-1}} \right)_{a, z} + R_i \quad (34)$$

where

$$R_i = \frac{(r-a)^i}{i!} \left(\frac{\partial^i f}{\partial r^i} \right)_{\xi, z} \quad (35)$$

and

$$\left| \xi - \frac{r+a}{2} \right| < \left| \frac{r-a}{2} \right| \quad (36)$$

Applying this expansion to the finite differences grid

$$f_{m+1, l} = f_{m, l} + \Delta r \left(\frac{\partial f}{\partial r} \right)_{m, l} + O(\Delta r^2) \quad (37)$$

$$f_{m-1, l} = f_{m, l} - \Delta r \left(\frac{\partial f}{\partial r} \right)_{m, l} + O(\Delta r^2) \quad (38)$$

Combining equations (37) and (38) gives

$$\left(\frac{\partial f}{\partial r} \right)_{m, l} = \frac{f_{m+1, l} - f_{m-1, l}}{2\Delta r} + O(\Delta r^2) \quad (39)$$

The functional symbol $O()$ indicates a truncation error which is proportional to the value of the argument of the function.

By a similar manipulation of Taylor series expansions, the following finite difference approximations may be derived with the order of their associated truncation error.

$$\left(\frac{\partial^2 f}{\partial r^2} \right)_{m, l} = \frac{3f_{m, l} - 4f_{m-1, l} + f_{m-2, l}}{2\Delta r^2} + O(\Delta r^2) \quad (40)$$

$$\left(\frac{\partial f}{\partial r} \right)_{m, l} = \frac{f_{m+1, l} - f_{m, l}}{\Delta r} + O(\Delta r) \quad (41)$$

$$\left(\frac{\partial^2 f}{\partial r^2}\right)_{m,l} = \frac{f_{m+1,l} - 2f_{m,l} + f_{m-1,l}}{\Delta r^2} + O(\Delta r^2) \quad (42)$$

$$\left(\frac{\partial f}{\partial r}\right)_{m+\frac{1}{2},l} = \frac{f_{m+1,l} - f_{m,l}}{\Delta r} + O(\Delta r^2) \quad (43)$$

A simple interchange results in approximations for derivatives with respect to z . For example

$$\left(\frac{\partial f}{\partial z}\right)_{m,l+\frac{1}{2}} = \frac{f_{m,l+1} - f_{m,l}}{\Delta z} + O(\Delta z^2) \quad (44)$$

Finite Difference Representation of the Motion Equation

Writing the equation of motion as

$$\rho u \frac{\partial u}{\partial z} = - \frac{dp}{dz} + \theta p + \mu \frac{\partial^2 u}{\partial r^2} + \left(\frac{\mu}{r} + \frac{\partial \mu}{\partial r} - \rho v \right) \frac{\partial u}{\partial r} \quad (45)$$

and adopting the notation

$$u_{m,l} = u[(m-1)\Delta r, (l-1)\Delta z] \quad (46)$$

$$v_{m,l} = v[(m-1)\Delta r, (l-1)\Delta z] \quad (47)$$

$$\rho_{m,l} = \rho[(m-1)\Delta r, (l-1)\Delta z] \quad (48)$$

$$\mu_{m,l} = \mu[(m-1)\Delta r, (l-1)\Delta z] \quad (49)$$

$$p_l = p[(l-1)\Delta z] \quad (50)$$

the motion equation can be approximated by

$$\begin{aligned}
\rho_{m,l+1} u_{m,l} \left(\frac{u_{m,l+1} - u_{m,l}}{\Delta z} \right) = & - \frac{p_{l+1} - p_l}{\Delta z} + \\
\mu_{m,l+1} \left(\frac{u_{m+1,l+1} - 2u_{m,l+1} + u_{m-1,l+1}}{\Delta r^2} \right) + & \left(\frac{\mu_{m,l+1}}{r_m} - \rho_{m,l+1} v_{m,l} + \right. \\
\left. \frac{u_{m+1,l+1} - \mu_{m-1,l+1}}{2\Delta r} \right) \left(\frac{u_{m+1,l+1} - u_{m-1,l+1}}{2\Delta r} \right) + & \theta_{p_{m,l+1}} \quad (51)
\end{aligned}$$

Rearranging this equation yields

$$\begin{aligned}
\left(- \frac{\mu_{m,l+1}}{\Delta r^2} + \frac{\mu_{m,l+1}}{2r_m \Delta r} - \frac{\rho_{m,l+1} v_{m,l}}{2\Delta r} + \frac{\mu_{m+1,l+1} - \mu_{m-1,l+1}}{4\Delta r^2} \right) u_{m-1,l+1} + \\
\left(\frac{\rho_{m,l+1} u_{m,l}}{\Delta z} + \frac{2\mu_{m,l+1}}{\Delta r^2} \right) u_{m,l+1} + \\
\left(- \frac{\mu_{m,l+1}}{\Delta r} - \frac{\mu_{m,l+1}}{2r_m \Delta r} + \frac{\rho_{m,l+1} v_{m,l}}{2\Delta r} - \frac{\mu_{m+1,l+1} - \mu_{m-1,l+1}}{4\Delta r^2} \right) u_{m+1,l+1} = \\
- \left(\frac{1}{\Delta z} \right) p_{l+1} + \frac{p_l + \rho_{m,l+1} u_{m,l}^2}{\Delta z} + \theta_{p_{m,l+1}} \quad (52)
\end{aligned}$$

At the wall $u_{N+1} = 0$. At the tube center line a limiting form of the equation of motion must be used since

$$\left(\frac{1}{r} \frac{\partial u}{\partial r} \right)_{r=0}$$

is undefined. By L'Hospital's rule

$$\lim_{r \rightarrow 0} \left(\frac{1}{r} \frac{\partial u}{\partial r} \right) = \frac{\partial^2 u}{\partial r^2} \quad (53)$$

and the equation of motion becomes at the tube center line

$$\rho u \left. \frac{\partial u}{\partial z} \right|_{r=0} = - \frac{dp}{dz} + \theta p \Big|_{r=0} + 2\mu \left. \frac{\partial^2 u}{\partial r^2} \right|_{r=0} \quad (54)$$

Upon substitution of the finite difference approximations the equation of motion at the center line becomes

$$\begin{aligned} \rho_{1,l+1} u_{1,l} \left(\frac{u_{1,l+1} - u_{1,l}}{\Delta z} \right) &= \left(\frac{p_{l+1} - p_l}{\Delta z} \right) + \theta p_{1,l+1} \\ &+ 2\mu_{1,l+1} \left(\frac{u_{2,l+1} - 2u_{1,l+1} + u_{0,l+1}}{\Delta r^2} \right) \end{aligned} \quad (55)$$

Noting that by symmetry conditions $u_{2,l+1} = u_{0,l+1}$

then rearrangement of equation (55) yields

$$\begin{aligned} \left(\frac{\rho_{1,l+1} u_{1,l}}{\Delta z} + \frac{4\mu_{1,l+1}}{\Delta r^2} \right) u_{1,l+1} &+ \left(-\frac{4\mu_{1,l+1}}{\Delta r^2} \right) u_{2,l+1} = \\ \left(-\frac{1}{\Delta z} \right) p_{l+1} &+ \left(\frac{p_l + \rho_{1,l+1} u_{1,l}^2}{\Delta z} \right) + \theta p_{1,l+1} \end{aligned} \quad (56)$$

The above system of equations can be written in vector-matrix notation as

$$\underline{A} \vec{u} = \vec{a} + \vec{b} p \quad (57)$$

where

$$\vec{u} = \begin{bmatrix} u_{1,l+1} \\ u_{2,l+1} \\ \vdots \\ u_{N,l+1} \end{bmatrix} \quad (58)$$

The matrix of coefficients is

$$\underline{A} = \begin{bmatrix} A_1 & B_1 & & & \\ C_2 & A_2 & B_2 & & \\ & \ddots & \ddots & \ddots & \\ & & C_{N-1} & A_{N-1} & B_{N-1} \\ & & & C_N & A_N \end{bmatrix} \quad (59)$$

where

$$A_1 = \left(\frac{\rho_{1,l+1}}{\Delta z} + \frac{4\mu_{1,l+1}}{\Delta r^2} \right) \quad (60)$$

$$B_1 = \left(-\frac{4\mu_{1,l+1}}{\Delta r^2} \right) \quad (61)$$

and for $2 \leq m \leq N$

$$A_m = \left(\frac{\rho_{m,l+1}}{\Delta z} + \frac{2u_{m,l+1}}{\Delta r^2} \right) \quad (62)$$

$$B_m = \left(-\frac{u_{m,l+1}}{\Delta r^2} - \frac{\mu_{m,l+1}}{2r_m \Delta r} + \frac{\rho_{m,l+1}}{2\Delta r} - \frac{\mu_{m+1,l+1} - \mu_{m,l+1}}{4\Delta r^2} \right) \quad (63)$$

$$C_m = \left(-\frac{\mu_{m,l+1}}{\Delta r^2} + \frac{\mu_{m,l+1}}{2r_m \Delta r} - \frac{\rho_{m,l+1}}{2\Delta r} + \frac{\mu_{m+1,l+1} - \mu_{m,l+1}}{4\Delta r^2} \right) \quad (64)$$

The vectors \vec{a} and \vec{b} are given by

$$\vec{a} = \begin{bmatrix} a_1 \\ a_2 \\ \vdots \\ a_N \end{bmatrix} \quad a_m = \left(\frac{p_\ell + \rho_{m,\ell+1} u_{m,\ell}^2}{\Delta z} \right) + \theta_{p_{m,\ell+1}} \quad (65)$$

and

$$\vec{b} = \begin{bmatrix} b_1 \\ b_2 \\ \vdots \\ b_N \end{bmatrix} \quad b_m = \left(-\frac{1}{\Delta z} \right) \quad (66)$$

The scalar p is the pressure at the $\ell+1$ step, $p_{\ell+1}$.

Finite Difference Representation of the Energy Equation

Writing the energy equation as

$$\rho c_p \text{Pr} u \frac{\partial T}{\partial z} = k \frac{\partial^2 T}{\partial r^2} + \left(\frac{k}{r} + \frac{\partial k}{\partial r} - \rho c_p \text{Pr} v \right) \frac{\partial T}{\partial r} \quad (67)$$

and adopting the notation

$$T_{m,\ell} = T[(m-1)\Delta r, (\ell-1)\Delta z] \quad (68)$$

$$k_{m,\ell} = k[(m-1)\Delta r, (\ell-1)\Delta z] \quad (69)$$

$$c_{p_{m,\ell}} = c_p[(m-1)\Delta r, (\ell-1)\Delta z] \quad (70)$$

the energy equation can be approximated by

$$\begin{aligned}
& \rho_{m,l} c_{p_{m,l}} \text{Pr } u_{m,l} \left(\frac{T_{m,l+1} - T_{m,l}}{\Delta z} \right) = \\
& k_{m,l} \left(\frac{T_{m+1,l+1} - 2T_{m,l+1} + T_{m-1,l+1}}{\Delta r^2} \right) + \left(\frac{k_{m,l}}{r_m} + \frac{k_{m+1,l} - k_{m-1,l}}{2\Delta r} \right. \\
& \left. - \rho_{m,l} c_{p_{m,l}} \text{Pr } v_{m,l} \right) \left(\frac{T_{m+1,l+1} - T_{m-1,l+1}}{2\Delta r} \right) \quad (71)
\end{aligned}$$

When rearranged this equation becomes

$$\begin{aligned}
& \left(-\frac{k_{m,l}}{\Delta r^2} + \frac{k_{m,l}}{2r_m \Delta r} + \frac{k_{m+1,l} - k_{m-1,l}}{4\Delta r^2} - \frac{\rho_{m,l} c_{p_{m,l}} \text{Pr } v_{m,l}}{2\Delta r} \right) T_{m-1,l+1} + \\
& \left(\frac{\rho_{m,l} c_{p_{m,l}} \text{Pr } u_{m,l}}{\Delta z} + \frac{2k_{m,l}}{\Delta r^2} \right) T_{m,l+1} + \left(-\frac{k_{m,l}}{2r_m \Delta r} \right. \\
& \left. - \frac{k_{m+1,l} - k_{m-1,l}}{4\Delta r^2} + \frac{\rho_{m,l} c_{p_{m,l}} \text{Pr } v_{m,l}}{2\Delta r} \right) T_{m+1,l+1} = \frac{\rho_{m,l} c_{p_{m,l}} \text{Pr } u_{m,l} T_{m,l}}{\Delta z} \quad (72)
\end{aligned}$$

As with the motion equation, a limiting value of the energy equation at the center line must be used. Therefore, applying L'Hospital's rule we get

$$\lim_{r \rightarrow 0} \left(\frac{1}{r} \frac{\partial T}{\partial r} \right) = \frac{\partial^2 T}{\partial r^2} \Big|_{r=0} \quad (73)$$

The energy equation at the center line becomes

$$\rho_1 c_p \text{Pr} u \left. \frac{\partial T}{\partial z} \right|_{r=0} = 2k \left. \frac{\partial^2 T}{\partial r^2} \right|_{r=0} \quad (74)$$

and the finite difference approximation is

$$\rho_1, l c_{p1, l} \text{Pr} u_{1, l} \left(\frac{T_{1, l+1} - T_{1, l}}{\Delta z} \right) = 2k_{1, l} \left(\frac{T_{2, l+1} - 2T_{1, l+1} + T_{0, l+1}}{\Delta r^2} \right) \quad (75)$$

Noting that by symmetry

$$T_{2, l+1} = T_{0, l+1}$$

rearrangement of equation (75) results in

$$\left(\frac{\rho_1, l c_{p1, l} \text{Pr} u_{1, l}}{\Delta z} + \frac{4k_{1, l}}{\Delta r^2} \right) T_{1, l+1} + \left(-\frac{4k_{1, l}}{\Delta r^2} \right) T_{2, l+1} =$$

$$\frac{\rho_1, l c_{p1, l} \text{Pr} u_{1, l} T_{1, l}}{\Delta z} \quad (76)$$

Since the radial velocity was expected to have a pronounced effect on the heat-transfer process and since the radial velocities for some situations are quite high near the wall of the tube, it was decided to add a fictitious mesh point one step past the wall. This procedure allows the use of the energy equation at the wall where the radial velocity is zero. At the wall the energy equation is

$$\left[\frac{\partial^2 T}{\partial r^2} + \left(\frac{1}{k} \frac{\partial k}{\partial r} + 2 \right) \frac{\partial T}{\partial r} \right]_{r=\frac{1}{2}} = 0 \quad (77)$$

Using difference approximations this equation becomes

$$\left[\frac{T_{N+2,l+1} - 2T_{N+1,l+1} + T_{N,l+1}}{\Delta r^2} \right] \quad (78)$$

$$+ \left[\frac{1}{k_{N+1,l}} \left(\frac{3k_{N+1,l} - 4k_{N,l} + k_{N-1,l}}{2\Delta r} \right) + 2 \right] \left[\frac{T_{N+2,l+1} - T_{N-1,l+1}}{2\Delta r} \right] = 0$$

or

$$\left(1 - \frac{3k_{N+1,l} - 4k_{N,l} + k_{N-1,l}}{4k_{N+1,l}} - \Delta r \right) T_{N,l+1} + \quad (79)$$

$$\left(1 + \frac{3k_{N+1,l} - 4k_{N,l} + k_{N-1,l}}{4k_{N+1,l}} + \Delta r \right) T_{N+2,l+1} = 2T_{N+1,l+1}$$

Note that

$$T_{N+1,l+1} = T_w$$

Let

$$T_{N+1,l+1}^* = T_{N+2,l+1} \quad (80)$$

Then the above system of equations may be written in vector-matrix notation as

$$\underline{B} \vec{t} = \vec{c} \quad (81)$$

where

$$\underline{B} = \begin{bmatrix} A_1 & B_1 & & & & \\ C_2 & A_2 & B_2 & & & \\ & \ddots & \ddots & \ddots & & \\ & & C_N & A_N & B_N^* & \\ & & & C_{N+1} & A_{N+1} & \end{bmatrix} \quad (82)$$

$$A_1 = \left(\frac{\rho_{1,l}^c p_{1,l}^{Pr} u_{1,l}}{\Delta z} + \frac{4k_{1,l}}{\Delta r^2} \right) \quad (83)$$

$$B_1 = \left(- \frac{4k_{1,l}}{\Delta r^2} \right) \quad (84)$$

for $2 \leq m \leq N$

$$A_m = \left(\frac{\rho_{m,l}^c p_{m,l}^{Pr} u_{m,l}}{\Delta z} + \frac{2k_{m,l}}{\Delta r^2} \right) \quad (85)$$

$$B_m = \left(- \frac{k_{m,l}}{\Delta r^2} - \frac{k_{m,l}}{2r_m \Delta r} - \frac{k_{m+1,l} - k_{m-1,l}}{4\Delta r^2} + \frac{\rho_{m,l}^c p_{m,l}^{Pr} v_{m,l}}{2\Delta r} \right) \quad (86)$$

$$C_m = \left(- \frac{k_{m,l}}{\Delta r^2} + \frac{k_{m,l}}{2r_m \Delta r} + \frac{k_{m+1,l} - k_{m-1,l}}{4\Delta r^2} - \frac{\rho_{m,l}^c p_{m,l}^{Pr} v_{m,l}}{2\Delta r} \right) \quad (87)$$

$$B_N^* = 0$$

and for $m = N + 1$

$$A_{N+1} = 1 + \frac{3k_{N+1,l} - 4k_{N,l} + k_{N-1,l}}{4k_{N+1,l}} + \Delta r \quad (88)$$

$$C_{N+1} = 1 - \frac{3k_{N+1,l} - 4k_{N,l} + k_{N-1,l}}{4k_{N+1,l}} - \Delta r \quad (89)$$

The vectors in equation (81) are

$$\vec{t} = \begin{bmatrix} T_{1,l+1} \\ T_{2,l+1} \\ \vdots \\ T_{N,l+1} \\ T_{N+1,l+1}^* \end{bmatrix} \quad (90)$$

$$\vec{c} = \begin{bmatrix} c_1^* \\ c_2^* \\ \vdots \\ c_N^* \\ c_{N+1}^* \end{bmatrix} \quad (91)$$

in which

$$c_m^* = \left(\frac{\rho_{m,l} c_{p_{m,l}} \text{Pr} u_{m,l} T_{m,l}}{\Delta z} \right) \quad 1 \leq m < N \quad (92)$$

$$c_N^* = \left(\frac{\rho_{N,l} c_{p_{N,l}} \text{Pr} u_{N,l} T_{N,l}}{\Delta z} - B_N T_w \right) \quad (93)$$

$$c_{N+1}^* = 2T_w \quad (94)$$

Finite Difference Representation of the Continuity Equation

The following finite difference approximations have a second order truncation error with respect to the grid point $(m + \frac{1}{2}, l + \frac{1}{2})$.

$$\frac{\partial(r\rho v)}{\partial r} = \left(\frac{r_{m+1}\rho_{m+1,l+1}v_{m+1,l+1} - r_m\rho_{m,l+1}v_{m,l+1}}{\Delta r} \right) + O(\Delta r^2) \quad (95)$$

$$\begin{aligned} r \frac{\partial(\rho u)}{\partial z} = & \frac{1}{2} \left(\frac{r_{m+1}(\rho_{m+1,l+1}u_{m+1,l+1} - \rho_{m+1,l}u_{m+1,l})}{\Delta z} \right. \\ & \left. + \frac{r_m(\rho_{m,l+1}u_{m,l+1} - \rho_{m,l}u_{m,l})}{\Delta z} \right) + O(\Delta r^2, \Delta z^2) \end{aligned} \quad (96)$$

These approximations can be substituted into the continuity equation

$$\frac{\partial(r\rho v)}{\partial r} + r \frac{\partial(\rho u)}{\partial z} = 0 \quad (97)$$

to yield

$$\begin{aligned} v_{m+1,l+1} = & \left(\frac{r_m\rho_{m,l+1}}{r_{m+1}\rho_{m+1,l+1}} \right) v_{m,l+1} - \left(\frac{\Delta r}{2\Delta z} \right) \left[u_{m+1,l+1} - \left(\frac{\rho_{m+1,l}}{\rho_{m+1,l+1}} \right) u_{m+1,l} \right. \\ & \left. + \left(\frac{r_m\rho_{m,l+1}}{r_{m+1}\rho_{m+1,l+1}} \right) u_{m,l+1} - \left(\frac{r_m\rho_{m,l}}{r_{m+1}\rho_{m+1,l+1}} \right) u_{m,l} \right] \end{aligned} \quad (98)$$

Writing the continuity equation in expanded form

$$\frac{\partial(\rho v)}{\partial r} + \frac{\rho v}{r} + \frac{\partial(\rho u)}{\partial z} = 0 \quad (99)$$

and noting that by L'Hospital's rule

$$\lim_{r \rightarrow 0} \left(\frac{\rho v}{r} \right) = \left. \frac{\partial(\rho v)}{\partial r} \right|_{r=0} \quad (100)$$

the equation

$$\left(2 \frac{\partial(\rho v)}{\partial r} + \frac{\partial(\rho u)}{\partial z} \right)_{r=0} = 0 \quad (101)$$

results. This equation can be put in finite difference form to get

$$2 \left(\frac{\rho_{2,l+1} v_{2,l+1} - \rho_{1,l+1} v_{1,l+1}}{\Delta r} \right) = - \frac{1}{2} \left(\frac{\rho_{2,l+1} u_{2,l+1} - \rho_{2,l} u_{2,l}}{\Delta z} + \frac{\rho_{1,l+1} u_{1,l+1} - \rho_{1,l} u_{1,l}}{\Delta z} \right) \quad (102)$$

Since

$$v_{1,l} = 0$$

then

$$v_{2,l+1} = - \left(\frac{\Delta r}{4\Delta z} \right) \left[u_{2,l+1} - \left(\frac{\rho_{2,l}}{\rho_{2,l+1}} \right) u_{2,l} + \left(\frac{\rho_{1,l+1}}{\rho_{2,l+1}} \right) u_{1,l+1} - \left(\frac{\rho_{1,l}}{\rho_{2,l+1}} \right) u_{1,l} \right] \quad (103)$$

The components of the vector

$$\vec{v} = \begin{bmatrix} v_{1,l+1} \\ v_{2,l+1} \\ \vdots \\ v_{N,l+1} \end{bmatrix} \quad (104)$$

are determined by recursive application of the above equations. These equations can be compactly represented in matrix-vector notation in terms

of \vec{u} as

$$\vec{v} = \underline{C} \vec{u} + \vec{d} \quad (105)$$

Although for computational purposes nothing would be gained by extracting the matrices \underline{C} and \vec{d} and cataloging their elements, it is noted that \underline{C} is a function of $(\frac{\Delta r}{\Delta z})$, r_m , $\rho_{m,\ell}$, and $\rho_{m,\ell+1}$; and \vec{d} , in addition, is a function of $u_{m,\ell}$.

Numerical Integration for Overall Material Balance

The statement

$$\int_0^{\frac{1}{2}} rpu \, dr = \frac{1}{8} \quad (106)$$

represents the overall mass balance which must be satisfied at any tube cross section. Denoting the integral by \mathcal{I}_u , it can be numerically calculated at the $\ell+1$ step as follows:

$$\mathcal{I}_u = \sum_{j=1}^{\frac{N-2}{2}} a_{2j-1} + a_N + a_{N+1} \quad (107)$$

where

$$a_m = \frac{\Delta r}{3} \left[(rpu)_{m,\ell+1} + 4(rpu)_{m+1,\ell+1} + (rpu)_{m+2,\ell+1} \right] \quad (108)$$

$$a_N = \left(\frac{\Delta r}{24} \right) \left[(rpu)_{N-3,\ell+1} - 5(rpu)_{N-2,\ell+1} + 19(rpu)_{N-1,\ell+1} + 9(rpu)_{N,\ell+1} \right] \quad (109)$$

and

$$\alpha_{N+1} = \frac{\Delta r}{720} \left[-19(rpu)_{N-2,l+1} + 106(rpu)_{N-2,l+1} - 264(rpu)_{N-1,l+1} + 646(rpu)_{N,l+1} + 251(rpu)_{N+1,l+1} \right] \quad (110)$$

The first term, the integration to $N-1$, is a straight forward application of Simpson's rule while α_N and α_{N+1} are high order quadrature formulas. The high order schemes were developed by Lee⁽¹⁾ to take into account the extreme variation in properties near the tube wall. In matrix-vector notation this calculation can be represented as the scalar product

$$\mathcal{Q}_u = (\vec{e}, \vec{u}) \quad (111)$$

where \vec{e} is a function of Δr , r_m , and $\rho_{m,l+1}$.

Solution of Systems of Equations

The difference approximations for the equations of motion and energy result in systems of linear algebraic equations for which the matrices of coefficients are tridiagonal in form. For this type of system a simple computational algorithm based on the Gaussian Elimination Scheme is available.⁽⁴³⁾ This scheme has high accuracy and is very economical with respect to computation time. An outline of this technique follows.

Consider the system of equations

$$\begin{bmatrix}
 A_1 & B_1 & & & \\
 C_2 & A_2 & B_2 & & \\
 & \ddots & \ddots & \ddots & \\
 & & C_{N-1} & A_{N-1} & B_{N-1} \\
 & & & C_N & A_N
 \end{bmatrix}
 \begin{bmatrix}
 x_1 \\
 x_2 \\
 \vdots \\
 x_{N-1} \\
 x_N
 \end{bmatrix}
 =
 \begin{bmatrix}
 D_1 \\
 D_2 \\
 \vdots \\
 D_N
 \end{bmatrix}
 \quad (112)$$

Then the computational algorithm is

$$\left.
 \begin{aligned}
 W_1 &= A_1 \\
 W_m &= A_m - C_m Q_{m-1} \quad (m = 2, 3, 4, \dots, N) \\
 Q_{m-1} &= \frac{B_{m-1}}{W_{m-1}} \\
 G_1 &= \frac{D_1}{W_1} \\
 G_m &= \frac{D_m - C_m G_{m-1}}{W_m} \quad (m = 2, 3, 4, \dots, N) \\
 x_N &= G_N \\
 x_m &= G_m - Q_m x_{m+1} \quad (m = N-1, N-2, \dots, 1)
 \end{aligned}
 \right\} \quad (113)$$

Notice that at the most three multiplications, three divisions, and three additions are required per grid point, and the amount of computational time is directly proportional to the number of grid points.

Newton's Method Calculation for \vec{u} and p

According to the overall material balance condition

$$\mathcal{Q}_u = \frac{1}{8} \quad (114)$$

hence

$$(\vec{e}, \vec{u}) = \frac{1}{8} \quad (115)$$

and for fixed values of \underline{A} , \vec{a} , \vec{b} , and \vec{e} then

$$F(p) = \frac{1}{8} - (\vec{e}, \vec{u}) \quad (116)$$

This implies the use of a Newton-Raphson iteration to choose the correct pressure. The iteration algorithm is

$$p^{i+1} = p^i - \frac{F(p^i)}{D_p F} \quad (117)$$

where

$$D_p F = -(\vec{e}, D_p \vec{u}) \quad (118)$$

$$\underline{A} D_p \vec{u} = \vec{b} \quad (119)$$

and $(\vec{e}, D_p \vec{u})$ is evaluated by the same numerical quadrature formula as \mathcal{I}_u .

Notice that $D_p \vec{u}$ is independent of p , and only one iteration is required for convergence to the correct value of p . The calculation is initiated by approximating $p_{\ell+1}$ by p_ℓ and calculating $F(p_\ell)$ and $D_p F(p_\ell)$. The correct value of $p_{\ell+1}$ is calculated by the Newton-Raphson algorithm and is used to compute \vec{u} . \mathcal{I}_u can then be calculated as a check.

It is possible to combine

$$(\vec{e}, \vec{u}) = \frac{1}{8} \quad (120)$$

and

$$\underline{A}\vec{u} = \vec{a} + \vec{b}p \quad (121)$$

in which p becomes an element of \vec{u} and $\frac{1}{8}$ becomes an element of \vec{a} to get

$$\underline{E}\vec{u} = \vec{a} \quad (122)$$

The matrix \underline{E} , however, is not tridiagonal and requires a much more complicated procedure than that for the tridiagonal system. Direct elimination methods are subject to round-off error for large systems such as considered in this work, and iterative methods, even when convergence is assured, require a large number of calculations. A detailed discussion of these problems may be found in Lapidus.⁽⁴³⁾

This Newton-Raphson approach was found to be very accurate and did not require excessive computation time. The difference, $\frac{1}{8} - \mathcal{J}_u$, was zero to at least eight decimal places.

Calculation Scheme for Velocity and Temperature Fields

The preceding equations can be summarized by

$$\begin{aligned} \underline{A}\vec{u} &= \vec{a} + \vec{b}p \\ \underline{B}\vec{t} &= \vec{c} \\ \vec{v} &= \underline{c}\vec{u} + \vec{d} \\ \mathcal{J}_u &= (\vec{e}, \vec{u}) \end{aligned} \quad (123)$$

The calculation procedure is as follows:

1. \underline{B} and \vec{c} are evaluated at step l and used to solve for \vec{t} .
2. With values of \vec{t} known, properties are evaluated at $l+1$.

3. \underline{A} , \vec{a} , \vec{b} and \vec{e} are evaluated and used to calculate \vec{u} and p .
4. \underline{C} and \vec{d} are used to calculate \vec{v} .
5. Velocities and temperatures are then used to calculate various heat transfer parameters.
6. The above steps are repeated in sequence.

The computer program for the implementation of this scheme is found in Appendix B.

Mean Temperature

Following Lee,⁽¹⁾ the mean temperature, T'_M , is defined by

$$Q' = W' \int_{T'_0}^{T'_M} c'_p dT' \quad (124)$$

and the first law of thermodynamics written for an element of volume fixed in space is

$$Q' = \int_{vol} \left(H' + \frac{\vec{V} \cdot \vec{V}}{2} + g_z z' \right) \rho' \vec{V} \cdot d\vec{A} \quad (125)$$

Neglecting potential and kinetic energy terms in comparison with the enthalpy term, this equation reduces to

$$Q' = \Delta \left(2\pi \int_0^{R'} \rho' u' r' H' dr' \right) = W' \int_{T'_0}^{T'_M} c'_p dT' \quad (126)$$

Choosing T'_0 as the reference temperature, the above equation in terms of dimensionless variables is

$$Q = \int_0^{\frac{1}{2}} H_p u r dr = \frac{1}{8} \int_0^{T'_M} c_p dT \quad (127)$$

where

$$H = \frac{H'}{c'_{p_o} (T'_w - T'_o)} \quad (128)$$

$$Q = \frac{Q'}{2\pi\rho'_o \bar{u}' D'^2 c'_{p_o} (T'_w - T'_o)} \quad (129)$$

and

$$H = \int_o^T c_p dT \quad (130)$$

If c'_p is a constant then

$$H = T \quad (131)$$

and

$$T_M = 8 \int_o^{\frac{1}{2}} H \rho u r dr \quad (132)$$

However, if

$$c'_p = c_o + c_1 T' \quad (133)$$

then denoting $(T'_w - T'_o)$ as $\Delta T'_{wo}$

$$c_p = \frac{c_o + c_1 T'_o + c_1 \Delta T'_{wo} T}{c'_{p_o}} \quad (134)$$

Integration yields

$$\int_o^{T_M} c_p dt = \frac{1}{c'_{p_o}} \left((c_o + c_1 T'_o) T_M + \frac{1}{2} (c_1 \Delta T'_{wo}) T_M^2 \right) \quad (135)$$

Letting

$$\mathcal{Q}_q = 8 \int_0^{\frac{1}{2}} H p u r dr \quad (136)$$

and solving equation (135) for T_M

$$T_M = \frac{-c'_{p_o} + \sqrt{(c'_{p_o})^2 + 2c_1 \Delta T'_{wo} c'_{p_o} \mathcal{Q}_q}}{c_1 \Delta T'_{wo}} \quad (137)$$

The integral \mathcal{Q}_q can be evaluated by the same scheme as \mathcal{Q}_u . The mean temperature as defined here is just a generalization of the cup-mixing temperature.

Nusselt Numbers

The local Nusselt number is defined by

$$Nu = \frac{h'D'}{k'_M} = \frac{D'k'_w \left. \frac{\partial T'}{\partial r} \right|_{r=D/2}}{k'_M (T'_w - T'_M)} \quad (138)$$

Putting this into dimensionless form

$$Nu = \frac{k_w \left. \frac{\partial T}{\partial r} \right|_{r=1/2}}{k_M (1 - T_M)} \quad (139)$$

A finite difference approximation for this equation is

$$Nu = \frac{k_{N+1} (3T_{N+1,l+1} - 4T_{N,l+1} + T_{N-1,l+1})}{2\Delta r k_M (1 - T_M)} \quad (140)$$

Defining the arithmetic mean heat-transfer coefficient as

$$Q' = h'_{AM} \pi D' z' \left[\frac{(T'_w - T'_o) + (T'_w - T'_M)}{2} \right] \quad (141)$$

and combining with equation (126)

$$2\pi \int_0^{\frac{D'}{2}} H' \rho' u' r' dr' = h'_{AM} \pi D' z' \left[\frac{2T'_w - T'_o - T'_M}{2} \right] \quad (142)$$

In dimensionless form the arithmetic mean Nusselt number is

$$Nu_{AM} = \frac{h'_{AM} D'}{k'_{AM}} = \frac{\frac{4Pr}{z} \int_0^{\frac{1}{2}} H \rho u r dr}{k_{AM} (2 - T_M)} \quad (143)$$

Similarly, define the logarithmic mean transfer coefficient by

$$Q' = h'_{LN} \pi D' z' \left[\frac{(T'_w - T'_o) - (T'_w - T'_M)}{\ln[(T'_w - T'_o)/(T'_w - T'_M)]} \right] \quad (144)$$

and in dimensionless form

$$Nu_{LN} = \frac{h'_{LN} D'}{k'_{LN}} = \frac{-2 \ln(1 - T_M) Pr \int_0^{\frac{1}{2}} H \rho u r dr}{z k_{LN} T_M} \quad (145)$$

For constant properties this expression may be reduced to

$$Nu_{LN} = \frac{Pr \ln\left(\frac{1}{1 - T_M}\right)}{4z} \quad (146)$$

Notice that for constant properties

$$Nu_{LN} = \left[\frac{(2 - T_M) \ln\left(\frac{1}{1 - T_M}\right)}{2T_M} \right] Nu_{AM} \quad (147)$$

For constant properties a very interesting relationship exists between Nu_{LN} and Nu . Since

$$h' \pi D' (T_M' - T_w') dz' = -\left(\frac{\pi}{4}\right) D'^2 \rho' c_p' \bar{u}' dT_M' \quad (148)$$

then

$$\int_0^{z'} h' dz' = - \int_{T_o'}^{T_M'} \frac{D' \rho' c_p' \bar{u}' dT_M'}{4(T_M' - T_w')} \quad (149)$$

Integrating

$$\int_0^{z'} h' dz' = \frac{-D' \rho' c_p' \bar{u}'}{4} \ln \left(\frac{T_M' - T_w'}{T_o' - T_w'} \right) \quad (150)$$

and rearranging

$$\int_0^{z'} h' dz' = \frac{D' \rho' c_p' \bar{u}'}{4} \left[\frac{\frac{(T_w' - T_o') - (T_w' - T_M')}{(T_w' - T_o') - (T_w' - T_M')}}{\ln \frac{T_w' - T_o'}{T_w' - T_M'}} \right] \quad (151)$$

or

$$\int_0^{z'} h' dz' = \frac{z' \left(\frac{D'^2}{4}\right) \rho' \bar{u}' \pi c_p' (T_M' - T_o')}{D' z' \pi (T_w' - T_M')_{LN}} \quad (152)$$

Then from equation (144)

$$\frac{1}{z'} \int_0^{z'} h' dz' = h'_{LN} \quad (153)$$

and

$$Nu_{LN} = \frac{1}{z} \int_0^z Nu dz \quad (154)$$

This integration can be performed in a straightforward manner by application of the Trapezoidal rule to get

$$(Nu_{LN})_{\ell+1} = (Nu_{LN})_{\ell} + \frac{\Delta z}{2z_{\ell}} \left((Nu)_{\ell+1} + (Nu)_{\ell} \right) \quad (155)$$

The starting value for the parabolic velocity profile case can be obtained from the L         solution.⁽³⁰⁾ It gives

$$T_M = 6.46 \left(\frac{Pr}{z} \right)^{-2/3} \quad (156)$$

or

$$Nu_{LN} = \frac{Pr \ln \left[\frac{1}{1 - 6.46 \left(\frac{Pr}{z} \right)^{-2/3}} \right]}{4z} \quad (157)$$

A starting value for the uniform velocity profile case can be obtained by taking the Pohlhausen flat plate solution to be a good approximation near the tube entrance. Modified for a log mean temperature⁽³²⁾ this solution gives

$$Nu_{LN} = - \left(\frac{Pr}{z} \right) \ln \left[1 - \frac{2.656}{Pr^{0.165} \left(\frac{Pr}{z} \right)^{0.5}} \right] \quad (158)$$

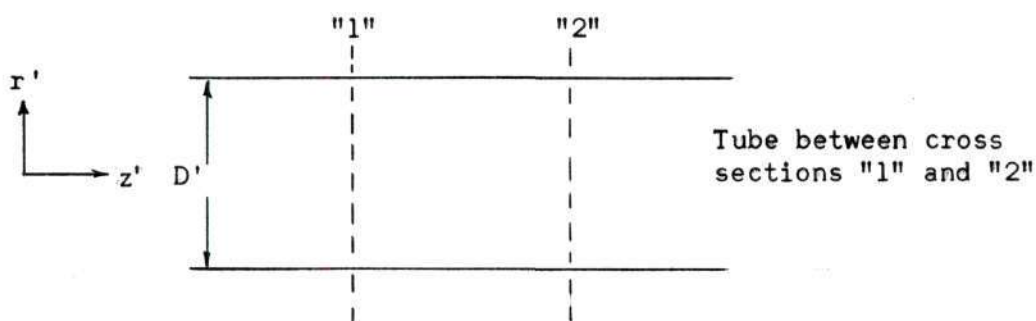
where

$$\lim_{\left(\frac{Pr}{z}\right) \rightarrow \infty} Nu_{LN} = 0.644 Pr^{-0.165} \left(\frac{Pr}{z}\right)^{0.5} \quad (159)$$

Step-by-Step Energy Balance

When the temperature and velocity fields are known it is possible to calculate the energy added to the system from one tube cross section to the other by two independent methods. One method is based on an integration of the heat flux at the wall, and the other one is based on using T_M to find the difference between the total energy entering and leaving from one cross section to the other.

Consider the system below.



Since

$$Nu = \frac{h'D'}{k'_M} \quad (160)$$

and

$$dQ' = h' \pi D' (T'_w - T'_M) dz' \quad (161)$$

then

$$dQ' = Nu k_M' \pi (T_w' - T_M') dz' \quad (162)$$

and in dimensionless form

$$dQ = \left(\frac{1}{2}\right) Pr Nu k_M (1 - T_M) dz \quad (163)$$

$$Q = \frac{Pr}{2} \int_{z_1}^{z_2} k_M Nu (1 - T_M) dz \quad (164)$$

In finite difference representation, using the Trapezoidal rule and making the calculation grid step by grid step

$$Q \Big|_{\ell}^{\ell+1} = \left(\frac{\Delta z}{4Pr}\right) \left((Nu k_M (1 - T_M))_{\ell} + (Nu k_M (1 - T_M))_{\ell+1} \right) \quad (165)$$

On the other hand

$$Q \Big|_{"1"}^{"2"} = \Delta \left[\frac{1}{8} \int_0^{T_M} c_p dT \right] \quad (166)$$

For constant c_p' this becomes

$$Q \Big|_{"1"}^{"2"} = \frac{1}{8} (T_{M_2} - T_{M_1}) \quad (167)$$

but for

$$c_p' = c_o + c_1 T' \quad (168)$$

then

$$c_p = 1 + \left(\frac{c_1 \Delta T'_{wo}}{c_{p_o}'} \right) T \quad (169)$$

Substitution in equation (216) and integrating gives

$$Q \left|_{1}^{2} \right. = \frac{1}{8} \left[T_{m_2} - T_{m_1} + \left(\frac{c_1 \Delta T_{wo}}{2c_p'} \right) (T_{M_2}^2 - T_{M_1}^2) \right] \quad (170)$$

If $c_1 = 0$, this reverts to equation (217). In finite difference form

$$Q \left|_{\ell}^{\ell+1} \right. = \frac{1}{8} \left[T_{M_{\ell+1}} - T_{M_{\ell}} + \left(\frac{c_1 \Delta T_{wo}}{2c_p'} \right) (T_{M_{\ell+1}}^2 - T_{M_{\ell}}^2) \right] \quad (171)$$

Denoting Q from the local Nusselt number calculation as Q_N and from the mean temperature calculation as Q_T , an error term can be defined as

$$E_q = \frac{\frac{Q_N - Q_T}{2}}{\frac{Q_N + Q_T}{2}} = \frac{Q_N - Q_T}{Q_N + Q_T} \quad (172)$$

Note that this error is essentially defined by

$$Q = Q_{\text{Average}} \pm E_q (Q_{\text{Average}})$$

Pressure Terms

Rearrangement of the equation of motion results in

$$\frac{dp}{dz} = - \left(\rho v \frac{\partial u}{\partial r} + \rho u \frac{\partial u}{\partial z} \right) + \frac{1}{r} \frac{\partial}{\partial r} \left(r \mu \frac{\partial u}{\partial r} \right) + \theta \rho \quad (173)$$

Now, averaging this across the tube and integrating with respect to z

$$\frac{\int_0^z \int_0^{\frac{1}{2}} \left(\frac{dp}{dz} \right) 2\pi r dr}{\pi \left(\frac{1}{2} \right)^2} = \frac{\int_0^z \int_0^{\frac{1}{2}} \left[- \left(\rho v \frac{\partial u}{\partial r} + \rho u \frac{\partial u}{\partial z} \right) + \frac{1}{r} \frac{\partial}{\partial r} \left(r \mu \frac{\partial u}{\partial r} \right) + \theta \rho \right] 2\pi r dr dz}{\pi \left(\frac{1}{2} \right)^2} \quad (174)$$

$$\begin{aligned} \frac{1}{8} \int_0^z dp = \int_0^z \int_0^{\frac{1}{2}} (\rho v \frac{\partial u}{\partial r} + \rho u \frac{\partial u}{\partial z}) r dr dz + \int_0^z (r \mu \frac{\partial u}{\partial r})_{r=\frac{1}{2}} dz \\ + \theta \int_0^z \int_0^{\frac{1}{2}} \rho r dr dz \end{aligned} \quad (175)$$

Hence

$$\begin{aligned} p = -8 \int_0^z \int_0^{\frac{1}{2}} (\rho v \frac{\partial u}{\partial r} + \rho u \frac{\partial u}{\partial z}) r dr dz + 4 \int_0^z (\mu \frac{\partial u}{\partial r})_{r=\frac{1}{2}} dz \\ + 8\theta \int_0^z \int_0^{\frac{1}{2}} \rho r dr dz \end{aligned} \quad (176)$$

and defining

$$p_{KE} = -8 \int_0^z \int_0^{\frac{1}{2}} (\rho v \frac{\partial u}{\partial r} + \rho u \frac{\partial u}{\partial z}) r dr dz \quad (\text{Kinetic Energy Effect}) \quad (177)$$

$$p_F = 4 \int_0^z (\mu \frac{\partial u}{\partial r})_{r=\frac{1}{2}} dz \quad (\text{Frictional Effect}) \quad (178)$$

$$p_G = 8\theta \int_0^z \int_0^{\frac{1}{2}} \rho r dr dz \quad (\text{Gravity Effect}) \quad (179)$$

then

$$p = p_{KE} + p_F + p_G \quad (180)$$

The term p_{KE} may be calculated by making the same difference approximation as in the equation of motion and evaluating the integral

$$(\mathcal{J}_{KE})_{\ell+\frac{1}{2}} = \int_0^{\frac{1}{2}} (\rho v \frac{\partial u}{\partial r} + \rho u \frac{\partial u}{\partial z})_{\ell+\frac{1}{2}} r dr \quad (181)$$

by the scheme represented in equations (107), (108), (109) and (110).

Then the term P_{KE} is given by the recursion formula

$$(p_{KE})_{l+1} = (p_{KE})_l - 8 \Delta z \mathcal{J}_{KE} \quad (182)$$

$$(p_{KE})_1 = 0$$

The term p_F is calculated for the parabolic entrance profile by

$$(p_F)_{l+1} = (p_F)_l - \left(\frac{\Delta z}{2}\right) (FRCTN_l + FRCTN_{l+1}) \quad (183)$$

where

$$FRCTN_l = \mu_w \left(\frac{3u_{N+1,l} - 4u_{N,l} + u_{N-1,l}}{2\Delta r} \right) \quad (184)$$

and

$$FRCTN_1 = -8\mu_o \quad (185)$$

For the flat entrance profile

$$\lim_{z \rightarrow 0^-} \left. \frac{\partial u}{\partial r} \right|_{r=\frac{1}{2}} = 0 \quad (186)$$

and

$$\lim_{z \rightarrow 0^+} \left. \frac{\partial u}{\partial r} \right|_{r=\frac{1}{2}} = \infty \quad (187)$$

However, the magnitude of this slope decreases rapidly and negligible error is introduced in the first step by taking

$$\text{FRCTN}_1 = \text{FRCTN}_2$$

Of course

$$(p_F)_1 = 0$$

The pressure drop due to gravity is calculated from

$$(p_G)_{l+1} = (p_G)_l + 4\theta\Delta z \left(\mathcal{J}_G \right)_l + \left(\mathcal{J}_G \right)_{l+1} \quad (188)$$

where

$$\left(\mathcal{J}_G \right)_l = \left[\int_0^{\frac{1}{2}} p r dr \right]_l \quad (189)$$

is evaluated by the scheme represented by equations (107), (108), (109), and (110). Also note that

$$(p_G)_1 = 0$$

and

$$\left(\mathcal{J}_G \right)_1 = \frac{1}{8}$$

Based on the foregoing pressure terms an apparent relative friction factor may be defined as

$$\frac{\Delta p_F + \Delta p_{KE}}{(\Delta p_F + \Delta p_{KE})_w} = \frac{f_{APP}}{f_{APPW}} \quad (190)$$

where the pressure drop calculated for variable properties is compared to the pressure drop if the fluid were flowing isothermally at the wall temperature.

For the parabolic entrance profile

$$\frac{f_{APP}}{f_{APPW}} = \frac{f_{APP}}{f_w} = \frac{\Delta p_F + \Delta p_{KE}}{-32 z \mu_w / \rho_w} \quad (191)$$

For the uniform entrance profile $(\Delta p_F + \Delta p_{KE})_w$ can be evaluated from Figure 6 by using

$$z_w = z \mu_w / \rho_w \quad (192)$$

The term $\Delta p_F + \Delta p_{KE}$ can be calculated directly or by the difference

$$\Delta p_F + \Delta p_{KE} = \Delta p - \Delta p_G \quad (193)$$

when Δp_G is small compared to Δp .

A suitable approximate calculation of the term p_G can be made by

$$p_G = \theta \int_0^z \rho_M dz \quad (194)$$

Truncation Error for Finite Difference Equations

Define a truncation error by

$$E_t = [\text{Finite Difference Equation}]_{m,l} - [\text{Partial Differential Equation}]_{m,l} \quad (195)$$

This error can be determined by expanding the point values in the finite difference equation in a Taylor series as previously described. Substitution of these terms into the finite difference equations retaining the remainder terms yields the truncation error. For the equations used in

this work the following errors are obtained.

$$(E_t)_{m,\ell+1} = O(\Delta z, \Delta r^2) \quad (\text{motion}) \quad (196)$$

$$(E_t)_{m+\frac{1}{2},\ell+\frac{1}{2}} = O(\Delta z^2, \Delta r^2) \quad (\text{continuity}) \quad (197)$$

$$(E_t)_{m,\ell+1} = O(\Delta z, \Delta r^2) \quad (\text{energy}) \quad (198)$$

Hence E_t vanishes unconditionally as Δz and Δr approach zero for all the approximations used.

Stability and Convergence

After O'Brian et al.⁽⁴⁴⁾ Let \mathcal{D} represent the exact solution of the partial differential equation, Δ represent the exact solution of the difference equation, and η represent the actual numerical solution. The truncation error for convergence $(\mathcal{D} - \Delta)$ is due to the finite mesh size.* Establishing conditions under which $(\mathcal{D} - \Delta) \rightarrow 0$ is convergence analysis. The numerical error $(\Delta - \eta)$ is due to the introduction of any numerical errors in the calculation, but it is primarily due to round-off errors made by the computer. Stability of the difference equation means that $(\Delta - \eta)$ can be kept small throughout the region of interest. Hence, in order to make

$$(\mathcal{D} - \eta) \equiv (\mathcal{D} - \Delta) + (\Delta - \eta) \quad (199)$$

small, the numerical scheme must be both convergent and stable.

* Notice that this truncation error is different from E_t which is the difference equation truncation error.

The questions of stability and convergence of numerical schemes for nonlinear partial differential equations with variable coefficients are difficult if not impossible to answer. However, in order to eliminate from consideration inherently poor numerical schemes so called heuristic arguments can be employed. The argument used here to reduce the equations of motion, continuity and energy to linear equations with constant coefficients has been attributed to von Neumann.⁽⁴⁴⁾ It involves examining the numerical scheme for the equation in small subregions in which the coefficients can be considered constant and the equation linear. If errors do not grow in this subregion where they are initiated, then they are assumed to remain bounded in the overall region and the numerical scheme is considered stable. Stability has been shown for many equations to imply convergence.

With these simplifications in mind, the linearized equations of motion, continuity, and energy become

$$\alpha \frac{\partial u}{\partial r} + \beta \frac{\partial u}{\partial z} = \frac{\partial^2 u}{\partial r^2} + \gamma \quad (200)$$

$$\frac{\partial v}{\partial r} + \frac{\partial u}{\partial z} = 0 \quad (201)$$

$$\alpha^* \frac{\partial I}{\partial r} + \beta^* \frac{\partial I}{\partial z} = \frac{\partial^2 I}{\partial r^2} \quad (202)$$

If the difference equations resulting from the numerical scheme as applied to these equations are stable and convergent, the difference equations for the nonlinear variable property equations will be assumed stable and convergent. The following discussion will be restricted to linear equations

with constant coefficients.

Now consider a difference equation of the form

$$\sum_s A_s u_{m+s, l+1} = \sum_s B_s u_{m+s, l} + c \quad (203)$$

where the summations are over a finite set of neighboring points around m on $l+1$ and l respectively. Introduction of round off errors yields

$$\sum_s A_s (u_{m+s, l+1} + \delta_{m+s, l+1}) = \sum_s B_s (u_{m+s, l} + \delta_{m+s, l}) + c \quad (204)$$

If equation (203) is subtracted from equation (204), the variation equation

$$\sum_s A_s \delta_{m+s, l+1} = \sum_s B_s \delta_{m+s, l} \quad (205)$$

results.

A complete description of the von Neumann stability analysis can be found in (44), and an outline in (45), but in essence a solution to equation (205) of the form

$$\delta_{m, l} = [\xi]^l e^{i\varphi m \Delta r}, \quad i = \sqrt{-1} \quad (206)$$

is assumed. This form is substituted into the equation, and if a solution is found, a necessary and sufficient condition that the errors do now grow as z increases is that

$$|\xi| \leq 1 \quad (207)$$

for all values of ϕ .

Lax⁽⁴⁶⁾ and Richtmyer⁽⁴⁷⁾ have extended the von Neumann stability analysis to include systems of equations and in addition have established the conditions under which stability for linear equations with constant coefficients implies convergence. Bodia⁽¹⁴⁾ has applied this procedure to a system similar to equations (200), (201), and (202).

The procedure consists of considering the set of K independent variables

$$\delta_{m,l}^{(1)}, \delta_{m,l}^{(2)} \dots \delta_{m,l}^{(n)} \dots \delta_{m,l}^{(K)}$$

and a set of K linear equations of the form

$$\begin{aligned} \sum_n \sum_s A_{s,n}^{(1)} \delta_{m+s,l+1}^{(n)} &= \sum_n \sum_s B_{s,n}^{(1)} \delta_{m+s,l}^{(n)} \\ &\vdots \\ \sum_n \sum_s A_{s,n}^{(K)} \delta_{m+s,l+1}^{(n)} &= \sum_n \sum_s B_{s,n}^{(K)} \delta_{m+s,l}^{(n)} \end{aligned} \quad (208)$$

Solutions of the form

$$\delta_{m,l}^{(n)} = [\xi_n]^l e^{i\phi m \Delta r} \quad (209)$$

are assumed and substituted into this system of equations. The common term $e^{i\phi m \Delta r}$ may be cancelled out and the resulting system of equations written as

$$\underline{H}_1 \vec{g}_1 = \underline{H}_0 \vec{g}_0 \quad (210)$$

where the vectors are

$$\vec{g}_1 = \begin{bmatrix} \xi_1^{l+1} \\ \xi_2^{l+1} \\ \vdots \\ \xi_K^{l+1} \end{bmatrix} \quad \text{and} \quad \vec{g}_0 = \begin{bmatrix} \xi_1^l \\ \xi_2^l \\ \vdots \\ \xi_K^l \end{bmatrix} \quad (211)$$

Defining the amplification matrix by

$$\underline{G} = \underline{H}^{-1} \underline{H}_0 \quad (212)$$

and denoting the eigenvalues of \underline{G} by λ_n , $n = 1, 2, \dots, K$.

Lax has shown that the von Neumann necessary condition for stability is

$$|\lambda_n| \leq 1 + O(\Delta r) \quad (213)$$

If in addition, all the elements in \underline{G} are bounded for all φ and if all of the eigenvalues with the possible exception of one satisfy

$$|\lambda_n| \leq 1 \quad (214)$$

then the condition is necessary and sufficient. Lax has also established the equivalence of stability and convergence for well posed problems which satisfy the consistency conditions. For linear equations the consistency conditions require that E_t vanish as Δz and Δr approach zero.

A trivial modification of Bodia's analysis yields for the difference system,

$$\alpha \left(\frac{u_{m+1,l+1} - u_{m-1,l+1}}{2\Delta r} \right) + \beta \left(\frac{u_{m,l+1} - u_{m,l}}{\Delta z} \right) = \left(\frac{u_{m+1,l+1} - 2u_{m,l+1} + u_{m-1,l+1}}{\Delta r^2} \right) + \gamma \quad (215)$$

$$\left(\frac{v_{m+1,l+1} - v_{m,l+1}}{\Delta r} \right) + \left(\frac{u_{m+1,l+1} - u_{m+1,l} + u_{m,l+1} - u_{m,l}}{2\Delta z} \right) = 0 \quad (216)$$

$$\begin{aligned} \alpha^* \left(\frac{T_{m+1,l+1} - T_{m-1,l+1}}{2\Delta r} \right) + \beta^* \left(\frac{T_{m,l+1} - T_{m,l}}{\Delta z} \right) \\ = \left(\frac{T_{m+1,l+1} - 2T_{m,l+1} + T_{m-1,l+1}}{\Delta r^2} \right) \end{aligned} \quad (217)$$

the amplification matrix

$$\underline{G} = \begin{bmatrix} \frac{1}{1-M} & \cdot & \cdot \\ \cdot & \frac{1}{1-M^*} & \cdot \\ \frac{-\left(\frac{\Delta r}{\Delta z}\right)(e^{i\phi\Delta r} + 1)(M)}{2(1-M)(e^{i\phi\Delta r} + 1)(e^{i\phi\Delta r-1})} & \cdot & \cdot \end{bmatrix} \quad (218)$$

The eigenvalues for this matrix are

$$\lambda_1 = \frac{1}{1-M} \quad (219)$$

$$\lambda_2 = \frac{1}{1-M^*} \quad (220)$$

$$\lambda_3 = 0 \quad (221)$$

where

$$M = \left(\frac{\Delta z}{\beta \Delta r^2} \right) \left((2 \cos \phi \Delta r - 2) - i \alpha \Delta r \sin \phi \Delta r \right) \quad (222)$$

and

$$M^* = \left(\frac{\Delta z}{\beta^* \Delta r^2} \right) \left((2 \cos \phi \Delta r - 2) - i \alpha^* \Delta r \sin \phi \Delta r \right) \quad (223)$$

An examination indicates that

$$|\lambda_1| \leq 1 \quad \text{for} \quad \beta > 0$$

$$|\lambda_2| \leq 1 \quad \text{for} \quad \beta^* > 0$$

By analogy the values of β and β^* can be related to the physical problem as

$$\beta = \frac{\rho u}{\mu} \quad (224)$$

and

$$\beta^* = \frac{Pr \rho c u}{k} \quad (225)$$

and the condition of stability becomes a restriction to nonnegative axial velocities. For β and β^* negative the eigenvalues can be shown to satisfy the stability criterion if certain restrictive conditions are placed on Δz , Δr , α and α^* , but due to the physical instability of the flow for negative axial velocities this is of little interest in this problem.

Since for $\beta \neq 0$ all the elements in \underline{G} are bounded functions of ϕ , the above conditions are necessary and sufficient for stability, and since the difference formulation satisfies the consistency condition, the difference scheme is convergent.⁽⁴⁷⁾

The results of this analysis in conjunction with the excellent results of the calculations imply that the difference scheme for the non-linear, variable property equations is stable and convergent.

APPENDIX B

COMPUTER APPLICATION OF CALCULATION SCHEME

Computer and Computer Language

The calculations were made on a Burroughs B-5000 Information Processing System operated by the Rich Electronic Computer Center at the Georgia Institute of Technology. The programming language was Extended Algol 60 described in references (48) and (49). A useful general introduction to Algol can also be found in McCracken.⁽⁵⁰⁾

Outline of Computer Program

The sections in the following outline of the computer program correspond to the sections found in the COMMENT statements in the program.

SECTION (I) In this section certain declarations and initial statements required by the programming language are made. In addition, computer procedures for implementation of equations (9), (10), and (12) and for forming the elements in the matrices (59) and (82) are set up. The property equations are also specified here.

SECTION (II) In this section the input data are read into the program. The input data consist of Re , D' , T'_0 , T'_w , z , c_1 , Fr , $(\Delta z)_0$, a constant which specifies the direction of flow (-1, up; +1, down; 0, Fr read in with data), a constant which specifies the initial velocity profile (0 Poiseuille, 1 flat), a constant that specifies how the radial net is to be modified, N , and a constant which allows θ to be set equal to zero. The finite difference scheme is initiated by calculating

certain starting values.

SECTION (III) Equation (10) is solved for \bar{t} in this section.

It is then used to calculate values of ρ , μ , k and c_p .

SECTION (IV) Equations (9) and (11) are solved for \bar{u} , \bar{v} and p in this section. For the first step, the values of the radial velocities are averaged with the values at $z = 0$ and used as a better starting value for SECTION (III).

SECTION (V) In this section the values of Nu , Nu_{AM} , T_M , E_q , P_{KE} , P_F , and P_G are calculated. Δz and Δr are changed in this section if certain prescribed conditions are met. If u_1 or u_N are less than zero, the program is stopped. The program is also stopped if $z < 5$; otherwise the numerical scheme is stepped Δz and cycled to SECTION III.

This program is to be regarded as a working tool for the calculation of the results presented in this work. It is presented more as reference material, to illustrate the practical implementation of the theoretical development, than as a finished program versatile enough to fit any application efficiently. However, the basic program can be easily modified to fit special cases.

Computer Program Nomenclature

$A[]$	-	A_m	CPA	-	$c_{p_{AM}}$
$B[]$	-	B_m	CPM	-	c_{p_M}
$C[]$	-	C_m	CPW	-	c_{p_w}
C_1	-	c_1	$D[]$	-	D_m
$CP[]$	-	c_{p_m}	DIA	-	D'

DIAV	-	$D_p F$	\emptyset	-	0
DL	-	Δz	P	-	p
DLO	-	$(\Delta z)_o$	PEN	-	Pe/z^*
DR	-	Δr	PENA	-	Pe_{AM}/z^*
DUP[]	-	$D_p u_m$	PENL	-	Pe_L/z^*
ERR	-	$2E_q$	PENM	-	Pe_M/z^*
FCN	-	F_c	PF	-	p_F
FCP	-	Heat capacity function	PG	-	p_G
FKT	-	Thermal conductivity function	PKEN	-	p_{KE}
FRH \emptyset	-	Density function	PRN	-	Pr
FRN	-	Fr	QN	-	QN
FVIS	-	Viscosity function	QT	-	QT
IAV	-	\mathcal{J}_u	RATI \emptyset	-	μ_r
KT[]	-	k_m	REN	-	Re
KTa	-	k_{AM}	RH \emptyset []	-	ρ_m
KTM	-	k_M	RH \emptyset O	-	ρ'_o
KTO	-	k'_o	RH \emptyset M	-	ρ_M
KTW	-	k_w	RH \emptyset W	-	ρ_w
L	-	z	T[]	-	T_m
N	-	N	TFCTS	-	Fictitious temperature
NUAM	-	Nu_{AM}	THETA	-	θ
NULM	-	Nu_{LN}	TM	-	T_M
NUN	-	Nu	TR[]	-	T'_m
O	-	Zero	TRM	-	T'_M

TRO - T'_O

TRW - T'_W

U[] - u_m

URHØ[] - $u_m \rho_m$

UM - \bar{u}'

V[] - v_m

VIS[] - μ_m

VISM - μ_M

VISO - μ'_O

VISW - μ_w

```

BEGIN
COMMENT SECTION (I) ;
COMMENT OIL A ;
COMMENT HT TRANSFR T A VRBL PRPRTY FLD N NTRRNC F VRTCL TUB ;
INTEGER I,J,M,MM,N,NN,S,X,Z,SGN ;
REAL ARRAY DATA1,DATA2,DATA3,DATA4,DATA5,DATA6,DATA7,DATA8[1:10] ;
INTEGER ARRAY DATA9,DATA10,DATA11,DATA12,DATA13[1:10] ;
REAL ARRAY A,B,C,D,E,F,G,H,W,DUP,VIS,KT,CP,RHØ,RHØ1,U1,U,V1,V,T1,T,TR,
PENL,URHØ[1:165] ;
REAL DL,DR,REN,DIA,TRO,TRW,C1,PRN,FRN,FCN,RATIØ,CPO,KTO,VISO,RHØO,L,
PEN,PENW,PENA,PENM,NUN,NUN1,NUAM,NULM,TFCTS,P,PG,PF,TM,TRM,IAV,ID,
ID1,HM,CPM,KTM,VISM,RHØM,KTA,CPA,PRNT,DIAV,UM,THETA,P1,VISW,RHØW,
CPW,KTW,DKT,QN,QT,ERR,TM1,DLO,KTM1,FRCTN,FRCTN1,KE,KE1,PKEN ;
LABEL NXTSTP,CRRCT,CYCL,BYPSS,RDVL,EXIT ;
REAL PRØCEDURE FCP(M,CPO,TR) ;
VALUE M,CPO ;
INTEGER M ; REAL CPO ;
ARRAY TR[1] ;
FCP←(0.15780+(5.31579@-4)*TR[M])/CPO ;
REAL PRØCEDURE FRHØ(M,RHØO,TR) ;
VALUE M, RHØO ;
INTEGER M ; REAL RHØO ;
ARRAY TR[1] ;
FRHO←(67.70978-(2.22667@-2)*TR[M])/RHØO ;

```



```

REAL PROCEDURE FKT(M,KTO,TR) ;
VALUE M,KTO ;
INTEGER M ; REAL KTO ;
ARRAY TR[1] ;
FKT←(0.085994-(2.19474@-5)*TR[M])/KTO ;
REAL PROCEDURE FVIS(M,VISO,TR) ;
VALUE M,VISO ;
INTEGER M ; REAL VISO ;
ARRAY TR[1] ;
FVIS←(((1.6274@-6)*EXP((4.9202@3)/TR[M])+(2.4605@-13)*EXP((1.3624@4)/
TR[M]))*3600)/VISO ;
PROCEDURE TOM(N,A,B,C,D,W,G,Y) ;
VALUE N ;
INTEGER N ;
ARRAY A,B,C,D,W,G,Y[1] ;
BEGIN INTEGER M ;

W[1]←A[1] ;
FOR M←2 STEP 1 UNTIL N DO W[M]←A[M]-(C[M]*B[M-1])/W[M-1] ;
G[1]←D[1]/W[1] ;
FOR M←2 STEP 1 UNTIL N DO G[M]←(D[M]-C[M]*G[M-1])/W[M] ;
Y[N]←G[N] ;
FOR M←N-1 STEP -1 UNTIL 1 DO Y[M]←G[M]-(B[M]*Y[M+1])/W[M] ;
END ;

```

```

PROCEDURE NTGRL(N,DR,RHØ,H,F,K) ;

VALUE N,DR ;
ARRAY RHØ,H,F[1] ;
BEGIN INTEGER M ;

K←0.0 ;
FOR M←1 STEP 2 UNTIL N-3 DØ K←K+(DR/3)×(F[M]×RHØ[M]×H[M]+4×F[M+
1]×RHØ[M+1]×H[M+1]+F[M+2]×RHØ[M+2]×H[M+2]) ;
K←K+(DR/24)×(F[N-3]×RHØ[N-3]×H[N-3]-5×F[N-2]×RHØ[N-2]×H[N-2]+
19×F[N-1]×RHØ[N-1]×H[N-1]+9×F[N]×RHØ[N]×H[N]) ;
K←K+(DR/720)×(-19×F[N-3]×RHØ[N-3]×H[N-3]+106×F[N-2]×RHØ[N-2]×H[N-2]-246×
F[N-1]×RHØ[N-1]×H[N-1]+646×F[N]×RHØ[N]×H[N]+251×F[N+1]×RHØ[N+1]×H[N+1]) ;
END ;

PROCEDURE CFFCNTS(N,DR,G,H,W,F,A,B,C) ;

VALUE N,DR ;
INTEGER N ; REAL DR ;
ARRAY G,H,W,F,A,B,C[1] ;
BEGIN INTEGER M ;

A[1]←G[1]+2×H[1] ;
B[1]←-2×H[1] ;
FOR M←2 STEP 1 UNTIL N DØ BEGIN A[M]←G[M]+H[M] ;
B[M]←-H[M]×(0.5+(0.25×DR/F[M]))-0.125×H[M+1]+0.125×H[M-1]+W[M] ;

```

```

C[M]←-H[M]×(0.5-(0.25×DR/F[M]))+0.125×H[M+1]-0.125×H[M-1]-W[M]      ;
END                                                                           ;
END                                                                           ;
FILE IN CARD (1,10)                                                         ;

FILE ØUT PRINT 1 (1,15)                                                     ;
LIST LST1(REN,PRN,DR,DL,FRN,SGN,FCN,RATIØ,DIA,TRO,TRW,CPO,KTO,VISO,      ;
RHØØ,C1,S,X)                                                                ;
LIST LST2(L,PEN,PENW,PENA,PENM,NUN,NUAM,PKEN,TFCTS,P,PG,PF,TM,TRM,      ;
IAV,ERR)                                                                    ;
LIST LST3(F[M],U[M],V[M],T[M],TR[M],URHO[M],PENL[M])                      ;
FØRMAT ØUT FMT1("REN=",E14.7,X5,"PRN=",E14.7,X5,"DR=",E14.7,X5,"DL=",
E14.7,X5,"FRN=",E14.7/X5,"SGN=",I2,X5,"FCN=",E14.7,X5,"RATIØ=",E14.7,X5.
"DIA=",E14.7,X5,"TRO=",E14.7/X5,"TRW=",E14.7,X5,"CPO=",E14.7,X5,"KTO=",
E14.7,X5,"VISO=",E14.7,X5,"RHØØ=",E14.7/X5,"C1=",E14.7,X5,"S=",I2,X5,
"X=",I2,X5,"ZERØ PARA"//)                                                  ;

FØRMAT ØUT FMT2("L=",E14.7,X5,"PEN=",E14.7,X5,"PENW=",E14.7,
X5,"PENA=",E14.7,X5,"PENM=",E14.7/X5,"NUN=",E14.7,X5,"NUAM=",E14.7,X5,
"PKEN=",E14.7,X5,"TFCTS=",E14.7,X5,"P=",E14.7/X5,"PG=",E14.7,X5,"PF=",E14.7,
X5,"TM=",E14.7,X5,"TRM=",E14.7,X5,"IAV=",E14.7/X5,"ERR=",E14.7//)        ;
FØRMAT ØUT FMT3(E14.7,E14.7,E14.7,F13.9,E14.7,E14.7,E14.7//)            ;

FØRMAT ØUT HEAD(X5,"R",X13,"U",X13,"V",X13,"T",X13,"TR",X13,"URHØ",

```

```

X13,"PENL"/) ;
COMMENT SECTION (II) ;
READ (CARD,/,NN) ;

READ (CARD,/,FOR M+1 STEP 1 UNTIL NN DØ [DATA1[M],DATA2[M],DATA3[M],
DATA4[M],DATA5[M],DATA6[M],DATA7[M],DATA8[M],DATA9[M], DATA10[M],
DATA11[M],DATA12[M],DATA13[M]]) ;
CLOSE (CARD,RELEASE) ;

FOR MM+1 STEP 1 UNTIL NN DØ
BEGIN
REN+DATA1[MM] ;
DIA+DATA2[MM] ;
TRO+DATA3[MM] ;
TRW+DATA4[MM] ;
DL+DATA5[MM] ;
C1+DATA6[MM] ;
FRN+DATA7[MM] ;
DLO+DATA8[MM] ;
SGN+DATA9[MM] ;
X+DATA10[MM] ;
S+DATA11[MM] ;

N+DATA12[MM] ;
I+DATA13[MM] ;

L+DL ;

```

```

DR←0.5/N ;
ID1←0.125 ;
PG←0.0 ;
TM1←0.0 ;
KTM1←1.0 ;
NUN1←0.0 ;
P-P1←0.0 ;
KE1←FRCTN1←PF←PKEN←0.0 ;
J←1 ;

Z←0 ;
V1[N+1]←V[N+1]←U1[N+1]←U[N+1]←0.0 ;
FOR M←1 STEP 1 UNTIL N DO BEGIN TR[M]←TRO ;
T1[M]←T[M]←V1[M]←V[M]←0.0 ;
END ;
TR[N+1]←TRW ;
T[N+1]←1.0 ;
CPO←KTO←VISO←RHØO←1.0 ;
M←1 ;
CPO←FCP(M,CPO,TR) ;
KTO←FKT(M,KTO,TR) ;
VISO←FVIS(M,VISO,TR) ;
RHØO←FRHO(M,RHØO,TR) ;
M←N+1 ;
CPW←FCP(M,CPO,TR) ;
KTW←FKT(M,KTO,TR) ;

```



```

VISW←FVIS(M,VISO,TR) ;
RHØW←FRHO(M,RHØO,TR) ;
FØR M←1 STEP 1 UNTIL N+1 DØ F[M]←(M-1)×DR ;

PRN←VISO×CPO/KTO ;

UM←REN×VISO/(DIA×RHØO×3600.0) ;
IF SGN ≠ 0 THEN
FRN←SGN×UM×UM/(32.17×DIA) ;
PEN←PRN/DL ;
RATIØ←1.0/VISW ;
THETA←REN×I/FRN ;
FCN←2.0×THETA×(RHØW-1.0)/(RHØW+1.0) ;
WRITE(PRINT,FMT1,LST1) ;
FØR M←1 STEP 1 UNTIL N+1 DØ BEGIN CP[M]←FCP(M,CPO,TR) ;
KT[M]←FKT(M,KTO,TR) ;
VIS[M]←FVIS(M,VISO,TR) ;
RHØ[M]←RHØ1[M]←FRHØ(M,RHØO,TR) ;
END ;

DKT←0.0 ;
IF X=0 THEN BEGIN FØR M←1 STEP 1 UNTIL N DØ U1[M]←2.0×(1.0-4×F[M]×F[M]) ;
FRCTN1←-8.0 ;
GØ TØ NXTSTP ;
END ;
FØR M←1 STEP 1 UNTIL N DØ BEGIN U1[M]←U[M]←1.0 ;
V1[M]←V[M]←0.0 ;
END ;

```

```

COMMENT SECTION (III) ;
NXTSTP: PEN←PRN/L ;
CRRCT: ;
FOR M←1 STEP 1 UNTIL N+1 DO BEGIN G[M]←RHØ[M]×CP[M]×PRN×U1[M]/DL ;
H[M]←2×KT[M]/(DR×DR) ;
W[M]←RHØ[M]×CP[M]×PRN×V1[M]/(2×DR) ;
END ;
IF Z=0 THEN
IF J=1 THEN H[N+1]←H[N-1] ;
CFFCNTS(N,DR,G,H,W,F,A,B,C) ;
FOR M←1 STEP 1 UNTIL N DO D[M]←G[M]×T1[M] ;
D[N]←D[N]-B[N]×T[N+1] ;
B[N]←0.0 ;
C[N+1]←1-DKT×DR×DR-DR ;
A[N+1]←1+DKT×DR×DR+DR ;
D[N+1]←2 ;
N←N+1 ;
TØM(N,A,B,C,D,W,G,T) ;
N←N-1 ;
FOR M←1 STEP 1 UNTIL N DO TR[M]←T[M]×(TRW-TRO)+TRO ;
FOR M←1 STEP 1 UNTIL N DO BEGIN CP[M]←FCP(M,CPO,TR) ;
KT[M]←FKT(M,KTO,TR) ;
VIS[M]←FVIS(M,VISO,TR) ;
RHØ[M]←FRHØ(M,RHØO,TR) ;
END ;

```

```

T[N+2]←T[N+1] ;
T[N+1]←1.0 ;
TR[N+2]←T[N+2]×(TRW-TRO)+TRO ;
KT[N+2]←FKT(N+2,KTO,TR) ;
DKT←(3×KT[N+1]-4×KT[N]+KT[N-1])/(4×KT[N+1]×DR×DR) ;
CØMMENT SECTION (IV) ;
FØR M←1 STEP 1 UNTIL N+1 DØ BEGIN G[M]←RHØ[M]×U1[M]/DL ;
H[M]←2×VIS[M]/(DR×DR) ;
W[M]←RHØ[M]×V1[M]/(2×DR) ;
E[M]←-1.0/DL ;
END ;
CFFCNTS(N,DR,G,H,W,F,A,B,C) ;
I←1 ;
CYCL: FØR M←1 STEP 1 UNTIL N DØ D[M]←E[M]×(P-P1-RHØ[M]×U1[M]×U1[M1])+ ;
THETA×RHØ[M] ;
TØM(N,A,B,C,D,W,G,U) ;
NTGRL(N,DR,RHØ,U,F,IAV) ;
IF I≥2 THEN GØ TØ RDVL ;
TØM(N,A,B,C,E,W,G,DUP) ;
DUP[N+1]←0.0 ;
NTGRL(N,DR,RHØ,DUP,F,DIIV) ;
P←P+(0.125-IAV)/DIIV ;
I←I+1 ;
GØ TØ CYCL ;
RDVL: V[1]←0.0 ;
V[2]←-(DR/(4×DL))×(U[2]-RHØ1[2]×U1[2]/RHØ[2]+RHØ[1]×U[1]/RHØ[2]- ;
RHØ1[1]×U1[1]/RHØ[2]) ;

```

```

FOR M=2 STEP 1 UNTIL N DO V[M+1]←F[M]×RHØ[M]×V[M]/(F[M+1]×RHØ[M+1]) -
(DR/(2×DL))×(U[M+1]-RHØ1[M+1]×U1[M+1]/RHØ[M+1]+F[M]×RHØ[M]×U[M]/(F[M+
1]×RHØ[M+1]))-F[M]×RHØ1[M]×U1[M]/(F[M+1]×RHØ[M+1]))
;
IF Z=0 THEN BEGIN
J←J+1
;
IF J<3 THEN BEGIN FOR M=1 STEP 1 UNTIL N DO V1[M]←V[M]
;
GO TO CRRCT
;
END
;
IF X≠0 THEN
FOR M=1 STEP 1 UNTIL N DO V[M]←V[M]/2.0
;
END
;
COMMENT SECTION (V)
;
FOR M=1 STEP 1 UNTIL N+1 DO BEGIN URHØ[M]←RHØ[M]×U[M]
;
PENL[M]←PEN×CP[M]/KT[M]
;
H[M]←U[M]×(T[M]+(C1×(TRW-TRO)/(2×CPO))×T[M]×T[M])
;
END
;
NTGRL(N,DR,RHØ,H,F,HM)
;
IF C1>0.0 THEN
TM←(-CPO+SQRT(CPO×CPO+2×C1×(TRW-TRO)×CPO×8×HM))/(C1×(TRW-TRO))
ELSE
TM←8×HM
;
FOR M=1 STEP 1 UNTIL N+1 DO H[M]←1.0
;
NTGRL(N,DR,RHO,H,F,ID)
;
PG←PG+THETA×4.0×DL×(ID+ID1)
;
H[1]←(U1[1]×(U[1]-U1[1]))/DL
;
FOR M=2 STEP 1 UNTIL N DO
H[M]←(V1[M]×(U[M+1]-U[M-1]))/(2×DR)+(U1[M]×(U[M]-U1[M]))/DL
;

```

```

H[N+1]←0.0 ;
NTGRL(N,DR,RHØ,H,F,KE) ;
PKEN←PKEN-8×DL×KE ;
FRCTN←VISW×((3×U[N+1]-4×U[N]+U[N-1])/(2×DR)) ;
IF (X≠0) AND (Z=0) THEN FRCTN1←FRCTN ;
PF←PF+2×DL×(FRCTN1+FRCTN) ;
TRM←TM×(TRW-TRO)+TRO ;
TR[N+3]←TRM ;
TR[N+4]←(TRO+TRM)×0.5 ;
CPM←CP[N+3]←FCP(N+3,CPO,TR) ;
KTM←KT[N+3]←FKT(N+3,KTO,TR) ;
VISM←VIS[N+3]←FVIS(N+3,VISO,TR) ;
RHØM←RHØ[N+3]←FRHØ(N+3,RHØO,TR) ;
KTA←KT[N+4]←FKT(N+4,KTO,TR) ;
CPA←CP[N+4]←FCP(N+4,CPO,TR) ;
PENW←PEN×CPW/KTW ;
PENM←PEN×CPM/KTM ;
PENA←PEN×CPA/KTA ;
NUN←KTW×(T[N+2]-T[N])/(2×DR×KTM×(1-TM)) ;
NUAM←4×PEN×HM/(KTA×(2-TM)) ;
QT←(TM-TM1+(C1×(TRW-TRO)×0.5/CPO)×(TM×TM-TM1×TM1))/8 ;
QN←(DL×((1-TM1)×NUN1×KTM1+(1-TM)×NUN×KTM))/(4×PRN) ;
ERR←2×(QN-QT)/(QN+QT) ;
TFCTS←T[N+2] ;
WRITE(PRINT,FMT2,LST2) ;
IF (Z-2×ENTIER(Z/2))<0.5 THEN

```



```

BEGIN
WRITE (PRINT,HEAD) ;
FOR M←1 STEP N DIV 20 UNTIL N-(N DIV 20)+1,N DO
BEGIN IF T[M] < 1@-45 THEN T[M]←0 ;
WRITE(PRINT,FMT3,LST3) ;
END ;
END ;
IF Z=0 THEN DL←DLO ;
IF Z>0 THEN
IF ((ABS((TM-TM1)/TM1)<0.05) AND (TM≤0.6)) OR ((ABS((TM-TM1)/TM1)≤0.005)
AND (TM>0.6)) THEN
DL←1.5×DL ;
IF L≥(10.0*(S-4)) THEN BEGIN S←S+1 ;
IF N>20 THEN BEGIN N←N DIV 2 ;
DR←0.5/N ;
FOR M←1 STEP 1 UNTIL N+1 DO BEGIN I←2×M-1 ;
U[M]←U[I] ;
U1[M]←U1[I] ;
V[M]←V[I] ;
V1[M]←V1[I] ;
T[M]←T[I] ;
T1[M]←T1[I] ;
TR[M]←TR[I] ;
CP[M]←CP[I] ;
KT[M]←KT[I] ;
VIS[M]←VIS[I] ;
RHØ[M]←RHØ[I] ;

```

```

RHØ1[M]←RHØ1[I] ;
F[M]←(M-1)×DR ;
END ; END ; END ;
P1←P ;

KE1←KE ;
FRCTN1←FRCTN ;
TM1←TM ;
KTM1←KTM ;
NUN1←NUN ;
ID1←ID ;
FØR M←1 STEP 1 UNTIL N+1 DØ BEGIN U1[M]←U[M] ;
V1[M]←V[M] ;
T1[M]←T[M] ;
RHØ1[M]←RHØ[M] ;
END ;
IF (U[1]<0.0) ØR (U[N] <0.0) THEN GØ TØ EXIT ;
IF PEN >5.0 THEN BEGIN Z←Z+1 ;
L←L+DL ;
GØ TØ NXTSTP ;
END ;
EXIT: ;
END ;
END.

```

APPENDIX C

EMPIRICAL PROPERTY EQUATIONS

This appendix contains the empirical equations used to describe the physical properties of the fluids studied. The equations for air, helium, water, and oil A are the same as those used by Lee.⁽¹⁾ However, one of the constants in the equation for the viscosity of helium appeared to be a typographical error and had to be empirically adjusted. The data for n-octane was taken from references (51) and (52). It was fitted by the equations given. In selecting materials for study, primary emphasis was placed on accurate density and viscosity data due to the relative importance of these properties. The equations fit the data within approximately one per cent.

Oil A*

$$\rho' = 67.70978 - 2.22667 \times 10^{-2} T' \quad (\text{lb/ft}^3, ^\circ\text{R})$$

$$c_p' = 0.15780 + 5.31579 \times 10^{-4} T' \quad (\text{Btu/lb-}^\circ\text{R}, ^\circ\text{R})$$

$$k' = 0.085994 - 2.19474 \times 10^{-5} T' \quad (\text{Btu/ft-hr-}^\circ\text{R}, ^\circ\text{R})$$

$$\mu' = 1.6274 \times 10^{-6} \exp(4.9202 \times 10^3/T') + 2.4605 \times 10^{-13} \exp(1.3624 \times 10^4/T') \quad (\text{lb/ft-sec}, ^\circ\text{R})$$

Water

$$\rho' = 46.85311 + 6.55268 \times 10^{-2} T' - 6.875 \times 10^{-5} T'^2 \quad (\text{lb/ft}^3, ^\circ\text{R})$$

$$c_p' = 1.000 \quad (\text{Btu/lb} - ^\circ\text{R})$$

$$k' = -0.49958 + 2.58911 \times 10^{-3} T' - 1.875 \times 10^{-6} T'^2 \quad (\text{Btu/ft-hr-}^\circ\text{R}, ^\circ\text{R})$$

$$\frac{1}{\mu'} = 2.1482 \left[(T' - 8.435) + \sqrt{8078.4 + (T' - 8.435)^2} \right] - 120 \quad (\text{poises}, ^\circ\text{C})$$

n-Octane

$$\rho' = 56.911107 - 2.088306 \times 10^{-2} T' - 7.1951738 \times 10^{-6} T'^2 \quad (\text{lb/ft}^3, ^\circ\text{R})$$

$$c_p' = 0.3234 + 3.80 \times 10^{-4} T' \quad (\text{Btu/lb-}^\circ\text{R}, ^\circ\text{R})$$

$$k' = 0.083 - 0.313 \times 10^{-4} (T' - 545.59) \quad (\text{Btu/ft-hr-}^\circ\text{R}, ^\circ\text{R})$$

$$\mu' = \exp(-5.818039 + 4.7222354 \times 10^3/T' - 1.61711622 \times 10^6/T'^2 + 3.0491151 \times 10^8/T'^3) \quad (\text{lb/ft-hr}, ^\circ\text{R})$$

*This oil was used by Martinelli et al.⁽²⁾ in their experiments.

Air

$$\rho' = 39.667215/T' \quad (\text{lb/ft}^3, \text{ } ^\circ\text{R})$$

$$c_p' = 0.22369358 = 2.6278162 \times 10^{-5} T' \quad (\text{Btu/lb-}^\circ\text{R})$$

$$k' = 1.002167 \times 10^{-3} + 2.8649806 \times 10^{-5} T' - 4.2876644 \times 10^{-9} T'^2$$

$$(\text{Btu/ft-hr-}^\circ\text{R}, \text{ } ^\circ\text{R})$$

$$\mu' = \frac{2.63142 \times 10^{-3} (T')^{1.5}}{(T' + 198.74)} \quad (\text{lb/ft-hr}, \text{ } ^\circ\text{R})$$

Helium

$$\rho' = 5.468830/T' \quad (\text{lb/ft}^3, \text{ } ^\circ\text{R})$$

$$c_p' = 1.242 \quad (\text{Btu/lb-}^\circ\text{R})$$

$$k' = 0.03383724 = 1.0399225 \times 10^{-4} T' - 1.25 \times 10^{-8} T'^2 \quad (\text{Btu/ft-hr-}^\circ\text{R}, \text{ } ^\circ\text{R})$$

$$\mu' = \frac{2.63142 \times 10^{-2} (T')^{1.5}}{(T' + 131.25)} \quad (\text{lb/ft-hr}, \text{ } ^\circ\text{R})$$

APPENDIX D

CALCULATED CONSTANT PROPERTY
FLUID FLOW AND HEAT TRANSFER RESULTS

This appendix contains the numerical values from which Figures 2, 6, 8, 9, and 10 were constructed along with additional similar calculations which were not convenient to include in the above figures.

Table 4. Constant Property Axial Velocity Calculations
Entrance Profile: Uniform

$\left(\frac{z^*}{Re}\right) \times 10^2$	r'/R'							
	0	0.2	0.4	0.6	0.7	0.8	0.9	0.95
0.0020	1.033	1.033	1.033	1.033	1.033	1.033	1.033	1.033
0.0050	1.052	1.052	1.052	1.052	1.052	1.052	1.051	0.935
0.0100	1.071	1.071	1.071	1.071	1.071	1.071	0.805	0.805
0.0147	1.083	1.038	1.038	1.038	1.038	1.038	1.043	0.731
0.207	1.098	1.098	1.098	1.098	1.098	1.097	1.014	0.658
0.0247	1.106	1.106	1.106	1.106	1.106	1.055	0.999	0.623
0.0497	1.146	1.146	1.146	1.146	1.146	1.131	0.872	0.499
0.1037	1.205	1.205	1.205	1.205	1.198	1.112	0.731	0.398
0.3037	1.339	1.339	1.338	1.308	1.215	0.980	0.565	0.298
0.6077	1.470	1.469	1.455	1.337	1.166	0.884	0.490	0.256
0.7997	1.535	1.532	1.502	1.335	1.141	0.851	0.466	0.243
1.0237	1.601	1.593	1.540	1.330	1.119	0.824	0.448	0.233
1.4077	1.690	1.672	1.581	1.319	1.091	0.793	0.427	0.221
1.7277	1.749	1.722	1.604	1.311	1.075	0.776	0.416	0.215
2.1117	1.805	1.767	1.623	1.304	1.062	0.762	0.407	0.210
2.4957	1.847	1.801	1.636	1.298	1.052	0.752	0.401	0.207
3.0077	1.890	1.834	1.648	1.293	1.042	0.742	0.394	0.203
3.5197	1.919	1.857	1.656	1.289	1.036	0.736	0.390	0.201
4.0317	1.940	1.873	1.662	1.286	1.031	0.731	0.387	0.199
4.5437	1.955	1.885	1.667	1.284	1.028	0.728	0.385	0.198
5.0557	1.967	1.894	1.670	1.282	1.025	0.726	0.384	0.197
6.0791	1.981	1.905	1.673	1.281	1.022	0.723	0.382	0.196
7.1037	1.989	1.911	1.676	1.280	1.021	0.721	0.380	0.196

Table 5. Constant Property Heat Transfer Calculations
Entrance Profile: Parabolic

Pe/z^*	Nu	Nu_{LN}	T_M
10000	22.5	33.6	0.0134
5000	17.7	26.6	0.0210
2059	13.0	19.6	0.0374
1000	10.2	15.3	0.0595
714	9.09	13.7	0.0737
360	7.26	10.8	0.1133
207	6.10	9.02	0.1598
101	4.96	7.16	0.2460
49.0	4.18	5.75	0.3745
20.9	3.73	4.65	0.5889
10.5	3.66	4.10	0.7908
6.82	3.66	3.85	0.8953

Table 6. Constant Property Heat Transfer Calculations
Entrance Profile: Uniform
Prandtl Number: 0.1

Pe/z^*	Nu	NU_{LN}	T_M
10000	78.8	84.3	0.0331
5000	33.9	63.8	0.0497
2000	20.9	41.3	0.0792
1000	15.3	29.4	0.1111
690	13.0	24.7	0.1333
339	9.65	17.7	0.1887
202	7.85	14.0	0.2427
101	6.10	10.4	0.3388
58.3	5.18	8.35	0.4362
21.0	4.27	5.88	0.6735
10.1	4.00	4.91	0.8563
4.97	3.81	4.29	0.9684

Table 7. Constant Property Heat Transfer Calculations
Entrance Profile: Uniform
Prandtl Number: 0.7

Pe/z^*	Nu	Nu_{LN}	T_M
40000	73.5	162	0.0161
15555	42.1	100	0.0255
10370	35.2	80.2	0.0305
5090	25.9	54.8	0.0421
2074	17.4	34.9	0.0651
1033	12.9	25.0	0.0919
701	10.9	20.8	0.1116
380	8.51	15.7	0.1518
199	6.63	11.8	0.2105
99.4	5.23	8.78	0.2977
49.7	4.32	6.72	0.4179
19.8	3.76	5.02	0.6357
10.6	3.67	4.34	0.8049
7.64	3.66	4.08	0.8816

Table 8. Constant Property Heat Transfer Calculations
Entrance Profile: Uniform
Prandtl Number: 1

Pe/z^*	Nu	Nu_{LN}	T_M
40000	62.3	166	0.0165
16666	41.3	100	0.0238
10000	33.1	75.6	0.0298
5128	24.8	53.1	0.0405
2020	16.5	33.2	0.0636
1005	12.2	23.7	0.0900
696.8	10.5	19.9	0.1083
379.5	8.23	15.1	0.1474
192.4	6.38	11.2	0.2080
96.9	5.07	8.44	0.2941
48.6	4.23	6.50	0.4139
19.0	3.72	4.87	0.6405
10.1	3.66	4.25	0.8131
5.70	3.66	3.9	0.9367
1.05	3.66	2.38	0.9998

Table 9. Constant Property Heat Transfer Calculations
Entrance Profile: Uniform
Prandtl Number: 5

Pe/z^*	Nu	Nu_{LN}	T_M
40000	76.1	143	0.0142
15385	31.6	96.0	0.0246
10526	26.6	75.5	0.0283
5000	19.6	48.4	0.0380
2083	13.9	29.9	0.0588
1000	10.5	20.7	0.0795
694	9.14	17.4	0.0954
357	7.19	12.9	0.134
212	6.03	10.3	0.177
105	4.91	7.82	0.257
52.3	4.19	6.12	0.374
20.1	3.72	4.69	0.608
10.4	3.66	4.15	0.796
7.0	3.66	3.94	0.894
4.9	3.66	3.81	0.955

Table 10. Constant Property Heat Transfer Calculations
 Entrance Profile: Uniform
 Prandtl Number: 10

Pe/z^*	Nu	Nu_{LN}	T_M
48192	46.4	160	0.0130
14981	29.1	77.7	0.0200
10554	25.4	63.3	0.0230
5031	18.9	42.3	0.0422
1989	13.2	26.5	0.0264
1017	10.2	19.3	0.0729
698	8.93	16.2	0.0887
387	7.26	12.6	0.1219
199	5.88	9.62	0.1754
104	4.92	7.55	0.2520

Table 11. Constant Property Heat Transfer Calculations
Entrance Profile: Uniform
Prandtl Number: 100

Pe/z^*	Nu	Nu_{LN}	T_M
42105	35.6	114	0.0108
15686	24.9	61.7	0.0156
10025	21.2	47.9	0.0189
5108	16.3	34.2	0.0264
2067	12.3	22.2	0.0421
1038	9.95	16.6	0.0620
503	8.63	11.5	0.0873
347	7.39	10.3	0.112
208	6.19	8.87	0.157
103	5.01	7.14	0.241
50.2	4.21	5.77	0.368
20.1	3.73	4.60	0.599
10.3	3.66	4.10	0.795
6.7	3.66	3.86	0.901

APPENDIX E

COMPARISON CONDITIONS AND COMPARISON RESULTS

Tables 12, 13, and 14 of this appendix give the flow and thermal conditions of the fluids which were compared for correlation purposes. These conditions were used for both parabolic and uniform entrance velocity cases. Additional comparisons used to justify the correlation scheme are shown in Figures 40 through 61.

Table 12. Conditions for Variable Property Comparison*
Calculations for Water

	Fc	μ_r	T'_o , °R	T'_w , °R	Pr	Re/Fr
Water	200	2.5	540.0	640.4	5.90	-7.52×10^3
	200	2.5	573.0	699.1	3.92	-4.52×10^3
	200	2.5	556.0	667.8	4.78	-5.82×10^3
	0.1	3.4	540.0	691.0	5.90	-2.10
	400	3.4	540.0	691.0	5.90	-8.45×10^3
	-100	2	540.0	610.0	5.90	6.50×10^3
	0.1	2	540.0	610.0	5.90	-6.50
	200	2	540.0	610.0	5.90	-1.30×10^4
	800	2	540.0	610.0	5.90	-5.21×10^4
	0.1	2	506.4	559.0	10.0	-15.3
	400	2	506.4	559.0	10.0	-6.14×10^4
	800	2	506.4	559.0	10.0	-1.23×10^5
	0.1	2	552.3	630.0	5.00	-5.03
	200	2	552.3	630.0	5.00	-1.00×10^4
	400	2	552.3	630.0	5.00	-2.00×10^4
	800	2	552.3	630.0	5.00	-4.01×10^4
	0.1	0.5	610.0	540.0	2.73	6.51
	200	0.5	610.0	540.0	2.73	1.3×10^4
	800	0.5	610.0	540.0	2.73	5.21×10^4

* Various of the values in this table were used with pseudo Prandtl numbers as explained in the text.

Table 13. Conditions for Variable Property Comparison*
Calculations for Air, Helium, n-Octane

	Fc	μ_r	T'_o , °R	T'_w , °R	Pr	Re/Fr
Air	0.1	1.5	1000.0	565.0	0.684	1.80×10^{-1}
	200	1.5	1000.0	565.0	0.684	3.60×10^2
	800	1.5	1000.0	565.0	0.684	1.44×10^3
	0.1	0.667	500.0	734.0	0.699	-1.85×10^{-1}
	200	0.667	500.0	734.0	0.699	-3.71×10^2
	800	0.667	500.0	734.0	0.699	-1.48×10^3
Helium	0.1	1.5	1460.0	752.0	0.721	1.56×10^{-1}
	200	1.5	1460.0	752.0	0.721	3.13×10^2
	800	1.5	1460.0	752.0	0.721	1.24×10^3
	0.1	0.667	752.0	1460.0	0.727	-1.56×10^{-1}
	200	0.667	752.0	1460.0	0.727	-3.12×10^2
	800	0.667	752.0	1460.0	0.727	-1.25×10^3
n-Octane	0.1	10	392.0	713.0	28.0	-4.65×10^{-1}
	800	10	392.0	713.0	28.0	-3.72×10^3
	0.1	2.0	497.6	609.7	10.0	-1.34×10^{-1}
	800	2.0	497.6	609.7	10.0	-1.07×10^4
	0.1	0.5	641.9	518.8	5.0	1.18
	800	0.5	641.9	518.8	5.0	9.44×10^3
	0.1	0.1	713.0	392.0	4.0	4.65×10^{-1}
	800	0.1	713.0	392.0	4.0	3.72×10^3

* Various of the values in this table were used with pseudo Prandtl numbers as explained in the text.

Table 14. Conditions for Variable Property Comparison*
Calculations for Oil A

	Fc	μ_r	$T'_o, ^\circ R$	$T'_w, ^\circ R$	Pr	Re/Fr
Oil A	0.1	10	550.0	671.0	583	-2.00
	800	10	550.0	671.0	583	-1.61×10^4
	0.1	5	540.0	602.6	800	-3.92
	0.1	5	565.0	649.2	384	-3.07
	0.1	5	589.0	700.3	324	-2.20
	0.1	3.4	610.0	701.0	153	-2.62
	400	3.4	610.0	701.0	153	-1.05×10^4
	-100	2.0	550.0	575.0	583	9.90×10^3
	0.1	2.0	550.0	575.0	583	-9.90
	200	2.0	550.0	575.0	583	-1.98×10^4
	800	2.0	550.0	575.0	583	-7.94×10^4
	0.1	0.5	575.0	550.0	302	9.90
	200	0.5	575.0	550.0	302	1.98×10^4
	800	0.5	575.0	550.0	302	7.94×10^4
	0.1	0.1	671.0	550.0	68.9	2.00
	800	0.1	671.0	550.0	68.9	1.61×10^4

* Various of the values in this table were used with pseudo Prandtl numbers as explained in the text.

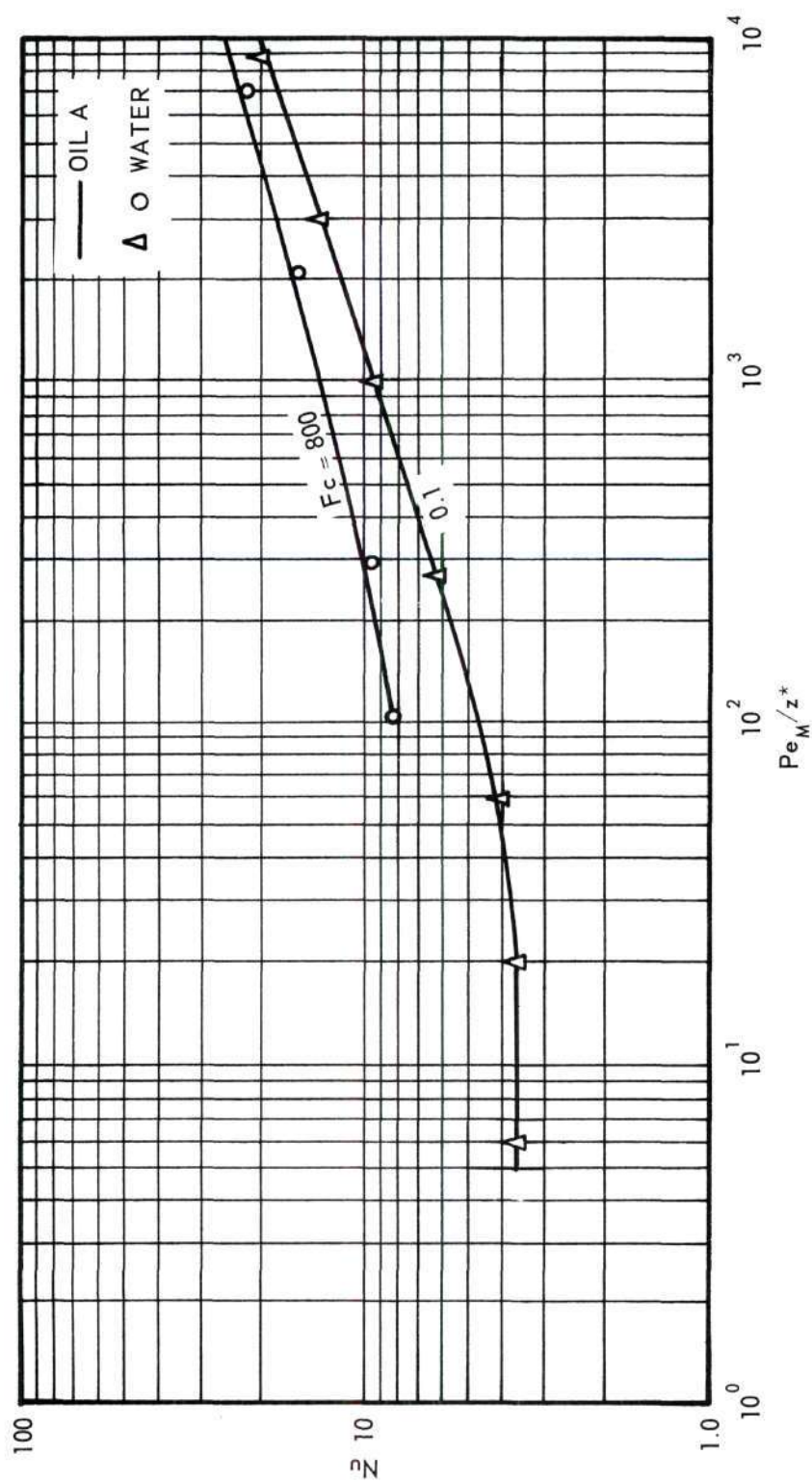


Figure 40. Comparison of Variable Property Local Nusselt Number Calculations for Oil A and Water. Entrance Profile: Parabolic. Viscosity Ratio: 0.5.

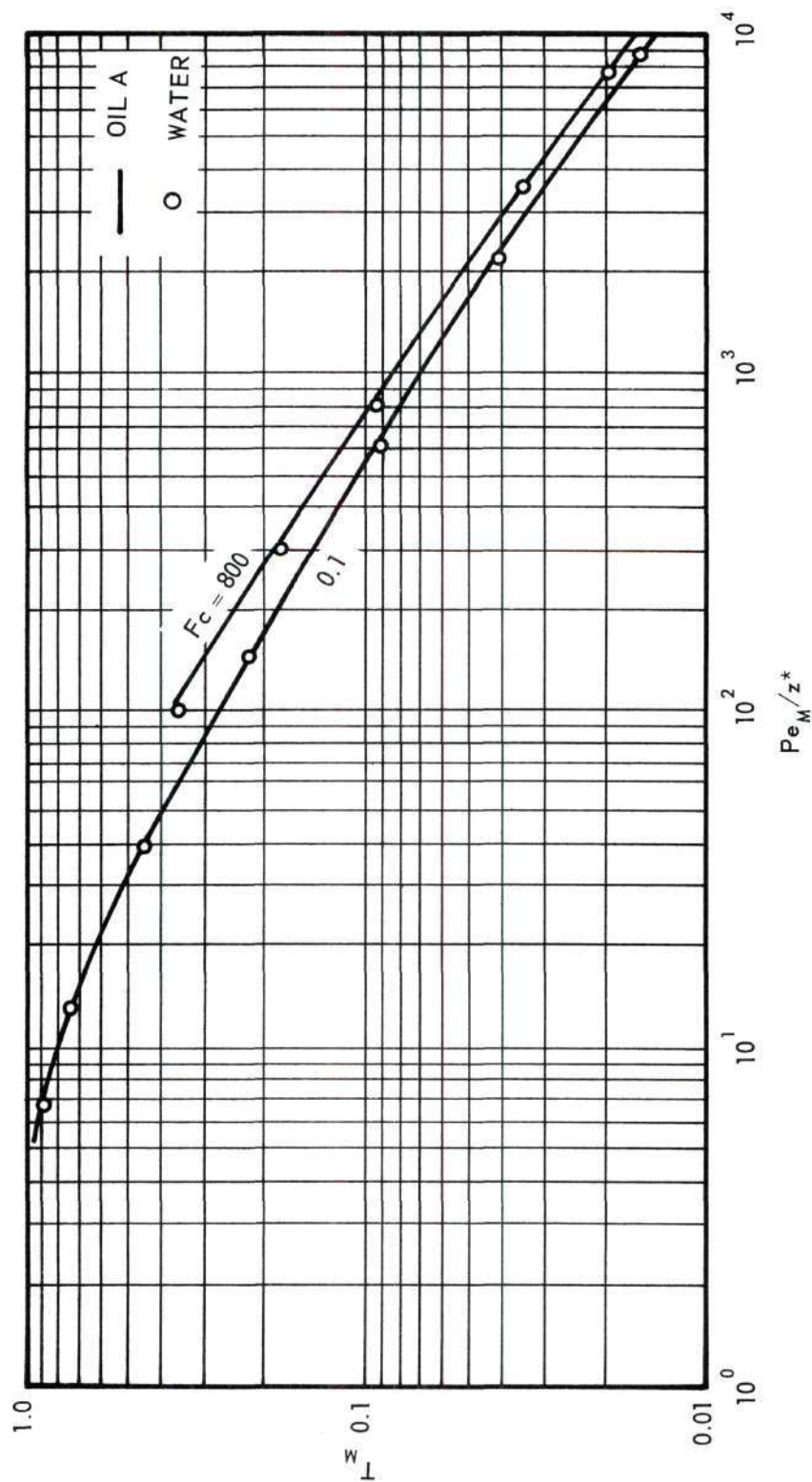


Figure 41. Comparison of Variable Property Mean Temperature Calculations for Oil A and Water.
Entrance Profile: Parabolic.
Viscosity Ratio: 3.4.

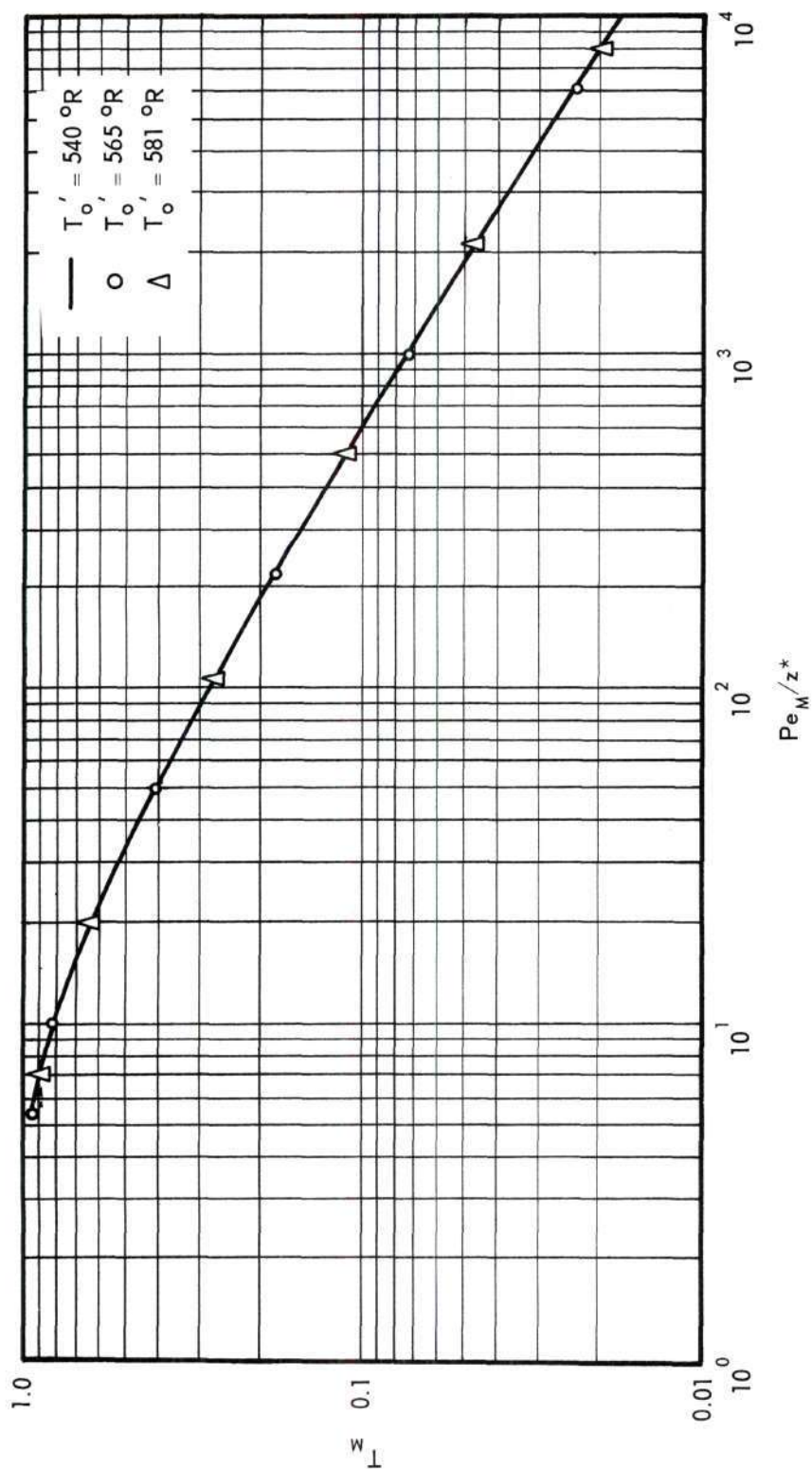


Figure 42. Comparison of Variable Property Mean Temperature Calculations for Oil A.
 Entrance Profile: Parabolic.
 Viscosity Ratio: 5.0.
 Free Convection Parameter: 0.1.

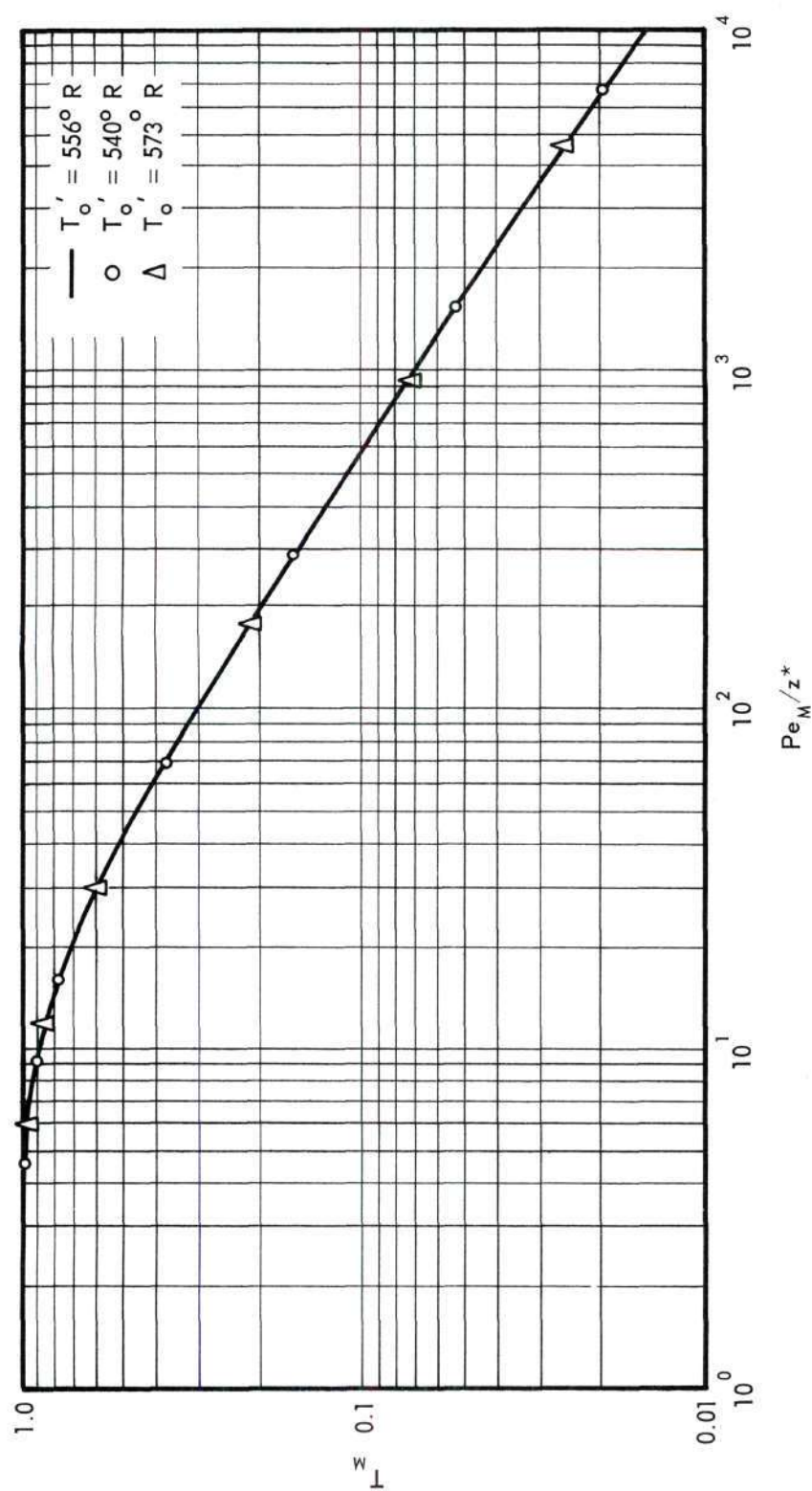


Figure 43. Comparison of Variable Property Mean Temperature Calculations for Water.
 Entrance Profile: Parabolic.
 Viscosity Ratio: 2.5.
 Free Convection Parameter: 200.

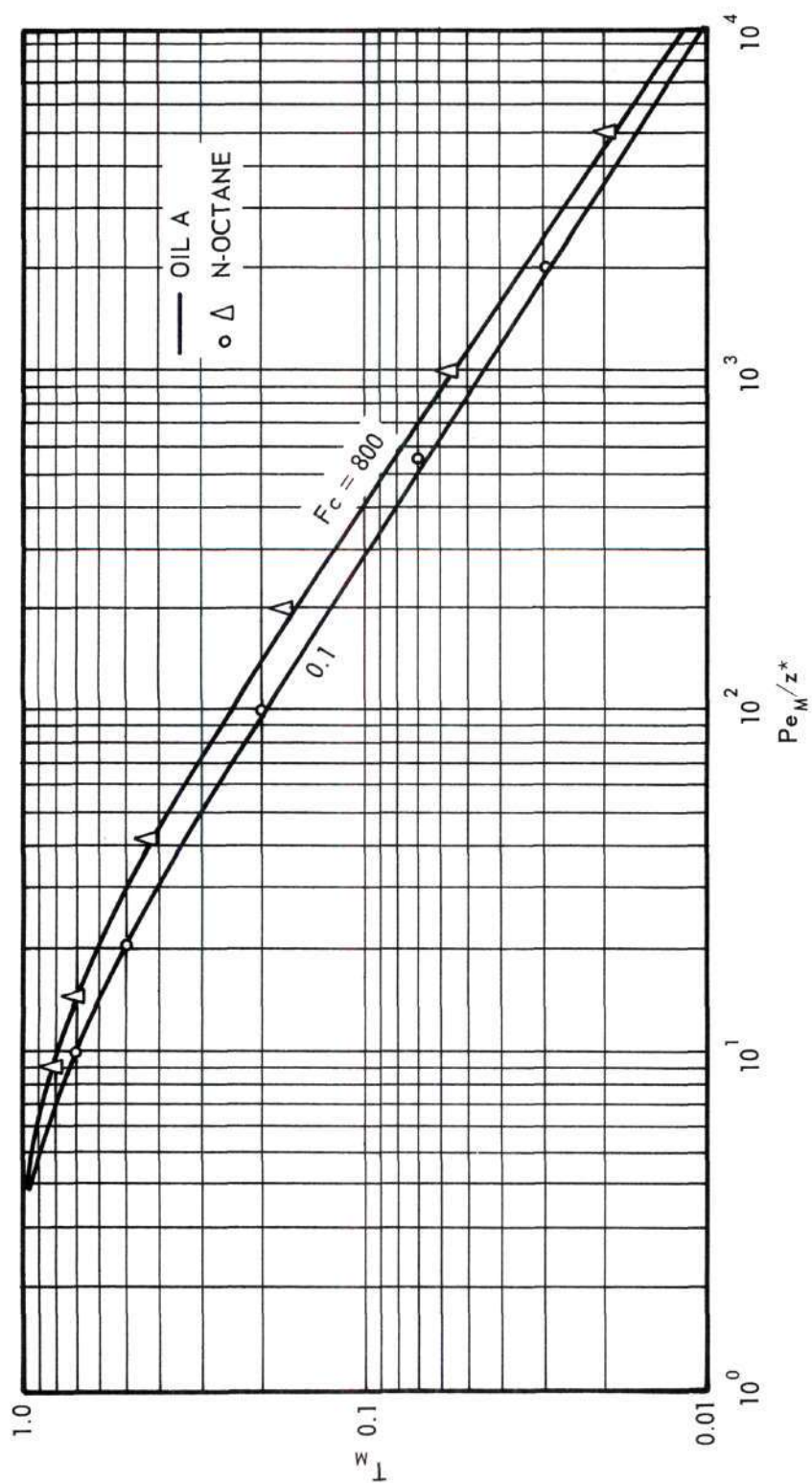


Figure 44. Comparison of Variable Property Mean Temperature Calculations for Oil A and N-Octane. Entrance Profile: Parabolic. Viscosity Ratio: 0.1.

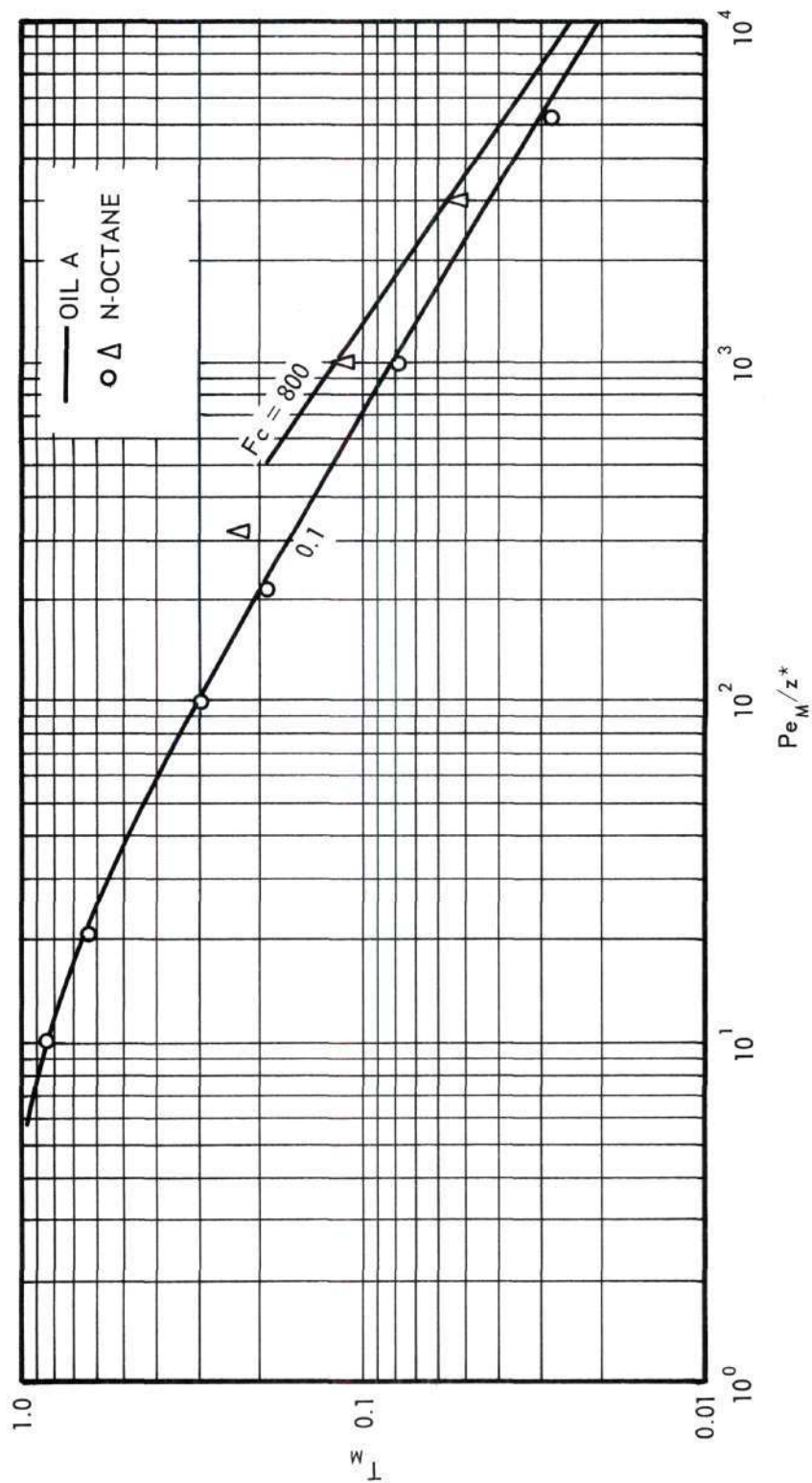


Figure 45. Comparison of Variable Property Mean Temperature Calculations for Oil A and n-octane.
Entrance Profile: Parabolic.
Viscosity Ratio: 10.

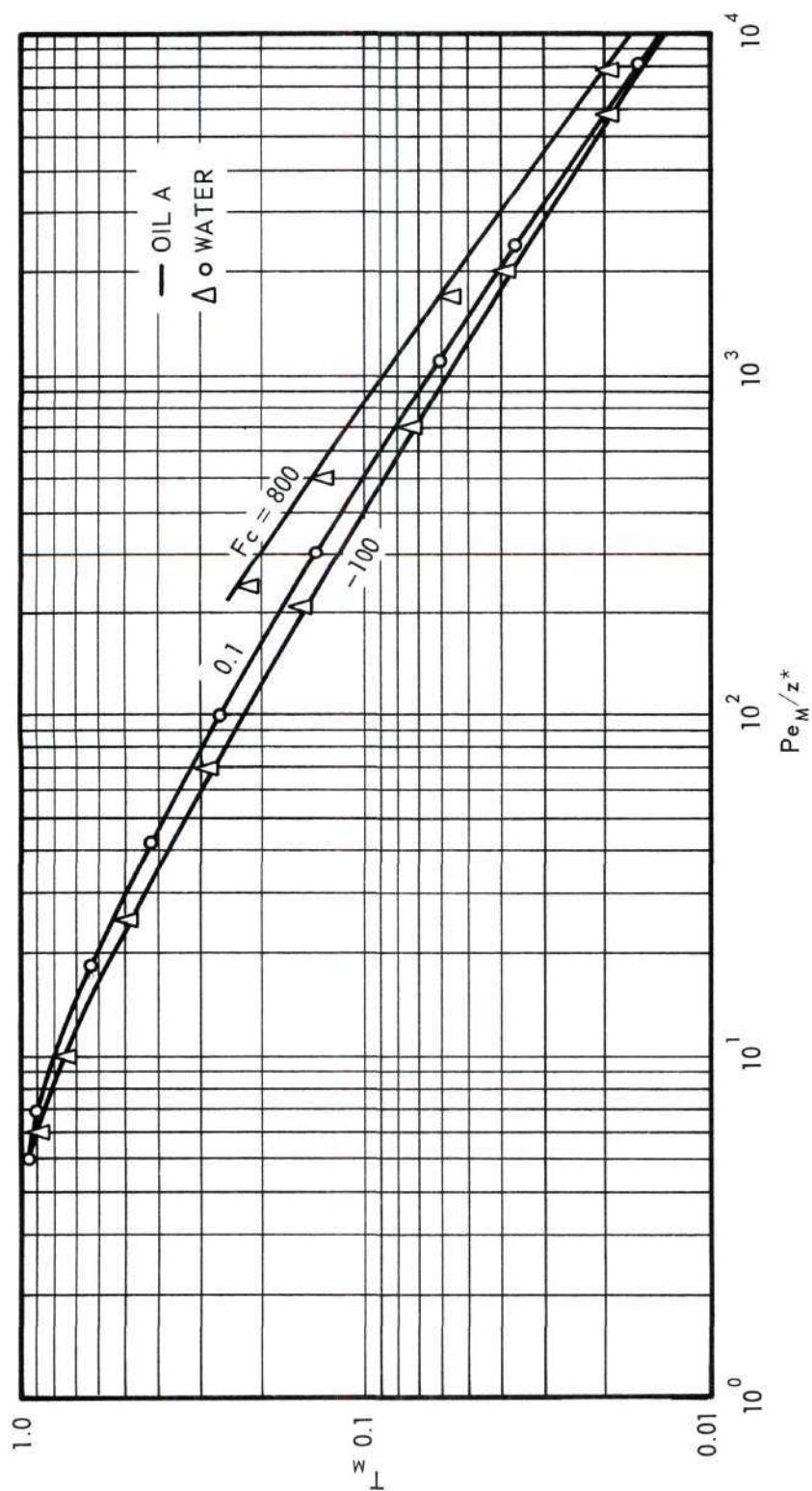


Figure 46. Comparison of Variable Property Mean Temperature Calculations for Oil A and Water.
Entrance Profile: Parabolic.
Viscosity Ratio: 2.

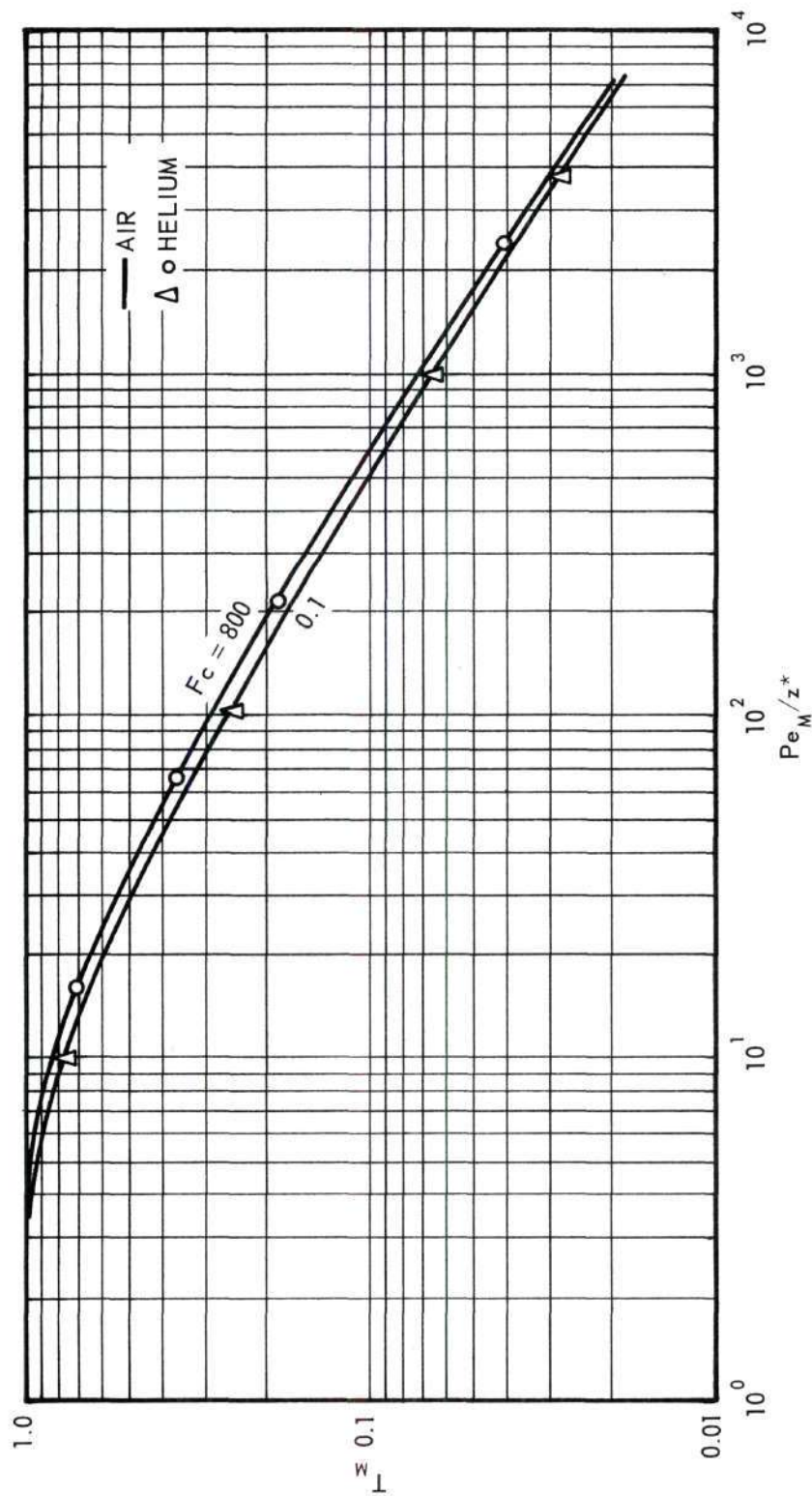


Figure 47. Comparison of Variable Property Mean Temperature Calculations for Air and Helium.
Entrance Profile: Parabolic.
Viscosity Ratio: 0.667.

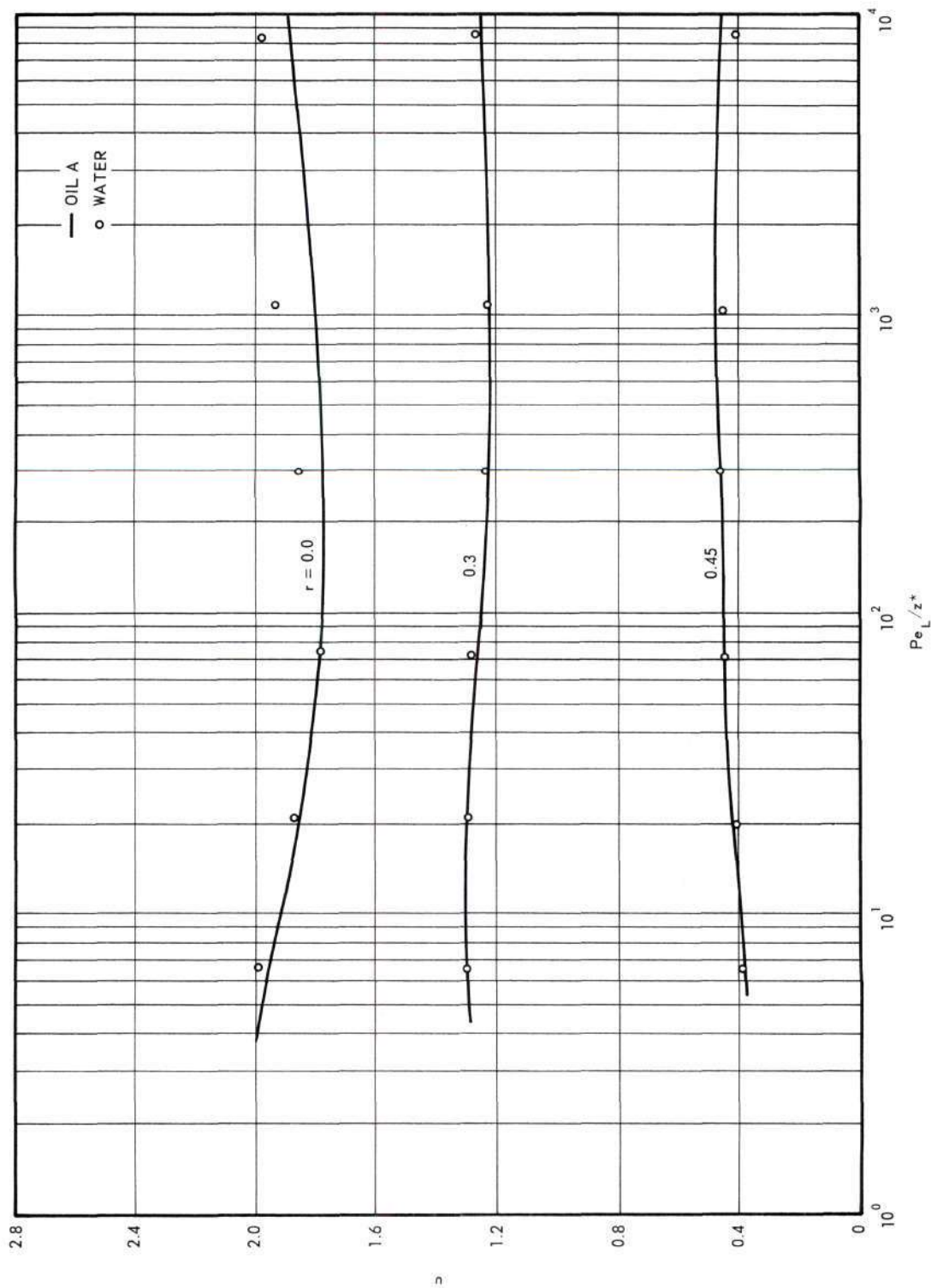


Figure 48. Comparison of Variable Property Velocity Profile Calculations for Oil A and Water. Entrance Profile: Parabolic. Viscosity Ratio: 2. Free Convection Parameter: 0.1.

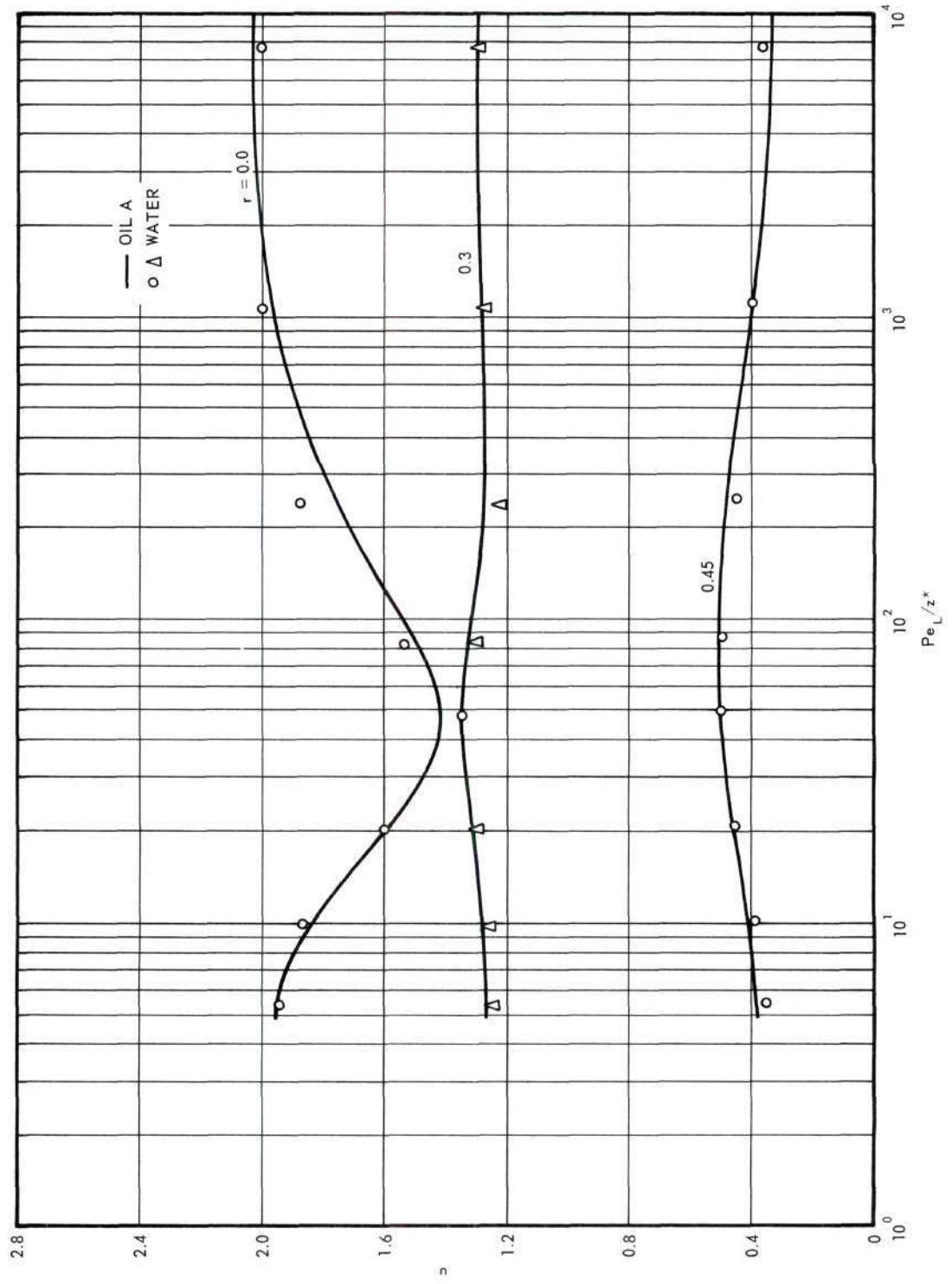


Figure 49. Comparison of Variable Property Velocity Profile Calculations for Oil A and Water. Entrance Profile: Parabolic. Viscosity Ratio: 0.5. Free Convection Parameter: 200.

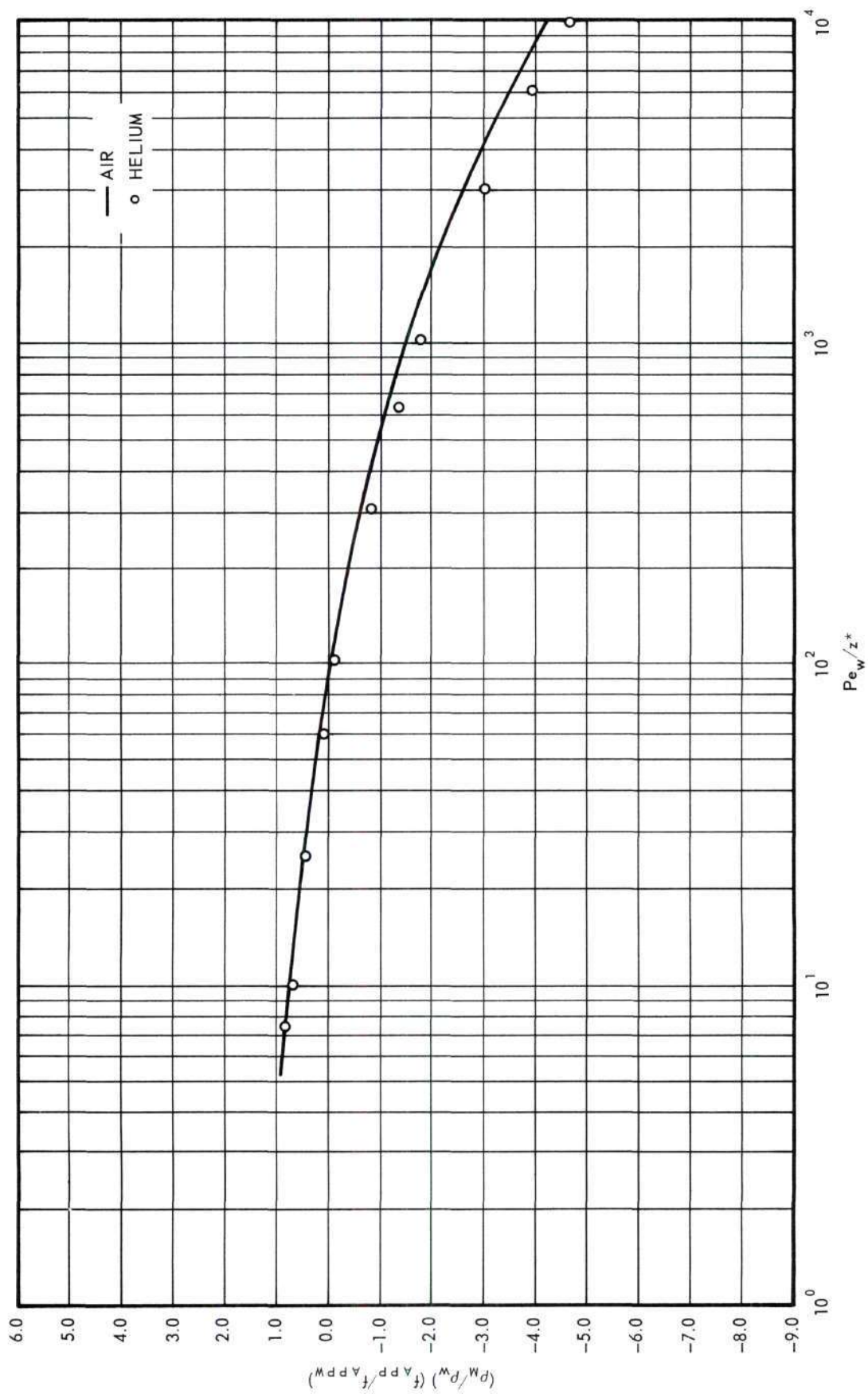


Figure 50. Comparison of Variable Property Friction Factor Calculations for Air and Helium. Entrance Profile: Parabolic. Viscosity Ratio: 1.5.

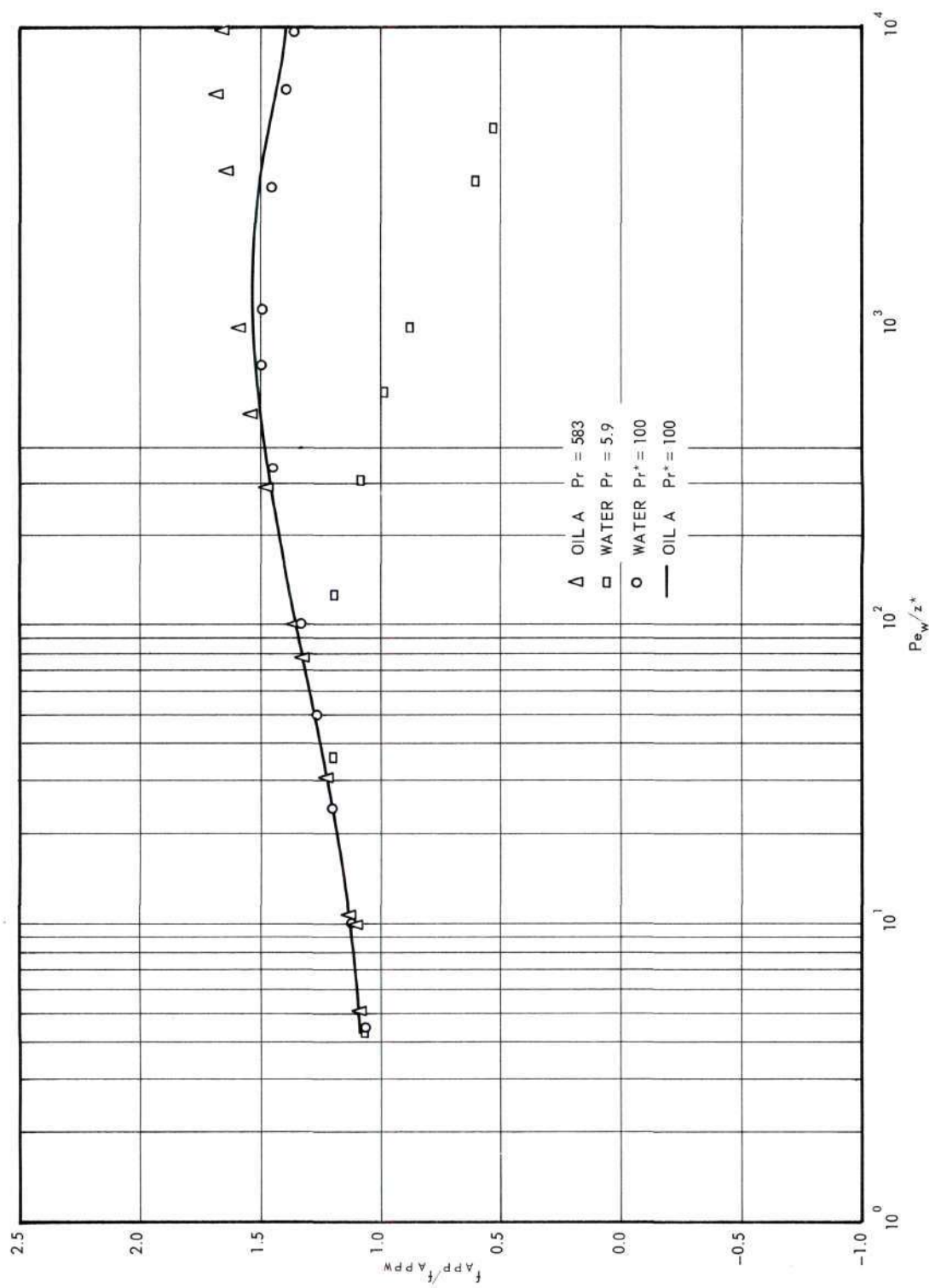


Figure 51. Comparison of Variable Property Friction Factor Calculations for Oil A and Water. Entrance Profile: Parabolic. Viscosity Ratio: 2. Prandtl Number: 100.

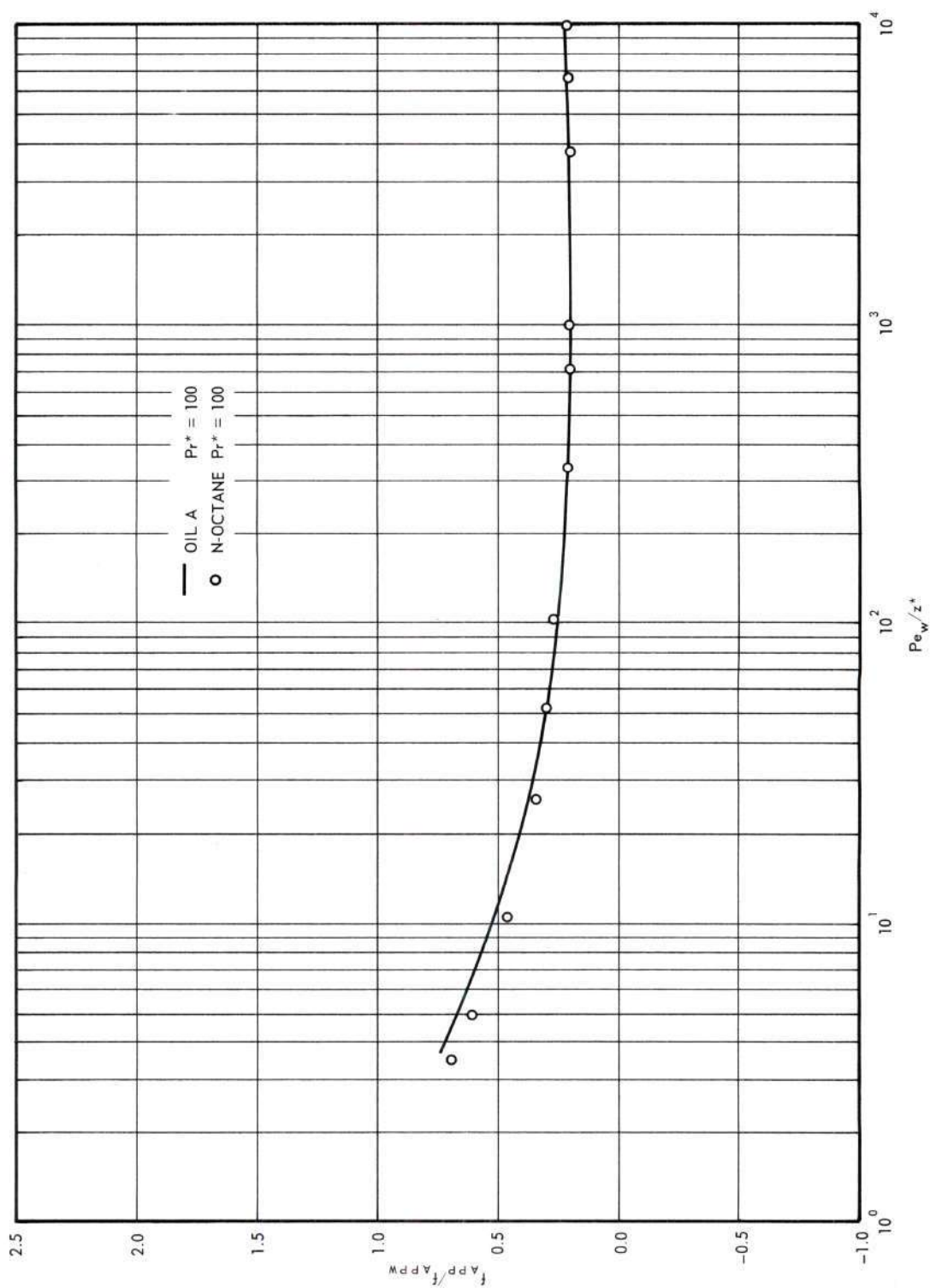


Figure 52. Comparison of Variable Property Friction Factor Calculations for Oil A and N-Octane. Entrance Profile: Parabolic. Viscosity Ratio: 0.1. Prandtl Number: 100.

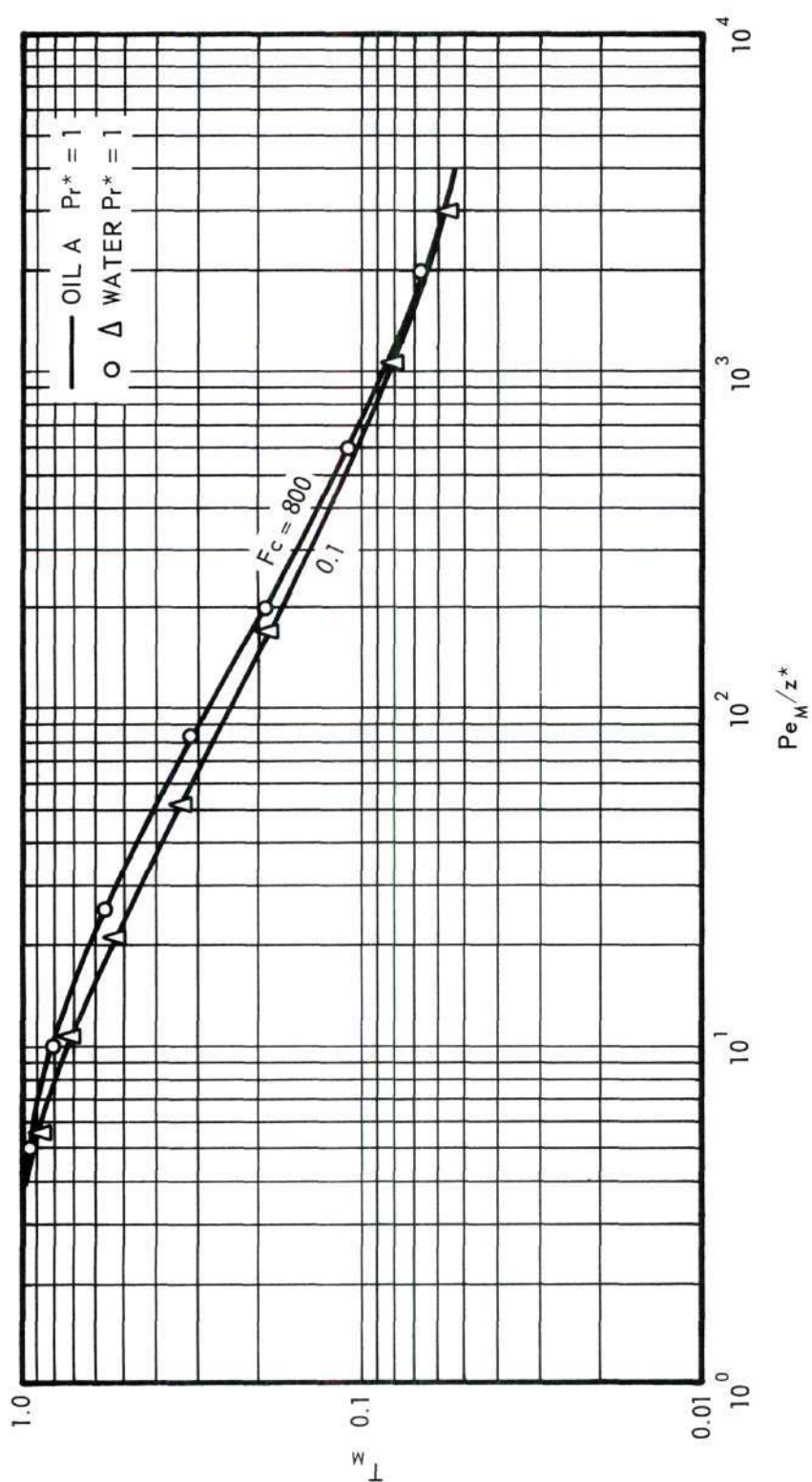


Figure 53. Comparison of Variable Property Mean Temperature Calculations for Oil A and n-Octane.
 Entrance Profile: Uniform.
 Viscosity Ratio: 0.1.
 Prandtl Number: 1.

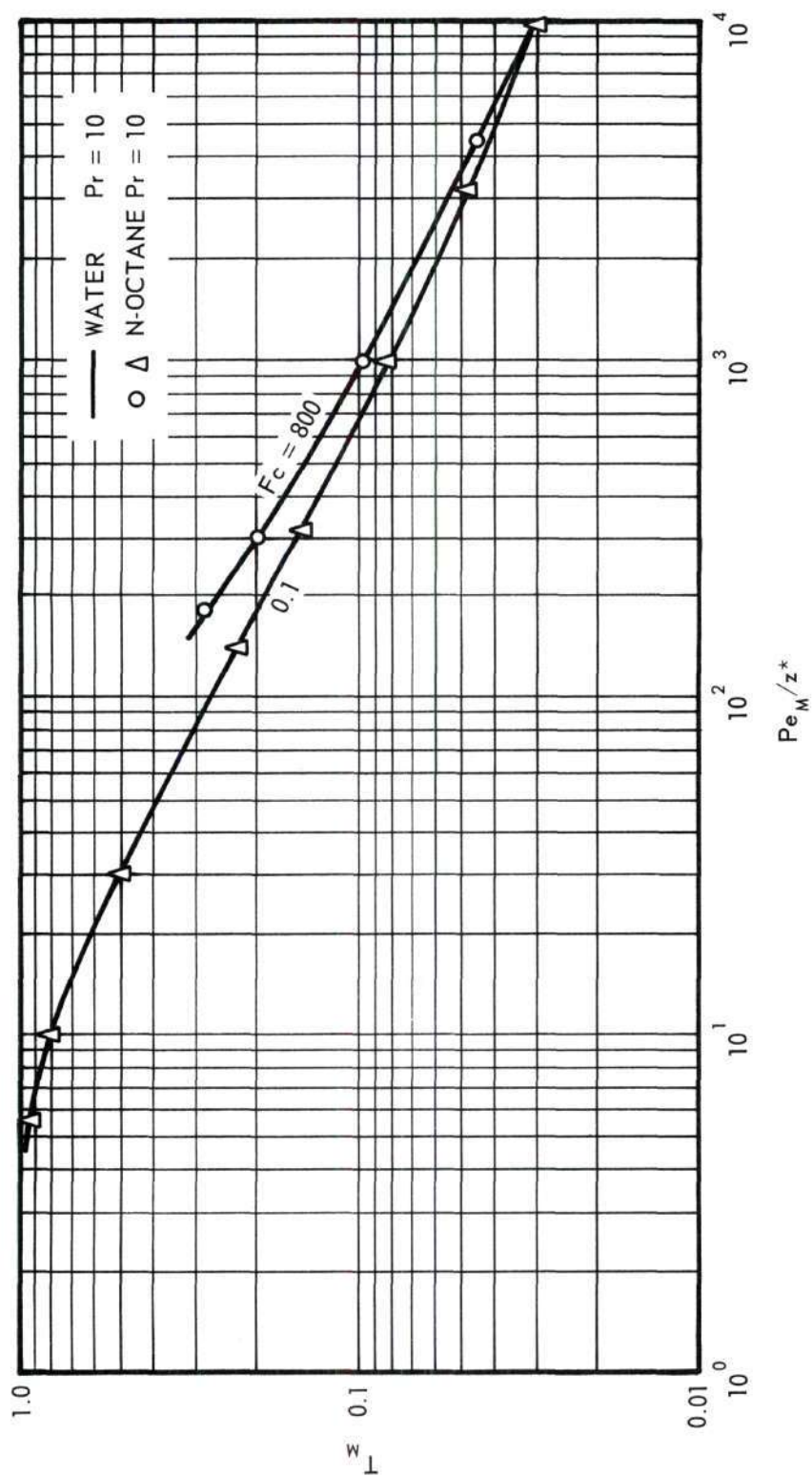


Figure 54. Comparison of Variable Property Mean Temperature Calculations for Water and n-Octane.
 Entrance Profile: Uniform.
 Viscosity Ratio: 2.
 Prandtl Number: 10.

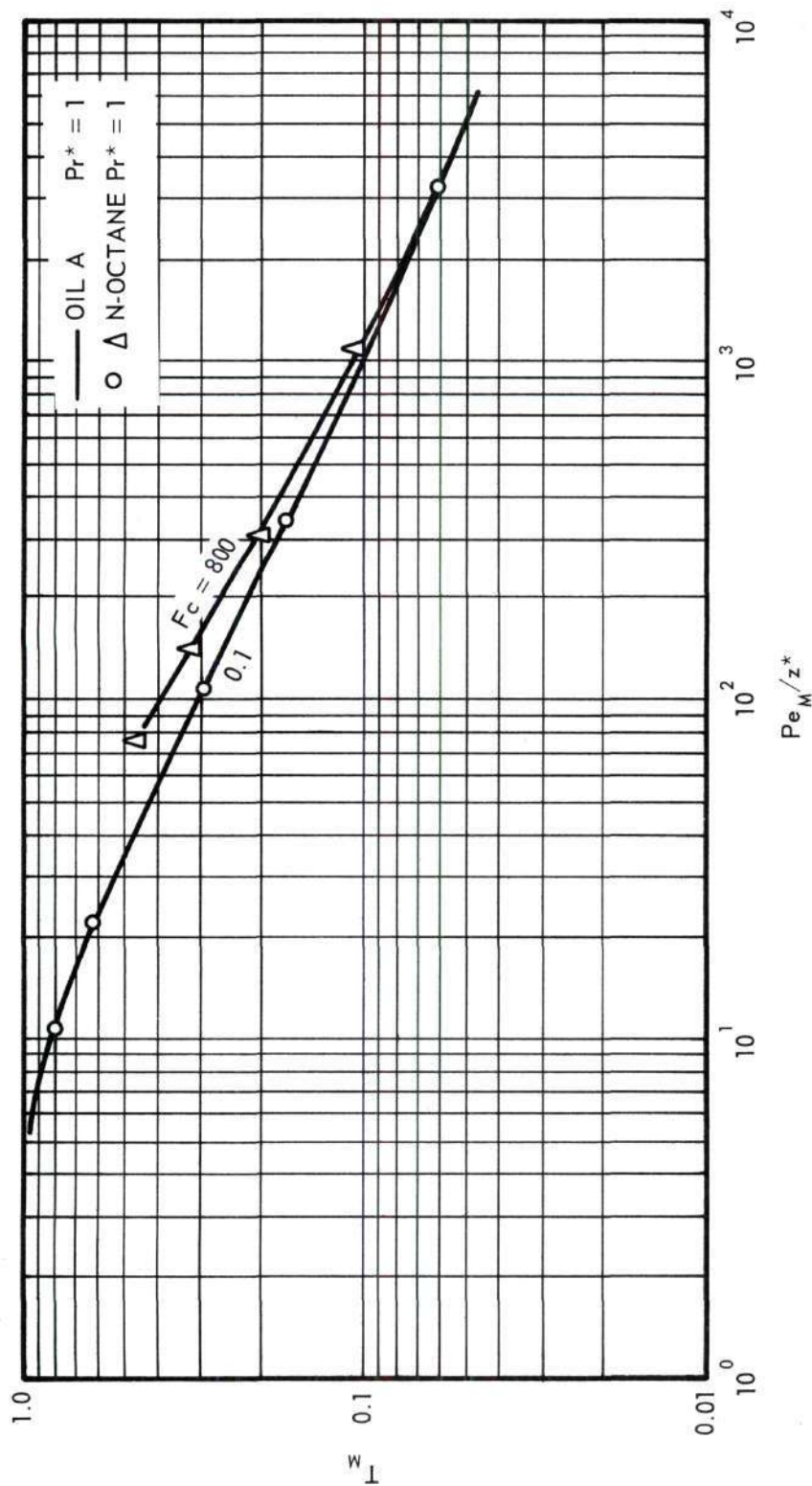


Figure 55. Comparison of Variable Property Mean Temperature Calculations for Oil A and Water.
 Entrance Profile: Uniform.
 Viscosity Ratio: 2.
 Prandtl Number: 1.

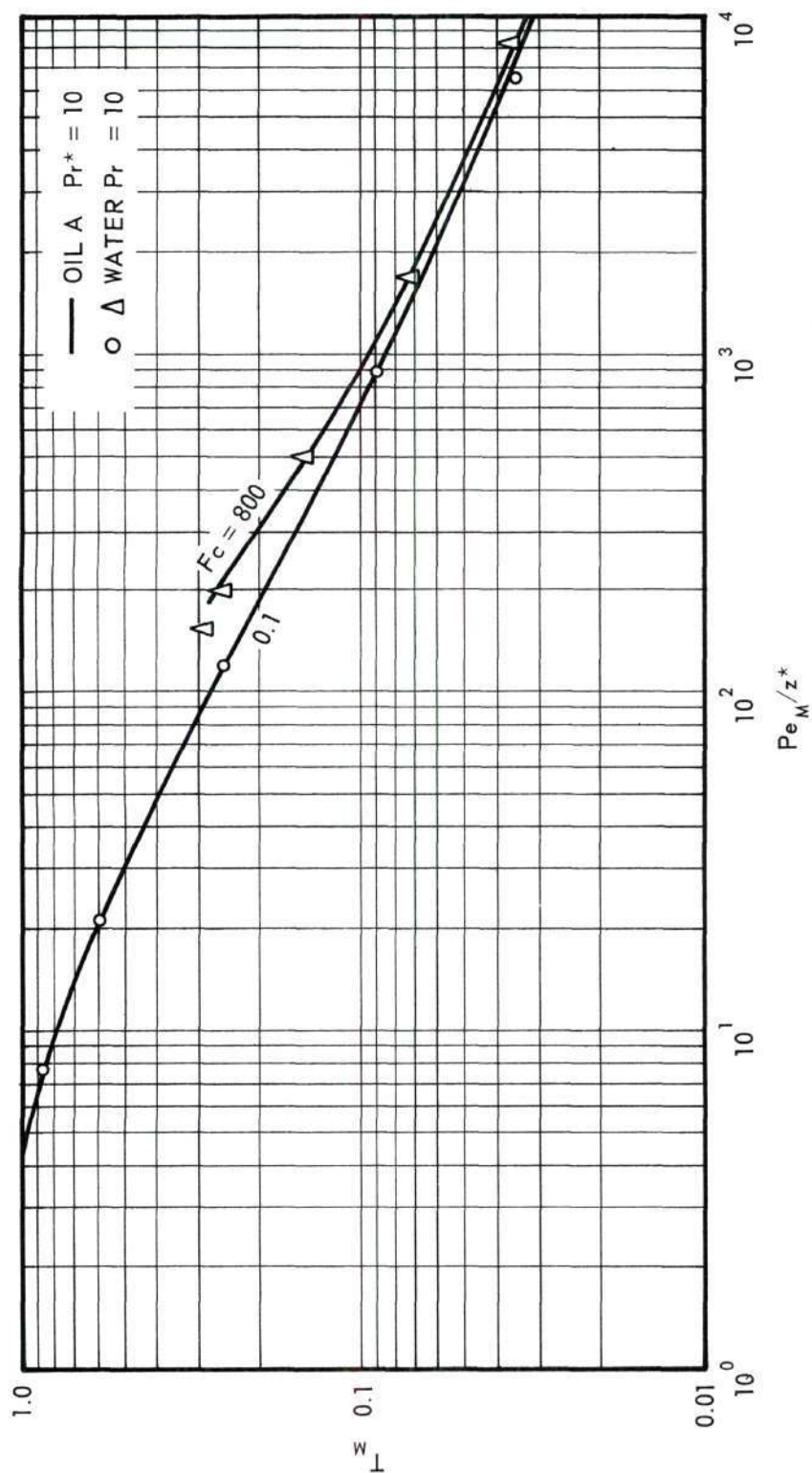


Figure 56. Comparison of Variable Property Mean Temperature Calculations for Oil A and Water.
 Entrance Profile: Uniform.
 Viscosity Ratio: 2.
 Prandtl Number: 10.

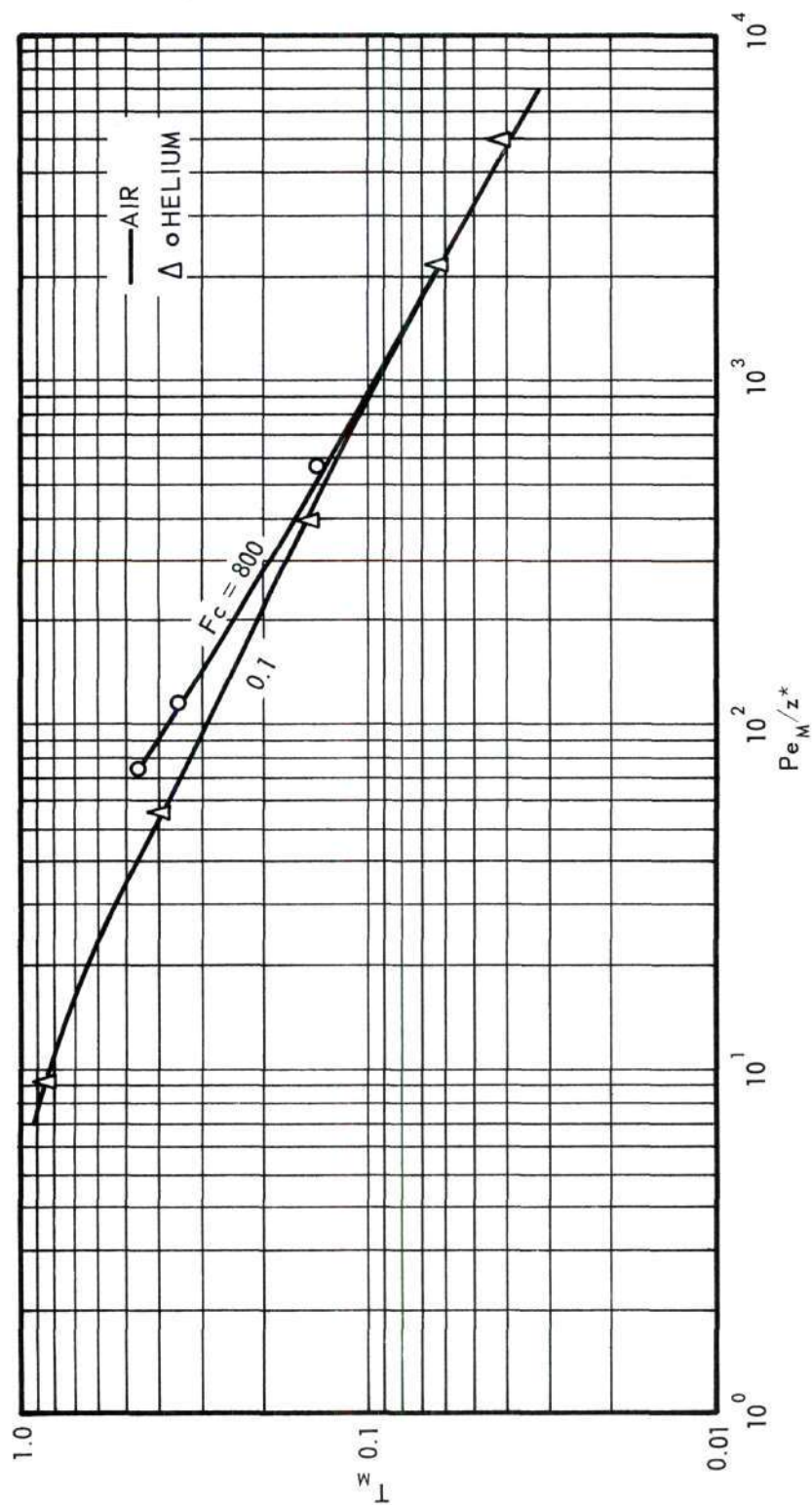


Figure 57. Comparison of Variable Property Mean Temperature Calculations for Air and Helium.
Entrance Profile: Uniform.
Viscosity Ratio: 1.5.

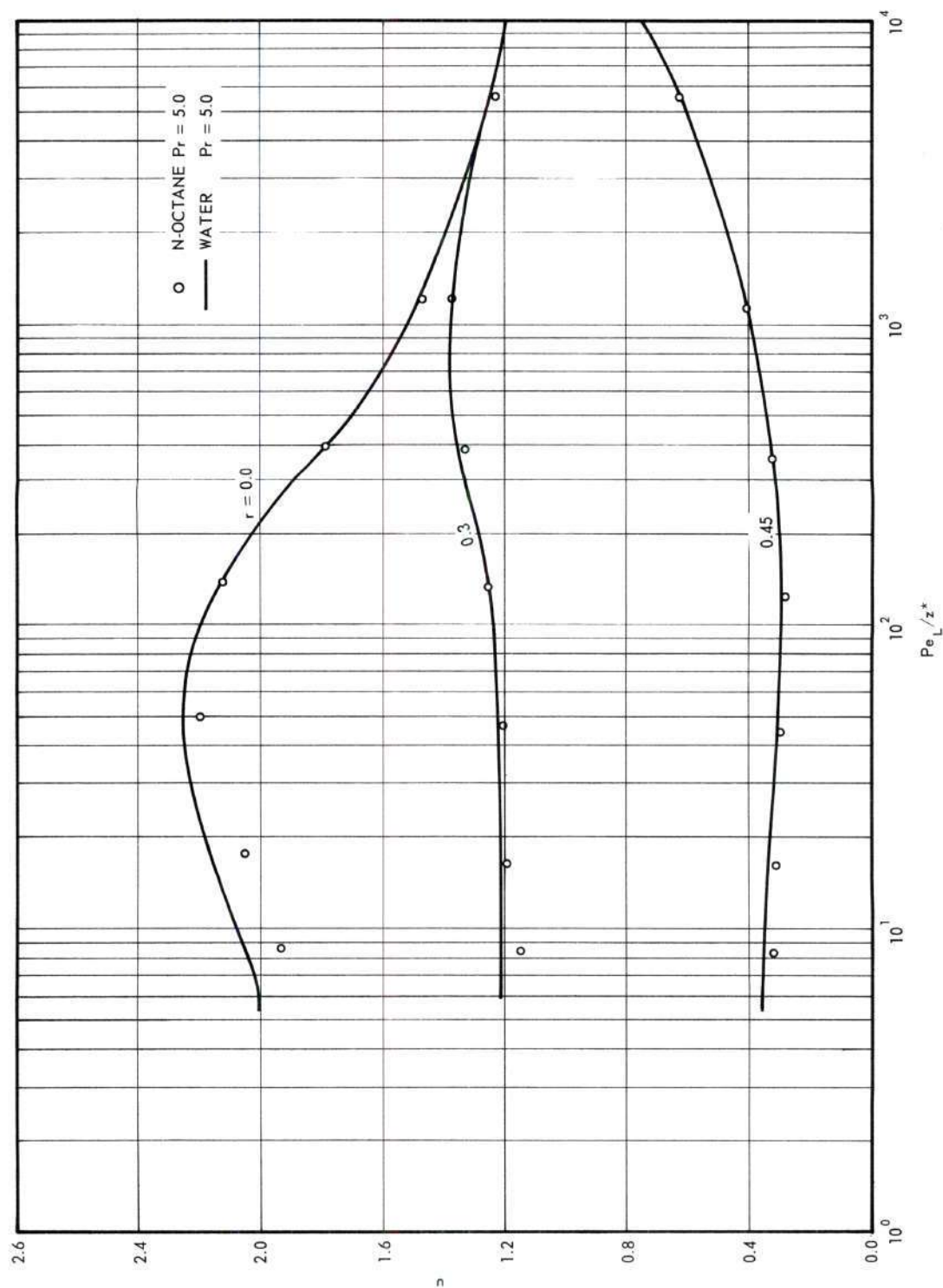


Figure 58. Comparison of Variable Property Velocity Profile Calculations for Water and n-Octane. Entrance Profile: Uniform. Viscosity Ratio: 0.5. Free Convection Parameter: 0.1. Prandtl Number: 5.

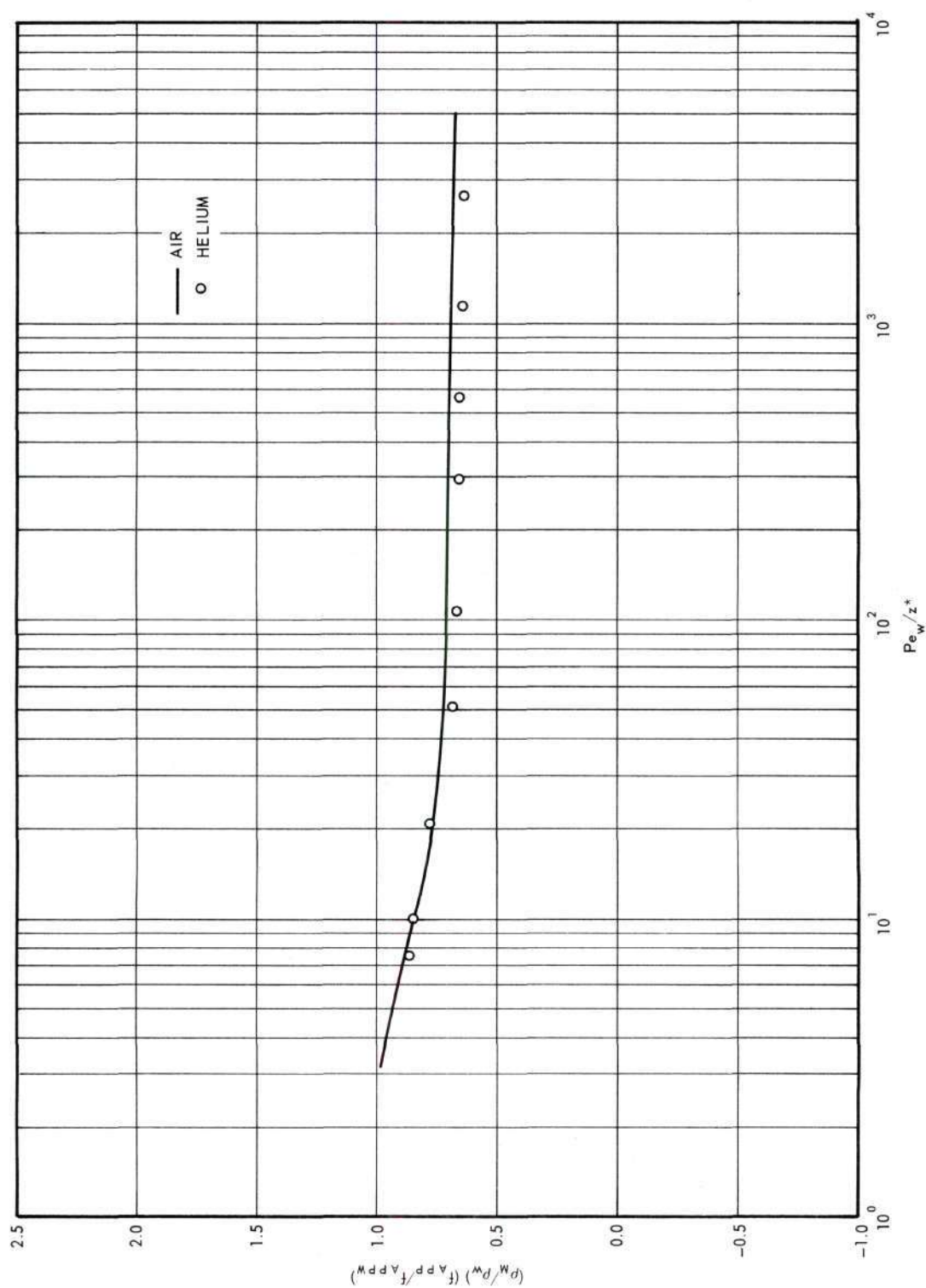


Figure 59. Comparison of Variable Property Friction Factor Calculations for Air and Helium. Entrance Profile: Uniform. Viscosity Ratio: 1.5.

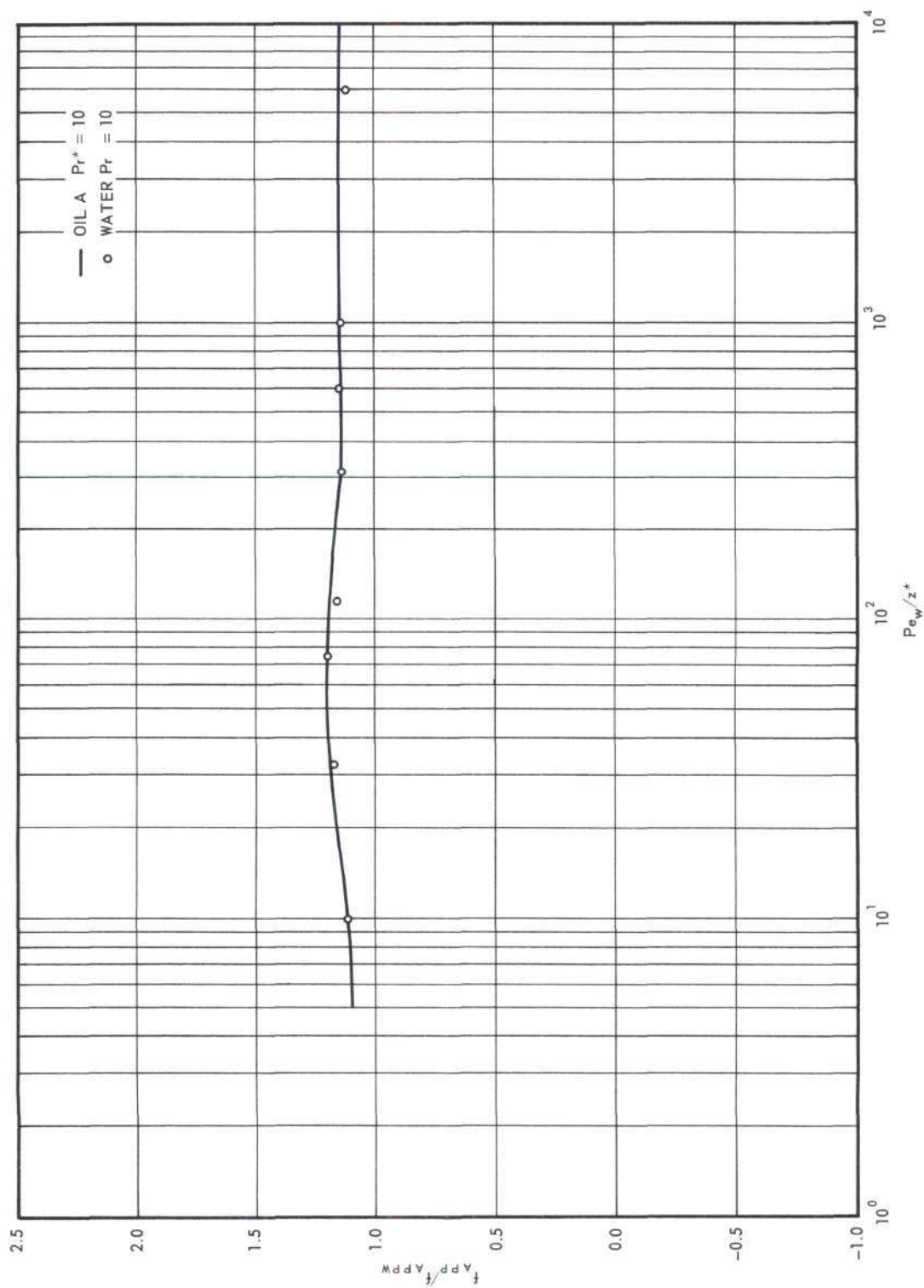


Figure 60. Comparison of Variable Property Friction Factor Calculations for Oil A and Water. Entrance Profile: Uniform. Viscosity Ratio: 2. Prandtl Number: 10.

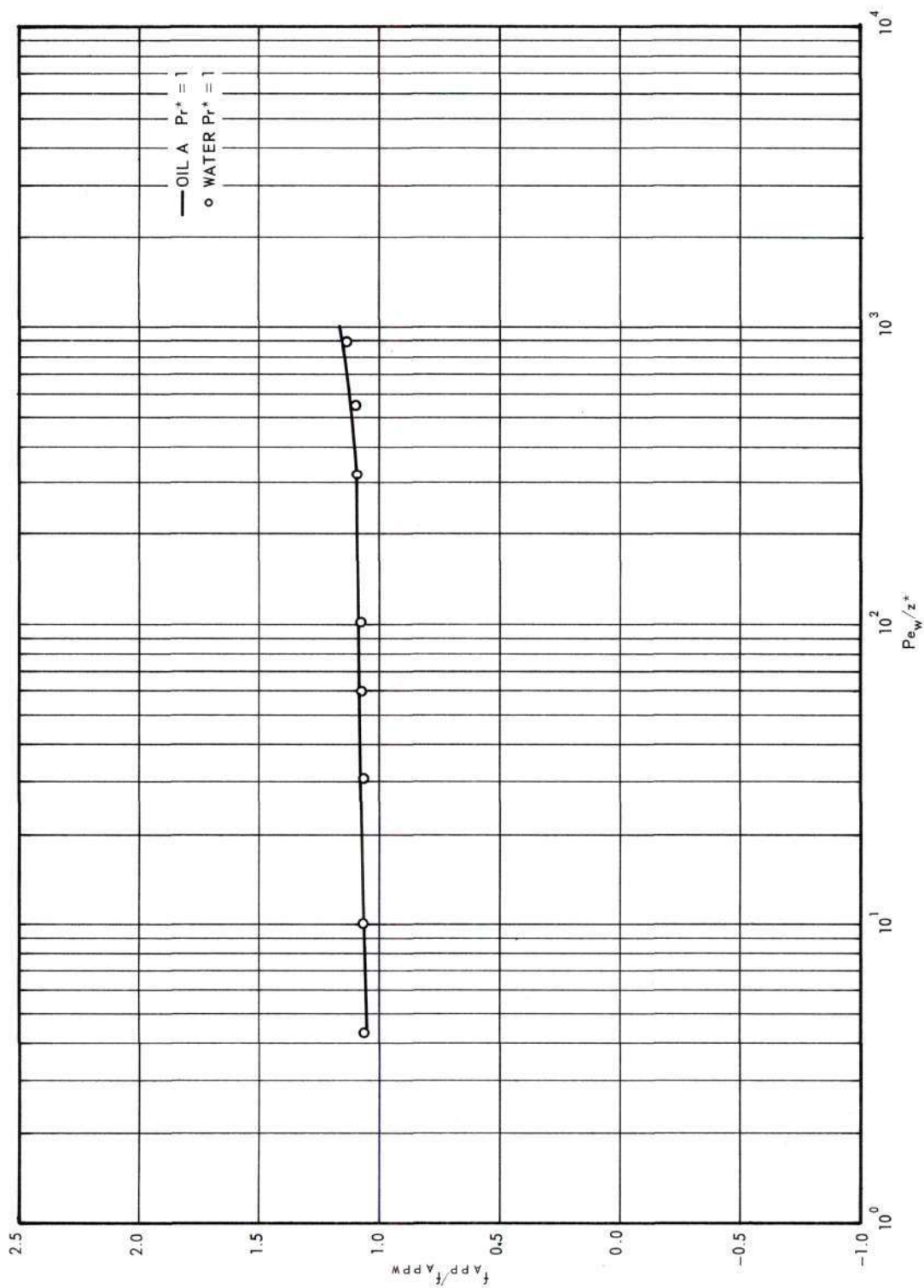


Figure 61. Comparison of Variable Property Friction Factor Calculations for Oil A and Water. Entrance Profile: Uniform. Viscosity Ratio: 2. Prandtl Number: 1.

APPENDIX F

VARIABLE PROPERTY FRICTION FACTOR CORRELATIONS

Correlated friction factor results are presented in graphical form in this appendix in Figures 62 through 69. The data included both liquids and gases and the parabolic and uniform entrance velocity profile cases for negligible free convection. Air was the correlating fluid for gases and oil A was used as the correlating fluid for liquids.

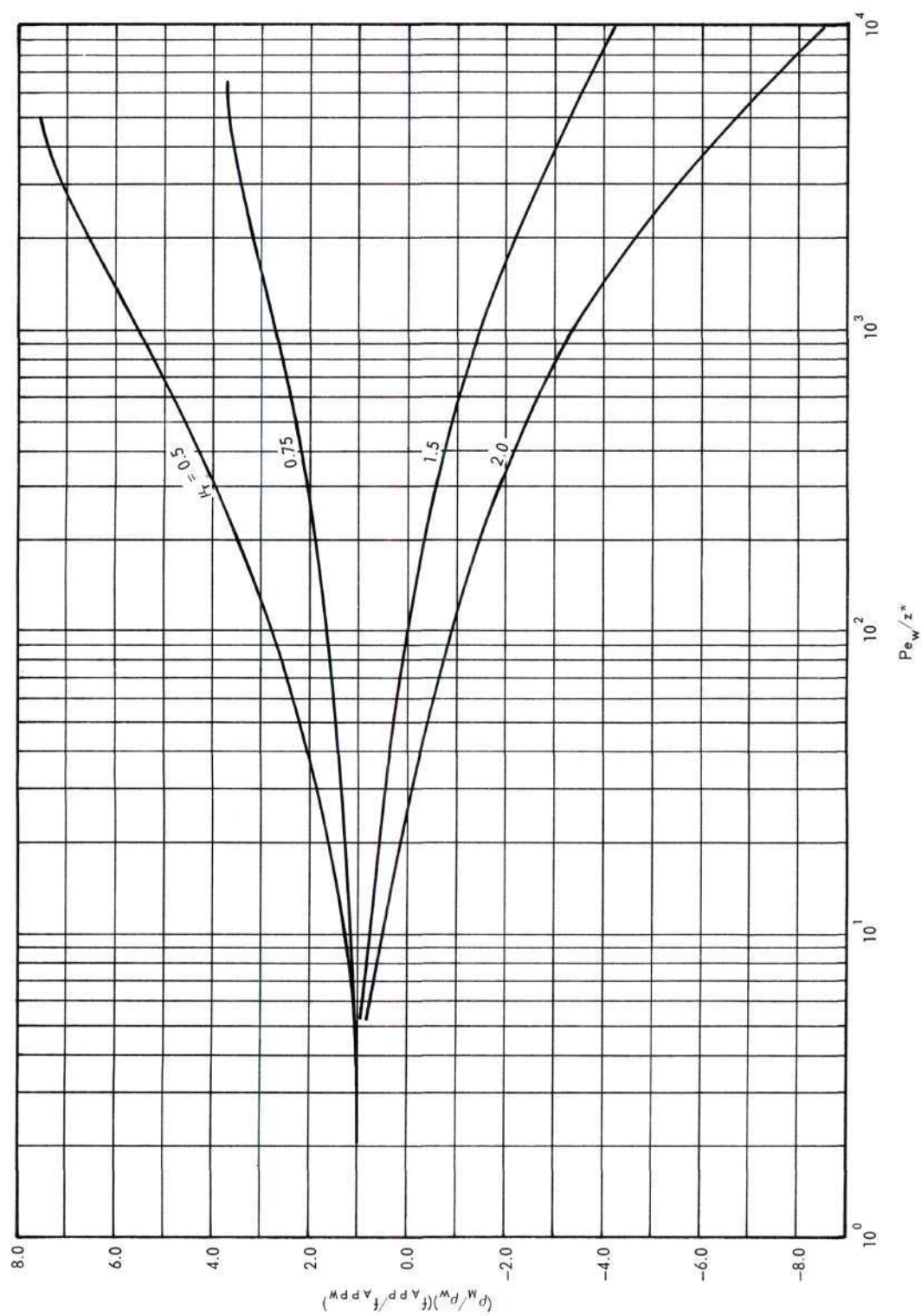


Figure 62. Variable Property Friction Factor Calculations for Gases.
Entrance Profile: Parabolic.

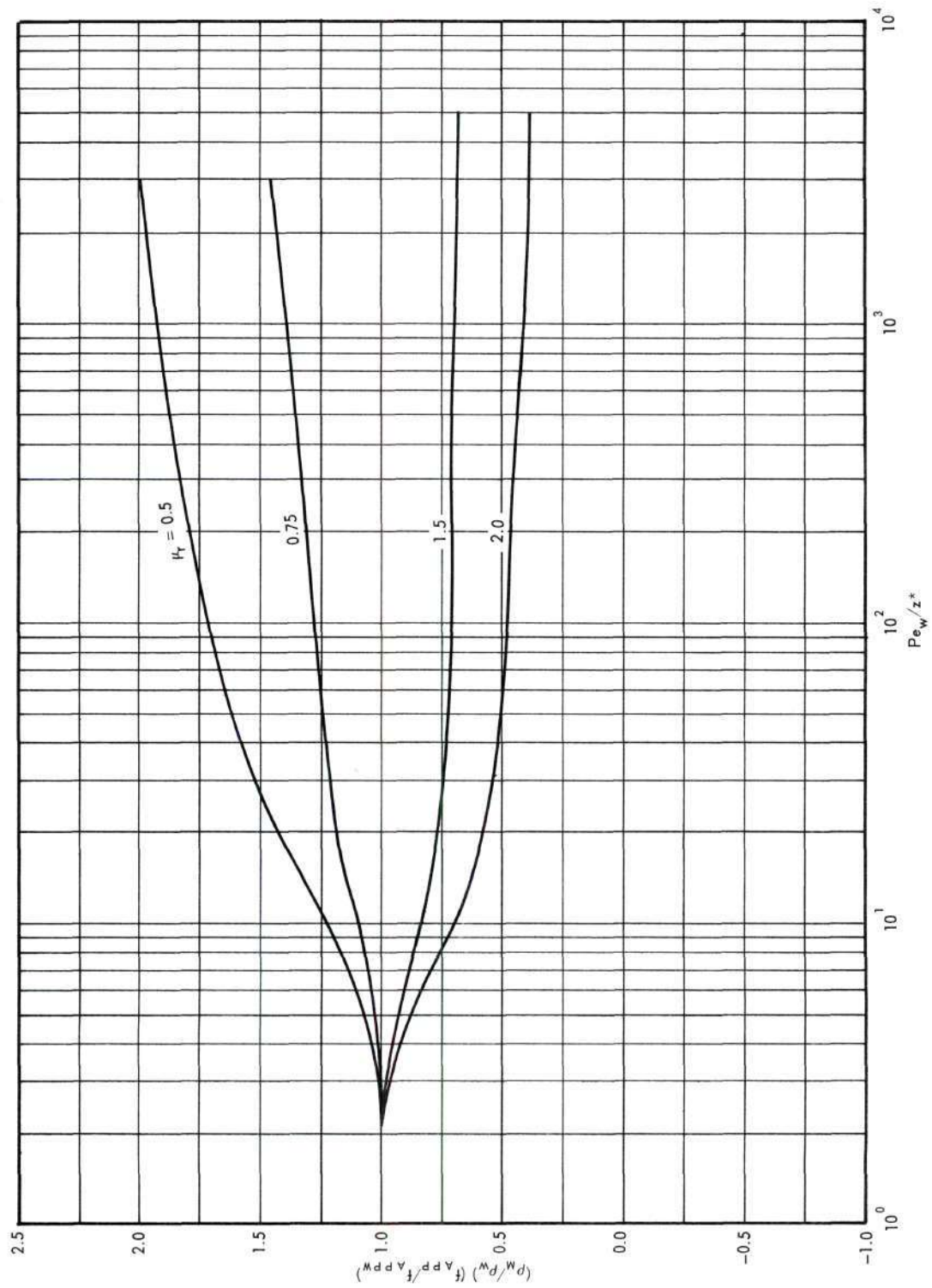


Figure 63. Variable Property Friction Factor Calculations for Gases.
Entrance Profile: Uniform.

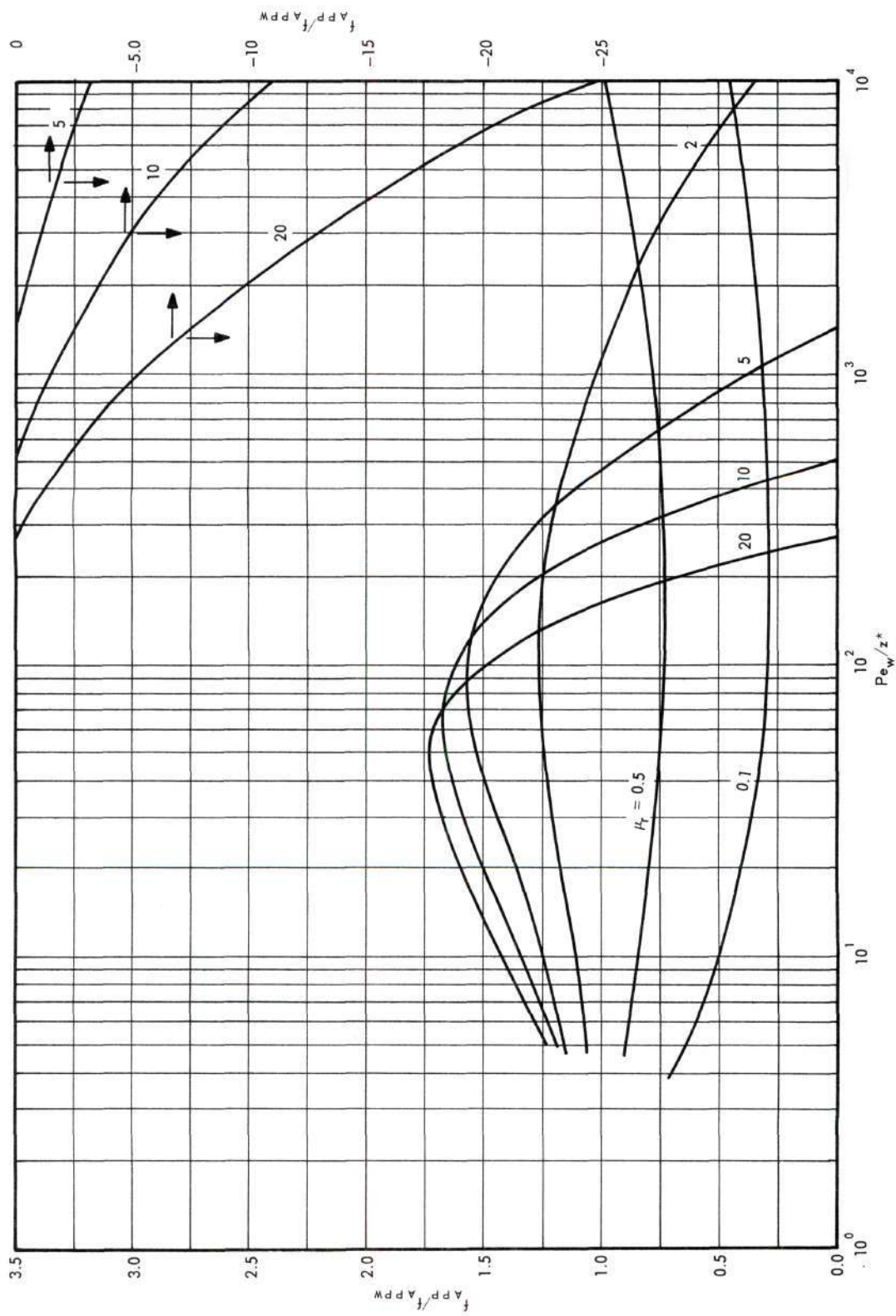


Figure 64. Variable Property Friction Factor Calculations for Liquids.
Entrance Profile: Parabolic. Prandtl Number: 10.

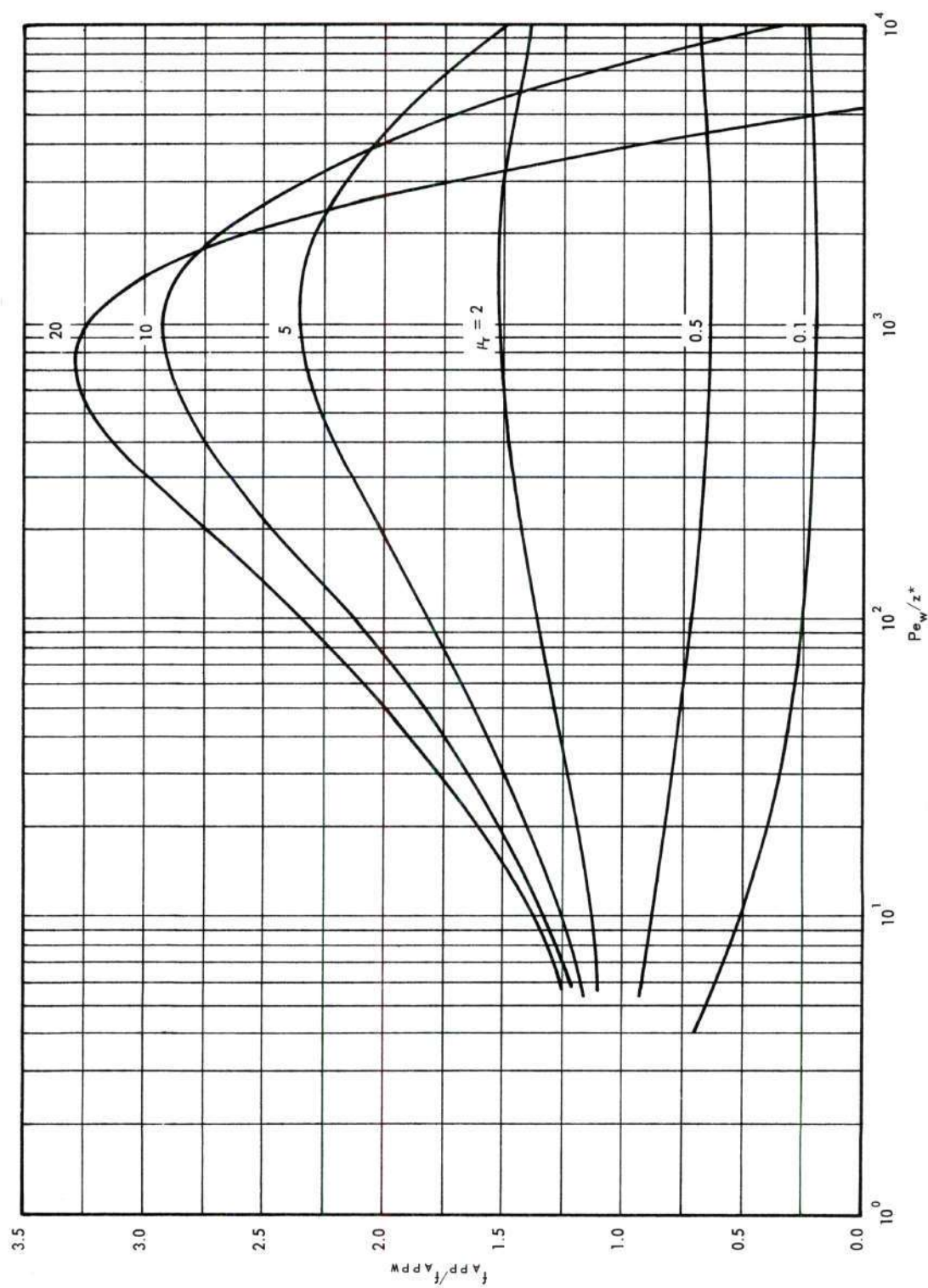


Figure 65. Variable Property Friction Factor Calculations for Liquids.
Entrance Profile: Parabolic. Prandtl Number: 100.

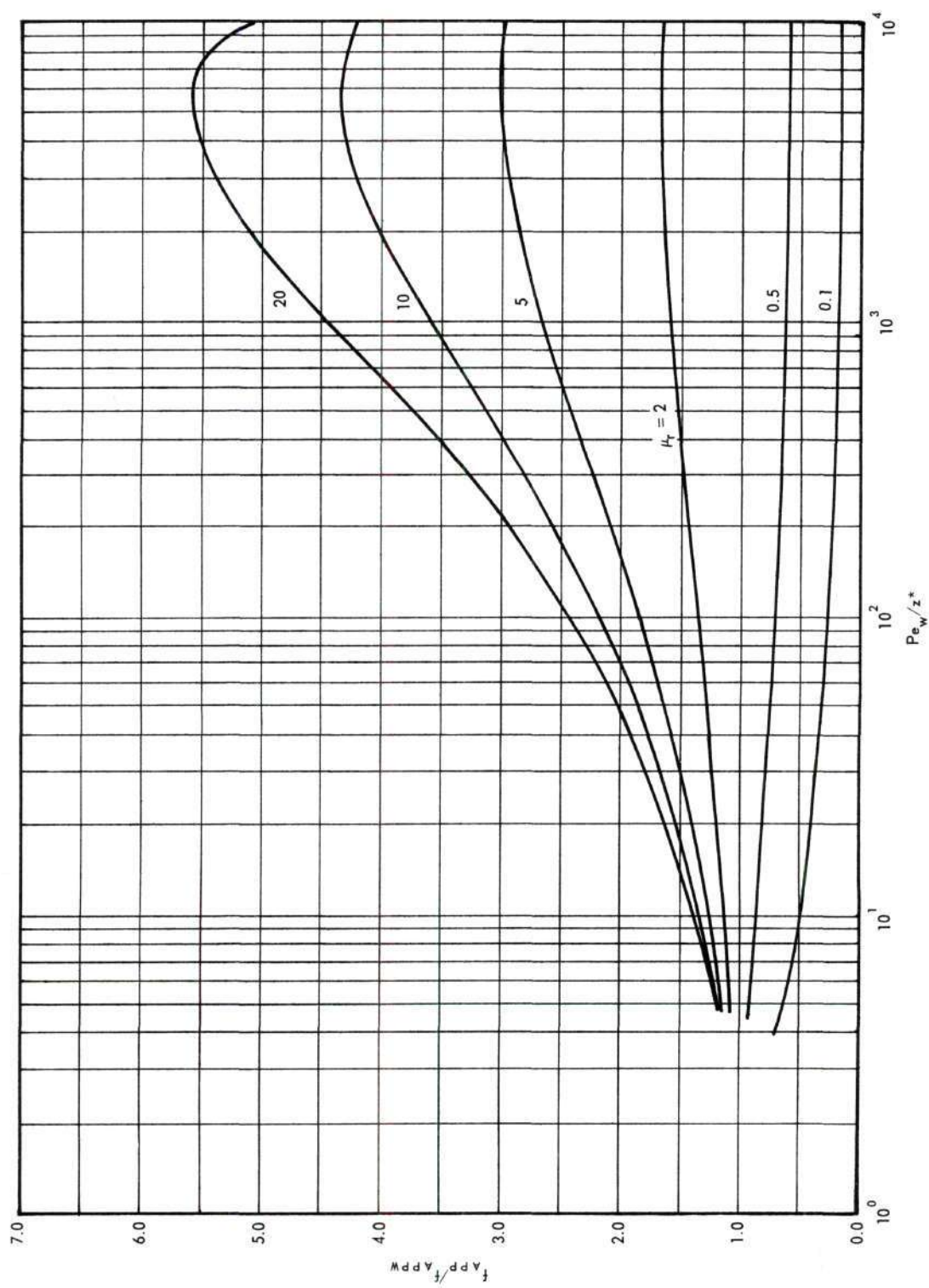


Figure 66. Variable Property Friction Factor Calculations for Liquids.
Entrance Profile: Parabolic. Prandtl Number: 500.

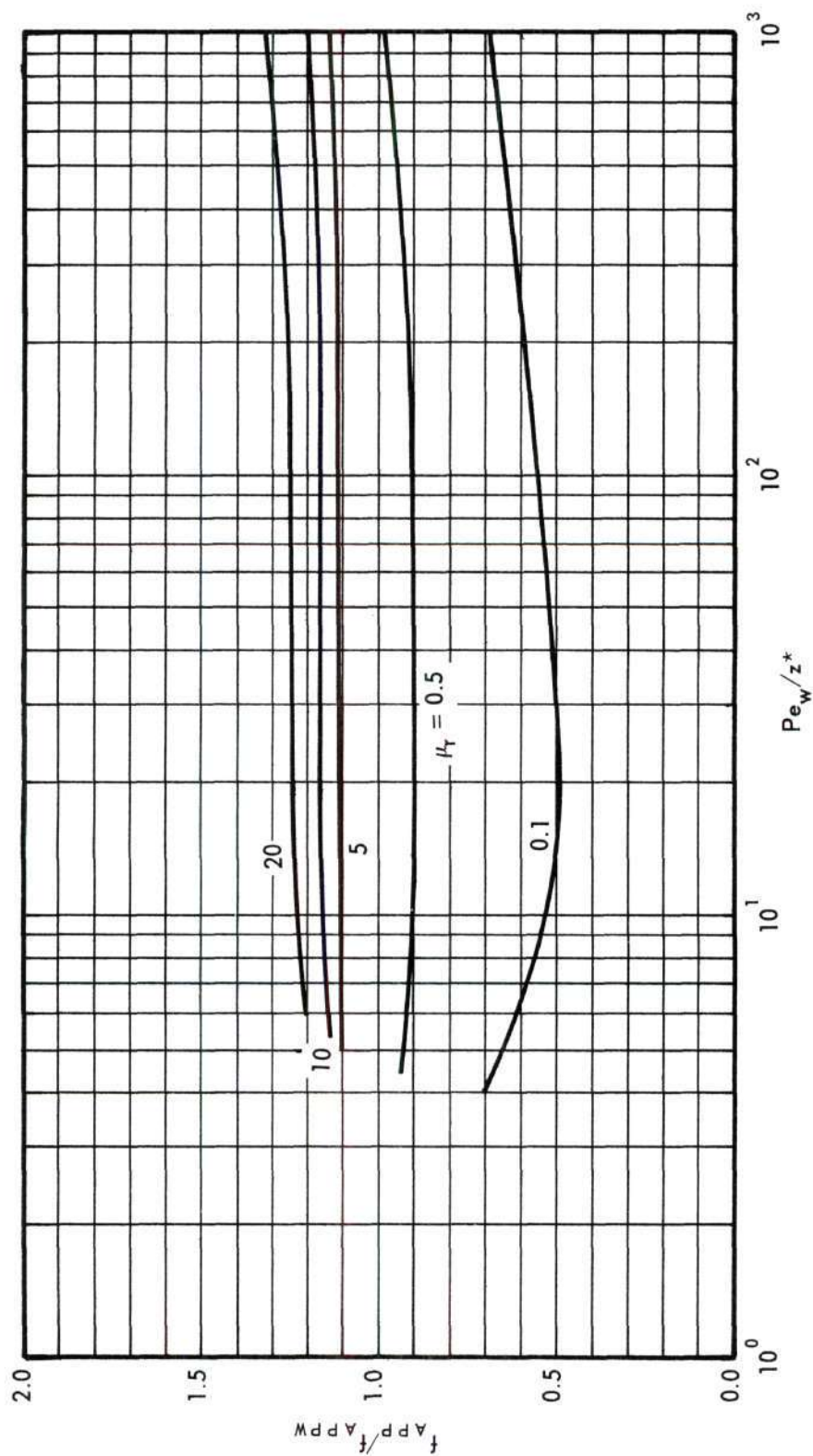


Figure 67. Variable Property Friction Factor Calculations for Liquids.
Entrance Profile: Uniform.
Prandtl Number: 1.

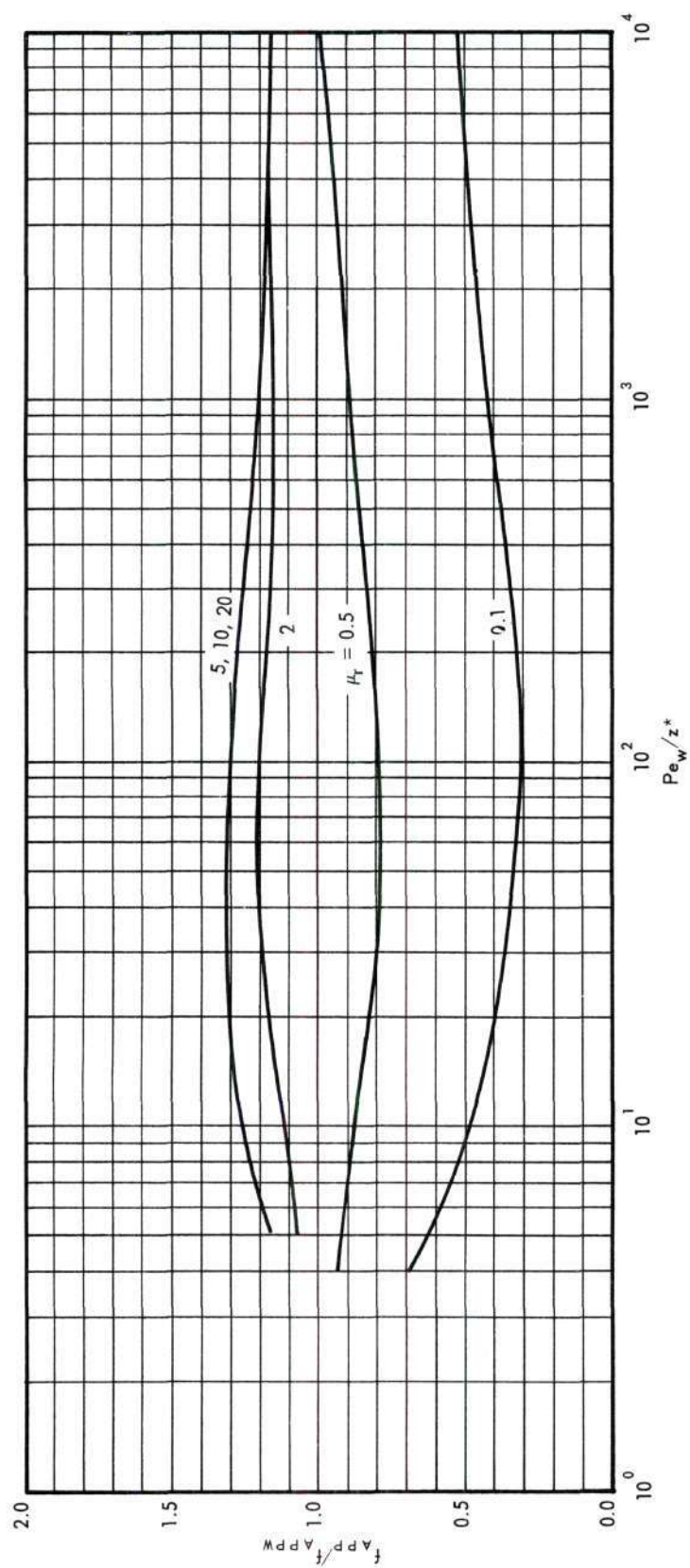


Figure 68. Variable Property Friction Factor Calculations for Liquids.
Entrance Profile: Uniform.
Prandtl Number: 10.

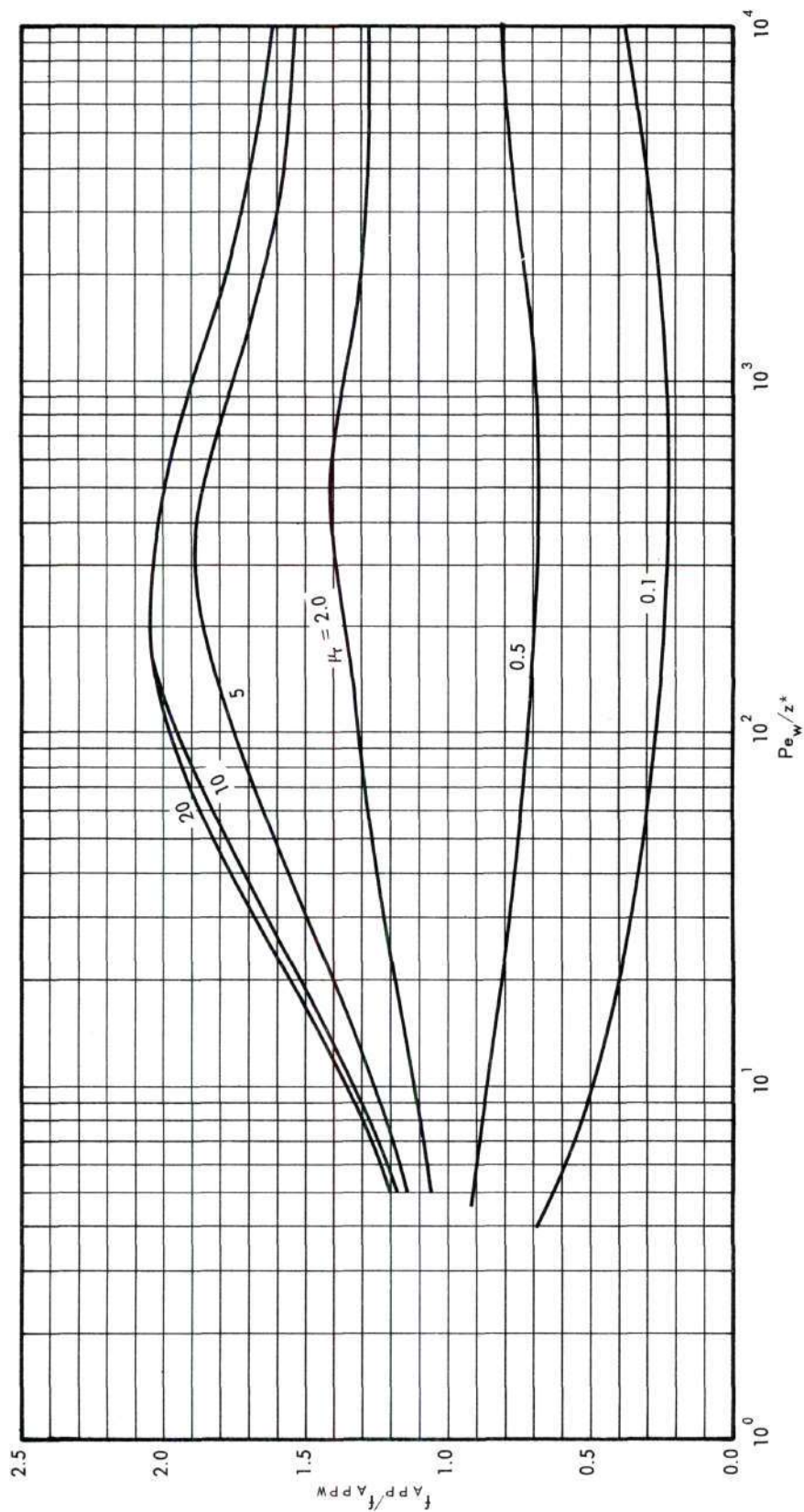


Figure 69. Variable Property Friction Factor Calculations for Liquids.
 Entrance Profile: Uniform.
 Prandtl Number: 100.

APPENDIX G

VARIABLE PROPERTY HEAT-TRANSFER CORRELATIONS

In this appendix correlated results for T_M and Nu are presented for both parabolic entrance profile and uniform entrance profile cases for gases and liquids for a wide range of μ_r and Fc . Air was the correlating fluid for gases and oil A was the correlating fluid for liquids.

Table 15. Variable Property Mean Temperature and Local
Nusselt Number Calculations for Liquids
Entrance Profile: Parabolic
Viscosity Ratio: 0.1

Fc	Pe_M/z^*	T_M	Nu	Fc	Pe_M/z^*	T_M	Nu
±0.1	10479	0.0100	16.6	800	10365	0.0115	20.0
	6253	0.0139	13.9		5943	0.0167	17.0
	3207	0.0214	11.1		3283	0.0248	14.4
	1360	0.0372	8.34		1450	0.0432	11.4
	633	0.0608	6.54		768	0.0664	9.55
	324	0.0932	5.37		338	0.115	7.79
	146	0.155	4.34		122	0.224	6.04
	66.8	0.252	3.66		60.0	0.347	5.18
	24.2	0.462	3.21		31.3	0.498	4.41
	10.3	0.714	3.26		12.4	0.749	3.67
	3.96	0.959	3.58		3.88	0.975	3.63
200	10337	0.0107	17.5	-200	10500	0.00999	15.1
	6214	0.0148	14.9		6058	0.0139	12.4
	3682	0.0208	12.6		3519	0.0194	10.1
	1603	0.0357	9.70		1556	0.0321	7.53
	703	0.0611	7.55		756	0.0501	5.88
	340	0.0979	6.12		341	0.0821	4.65
	128	0.183	4.71		129	0.151	3.72
	63.4	0.282	4.00		60.0	0.246	3.26
	30.9	0.429	3.52		30.2	0.377	3.03
	12.8	0.674	3.34		12.1	0.638	3.10
	3.95	0.964	3.60		3.98	0.953	3.56
400	10612	0.0108	18.6				
	6025	0.0156	15.6				
	3309	0.0232	13.0				
	1455	0.0399	10.2				
	771	0.0608	8.44				
	338.8	0.104	6.70				
	143.1	0.182	5.34				
	63.8	0.300	4.41				
	30.9	0.455	3.80				
	12.4	0.707	3.46				
	3.97	0.967	3.61				

Table 16. Variable Property Mean Temperature and Local
Nusselt Number Calculations for Liquids
Entrance Profile: Parabolic
Viscosity Ratio: 0.5

Fc	Pe_M/z^*	T_M	Nu	Fc	Pe_M/z^*	T_M	Nu
±0.1	10132	0.0121	20.4	800	10068	0.0141	25.5
	6133	0.0168	17.2		6265	0.0196	22.2
	3180	0.0258	13.7		3555	0.0290	18.9
	1460	0.0426	10.6		1450	0.0540	14.8
	672	0.0700	8.17		702	0.0890	12.3
	313	0.114	6.43		342	0.146	10.4
	152	0.178	5.23		150	0.252	8.80
	67.9	0.290	4.27		96.4	0.335	8.23
	24.8	0.512	3.66	-200	10754	0.0112	18.7
	10.3	0.773	3.58		5748	0.0165	14.7
200	4.78	0.950	3.64		3320	0.0231	11.8
	10222	0.0127	22.1		1477	0.0378	8.54
	5903	0.0183	18.5		717	0.0585	6.42
	3277	0.0270	15.4		342	0.0911	4.98
	1454	0.0463	12.0		125	0.168	3.88
	703	0.0749	9.62		61.1	0.261	3.42
	331	0.122	7.76		29.7	0.405	3.18
	119	0.235	5.90		12.3	0.664	3.26
	61.6	0.348	5.07		4.54	0.943	3.58
	28.0	0.535	4.32				
400	12.2	0.769	3.86				
	4.45	0.969	3.68				
	10221	0.0132	23.4				
	6325	0.0182	20.2				
	3277	0.0284	16.6				
	1586	0.0464	13.4				
	703	0.0804	10.7				
	342	0.130	8.80				
	133	0.240	7.01				
	59.9	0.389	5.94				
	29.5	0.567	5.04				
	12.4	0.801	4.10				
	4.38	0.976	3.70				

Table 17. Variable Property Mean Temperature and Local
Nusselt Number Calculations for Liquids
Entrance Profile: Parabolic
Viscosity Ratio: 1

Fc	Pe_M/z^*	T_M	Nu	Fc	Pe_M/z^*	T_M	Nu
±0.1	10359	0.0130	22.7	800	10679	0.0151	29.9
	6254	0.0181	19.1		6118	0.0224	25.4
	3193	0.0280	15.1		3020	0.0368	20.7
	1484	0.0460	11.6		1448	0.0614	16.9
	628	0.0797	8.72		648	0.107	13.7
	309	0.124	6.92		312	0.176	11.6
	140	0.203	5.44		152	0.284	10.2
	65.7	0.318	4.46				
	30.3	0.490	3.88		10771	0.0122	21.5
	10.3	0.801	3.67		6401	0.0170	17.7
	5.46	0.942	3.66		3230	0.0263	13.8
					1456	0.0433	10.2
					653	0.0710	7.63
					315	0.111	5.94
200	10202	0.0139	24.9	-100	10771	0.0122	21.5
	6197	0.0195	21.2		6401	0.0170	17.7
	3038	0.0315	16.9		3230	0.0263	13.8
	1450	0.0517	13.4		1456	0.0433	10.2
	647	0.0882	10.5		653	0.0710	7.63
	322	0.139	8.58		315	0.111	5.94
	150	0.226	6.97		105	0.216	4.30
	65.5	0.372	5.73		62.4	0.294	3.83
	26.2	0.603	4.70		23.9	0.511	3.42
	10.4	0.850	3.96		10.4	0.767	3.48
	5.48	0.959	3.74		5.49	0.930	3.60
400	10071	0.0147	26.6				
	6149	0.0207	22.8				
	3026	0.0336	18.4				
	1448	0.0555	14.8				
	697	0.0911	12.0				
	312	0.156	9.71				
	121	0.286	7.84				
	58.2	0.444	6.82				
	20.8	0.725	5.12				
	10.2	0.888	4.14				
	5.35	0.970	3.77				

Table 18. Variable Property Mean Temperature and Local
Nusselt Number Calculations for Liquids
Entrance Profile: Parabolic
Viscosity Ratio: 2

Fc	Pe_M/z^*	T_M	Nu	Fc	Pe_M/z^*	T_M	Nu
±0.1	10848	0.0144	26.5	800	10571	0.0173	34.7
	6430	0.0203	22.1		6078	0.0257	29.4
	3005	0.0330	16.8		3005	0.0423	24.0
	1499	0.0514	13.1		1550	0.0670	19.9
	689	0.0836	9.92		750	0.110	16.5
	312	0.136	7.54		501	0.145	15.0
	146	0.213	5.89		224	0.250	12.9
	67.0	0.333	4.72				
	30.3	0.508	4.03				
	14.9	0.704	3.78				
200	5.12	0.953	3.67	-100	10994	0.0136	25.0
					5914	0.0202	19.6
					3494	0.0281	15.9
					1569	0.0459	11.5
					746	0.0715	8.43
					349	0.111	6.22
					58.7	0.307	3.67
					29.6	0.450	3.35
					12.3	0.704	3.35
					5.03	0.939	3.57
400	10668	0.0154	29.3				
	6109	0.0224	24.4				
	3012	0.0361	19.4				
	1552	0.0561	15.7				
	729	0.0921	12.4				
	343	0.150	9.94				
	120	0.288	7.59				
	63.4	0.418	6.64				
	29.6	0.615	5.63				
	12.0	0.849	4.37				
400	5.02	0.974	3.77				
	10668	0.0161	31.5				
	6109	0.0237	26.4				
	3471	0.0350	22.1				
	1552	0.0604	17.4				
	750	0.0986	14.1				
	334	0.168	11.4				
	119	0.325	9.30				
	82.6	0.405	8.82				

Table 19. Variable Property Mean Temperature and Local
Nusselt Number Calculations for Liquids
Entrance Profile: Parabolic
Viscosity Ratio: 5

Fc	Pe_M/z^*	T_M	Nu	Fc	Pe_M/z^*	T_M	Nu
±0.1	10848	0.0171	31.7	800	10493	0.0207	41.8
	6437	0.0240	26.1		6060	0.0307	35.3
	3013	0.0386	19.6		3008	0.0502	28.6
	1505	0.0595	14.9		1557	0.0792	23.8
	658	0.0982	10.8		756	0.130	19.8
	349	0.142	8.52		370	0.211	17.1
	135	0.245	6.07				
	62.0	0.372	4.82	-100	10904	0.0162	29.7
	26.9	0.564	4.08		7122	0.0212	24.8
	12.1	0.783	3.80		3492	0.0328	18.1
	5.35	0.953	3.68		1455	0.0546	11.8
					808	0.0750	8.59
					479	0.0980	6.32
200	10585	0.0183	35.1				
	6089	0.0267	29.0				
	3226	0.0408	23.4				
	1494	0.0676	18.1				
	746	0.106	14.5				
	349	0.172	11.7				
	156	0.283	9.61				
	70.2	0.453	8.46				
	31.6	0.676	7.26				
	14.8	0.865	5.33				
400	5.10	0.983	3.84				
	10586	0.0192	37.8				
	6090	0.0282	31.6				
	3015	0.0457	25.2				
	1558	0.0712	20.6				
	756	0.115	16.7				
	352	0.190	13.8				
	151	0.328	12.0				

Table 20. Variable Property Mean Temperature and Local
Nusselt Number Calculations for Liquids
Entrance Profile: Parabolic
Viscosity Ratio: 10

Fc	Pe_M/z^*	T_M	Nu	Fc	Pe_M/z^*	T_M	Nu
±0.1	10420	0.0200	35.5	800	10421	0.0237	47.6
	6292	0.0276	29.0		6047	0.0350	40.1
	3104	0.0426	22.0		3016	0.0570	32.5
	1486	0.0668	16.0		1457	0.0940	26.5
	626	0.111	11.2		708	0.154	22.2
	323	0.160	8.66		515	0.191	20.9
	148	0.247	6.42	-100	10550	0.0188	33.0
	65.8	0.377	4.98		6144	0.0262	25.7
	30.2	0.550	4.21		3209	0.0383	18.5
	12.4	0.788	3.83		1590	0.0557	12.1
	5.79	0.947	3.70		1006	0.0684	8.30
200	10604	0.0208	40.0				
	6488	0.0291	33.5				
	3605	0.0429	27.2				
	1551	0.0742	20.4				
	726	0.120	16.0				
	302	0.210	12.6				
	82.6	0.461	10.5				
400	10511	0.0220	42.9				
	7123	0.0288	37.6				
	3020	0.0517	28.4				
	1456	0.0841	22.6				
	730	0.132	18.6				
	324	0.226	15.5				
	212	0.297	14.6				

Table 21. Variable Property Mean Temperature and Local
Nusselt Number Calculations for Liquids
Entrance Profile: Parabolic
Viscosity Ratio: 20

Fc	Pe_M/z^*	T_M	Nu	Fc	Pe_M/z^*	T_M	Nu
±0.1	10338	0.0229	39.5	-100	10906	0.0206	35.7
	6115	0.0317	31.4		6272	0.0287	27.8
	3072	0.0476	23.9		3142	0.0418	18.3
	1486	0.0726	16.8		1757	0.0528	10.8
	693	0.113	12.0				
	148	0.259	6.52				
	64.2	0.395	5.00				
	32.3	0.548	4.30				
	10.4	0.843	3.81				
	6.12	0.943	3.71				
200	10368	0.0243	43.8				
	6099	0.0344	36.1				
	3176	0.0523	28.6				
	1574	0.0818	22.5				
	720	0.134	17.7				
	347	0.213	14.7				
	122	0.410	12.9				
400	10542	0.0249	48.1				
	6481	0.0347	40.7				
	3131	0.0566	31.9				
	1492	0.0924	25.3				
	747	0.145	21.0				
	342	0.243	18.0				
	270	0.284	17.4				

Table 22. Variable Property Mean Temperature and Local
Nusselt Number Calculations for Gases
Entrance Profile: Parabolic
Viscosity Ratio: 0.5

Fc	Pe_M/z^*	T_M	Nu^*	Fc	Pe_M/z^*	T_M	Nu
±0.1	7551	0.0217	28.5	800	6446	0.0248	27.5
	2825	0.0398	18.2		2818	0.0417	19.7
	1389	0.0609	14.0		1349	0.0655	15.2
	791.1	0.0848	11.4		774.1	0.0915	12.6
	380.1	0.129	8.72		358.7	0.144	9.69
	106.6	0.259	5.57		102.5	0.289	6.45
	59.11	0.350	4.63		53.55	0.403	5.37
	26.36	0.515	3.83		25.38	0.570	4.46
	12.92	0.698	3.58		12.39	0.756	3.88
	2.08	0.997	3.65		2.18	0.997	3.65
200	6781	0.0234	27.0	-100	6784	0.0231	26.4
	2823	0.0403	18.6		2826	0.0395	18.0
	1414	0.0611	14.4		1390	0.0604	13.8
	798.8	0.0857	11.8		791.8	0.0841	11.2
	366.7	0.135	8.90		380.7	0.128	8.58
	104.8	0.267	5.76		106.9	0.256	5.47
	54.94	0.372	4.72		55.92	0.356	4.47
	26.05	0.529	3.96		26.46	0.509	3.76
	12.88	0.712	3.66		12.33	0.707	3.54
	2.10	0.998	3.65		2.12	0.997	3.65
400	6779	0.0236	27.4				
	2822	0.0408	19.0				
	1413	0.0620	14.8				
	840.5	0.0845	12.3				
	370.3	0.136	9.22				
	104.6	0.274	5.99				
	54.67	0.381	4.92				
	25.88	0.542	4.12				
	11.51	0.754	3.72				
	2.12	0.998	3.65				

Table 23. Variable Property Mean Temperature and Local
Nusselt Number Calculations for Gases
Entrance Profile: Parabolic
Viscosity Ratio: 0.75

Fc	Pe_M/z^*	T_M	Nu	Fc	Pe_M/z^*	T_M	Nu
±0.1	8179	0.0163	27.4	800	7720	0.0178	28.2
	4507	0.0248	19.2		4468	0.0265	21.4
	2512	0.0362	15.3		2615	0.0380	17.6
	1365	0.0532	12.3		1364	0.0582	14.3
	662.2	0.0834	9.58		663.5	0.0934	11.5
	268.0	0.144	7.07		252.9	0.173	8.83
	126.1	0.225	5.57		122.4	0.272	7.50
	61.75	0.335	4.56		58.86	0.420	6.79
	21.80	0.568	3.76		21.68	0.691	5.43
	10.37	0.776	3.63		10.57	0.866	4.22
	3.89	0.973	3.65		3.34	0.992	3.68
200	7722	0.0173	26.5	-100	7723	0.0170	25.7
	4507	0.0252	19.8		4508	0.0246	18.9
	2769	0.0347	16.4		2678	0.0343	15.4
	1364	0.0545	12.9		1342	0.0530	11.9
	626.0	0.0891	9.92		644.9	0.0834	9.22
	256.8	0.154	7.48		260.7	0.144	6.75
	120.8	0.241	5.99		122.2	0.223	5.27
	60.14	0.358	5.02		60.86	0.329	4.32
	23.51	0.576	4.22		23.85	0.531	3.61
	8.88	0.841	3.80		10.37	0.763	3.51
	3.71	0.981	3.67		3.56	0.979	3.64
400	7721	0.0174	27.1				
	4470	0.0257	20.3				
	2579	0.0370	16.5				
	1337	0.0566	13.2				
	660.7	0.0888	10.6				
	259.2	0.160	7.96				
	124.6	0.249	6.52				
	57.74	0.386	5.50				
	21.64	0.633	4.65				
	10.58	0.826	4.02				
	3.47	0.988	3.68				

Table 24. Variable Property Mean Temperature and Local
Nusselt Number Calculations for Gases
Entrance Profile: Parabolic
Viscosity Ratio: 1

Fc	Pe_M/z^*	T_M	Nu	Fc	Pe_M/z^*	T_M	Nu
± 0.1	7545	0.0222	29.6	800	7537	0.0231	31.6
	4401	0.0313	22.6		3219	0.0399	21.9
	2510	0.0440	18.1		1569	0.0623	17.0
	1265	0.0664	14.1		945.9	0.0848	14.3
	584.0	0.105	10.6		530.3	0.120	11.8
	225.0	0.179	7.54		161.9	0.237	8.04
	98.10	0.279	5.66		77.34	0.352	6.52
	43.30	0.419	4.41		38.15	0.501	5.59
	15.40	0.666	3.78		17.33	0.702	4.60
	7.12	0.873	3.73		9.55	0.852	4.07
	2.12	0.996	3.66		2.71	0.995	3.67
200	7543	0.0225	30.1	-100	7547	0.0221	29.3
	4632	0.0307	23.6		2969	0.0395	19.1
	2090	0.0500	17.4		1470	0.0602	14.7
	939.6	0.0807	13.1		878.1	0.0815	12.1
	369.3	0.139	9.37		429.3	0.123	9.32
	136.9	0.241	6.65		122.2	0.245	5.94
	50.00	0.403	4.88		62.60	0.345	4.79
	20.60	0.605	4.07		28.18	0.506	8.95
	8.13	0.852	3.81		12.93	0.707	3.68
	2.20	0.997	3.66		7.39	0.859	3.70
					2.10	0.998	3.65
400	7541	0.0227	30.6				
	4397	0.0321	23.6				
	2562	0.0440	19.2				
	1276	0.0680	15.0				
	604.1	0.106	11.6				
	221.7	0.190	8.17				
	102.5	0.288	6.35				
	45.62	0.433	5.05				
	14.80	0.709	4.11				
	6.98	0.896	3.83				
	2.17	0.997	3.66				

Table 25. Variable Property Mean Temperature and Local
Nusselt Number Calculations for Gases
Entrance Profile: Parabolic
Viscosity Ratio: 1.5

Fc	Pe_M/z^*	T_M	Nu	Fc	Pe_M/z^*	T_M	Nu
±0.1	6541	0.0134	21.6	800	2774	0.0290	17.0
	2718	0.0269	13.7		1415	0.0486	13.7
	1352	0.0437	10.5		699.1	0.0813	11.3
	694.2	0.0680	8.32		290.5	0.153	9.33
	280.8	0.122	6.20		150.0	0.247	8.68
	145.2	0.185	5.11		75.63	0.414	9.37
	71.77	0.288	4.30		59.66	0.499	10.5
	32.48	0.466	3.81				
	16.98	0.664	3.71		6541	0.0134	21.1
	7.24	0.908	3.68		2652	0.0269	13.1
					1365	0.0423	10.1
					648.6	0.0685	7.62
					285.0	0.115	8.54
					145.8	0.173	4.53
200	4511	0.0187	18.2	-100	73.39	0.261	3.67
	2759	0.0274	14.7		30.65	0.432	3.00
	1334	0.0461	11.3		16.55	0.601	2.85
	698.6	0.0719	9.22		6.93	0.869	3.09
	280.8	0.133	7.14				
	145.0	0.207	6.16				
	74.92	0.322	5.64				
	33.04	0.554	5.96				
	18.41	0.769	6.13				
	7.29	0.961	4.34				
400	6542	0.0135	23.5				
	2706	0.0285	15.4				
	1336	0.0478	12.1				
	674.6	0.0773	9.88				
	277.6	0.143	7.92				
	146.6	0.223	7.09				
	75.52	0.355	6.91				
	40.58	0.557	8.25				

Table 26. Variable Property Mean Temperature and Local
Nusselt Number Calculations for Gases
Entrance Profile: Parabolic
Viscosity Ratio: 2

Fc	Pe_M/z^*	T_M	Nu	Fc	Pe_M/z^*	T_M	Nu
±0.1	3318	0.0213	15.8	800	3350	0.0225	20.0
	1145	0.0461	9.96		1134	0.0541	13.4
	559.0	0.0745	7.62		572.0	0.0906	11.1
	263.2	0.122	5.93		267.2	0.159	9.56
	118.9	0.202	4.72		119.1	0.295	9.23
	61.43	0.308	4.11		61.55	0.514	11.9
	25.45	0.531	3.72				
	14.25	0.730	3.71	-100	3260	0.0214	15.0
	8.56	0.887	3.70		1169	0.0440	9.39
					545.7	0.0720	6.91
200	3329	0.0218	17.0		251.2	0.117	5.13
	1183	0.0474	11.1		109.8	0.192	3.78
	544.5	0.0817	8.64		93.00	0.211	3.55
	250.0	0.140	6.99				
	110.7	0.245	6.05				
	60.74	0.384	6.01				
	28.84	0.655	8.02				
400	3369	0.0219	18.2				
	1156	0.0502	12.0				
	539.6	0.0870	9.52				
	266.7	0.144	8.05				
	117.4	0.260	7.25				
	63.00	0.415	7.83				
	44.33	0.558	9.72				

Table 27. Variable Property Mean Temperature and Local
Nusselt Number Calculations for Liquids

Entrance Profile: Uniform

Viscosity Ratio: 0.1

Prandtl Number: 1

Fc	Pe_M/z^*	T_M	Nu	Fc	Pe_M/z^*	T_M	Nu
±0.1	3045	0.0544	13.1	800	3045	0.0547	14.3
	1117	0.0804	9.09		1174	0.0803	10.6
	479.6	0.116	6.78		505.9	0.119	8.31
	214.9	0.169	5.20		210.1	0.186	6.56
	100.2	0.247	4.14		94.16	0.287	5.45
	38.48	0.398	3.35		37.07	0.468	4.59
	20.10	0.547	3.16		18.74	0.644	3.96
	8.99	0.778	3.31		8.65	0.845	3.60
	3.93	0.963	3.59		3.93	0.975	3.63
200	3045	0.0544	13.4	-200	3045	0.0543	12.8
	1174	0.0790	9.61		1117	0.0799	8.71
	489.9	0.116	7.20		457.9	0.117	6.29
	216.9	0.172	5.58		204.0	0.170	4.75
	100.5	0.254	4.48		102.5	0.237	3.85
	38.41	0.414	3.62		38.93	0.382	3.11
	20.02	0.568	3.36		20.28	0.527	2.97
	8.97	0.794	3.39		8.56	0.777	3.24
	3.81	0.970	3.61		3.99	0.956	3.57
400	3045	0.0545	13.7				
	1174	0.0794	9.96				
	506.2	0.116	7.64				
	210.5	0.178	5.88				
	98.93	0.264	4.80				
	38.06	0.431	3.92				
	19.11	0.599	3.66				
	8.75	0.816	3.47				
	3.87	0.971	3.61				

Table 28. Variable Property Mean Temperature and Local
Nusselt Number Calculations for Liquids
Entrance Profile: Uniform
Viscosity Ratio: 0.5
Prandtl Number: 1

Fc	Pe_M/z^*	T_M	Nu	Fc	Pe_M/z^*	T_M	Nu
±0.1	3044	0.0571	16.9	800	3043	0.0580	18.7
	1131	0.0872	11.3		1168	0.0896	13.6
	502.8	0.127	8.34		488.2	0.139	10.5
	222.6	0.188	6.22		216.9	0.217	8.64
	116.1	0.259	5.03		112.7	0.314	7.74
	48.04	0.400	4.01		62.29	0.441	7.58
	24.26	0.553	3.63				
	9.46	0.812	3.58				
200				-200	3044	0.0568	16.4
					1131	0.0861	10.7
	3044	0.0573	17.4		487.0	0.125	7.55
	1130	0.0882	11.9		234.8	0.176	5.64
	502.7	0.129	8.97		106.6	0.256	4.24
	235.4	0.189	7.01		42.84	0.394	3.35
	113.3	0.275	5.69		21.44	0.547	3.12
	44.22	0.444	4.64		9.98	0.763	3.30
	22.56	0.610	4.18		4.44	0.954	3.59
	10.18	0.824	3.82				
400							
	3043	0.0575	17.8				
	1168	0.0878	12.6				
	488.4	0.134	9.47				
	210.4	0.207	7.42				
	112.4	0.290	6.38				
	50.28	0.443	5.56				
	22.41	0.651	4.77				
	10.53	0.847	4.02				
	4.42	0.976	3.70				

Table 29. Variable Property Mean Temperature and Local
Nusselt Number Calculations for Liquids
Entrance Profile: Uniform
Viscosity Ratio: 1
Prandtl Number: 1

Fc	Pe_M/z^*	T_M	Nu	Fc	Pe_M/z^*	T_M	Nu
±0.1	3078	0.0585	18.6	800	4007	0.0530	22.9
	1188	0.0891	12.6		1259	0.0908	15.3
	476.1	0.137	8.77		450.9	0.155	11.3
	222.8	0.198	6.63		224.5	0.230	9.69
	112.8	0.278	5.29		107.5	0.354	8.86
	43.25	0.444	4.13		74.64	0.440	9.05
	21.80	0.610	3.77				
	11.06	0.798	3.67	-100	3078	0.0584	18.3
200	5.40	0.948	3.66		1150	0.0898	12.0
					437.5	0.141	8.07
	3078	0.0588	19.2		227.6	0.192	6.22
	1189	0.0903	13.2		103.0	0.281	4.68
	458.1	0.143	9.44		46.57	0.410	3.76
	219.0	0.209	7.45		21.12	0.592	3.40
	107.0	0.304	6.13		11.42	0.763	3.44
	42.54	0.488	5.12		5.36	0.939	3.60
400	21.69	0.665	4.59				
	11.05	0.842	4.06				
	5.43	0.961	3.75				
	3078	0.0590	19.7				
	1189	0.0914	13.9				
	458.2	0.148	10.2				
	219.2	0.218	8.25				
	107.2	0.322	7.07				
	43.97	0.519	6.37				
	21.41	0.719	5.31				
	11.35	0.871	4.34				
	5.34	0.972	3.79				

Table 30. Variable Property Mean Temperature and Local
Nusselt Number Calculations for Liquids
Entrance Profile: Uniform
Viscosity Ratio: 5
Prandtl Number: 1

Fc	Pe_M/z^*	T_M	Nu	Fc	Pe_M/z^*	T_M	Nu
±0.1	6352	0.0431	34.4	800	6352	0.0434	35.8
	2928	0.0633	23.3		3040	0.0636	26.4
	1118	0.101	15.0		1088	0.110	18.5
	465.0	0.155	10.3		456.5	0.179	14.5
	214.1	0.227	7.61		217.5	0.278	12.7
	107.1	0.317	5.95		106.5	0.432	12.7
	42.33	0.491	4.62		97.21	0.458	12.9
	23.11	0.637	4.17				
	11.39	0.821	3.91		6352	0.0431	34.2
	5.25	0.961	3.74		2928	0.0630	22.9
200				-100	1192	0.0967	14.8
	6352	0.0432	34.7		486.9	0.148	9.75
	3040	0.0636	24.4		218.4	0.215	6.73
	1134	0.102	16.1		108.0	0.296	4.96
	450.5	0.165	11.6		44.02	0.441	3.65
	217.7	0.230	9.51		23.51	0.575	3.24
	107.1	0.353	7.91		11.16	0.765	3.13
	44.09	0.564	7.44		5.49	0.927	3.28
	22.97	0.755	7.02				
	11.40	0.914	5.22				
400	5.43	0.983	4.10				
	6352	0.0433	35.1				
	3040	0.0630	25.1				
	1088	0.106	16.8				
	443.4	0.172	12.6				
	216.3	0.256	10.6				
	110.6	0.376	9.68				
	63.20	0.520	10.1				

Table 31. Variable Property Mean Temperature and Local
Nusselt Number Calculations for Liquids
Entrance Profile: Uniform
Viscosity Ratio: 10
Prandtl Number: 1

Fc	Pe_M/z^*	T_M	Nu	Fc	Pe_M/z^*	T_M	Nu
±0.1	7131	0.0406	38.1	800	3288	0.0620	29.2
	3054	0.0631	25.7		1188	0.109	20.6
	1167	0.102	16.3		469.0	0.186	15.9
	441.0	0.166	10.7		223.8	0.291	14.0
	231.4	0.228	8.24		101.0	0.480	14.6
	116.9	0.317	6.43				
	51.74	0.465	5.06	-100	7131	0.0405	38.0
	23.43	0.654	4.37		3054	0.629	25.3
	11.87	0.828	4.07		1142	0.102	15.4
	5.70	0.958	3.85		453.2	0.158	9.80
					234.4	0.215	7.07
					113.3	0.297	5.00
200	7131	0.0406	38.4		45.87	0.437	3.55
	3134	0.0627	26.8		24.58	0.565	3.09
	1219	0.102	17.9				
	450.7	0.173	12.4				
	220.7	0.254	10.1				
	109.8	0.371	8.77				
	46.05	0.593	8.83				
	36.61	0.664	9.15				
400	7131	0.0407	38.7				
	3261	0.0618	27.9				
	1184	0.106	18.8				
	446.4	0.181	13.7				
	220.1	0.270	11.6				
	116.4	0.391	10.8				
	64.81	0.551	11.7				

Table 32. Variable Property Mean Temperature and Local
Nusselt Number Calculations for Liquids

Entrance Profile: Uniform

Viscosity Ratio: 20

Prandtl Number: 1

Fc	Pe_M/z^*	T_M	Nu	Fc	Pe_M/z^*	T_M	Nu
±0.1	7286	0.0399	39.5	-100	7286	0.0398	39.3
	3306	0.0612	28.0		3306	0.0610	27.7
	1160	0.106	17.3		1136	0.105	16.4
	445.8	0.171	11.3		457.7	0.163	10.1
	236.1	0.234	8.68		221.1	0.226	6.89
	120.5	0.325	6.78		119.9	0.295	5.00
	54.04	0.473	5.35		55.78	0.388	3.74
	25.97	0.648	4.64				
	13.43	0.834	4.30				
	6.25	0.956	4.03				
200	7286	0.0399	29.7				
	3307	0.0615	28.7				
	1199	0.106	18.9				
	454.3	0.179	13.2				
	225.4	0.263	10.8				
	113.7	0.384	9.59				
	53.24	0.584	9.92				
	41.79	0.665	10.6				
400	7286	0.0399	40.0				
	3307	0.0618	29.4				
	1200	0.108	20.1				
	455.2	0.187	14.7				
	226.4	0.279	12.5				
	121.1	0.404	11.9				
	68.39	0.568	13.0				

Table 33. Variable Property Mean Temperature and Local
Nusselt Number Calculations for Liquids

Entrance Profile: Uniform

Viscosity Ratio: 0.1

Prandtl Number: 10

Fc	Pe_M/z^*	T_M	Nu	Fc	Pe_M/z^*	T_M	Nu
±0.1	5265	0.0373	12.2	800	5524	0.0359	15.2
	1066	0.0676	7.26		1023	0.0719	9.72
	409.0	0.104	5.46		398.5	0.118	7.68
	81.90	0.240	3.72		87.62	0.285	5.55
200	5265	0.0370	13.0	-200	5726	0.0363	11.7
	989.1	0.0703	7.86		992.1	0.0685	6.28
	437.2	0.103	6.23		392.9	0.102	4.68
	82.98	0.253	4.16		83.91	0.222	3.33
400	5265	0.0368	13.7				
	1011	0.0705	8.57				
	413.6	0.110	6.73				
	85.89	0.262	4.64				

Table 34. Variable Property Mean Temperature and Local
 Nusselt Number Calculations for Liquids
 Entrance Profile: Uniform
 Viscosity Ratio: 0.5
 Prandtl Number: 10

Fc	Pe_M/z^*	T_M	Nu	Fc	Pe_M/z^*	T_M	Nu
±0.1	3417	0.0432	13.8	800	3413	0.0450	17.7
	1021	0.0732	9.05		1120	0.0785	13.2
	473.6	0.107	7.03		430.1	0.136	10.5
	92.10	0.256	4.49		96.92	0.339	8.21
200	4013	0.0407	15.8	-200	3417	0.0427	12.4
	1231	0.0691	10.9		1069	0.0691	7.64
	466.9	0.114	8.19		414.7	0.106	5.26
	91.86	0.284	5.47		90.38	0.227	3.53
400	3654	0.0430	16.3				
	1104	0.0753	11.5				
	446.9	0.123	9.06				
	90.85	0.311	6.40				

Table 35. Variable Property Mean Temperature and Local
 Nusselt Number Calculations for Liquids
 Entrance Profile: Uniform
 Viscosity Ratio: 1
 Prandtl Number: 10

Fc	Pe_M/z^*	T_M	Nu	Fc	Pe_M/z^*	T_M	Nu
±0.1	4258	0.0410	16.7	800	4110	0.0434	21.1
	1019	0.0777	9.92		1037	0.0885	14.6
	435.0	0.119	7.42		417.7	0.152	17.1
	233.7	0.165	6.11		209.3	0.235	10.5
	93.48	0.271	4.78		135.7	0.309	9.98
200	4460	0.0406	18.4	-100	4092	0.0415	15.7
	1107	0.0777	11.7		1054	0.0746	9.11
	415.0	0.131	8.79		419.1	0.116	6.39
	212.7	0.192	7.39		215.7	0.162	5.10
	90.26	0.315	6.09		94.39	0.249	4.09
400	4110	0.0425	19.1				
	1085	0.0814	12.8				
	412.1	0.140	9.96				
	217.0	0.205	8.63				
	96.39	0.334	7.44				

Table 36. Variable Property Mean Temperature and Local
Nusselt Number Calculations for Liquids

Entrance Profile: Uniform

Viscosity Ratio: 5

Prandtl Number: 10

Fc	Pe_M/z^*	T_M	Nu	Fc	Pe_M/z^*	T_M	Nu
±0.1	8862	0.0337	30.0	800	8242	0.0362	35.4
	4163	0.0467	21.9		4183	0.0504	28.7
	1089	0.0881	12.7		1064	0.109	19.9
	429.7	0.140	8.86		423.3	0.192	22.3
	209.3	0.203	6.87		253.7	0.268	15.7
	93.54	0.308	5.35				
200				-100	8862	0.0334	28.9
	8862	0.0341	31.8		4055	0.0466	20.3
	4335	0.0470	24.4		1077	0.0844	10.7
	1068	0.0854	15.2		412.6	0.130	14.3
	410.4	0.162	11.6		207.0	0.177	4.52
	212.1	0.238	9.97				
400	90.70	0.392	8.67				
	8242	0.0355	32.6				
	4182	0.0487	25.9				
	1096	0.0990	17.3				
	427.5	0.172	13.7				
	212.1	0.264	12.2				
	137.2	0.347	11.7				

Table 37. Variable Property Mean Temperature and Local
Nusselt Number Calculations for Liquids

Entrance Profile: Uniform

Viscosity Ratio: 10

Prandtl Number: 10

Fc	Pe_M/z^*	T_M	Nu	Fc	Pe_M/z^*	T_M	Nu
±0.1	10154	0.0330	35.6	800	11420	0.0325	44.5
	6175	0.0411	28.6		6356	0.0433	36.6
	1019	0.0969	13.2		1033	0.121	22.3
	375.7	0.160	8.89		383.2	0.226	18.8
	94.2	0.322	5.53		300.9	0.266	18.5
200	10673	0.0327	38.5	-100	11110	0.0315	35.8
	6630	0.0406	31.9		6795	0.0389	28.4
	3110	0.0587	24.0		1106	0.0872	11.0
	971.5	0.108	16.4		383.7	0.136	5.37
	304.5	0.211	12.1				
	135.4	0.342	10.6				
	78.9	0.471	10.3				
400	11179	0.0323	41.0				
	6279	0.0424	33.2				
	1098	0.107	19.3				
	367.0	0.207	15.1				
	167.7	0.340	16.7				

Table 38. Variable Property Mean Temperature and Local
Nusselt Number Calculations for Liquids

Entrance Profile: Uniform

Viscosity Ratio: 20

Prandtl Number: 10

Fc	Pe_M/z^*	T_M	Nu	Fc	Pe_M/z^*	T_M	Nu
±0.1	10429	0.0337	39.9	-100	10428	0.0334	38.4
	5828	0.0441	30.2		5827	0.0434	28.4
	1109	0.0981	14.5		1091	0.0901	10.5
	420.5	0.159	9.69		645.6	0.110	6.64
	99.38	0.326	5.74				
200	11137	0.0331	43.6				
	6282	0.0437	34.3				
	1072	0.110	18.4				
	451.9	0.181	14.8				
400	10483	0.0345	44.6				
	6070	0.0453	36.2				
	1104	0.115	21.3				
	432.5	0.203	17.5				

Table 39. Variable Property Mean Temperature and Local
Nusselt Number Calculations for Gases

Entrance Profile: Uniform

Viscosity Ratio: 0.5

Prandtl Number: 0.7

Fc	Pe_M/z^*	T_M	Nu	Fc	Pe_M/z^*	T_M	Nu
±0.1	2488	0.0718	19.1	800	3121	0.0662	22.4
	1140	0.101	13.7		1181	0.101	15.2
	490.8	0.146	9.82		530.9	0.146	11.4
	219.2	0.211	7.21		212.9	0.226	8.29
	99.30	0.303	5.45		96.51	0.329	6.42
	32.49	0.495	3.99		41.70	0.479	5.05
	11.19	0.754	3.58		15.37	0.712	3.98
	5.89	0.909	3.63		6.92	0.898	3.70
	2.11	0.997	3.65		2.23	0.997	3.66
200	2487	0.0720	19.4	-100	1698	0.0843	16.0
	1139	0.101	14.1		1141	0.100	13.6
	490.0	0.148	10.1		554.7	0.138	10.1
	218.5	0.215	7.48		219.5	0.210	7.08
	98.82	0.309	5.67		99.54	0.300	5.34
	42.74	0.448	4.42		43.16	0.434	4.17
	15.69	0.675	3.71		15.83	0.658	3.56
	6.98	0.879	3.64		7.01	0.869	3.60
	2.17	0.997	3.65		2.14	0.997	3.65
400	2486	0.0724	19.7				
	1182	0.100	14.6				
	563.5	0.140	11.0				
	219.7	0.217	7.79				
	98.75	0.314	5.92				
	42.54	0.458	4.61				
	15.60	0.687	3.80				
	6.97	0.885	3.66				
	2.14	0.997	3.65				

Table 40. Variable Property Mean Temperature and Local
Nusselt Number Calculations for Gases

Entrance Profile: Uniform

Viscosity Ratio: 0.75

Prandtl Number: 0.7

Fc	Pe_M/z^*	T_M	Nu	Fc	Pe_M/z^*	T_M	Nu
±0.1	2660	0.0663	18.7	800	2661	0.0675	20.3
	1249	0.0922	13.6		1165	0.0984	15.1
	557.2	0.133	9.88		486.5	0.151	11.4
	244.2	0.197	7.25		206.0	0.237	8.94
	112.5	0.285	5.54		99.81	0.347	7.63
	43.89	0.442	4.27		43.49	0.527	6.98
	16.71	0.668	3.69		15.79	0.785	4.71
	8.06	0.856	3.67		8.11	0.916	3.97
	3.64	0.980	3.65		3.39	0.991	3.69
200	2954	0.0637	20.0	-100	2661	0.0661	18.5
	1249	0.0930	14.1		1249	0.0918	13.3
	556.7	0.136	10.4		601.2	0.128	9.91
	232.2	0.207	7.66		240.4	0.196	6.93
	109.5	0.299	6.04		121.5	0.270	5.42
	50.01	0.435	4.86		60.98	0.372	4.38
	17.08	0.689	4.04		20.95	0.597	3.59
	8.15	0.872	3.77		10.88	0.769	3.53
	3.66	0.983	3.67		3.56	0.980	3.65
400	2662	0.0669	19.5				
	1249	0.0938	14.6				
	501.6	0.145	10.5				
	209.5	0.224	7.95				
	109.2	0.310	6.60				
	45.78	0.474	5.44				
	16.62	0.725	4.35				
	8.32	0.887	3.87				
	3.55	0.987	3.68				

Table 41. Variable Property Mean Temperature and Local
Nusselt Number Calculations for Gases
Entrance Profile: Uniform
Viscosity Ratio: 1
Prandtl Number: 0.7

Fc	Pe_M/z^*	T_M	Nu	Fc	Pe_M/z^*	T_M	Nu
±0.1	3121	0.0668	22.9	800	3320	0.0619	53.6
	1333	0.0968	15.8		1454	0.0903	34.9
	562.1	0.143	11.1		601.4	0.139	23.1
	251.0	0.207	8.08		287.9	0.204	10.2
	109.1	0.302	5.95		125.4	0.317	8.40
	42.61	0.456	4.49		59.98	0.468	7.71
	11.98	0.753	3.76		49.48	0.516	7.61
	5.45	0.932	3.71				
	2.14	0.998	3.66				
200				-100	3121	0.0666	22.7
					1333	0.0965	15.6
	3120	0.0671	23.3		562.7	0.142	10.9
	1332	0.0975	16.2		251.5	0.205	7.90
	530.1	0.148	11.2		109.4	0.298	5.80
	243.2	0.213	8.36		41.33	0.457	4.32
	106.9	0.311	6.24		13.66	0.712	3.70
	36.20	0.500	4.50		5.36	0.932	3.69
	13.65	0.732	3.91		2.12	0.998	3.66
	5.37	0.940	3.73				
	2.22	0.997	3.66				
400	3320	0.0614	22.4				
	1455	0.0889	16.0				
	602.2	0.135	11.7				
	288.8	0.195	9.13				
	134.8	0.287	7.28				
	51.55	0.461	5.80				
	20.88	0.680	4.84				
	7.74	0.909	3.92				
	3.66	0.987	3.69				

Table 42. Variable Property Mean Temperature and Local
Nusselt Number Calculations for Gases

Entrance Profile: Uniform

Viscosity Ratio: 1.5

Prandtl Number: 0.7

Fc	Pe_M/z^*	T_M	Nu	Fc	Pe_M/z^*	T_M	Nu
±0.1	6736	0.0346	39.2	800	6736	0.0346	39.7
	3201	0.0534	22.7		2978	0.0560	23.3
	1528	0.0773	15.2		1623	0.0773	17.7
	630.2	0.119	10.2		718.4	0.120	13.4
	299.7	0.172	7.55		324.1	0.188	10.9
	140.0	0.252	5.72		170.2	0.279	9.94
	65.64	0.369	4.73		111.4	0.366	9.97
	27.32	0.567	3.89		81.67	0.452	10.7
	13.32	0.770	3.73				
	7.06	0.921	3.68				
200				-100	6736	0.0346	38.1
					3201	0.0533	22.5
	6736	0.0346	39.3		1528	0.0770	14.9
	3202	0.0535	23.1		629.9	0.118	9.78
	1528	0.0780	15.8		323.9	0.162	7.25
	654.6	0.120	11.2		148.4	0.235	5.16
	326.5	0.172	8.75		66.85	0.343	3.92
	161.0	0.251	7.16		29.96	0.495	3.07
	100.7	0.326	6.51		16.01	0.654	2.90
	47.67	0.496	6.19		6.93	0.883	3.13
400							
	6736	0.0346	39.5				
	3945	0.0479	26.6				
	1622	0.0763	16.7				
	638.4	0.124	11.8				
	323.0	0.179	9.54				
	160.8	0.266	8.18				
	71.57	0.431	8.32				
	50.69	0.534	8.44				

Table 43. Variable Property Mean Temperature and Local
Nusselt Number Calculations for Gases
Entrance Profile: Uniform
Viscosity Ratio: 2
Prandtl Number: 0.7

Fc	Pe_M/z^*	T_M	Nu	Fc	Pe_M/z^*	T_M	Nu
±0.1	3432	0.0478	29.2	800	3528	0.0471	31.3
	1171	0.0857	14.7		1221	0.0868	17.5
	553.7	0.126	10.1		560.4	0.135	13.2
	266.2	0.182	7.36		273.4	0.208	11.1
	126.0	0.266	5.53		131.4	0.336	10.6
	66.81	0.366	5.21		83.83	0.467	12.1
	25.57	0.592	3.88				
	14.19	0.769	3.74	-100	3432	0.0477	29.0
200	8.77	0.896	3.70		2104	0.0628	20.6
					1147	0.0861	14.2
	3432	0.0478	29.6		491.9	0.120	9.96
	1172	0.0866	15.5		273.8	0.174	6.73
	572.7	0.127	11.2		153.2	0.228	5.06
	259.6	0.194	8.48		122.6	0.253	4.51
	133.0	0.282	7.20		65.90	0.335	3.74
	64.00	0.435	6.89		41.21	0.410	2.78
400	32.19	0.669	8.29				
	3528	0.0471	30.6				
	1350	0.0809	17.2				
	559.4	0.131	11.9				
	257.4	0.203	9.45				
	125.1	0.314	8.46				
	67.86	0.466	9.08				
	57.25	0.527	9.76				

APPENDIX H

VARIABLE PROPERTY TEMPERATURE AND
VELOCITY PROFILE CORRELATION

This appendix contains the correlated temperature and velocity profiles under the same conditions as found in Appendix G.

Table 44. (Continued)

r = 0.0			r = 0.2			r = 0.3			r = 0.4			r = 0.45			
Fc	Pe _L /z*	T	u	Pe _L /z*	T	u	Pe _L /z*	T	u	Pe _L /z*	T	u	Pe _L /z*	T	u
-200	10523	0.000	2.103	10523	0.000	1.783	10523	0.000	1.373	10513	0.004	0.662	9902	0.278	0.184
	6077	0.000	2.162	6077	0.000	1.840	6077	0.000	1.399	6040	0.028	0.594	5570	0.396	0.148
	3524	0.000	2.256	3534	0.000	1.919	3534	0.000	1.413	3462	0.095	0.508	3163	0.502	0.120
	1567	0.000	2.509	1567	0.000	2.072	1566	0.002	1.386	1480	0.262	0.380	1361	0.633	0.089
	696	0.000	2.898	696	0.000	2.224	691	0.034	1.280	632	0.433	0.291	691	0.728	0.072
	315	0.000	3.289	315	0.005	2.311	306	0.136	1.144	278	0.560	0.253	264	0.791	0.070
	146	0.000	3.579	144	0.042	2.298	137	0.272	1.051	126	0.653	0.256	121	0.836	0.081
	69.7	0.005	3.712	67.7	0.139	2.205	63.8	0.409	1.016	59.3	0.727	0.290	57.3	0.871	0.105
	24.1	0.142	3.376	22.8	0.378	2.007	21.7	0.605	1.056	20.6	0.821	0.388	20.2	0.916	0.164
	11.1	0.462	2.710	10.7	0.621	1.836	10.4	0.760	1.125	10.0	0.891	0.497	9.9	0.948	0.232
	4.0	0.916	1.979	4.0	0.939	1.609	4.0	0.960	1.185	4.0	0.982	0.642	3.9	0.991	0.332

Table 45. (Continued)

r = 0.0				r = 0.2				r = 0.3				r = 0.45			
Fc	Pe_L/z^*	T	u	Pe_L/z^*	T	u	Pe_L/z^*	T	u	Pe_L/z^*	T	u	Pe_L/z^*	T	u
400	10233	0.000	2.000	10233	0.000	1.680	10233	0.000	1.279	10233	0.000	0.717	10160	0.082	0.380
	6335	0.000	1.994	6335	0.000	1.674	6335	0.000	1.273	6334	0.001	0.7.8	6255	0.146	0.392
	3032	0.000	1.972	3032	0.000	1.652	3032	0.000	1.258	3029	0.011	0.732	2962	0.267	0.422
	1460	0.000	1.912	1462	0.000	1.604	1460	0.000	1.240	1453	0.053	0.770	1411	0.392	0.467
	708	0.000	1.774	708	0.000	1.519	708	0.001	1.226	699	0.142	0.840	677	0.508	0.525
	346	0.000	1.545	346	0.000	1.396	346	0.012	1.228	338	0.265	0.936	328	0.610	0.589
	125	0.000	1.048	124	0.014	1.182	124	0.111	1.292	120	0.468	1.083	117	0.735	0.671
	56.6	0.038	0.691	56.2	0.122	1.115	55.3	0.304	1.367	53.7	0.633	1.122	52.8	0.821	0.681
	21.3	0.386	1.137	21.1	0.505	1.336	20.8	0.653	1.329	20.5	0.832	0.944	20.3	0.919	0.549
	10.4	0.714	1.612	10.4	0.784	1.509	10.3	0.856	1.277	10.2	0.932	0.801	10.2	0.968	0.445
800	4.6	0.948	1.889	4.6	0.962	1.611	4.6	0.975	1.248	4.6	0.988	0.716	4.6	0.994	0.382
	10906	0.000	1.981	10906	0.000	1.662	10906	0.000	1.262	10906	0.000	0.718	10858	0.051	0.415
	6754	0.000	1.966	6754	0.000	1.646	6754	0.000	1.249	6754	0.000	0.726	6695	0.100	0.442
	3269	0.000	1.915	3269	0.000	1.598	3269	0.000	1.221	3268	0.004	0.759	3212	0.202	0.503
	1249	0.000	1.727	1249	0.000	1.462	1249	0.000	1.180	1245	0.040	0.867	1211	0.357	0.622
	598	0.000	1.419	598	0.000	1.286	598	0.000	1.160	592	0.114	1.015	574	0.473	0.739
-200	288	0.000	0.962	288	0.000	1.043	288	0.009	1.166	282	0.228	1.211	274	0.579	0.865
	110	0.003	0.064	110	0.014	0.652	109	0.087	1.279	106	0.419	1.490	103	0.705	1.015
	11712	0.000	2.040	11712	0.000	1.720	11712	0.000	1.318	11712	0.000	1.047	11567	0.144	0.296
	6872	0.000	2.066	6872	0.000	1.746	6872	0.000	1.335	6869	0.004	0.686	6721	0.255	0.266
	3068	0.000	2.143	3068	0.000	1.813	3068	0.000	1.358	3053	0.056	0.620	2954	0.435	0.215
	1366	0.000	2.312	1366	0.000	1.922	1366	0.001	1.363	1342	0.209	0.522	1297	0.592	0.164

Table 46. (Continued)

		r = 0.0				r = 0.2				r = 0.3				r = 0.4				r = 0.45			
		Fc		Pe _L /z*		T		u		Pe _L /z*		T		u		Pe _L /z*		T		u	
		11571	0.000	1.916	11571	0.000	1.618	11571	0.000	1.253	11571	0.000	0.751	11614	0.035	0.450					
		7218	0.000	1.877	7218	0.000	1.594	7218	0.000	1.246	7218	0.000	0.766	7276	0.076	0.476					
		3477	0.000	1.798	3477	0.000	1.545	3477	0.000	1.232	3478	0.002	0.800	3541	0.174	0.528					
		1344	0.000	1.640	1344	0.000	1.448	1344	0.000	1.209	1349	0.034	0.876	1392	0.334	0.621					
		641	0.000	1.451	641	0.000	1.335	641	0.000	1.191	648	0.111	0.972	672	0.460	0.710					
		307	0.000	1.176	307	0.000	1.180	307	0.011	1.185	314	0.231	1.102	326	0.575	0.808					
		107	0.002	0.588	107	0.020	0.915	108	0.112	1.249	112	0.446	1.316	115	0.718	0.934					
		62.4	0.040	0.326	62.8	0.096	0.848	63.7	0.242	1.314	65.9	0.569	1.372	67.3	0.786	0.946					
		24.1	0.408	0.750	24.4	0.495	1.138	24.7	0.625	1.370	25.1	0.809	1.168	25.4	0.908	0.740					
		10.1	0.791	1.550	10.1	0.840	1.519	10.2	0.892	1.349	10.2	0.949	0.894	10.3	0.975	0.511					
		5.3	0.946	1.923	5.3	0.960	1.673	5.4	0.974	1.325	5.4	0.988	0.780	5.4	0.994	0.421					
		9969	0.000	1.837	9969	0.000	1.562	9969	0.000	1.230	9969	0.000	0.779	9998	0.027	0.511					
		6104	0.000	1.765	6104	0.000	1.518	6104	0.000	1.217	6104	0.000	0.806	6144	0.064	0.559					
		3008	0.000	1.630	3008	0.000	1.434	3008	0.000	1.193	3009	0.002	0.863	3055	0.147	0.649					
		1438	0.000	1.429	1438	0.000	1.308	1438	0.000	1.160	1440	0.015	0.956	1478	0.260	0.774					
		690	0.000	1.136	690	0.000	1.129	690	0.000	1.123	694	0.062	1.102	718	0.383	0.929					
		332	0.000	0.709	332	0.000	0.880	332	0.003	1.094	338	0.153	1.312	350	0.500	1.108					
		161	0.000	0.087	161	0.002	0.551	162	0.029	1.110	166	0.280	1.583	172	0.608	1.297					
		9733	0.000	2.036	9734	0.000	1.706	9734	0.000	1.291	9734	0.000	0.707	9852	0.116	0.351					
		5843	0.000	2.054	5843	0.000	1.718	5843	0.000	1.294	5844	0.003	0.699	5971	0.209	0.339					
		3467	0.000	2.080	3467	0.000	1.734	3467	0.000	1.299	3474	0.018	0.687	3583	0.316	0.324					
		1562	0.000	2.138	1562	0.000	1.768	1562	0.000	1.306	1579	0.103	0.659	1641	0.477	0.297					

Table 47. Variable Property Velocity and Temperature
Profile Calculations for Liquids
Entrance Profile: Parabolic
Viscosity Ratio: 2

<hr/>																			
$r = 0.0$				$r = 0.2$				$r = 0.3$				$r = 0.4$				$r = 0.45$			
F_c	Pe_L/z^*	T	u	Pe_L/z^*	T	u	Pe_L/z^*	T	u	Pe_L/z^*	T	u	Pe_L/z^*	T	u				
<hr/>																			
±0.1	10842	0.000	1.893	10842	0.000	1.608	10842	0.000	1.251	10842	0.000	0.758	10860	0.044	0.460				
	6425	0.000	1.874	6425	0.000	1.595	6425	0.000	1.250	6424	0.000	0.769	6450	0.106	0.473				
	3282	0.000	1.848	3282	0.000	1.580	3282	0.000	1.248	3283	0.006	0.783	3310	0.222	0.485				
	1365	0.000	1.814	1365	0.000	1.562	1365	0.000	1.248	1368	0.061	0.805	1385	0.401	0.494				
	687	0.000	1.790	687	0.000	1.551	687	0.002	1.253	692	0.169	0.818	701	0.532	0.492				
	345	0.000	1.773	345	0.000	1.547	345	0.024	1.262	349	0.315	0.823	353	0.644	0.482				
	131	0.000	1.767	131	0.023	1.558	132	0.156	1.282	134	0.526	0.815	135	0.767	0.461				
	59.7	0.020	1.790	60.0	0.134	1.584	60.5	0.350	1.294	61.2	0.674	0.797	61.6	0.843	0.441				
	27.0	0.191	1.845	27.2	0.368	1.620	27.4	0.570	1.298	27.6	0.796	0.774	27.7	0.902	0.421				
	12.8	0.543	1.922	12.8	0.659	1.656	12.9	0.775	1.296	12.9	0.895	0.752	13.0	0.950	0.403				
5.3	0.905	1.998	5.3	0.930	1.688	5.3	0.954	1.293	5.4	0.978	0.732	5.4	0.990	0.387					
<hr/>																			
200	12382	0.000	1.858	12382	0.000	1.577	12382	0.000	1.235	12382	0.000	0.771	12391	0.019	0.494				
	7714	0.000	1.812	7714	0.000	1.550	7714	0.000	1.229	7714	0.000	0.788	7729	0.052	0.522				
	3008	0.000	1.706	3008	0.000	1.484	3008	0.000	1.212	3008	0.003	0.834	3028	0.180	0.590				
	1438	0.000	1.595	1438	0.000	1.417	1438	0.000	1.196	1440	0.027	0.887	1454	0.313	0.654				
	672	0.000	1.443	672	0.000	1.325	672	0.005	1.180	675	0.105	0.963	684	0.453	0.728				
	314	0.000	1.236	314	0.000	1.207	314	0.012	1.171	317	0.238	1.063	321	0.580	0.808				
	143	0.000	0.948	143	0.009	1.062	143	0.080	1.186	145	0.406	1.184	146	0.694	0.883				
	62.5	0.032	0.634	62.6	0.103	0.949	63.0	0.264	1.245	63.8	0.590	1.279	64.3	0.797	0.912				
	23.5	0.389	0.826	23.6	0.490	1.130	23.7	0.628	1.324	23.9	0.813	1.148	24.0	0.910	0.742				
	5.0	0.952	1.892	5.0	0.964	1.645	5.0	0.977	1.301	5.0	0.989	0.765	5.0	0.995	0.413				
<hr/>																			

Table 47. (Continued)

		r = 0.0				r = 0.2				r = 0.3				r = 0.4				r = 0.45			
Fc	Pe _L /z*	T	u	Pe _L /z*	T	u	Pe _L /z*	T	u	Pe _L /z*	T	u	Pe _L /z*	T	u	Pe _L /z*	T	u			
400	12382	0.000	1.821	12382	0.000	1.549	12382	0.000	1.222	12382	0.000	0.782	12387	0.013	0.523						
	6104	0.000	1.722	6104	0.000	1.490	6104	0.000	1.206	6104	0.000	0.819	6116	0.056	0.581						
	3008	0.000	1.601	3008	0.000	1.414	3008	0.000	1.184	3008	0.001	0.869	3024	0.142	0.666						
	1438	0.000	1.434	1438	0.000	1.309	1438	0.000	1.156	1439	0.016	0.945	1452	0.264	0.772						
	690	0.000	1.203	690	0.000	1.167	690	0.000	1.124	692	0.069	1.056	700	0.394	0.900						
	332	0.000	0.885	332	0.000	0.978	332	0.005	1.096	334	0.172	1.210	339	0.519	1.047						
800	153	0.000	0.409	154	0.004	0.720	154	0.045	1.091	155	0.322	1.424	157	0.637	1.210						
	90.8	0.015	0.031	90.8	0.035	0.542	91.1	0.123	1.122	92.2	0.440	1.572	93.1	0.711	1.295						
	10565	0.000	1.731	10565	0.000	1.486	10565	0.000	1.196	10565	0.000	0.812	10569	0.010	0.588						
	6665	0.000	1.637	6665	0.000	1.429	6665	0.000	1.179	6665	0.000	0.845	6672	0.028	0.648						
	3212	0.000	1.457	3212	0.000	1.316	3212	0.000	1.145	3212	0.000	0.915	3223	0.090	0.770						
	1220	0.000	1.117	1220	0.000	1.099	1220	0.000	1.082	1220	0.010	1.060	1230	0.228	0.996						
-100	598	0.000	0.748	598	0.000	0.870	598	0.000	1.023	599	0.048	1.231	605	0.348	1.216						
	222	0.000	0.028	222	0.000	0.405	222	0.000	0.944	223	0.172	1.602	226	0.514	1.595						
	10988	0.000	1.931	10988	0.000	1.633	10988	0.000	1.263	10988	0.000	0.747	11011	0.056	0.434						
	6471	0.000	1.926	6471	0.000	1.632	6471	0.000	1.265	6471	0.000	0.751	6503	0.134	0.433						
	2929	0.000	1.939	2929	0.000	1.643	2929	0.000	1.272	2930	0.016	0.752	2961	0.301	0.415						
	1271	0.000	1.986	1271	0.000	1.676	1271	0.000	1.287	1276	0.112	0.735	1294	0.487	0.370						
	744	0.000	2.042	744	0.000	1.714	744	0.003	1.302	751	0.226	0.708	761	0.591	0.330						
	320	0.000	2.180	320	0.001	1.801	321	0.055	1.324	325	0.428	0.635	328	0.719	0.259						
	129	0.000	2.376	130	0.036	1.910	130	0.222	1.321	132	0.605	0.549	133	0.811	0.201						
	52.3	0.026	2.548	52.6	0.182	1.976	53.1	0.429	1.291	53.7	0.730	0.503	53.9	0.872	0.184						
	21.4	0.235	2.557	21.5	0.431	1.947	21.7	0.628	1.267	21.8	0.829	0.529	21.9	0.918	0.220						
12.2	0.494	2.433	12.2	0.630	1.876	12.3	0.761	1.266	12.4	0.890	0.585	12.4	0.948	0.270							
5.2	0.881	2.135	5.2	0.913	1.742	5.2	0.943	1.283	5.2	0.974	0.690	5.2	0.987	0.355							

Table 48. Variable Property Velocity and Temperature
Profile Calculations for Liquids
Entrance Profile: Parabolic
Viscosity Ratio: 5

<hr/>															
$r = 0.0$				$r = 0.2$				$r = 0.3$				$r = 0.45$			
F_c	Pe_L/z^*	T	u	Pe_L/z^*	T	u	Pe_L/z^*	T	u	Pe_L/z^*	T	u	Pe_L/z^*	T	u
± 0.1	11920	0.000	1.759	11920	0.000	1.509	11920	0.000	1.208	11920	0.000	0.805	11936	0.013	0.566
	6990	0.000	1.702	6990	0.000	1.478	6990	0.000	1.204	6990	0.000	0.828	7024	0.047	0.600
	3281	0.000	1.640	3281	0.000	1.443	3281	0.000	1.199	3282	0.002	0.860	3335	0.154	0.634
	1365	0.000	1.579	1365	0.000	1.410	1365	0.000	1.200	1370	0.038	0.902	1414	0.340	0.655
	651	0.000	1.542	651	0.000	1.396	651	0.002	1.212	661	0.144	0.931	686	0.500	0.644
	309	0.000	1.527	309	0.001	1.399	310	0.026	1.236	319	0.307	0.938	330	0.634	0.612
	145	0.000	1.540	145	0.017	1.428	147	0.128	1.271	153	0.488	0.922	157	0.744	0.566
	66.3	0.017	1.595	67.0	0.116	1.487	68.4	0.319	1.302	70.7	0.649	0.884	72.0	0.830	0.516
	22.9	0.281	1.745	23.3	0.444	1.591	23.7	0.623	1.320	24.2	0.821	0.820	24.4	0.914	0.455
	10.6	0.661	1.915	10.7	0.747	1.667	10.8	0.833	1.320	10.9	0.922	0.775	11.0	0.963	0.418
200	5.3	0.915	2.021	5.3	0.937	1.713	5.4	0.959	1.317	5.4	0.981	0.749	5.4	0.991	0.397
	10565	0.000	1.687	10565	0.000	1.458	10565	0.000	1.187	10565	0.000	0.827	10575	0.009	0.617
	6665	0.000	1.610	6665	0.000	1.414	6665	0.000	1.176	6665	0.000	0.855	6686	0.030	0.664
	3212	0.000	1.488	3212	0.000	1.339	3212	0.000	1.156	3212	0.000	0.906	3248	0.106	0.745
	1483	0.000	1.340	1483	0.000	1.246	1483	0.000	1.132	1485	0.012	0.973	1520	0.236	0.842
	682	0.000	0.153	682	0.000	1.132	682	0.000	1.105	687	0.068	1.063	710	0.385	0.954
	316	0.000	0.915	316	0.000	0.987	316	0.008	1.077	322	0.185	1.182	332	0.525	1.084
	139	0.000	0.567	140	0.009	0.785	140	0.065	1.053	145	0.354	1.361	149	0.655	1.239
	59.9	0.074	0.139	60.2	0.122	0.569	61.0	0.249	1.086	62.9	0.554	1.567	64.4	0.774	1.337
	26.5	0.479	0.235	26.6	0.522	0.748	26.9	0.618	1.260	27.4	0.793	1.462	27.6	0.898	1.074
	11.9	0.812	1.047	12.0	0.849	1.276	12.0	0.893	1.363	12.1	0.948	1.077	12.1	0.975	0.666
	5.6	0.960	1.802	5.7	0.970	1.624	5.7	0.980	1.333	5.7	0.990	0.818	5.7	0.996	0.451

Table 49. (Continued)

		r = 0.0				r = 0.2				r = 0.3				r = 0.4				r = 0.45			
Fc	Pe _L /z*	T	u	Pe _L /z*	T	u	Pe _L /z*	T	u	Pe _L /z*	T	u	Pe _L /z*	T	u	Pe _L /z*	T	u	Pe _L /z*	T	u
400	11237	0.000	1.517	11237	0.000	1.335	11237	0.000	1.130	11237	0.000	0.876	11240	0.001	0.736						
	7086	0.000	1.394	7086	0.000	1.264	7086	0.000	1.112	7086	0.000	0.917	7096	0.008	0.808						
	3446	0.000	1.208	3446	0.000	1.147	3446	0.000	1.076	3446	0.000	0.985	3473	0.044	0.931						
	1297	0.000	0.913	1297	0.000	0.957	1297	0.000	1.014	1298	0.005	1.097	1335	0.165	1.141						
	615	0.000	0.620	615	0.000	0.766	615	0.000	0.949	619	0.035	1.210	648	0.293	1.368						
	218	0.000	0.031	218	0.000	0.375	218	0.009	0.808	224	0.154	1.467	237	0.476	1.848						
800	12000	0.000	1.454	12000	0.000	1.285	12000	0.000	1.103	12000	0.000	0.892	12000	0.000	0.783						
	6009	0.000	1.212	6009	0.000	1.140	6009	0.000	1.061	6009	0.000	0.970	6015	0.005	0.925						
	3717	0.000	1.039	3717	0.000	1.030	3717	0.000	1.025	3717	0.000	1.029	3730	0.020	1.038						
	1433	0.000	0.627	1433	0.000	0.761	1433	0.000	0.930	1433	0.001	1.173	1458	0.098	1.326						
	894	0.000	0.371	894	0.000	0.592	894	0.000	0.870	895	0.006	1.262	920	0.160	1.517						
	543	0.000	0.045	543	0.000	0.376	543	0.000	0.790	545	0.020	1.377	566	0.238	1.774						
-100	12184	0.000	1.676	12184	0.000	1.451	12184	0.000	1.186	12184	0.000	0.834	12199	0.007	0.628						
	7451	0.000	1.623	7451	0.000	1.426	7451	0.000	1.186	7451	0.000	0.858	7497	0.034	0.658						
	3187	0.000	1.597	3187	0.000	1.420	3187	0.000	1.200	3189	0.003	0.892	3292	0.184	0.666						
	1276	0.000	1.688	1276	0.000	1.500	1276	0.000	1.265	1298	0.095	0.909	1386	0.475	0.509						

Table 50. Variable Property Velocity and Temperature
Profile Calculations for Liquids
Entrance Profile: Parabolic
Viscosity Ratio: 20

±0.1	10273	0.000	1.476	10273	0.000	1.316	10273	0.000	1.131	10273	0.000	0.894	10284	0.004	0.759
	6062	0.000	1.398	6062	0.000	1.275	6062	0.000	1.127	6062	0.000	0.927	6102	0.024	0.807
	3319	0.000	1.335	3319	0.000	1.239	3319	0.000	1.121	3320	0.000	0.958	3396	0.084	0.848
	1332	0.000	1.293	1332	0.000	1.222	1332	0.000	1.134	1341	0.025	1.009	1438	0.283	0.868
	612	0.000	1.287	612	0.000	1.232	612	0.002	1.163	634	0.130	1.044	694	0.473	0.829
	314	0.000	1.298	314	0.001	1.253	316	0.024	1.196	338	0.275	1.051	368	0.603	0.778
	138	0.000	1.359	139	0.022	1.323	143	0.135	1.259	157	0.482	1.026	167	0.739	0.680
	58.3	0.035	1.476	60.2	0.150	1.431	63.5	0.352	1.320	68.8	0.665	0.966	71.7	0.837	0.589
	23.1	0.304	1.694	24.0	0.457	1.581	25.1	0.627	1.361	26.4	0.821	0.888	27.0	0.914	0.506
	10.6	0.696	1.948	10.8	0.772	1.716	11.0	0.848	1.378	11.2	0.929	0.823	11.3	0.966	0.448
	6.1	0.898	2.086	6.1	0.924	1.781	6.1	0.950	1.381	6.2	0.977	0.792	6.2	0.989	0.422
200	11040	0.000	1.424	11040	0.000	1.274	11040	0.000	1.108	11040	0.000	0.905	11044	0.001	0.796
	6629	0.000	1.304	6629	0.000	1.206	6629	0.000	1.092	6629	0.000	0.947	6645	0.009	0.865
	3130	0.000	1.156	3130	0.000	1.115	3130	0.000	1.066	3130	0.000	1.004	3178	0.056	0.965
	1431	0.000	0.997	1431	0.000	1.013	1431	0.000	1.034	1433	0.005	1.066	1496	0.163	1.083
	644	0.000	0.801	644	0.000	0.883	644	0.000	0.987	652	0.043	1.138	699	0.307	1.253
	356	0.000	0.612	356	0.000	0.753	357	0.003	0.930	367	0.107	1.211	398	0.414	1.443
	121	0.040	0.400	121	0.013	0.339	122	0.056	0.743	130	0.290	1.531	141	0.593	1.999

Table 50. (Continued)

r = 0.0		r = 0.2		r = 0.3		r = 0.4		r = 0.45							
Fc	Pe_L/z^*	T	u	Pe_L/z^*	T	u	Pe_L/z^*	T	u	Pe_L/z^*	T	u			
400	11237	0.000	1.375	11237	0.000	1.236	11237	0.000	1.088	11237	0.000	0.917	11238	0.000	0.829
	7086	0.000	1.236	7086	0.000	1.156	7086	0.000	1.067	7086	0.000	0.962	7093	0.004	0.908
	3307	0.000	1.029	3307	0.000	1.026	3307	0.000	1.026	3307	0.000	1.034	3336	0.031	1.042
	1568	0.000	0.808	1568	0.000	0.881	1568	0.000	0.974	1569	0.001	1.108	1614	0.105	1.199
	718	0.000	0.522	718	0.000	0.689	718	0.000	0.898	722	0.018	1.197	762	0.222	1.435
-100	422	0.000	0.272	422	0.000	0.516	423	0.000	0.822	428	0.051	1.273	459	0.312	1.676
	250	0.000	0.044	250	0.000	0.292	251	0.004	0.715	258	0.104	1.387	278	0.400	2.010
	11669	0.000	1.552	11669	0.000	1.366	11669	0.000	1.151	11669	0.000	0.874	11682	0.004	0.715
	6851	0.000	1.489	6851	0.000	1.338	6851	0.000	1.154	6851	0.000	0.905	6905	0.028	0.752
	3908	0.000	1.476	3908	0.000	1.339	3908	0.000	1.169	3908	0.001	0.931	4033	0.116	0.763
	1987	0.000	1.546	1987	0.000	1.404	1987	0.000	1.225	2003	0.030	0.966	2181	0.349	0.657

Table 51. Variable Property Velocity and Temperature
Profile Calculations for Gases
Entrance Profile: Parabolic
Viscosity Ratio: 0.5

$r = 0.0$				$r = 0.3$				$r = 0.4$				$r = 0.45$			
F_c	Pe_L/z^*	T	ρu	Pe_L/z^*	T	ρu	Pe_L/z^*	T	ρu	Pe_L/z^*	T	ρu	Pe_L/z^*	T	ρu
±0.1	7772	0.000	2.021	7772	0.000	1.703	7772	0.000	1.306	7601	0.016	0.734	5717	0.285	0.446
	1502	0.000	2.075	1502	0.000	1.757	1501	0.000	1.359	1164	0.227	0.621	868.0	0.635	0.259
	444.6	0.000	2.185	444.6	0.000	1.866	412.6	0.058	1.358	276.8	0.510	0.552	239.1	0.777	0.260
	84.1	0.005	2.613	69.6	0.167	1.883	54.4	0.464	1.173	45.8	0.766	0.573	43.3	0.892	0.287
	52.8	0.039	2.712	40.6	0.295	1.819	33.4	0.566	1.179	29.4	0.811	0.594	28.2	0.912	0.301
	9.3	0.649	2.174	8.8	0.756	1.727	8.4	0.847	1.258	8.1	0.931	0.679	8.0	0.967	0.352
200	2.1	0.995	2.000	2.1	0.996	1.679	2.1	0.997	1.278	2.1	0.998	0.718	2.1	0.999	0.379
	7772	0.000	2.019	7772	0.000	1.700	7772	0.000	1.303	7613	0.015	0.733	5754	0.277	0.309
	1530	0.000	2.062	1530	0.000	1.744	1529	0.000	1.346	1205	0.209	0.638	890.0	0.623	0.278
	455.3	0.000	2.141	455.2	0.000	1.822	427.8	0.048	1.344	287.1	0.490	0.588	246.0	0.767	0.288
	148.9	0.000	2.289	140.5	0.044	1.871	108.5	0.296	1.221	83.8	0.684	0.607	77.3	0.855	0.309
	59.5	0.026	2.413	46.7	0.252	1.767	37.9	0.531	1.217	32.9	0.795	0.643	31.3	0.905	0.332
400	20.9	0.298	2.235	17.6	0.532	1.727	15.9	0.715	1.250	14.8	0.874	0.674	14.4	0.941	0.351
	2.1	0.995	1.999	2.1	0.996	1.679	2.1	0.997	1.278	2.1	0.998	0.718	2.1	0.999	0.379
	7772	0.000	2.016	7772	0.000	1.698	7772	0.000	1.300	7625	0.014	0.731	5791	0.270	0.318
	1530	0.000	2.051	1530	0.000	1.732	1529	0.000	1.334	1219	0.197	0.651	894.6	0.614	0.296
	436.4	0.000	2.105	436.3	0.000	1.785	410.7	0.046	1.321	276.4	0.483	0.624	236.1	0.763	0.317
	106.5	0.001	2.172	95.1	0.092	1.743	73.3	0.370	1.241	59.0	0.719	0.678	55.1	0.870	0.356
	52.3	0.049	2.088	41.0	0.279	1.691	33.8	0.547	1.267	29.5	0.801	0.706	28.2	0.907	0.371
	20.5	0.320	2.013	17.6	0.539	1.688	15.9	0.717	1.278	14.8	0.875	0.712	14.4	0.941	0.374
	2.1	0.995	1.999	2.1	0.996	1.678	2.1	0.997	1.278	2.1	0.999	0.719	2.1	0.999	0.379

Table 51. (Continued)

$r = 0.0$		$r = 0.2$		$r = 0.3$		$r = 0.4$		$r = 0.45$	
Fc	Pe_L/z^*	T	ρu	Pe_L/z^*	T	ρu	Pe_L/z^*	T	ρu
800	7772	0.000	2.012	7772	0.000	1.294	7647	0.012	0.729
	1549	0.000	2.030	1549	0.000	1.312	1266	0.172	0.673
	689.3	0.000	2.035	689.3	0.000	1.716	478.8	0.355	0.673
	207.4	0.000	1.903	204.9	0.009	1.653	122.7	0.594	0.751
	99.3	0.002	1.787	89.1	0.088	1.531	55.4	0.708	0.813
	20.9	0.350	1.634	18.3	0.542	1.613	15.4	0.872	0.778
-100	2.2	0.995	1.998	2.2	0.996	1.678	2.2	0.998	0.719
	6995	0.000	2.025	6995	0.000	1.310	6813	0.019	0.734
	444.6	0.000	2.207	444.4	0.000	1.887	275.4	0.518	0.534
	114.7	0.000	2.586	101.6	0.098	1.973	63.4	0.734	0.534
	52.9	0.038	2.860	40.4	0.299	1.848	29.4	0.813	0.568
	10.3	0.596	2.253	9.6	0.723	1.744	8.9	0.923	0.665
-100	2.1	0.994	2.000	2.1	0.996	1.679	2.1	0.998	0.718
	5002	0.319	0.290	5002	0.319	0.290	5002	0.319	0.290
	238.7	0.780	0.246	238.7	0.780	0.246	238.7	0.780	0.246
	59.1	0.877	0.262	59.1	0.877	0.262	59.1	0.877	0.262
	28.2	0.913	0.284	28.2	0.913	0.284	28.2	0.913	0.284
	8.6	0.963	0.342	8.6	0.963	0.342	8.6	0.963	0.342
-100	2.2	0.999	0.379	2.2	0.999	0.379	2.2	0.999	0.379
	5866	0.256	0.335	5866	0.256	0.335	5866	0.256	0.335
	916.2	0.584	0.333	916.2	0.584	0.333	916.2	0.584	0.333
	384.8	0.700	0.358	384.8	0.700	0.358	384.8	0.700	0.358
	109.7	0.813	0.411	109.7	0.813	0.411	109.7	0.813	0.411
	51.5	0.865	0.443	51.5	0.865	0.443	51.5	0.865	0.443
-100	15.0	0.940	0.416	15.0	0.940	0.416	15.0	0.940	0.416
	2.2	0.999	0.379	2.2	0.999	0.379	2.2	0.999	0.379
	5866	0.256	0.335	5866	0.256	0.335	5866	0.256	0.335
	916.2	0.584	0.333	916.2	0.584	0.333	916.2	0.584	0.333
	384.8	0.700	0.358	384.8	0.700	0.358	384.8	0.700	0.358
	109.7	0.813	0.411	109.7	0.813	0.411	109.7	0.813	0.411

Table 53. Variable Property Velocity and Temperature
Profile Calculations for Gases
Entrance Profile: Parabolic
Viscosity Ratio: 1

r = 0.0			r = 0.2			r = 0.3			r = 0.4			r = 0.45			
Fc	Pe_L/z^*	T	ρu	Pe_L/z^*	T	ρu	Pe_L/z^*	T	ρu	Pe_L/z^*	T	ρu	Pe_L/z^*	T	ρu
±0.1	7777	0.000	2.016	7772	0.000	1.697	7772	0.000	1.300	7629	0.013	0.731	5807	0.267	0.317
	2658	0.000	2.037	2658	0.000	1.718	2658	0.000	1.321	2377	0.089	0.690	1641	0.523	0.292
	664.9	0.000	2.103	664.9	0.000	1.784	652.1	0.014	1.359	445.9	0.403	0.595	366.4	0.726	0.299
	132.5	0.000	2.331	122.5	0.061	1.861	94.1	0.329	1.187	74.1	0.700	0.621	68.7	0.862	0.328
	55.9	0.033	2.480	43.5	0.271	1.725	35.6	0.545	1.199	31.1	0.800	0.665	29.6	0.907	0.352
	20.9	0.297	2.173	17.7	0.520	1.678	16.0	0.713	1.256	14.8	0.873	0.708	14.4	0.940	0.375
	2.5	0.990	1.992	2.5	0.993	1.676	2.5	0.995	1.279	2.5	0.997	0.720	2.5	0.999	0.380
200	7772	0.000	2.013	7772	0.000	1.694	7772	0.000	1.296	7642	0.012	0.729	5854	0.258	0.326
	2229	0.000	2.033	2229	0.000	1.715	2229	0.000	1.316	1946	0.110	0.679	1359	0.543	0.311
	436.4	0.000	2.094	436.3	0.000	1.775	411.6	0.045	1.309	277.7	0.477	0.630	236.6	0.759	0.345
	88.6	0.004	2.193	75.8	0.133	1.686	59.1	0.417	1.207	48.7	0.741	0.719	45.7	0.880	0.396
	9.9	0.660	1.837	9.4	0.757	1.627	9.0	0.845	1.298	8.7	0.930	0.758	8.6	0.967	0.406
	2.2	0.994	1.993	2.2	0.996	1.677	2.2	0.997	1.279	2.2	0.998	0.720	2.2	0.999	0.380
400	7772	0.000	2.010	7772	0.000	1.691	7772	0.000	1.293	7654	0.011	0.727	5901	0.249	0.335
	2046	0.000	2.027	2046	0.000	1.707	2045	0.000	1.309	1775	0.116	0.678	1244	0.547	0.330
	910.8	0.000	2.040	910.8	0.000	1.721	907.4	0.002	1.318	665.3	0.293	0.645	517.3	0.667	0.355
	306.5	0.000	2.054	305.8	0.001	1.731	274.5	0.087	1.247	188.5	0.529	0.691	164.3	0.783	0.401
	68.0	0.016	1.874	55.8	0.190	1.530	44.5	0.466	1.258	37.6	0.762	0.823	35.6	0.890	0.465
	2.2	0.995	1.992	2.2	0.996	1.676	2.2	0.997	1.279	2.2	0.999	0.720	2.2	0.999	0.380

Table 54. Variable Property Velocity and Temperature
Profile Calculations for Gases
Entrance Profile: Parabolic
Viscosity Ratio: 1.5

r = 0.0				r = 0.2				r = 0.3			

Table 55. (Continued)

$r = 0.0$			$r = 0.2$			$r = 0.3$			$r = 0.4$			$r = 0.45$		
Fc	Pe_L/z^*	T	ρu	Pe_L/z^*	T	ρu	Pe_L/z^*	T	ρu	Pe_L/z^*	T	ρu	Pe_L/z^*	T
400	105.7	0.000	1.449	106.2	0.014	1.156	109.0	0.085	0.909	121.8	0.335	0.932	142.6	0.593
	52.7	0.020	0.802	53.7	0.071	0.691	56.1	0.180	0.764	63.9	0.440	1.257	75.0	0.671
	37.6	0.096	0.105	38.3	0.147	0.294	40.1	0.249	0.697	45.7	0.492	1.534	53.4	0.704
800	3323	0.000	1.968	3323	0.000	1.648	3323	0.000	1.248	3326	0.002	0.696	3452	0.103
	1113	0.000	1.917	1113	0.000	1.597	1113	0.000	1.197	1126	0.034	0.670	1230	0.249
	518.0	0.000	1.835	518.0	0.000	1.515	518.3	0.001	1.117	536.0	0.094	0.672	602.1	0.351
	235.1	0.000	1.655	235.1	0.000	1.336	236.4	0.016	0.965	251.9	0.179	0.741	288.8	0.449
	105.5	0.000	1.225	105.8	0.010	0.935	107.8	0.062	0.719	118.2	0.278	0.966	137.2	0.540
-100	54.0	0.021	0.241	54.7	0.055	0.221	56.4	0.135	0.482	62.9	0.369	1.418	73.6	0.615
	3236	0.000	1.986	3236	0.000	1.666	3236	0.000	1.266	3243	0.006	0.711	3443	0.163
	1051	0.000	1.975	1051	0.000	1.655	1051	0.000	1.255	1080	0.076	0.726	1234	0.369
	531.8	0.000	1.966	531.8	0.000	1.646	532.7	0.004	1.249	569.2	0.177	0.749	669.0	0.488
	218.6	0.000	1.957	218.8	0.002	1.639	222.8	0.053	1.270	253.5	0.347	0.773	302.4	0.627
	102.0	0.000	1.971	103.2	0.033	1.677	108.9	0.171	1.333	129.3	0.500	0.751	153.3	0.728
	85.7	0.002	1.983	87.2	0.051	1.699	92.8	0.207	1.351	110.9	0.534	0.736	131.1	0.749

Table 56. Variable Property Velocity and Temperature
Profile Calculations for Liquids
Entrance Profile: Uniform
Viscosity Ratio: 0.1
Prandtl Number: 1

$r = 0.0$				$r = 0.2$				$r = 0.3$				$r = 0.4$				$r = 0.45$			

Table 56. (Continued)

		r = 0.0				r = 0.2				r = 0.3				r = 0.4				r = 0.45			
Fc		Pe_L/z^*	T	u	Pe_L/z^*	T	u	Pe_L/z^*	T	u	Pe_L/z^*	T	u	Pe_L/z^*	T	u	Pe_L/z^*	T	u		
800	2621	0.000	1.250	2621	0.000	1.250	2621	0.000	1.250	2587	0.059	1.144	2408	0.385	0.587						
	740.9	0.000	1.350	740.9	0.000	1.350	739.7	0.007	1.341	705.5	0.224	0.989	650.4	0.586	0.454						
	135.4	0.000	1.352	134.6	0.027	1.389	130.7	0.162	1.390	120.2	0.538	0.885	113.8	0.776	0.426						
	49.4	0.063	0.933	48.2	0.182	1.399	46.0	0.395	1.459	42.8	0.703	0.863	41.3	0.959	0.424						
	19.9	0.374	1.520	19.3	0.515	1.573	18.6	0.673	1.299	17.9	0.846	0.719	17.5	0.927	0.366						
	3.9	0.954	1.891	3.9	0.966	1.575	9.8	0.978	1.190	3.9	0.989	0.664	3.9	0.995	0.349						
-200	2621	0.000	1.302	2621	0.000	1.302	2621	0.000	1.301	2573	0.085	1.120	2376	0.444	0.466						
	686.5	0.000	1.548	686.5	0.000	1.548	683.3	0.021	1.495	637.2	0.340	0.753	590.9	0.671	0.255						
	136.5	0.001	2.271	134.8	0.061	2.058	128.4	0.282	1.311	118.1	0.652	0.429	113.1	0.834	0.159						
	46.1	0.055	3.142	44.0	0.270	2.083	41.6	0.523	1.086	39.1	0.782	0.373	38.1	0.897	0.151						
	19.3	0.271	3.211	18.4	0.390	1.941	17.6	0.680	1.067	16.9	0.855	0.421	16.6	0.931	0.186						
	4.0	0.924	1.971	4.0	0.944	1.605	4.0	0.963	1.184	4.0	0.983	0.643	3.9	0.992	0.334						

Table 57. Variable Property Velocity and Temperature
Profile Calculations for Liquids
Entrance Profile: Uniform
Viscosity Ratio: 0.5
Prandtl Number: 1

r = 0.0			r = 0.2			r = 0.3			r = 0.4			r = 0.45			
Fc	Pe_L/z^*	T	u	Pe_L/z^*	T	u	Pe_L/z^*	T	u	Pe_L/z^*	T	u	Pe_L/z^*	T	u
±0.1	3059	0.000	1.165	3059	0.000	1.165	3-59	0.000	1.165	3053	0.020	1.139	2989	0.262	0.824
	719.4	0.000	1.310	719.4	0.000	1.310	719.0	0.005	1.303	706.4	0.208	1.020	684.2	0.569	0.543
	118.7	0.001	1.710	118.2	0.053	1.634	116.3	0.234	1.343	112.6	0.600	0.737	110.6	0.806	0.372
	40.5	0.090	2.068	39.9	0.272	1.724	39.1	0.501	1.261	38.2	0.764	0.663	37.8	0.887	0.336
	16.4	0.405	2.129	16.1	0.563	1.705	15.9	0.715	1.237	15.7	0.868	0.660	15.6	0.937	0.339
	4.8	0.916	1.967	4.8	0.938	1.640	4.8	0.959	1.241	4.8	0.981	0.693	3.8	0.991	0.364
200	3059	0.000	1.157	3059	0.000	1.157	3059	0.000	1.157	3054	0.019	1.134	2992	0.251	0.844
	719.4	0.000	1.270	719.4	0.000	1.270	719.1	0.004	1.266	707.8	0.185	1.050	685.7	0.545	0.610
	104.3	0.003	1.440	103.8	0.055	1.425	102.3	0.224	1.313	99.1	0.583	0.892	97.2	0.796	0.507
	36.3	0.129	1.407	35.8	0.287	1.446	35.2	0.496	1.317	34.4	0.755	0.866	34.0	0.883	0.487
	13.3	0.559	1.677	13.2	0.667	1.545	13.0	0.779	1.277	12.9	0.896	0.778	12.8	0.950	0.425
	4.4	0.948	1.918	4.4	0.961	1.621	4.4	0.974	1.244	4.4	0.988	0.706	4.4	0.994	0.374
400	3059	0.000	1.150	3059	0.000	1.150	3059	0.000	1.150	3054	0.017	1.130	2995	0.240	0.862
	610.0	0.000	1.244	610.0	0.000	1.244	609.7	0.005	1.240	599.7	0.195	1.061	581.2	0.550	0.663
	115.3	0.001	1.182	115.0	0.035	1.219	113.6	0.169	1.270	110.1	0.526	1.051	107.8	0.765	0.652
	42.1	0.109	0.755	41.7	0.226	1.142	41.0	0.418	1.361	40.0	0.705	1.091	39.4	0.857	0.657
	17.3	0.495	1.200	17.2	0.600	1.368	17.0	0.723	1.323	16.8	0.867	0.914	16.6	0.936	0.525
	4.7	0.949	1.881	4.7	0.962	1.607	4.7	0.975	1.247	4.7	0.988	0.717	4.6	0.994	0.382

Table 58. Variable Property Velocity and Temperature
Profile Calculations for Liquids
Entrance Profile: Uniform
Viscosity Ratio: 1
Prandtl Number: 1

	r = 0.0				r = 0.2				r = 0.3				r = 0.4				r = 0.45			
Fc	Pe _L /z*	T	u		Pe _L /z*	T	u		Pe _L /z*	T	u		Pe _L /z*	T	u		Pe _L /z*	T	u	
-0.1	3059	0.000	1.133		3059	0.000	1.133		3059	0.000	1.133		3063	0.013	1.120		3127	0.210	0.917	
	734.4	0.000	1.347		734.4	0.000	1.247		734.7	0.003	1.243		747.2	0.165	1.078		775.0	0.521	0.674	
	122.7	0.001	1.556		123.2	0.043	1.516		125.3	0.201	1.343		130.0	0.563	0.855		132.9	0.785	0.470	
	41.7	0.088	1.857		42.4	0.254	1.651		43.4	0.474	0.474		44.6	0.745	0.767		45.2	0.878	0.410	
	15.3	0.466	2.021		15.5	0.601	1.707		15.7	0.736	1.307		16.0	0.877	0.738		16.0	0.941	0.390	
	5.4	0.907	2.052		5.4	0.931	1.724		5.4	0.955	1.314		5.4	0.979	0.740		5.4	0.990	0.390	
200	3059	0.000	1.126		3059	0.000	1.126		3059	0.000	1.126		3063	0.012	1.115		3123	0.200	0.932	
	758.2	0.000	1.207		758.2	0.000	1.207		758.4	0.002	1.205		769.3	0.138	1.094		797.4	0.487	0.752	
	115.4	0.001	1.276		115.8	0.037	1.284		117.4	0.173	1.270		121.7	0.524	1.034		124.7	0.762	0.665	
	40.9	0.106	1.107		41.5	0.238	1.268		42.3	0.434	1.333		43.5	0.713	1.055		44.2	0.861	0.652	
	15.3	0.544	1.399		15.5	0.644	1.458		15.6	0.755	1.356		15.8	0.883	0.930		15.9	0.944	0.538	
	5.4	0.929	1.945		5.4	0.947	1.684		5.4	0.965	1.324		5.4	0.984	0.771		5.4	0.992	0.414	
400	3059	0.000	1.119		3059	0.000	1.119		3059	0.000	1.119		3062	0.011	1.110		3120	0.191	0.945	
	758.2	0.000	1.175		758.2	0.000	1.175		758.4	0.001	1.175		768.2	0.122	1.102		795.5	0.463	0.817	
	115.4	0.001	1.020		115.7	0.029	1.069		117.0	0.141	1.188		121.2	0.478	1.200		124.4	0.735	0.863	
	42.2	0.130	0.386		42.6	0.216	0.877		43.3	0.381	1.325		44.6	0.669	1.352		45.4	0.838	0.914	
	16.8	0.588	0.972		16.9	0.662	1.267		17.0	0.758	1.380		17.2	0.881	1.075		17.4	0.942	0.654	
	5.6	0.941	1.874		5.6	0.955	1.657		5.6	0.970	1.330		5.6	0.986	0.792		5.6	0.993	0.430	

Table 60. Variable Property Velocity and Temperature
Profile Calculations for Liquids
Entrance Profile: Uniform
Viscosity Ratio: 10
Prandtl Number: 1

	r = 0.0				r = 0.2				r = 0.3				r = 0.4				r = 0.45			
Fc	Pe_L/z^*	T	u	Pe_L/z^*	T	u	Pe_L/z^*	T	u	Pe_L/z^*	T	u	Pe_L/z^*	T	u	Pe_L/z^*	T	u		
±0.1	6324	0.000	1.045	6324	0.000	1.045	6324	0.000	1.045	6324	0.000	1.045	6325	0.000	1.045	6371	0.041	1.029		
	2247	0.000	1.062	2247	0.000	1.062	2247	0.000	1.062	2247	0.000	1.062	2250	0.007	1.060	2310	0.156	1.023		
	601.5	0.000	1.107	601.5	0.000	1.107	601.8	0.002	1.107	601.8	0.002	1.107	615.5	0.129	1.090	652.2	0.463	0.983		
	124.0	0.001	1.215	124.7	0.034	1.213	127.6	0.162	0.203	127.6	0.162	0.203	135.4	0.506	1.099	141.1	0.751	0.800		
	48.4	0.076	1.327	49.5	0.213	1.318	51.3	0.416	1.279	51.3	0.416	1.279	53.9	0.702	1.042	55.2	0.855	0.669		
200	20.3	0.399	1.492	20.8	0.533	1.457	21.3	0.679	1.344	21.3	0.679	1.344	21.9	0.846	0.954	22.2	0.926	0.560		
	5.7	0.924	1.859	5.7	0.943	1.679	5.7	0.962	1.368	5.7	0.962	1.368	5.7	0.982	0.816	5.7	0.991	0.440		
	6324	0.000	1.043	6324	0.000	1.043	6324	0.000	1.043	6324	0.000	1.043	6325	0.000	1.043	6370	0.040	1.029		
	2290	0.000	1.053	2290	0.000	1.053	2290	0.000	1.053	2290	0.000	1.053	2293	0.006	1.052	2349	0.142	1.027		
	658.4	0.000	1.061	658.4	0.000	1.061	658.6	0.001	1.061	658.6	0.001	1.061	669.2	0.091	1.066	706.4	0.401	1.050		
400	128.7	0.001	0.902	129.2	0.020	0.922	131.2	0.105	0.988	131.2	0.105	0.988	138.2	0.406	1.198	144.8	0.682	1.263		
	46.7	0.116	0.278	47.3	0.190	0.530	48.4	0.329	0.912	48.4	0.329	0.912	50.8	0.608	1.546	52.4	0.800	1.607		
	38.0	0.226	0.069	38.4	0.283	0.416	39.2	0.405	0.913	39.2	0.405	0.913	40.9	0.655	1.656	42.1	0.825	1.679		
	6324	0.000	1.041	6324	0.000	1.041	6324	0.000	1.041	6324	0.000	1.041	6325	0.000	1.041	6369	0.039	1.029		
	2359	0.000	1.046	2359	0.000	1.046	2359	0.000	1.046	2359	0.000	1.046	2361	0.005	1.045	2413	0.129	1.030		
	706.2	0.000	1.032	706.2	0.000	1.032	706.3	0.000	1.032	706.3	0.000	1.032	715.0	0.069	1.047	751.9	0.356	1.085		
	121.6	0.001	0.660	121.9	0.017	0.703	123.4	0.086	0.831	123.4	0.086	0.831	129.5	0.359	1.251	135.9	0.645	1.598		
	65.0	0.050	0.033	65.4	0.087	0.293	66.6	0.186	0.701	66.6	0.186	0.701	69.9	0.469	1.555	72.9	0.716	2.041		

Table 61. Variable Property Velocity and Temperature
Profile Calculations for Liquids
Entrance Profile: Uniform
Viscosity Ratio: 20
Prandtl Number: 1

r = 0.0			r = 0.2			r = 0.3			r = 0.4			r = 0.45			
Fc	Pe_L/z^*	T	u	Pe_L/z^*	T	u	Pe_L/z^*	T	u	Pe_L/z^*	T	u	Pe_L/z^*	T	u
±0.1	6425	0.000	1.040	6425	0.000	1.040	6425	0.000	1.040	6426	0.000	1.039	6489	0.036	1.029
	2373	0.000	1.050	2373	0.000	1.050	2373	0.000	1.050	2376	0.005	1.049	2457	0.129	1.029
	673.6	0.000	1.081	6736	0.000	1.081	673.8	0.001	1.081	691.4	0.095	1.075	751.2	0.410	1.028
	140.7	0.000	1.160	141.5	0.022	1.160	145.6	0.126	1.158	158.8	0.457	1.124	169.7	0.720	0.925
	54.1	0.056	1.244	55.9	0.177	1.243	58.8	0.371	1.235	63.4	0.668	1.119	66.1	0.837	0.796
	21.9	0.379	1.385	22.6	0.510	1.378	23.5	0.658	1.335	24.5	0.833	1.056	25.1	0.919	0.657
	6.2	0.918	1.718	6.2	0.938	1.639	6.2	0.958	1.422	6.3	0.980	0.901	6.3	0.990	0.469
200	6425	0.000	1.038	6425	0.000	1.038	6425	0.000	1.038	6426	0.000	1.038	6488	0.035	1.029
	2373	0.000	1.043	2373	0.000	1.043	2373	0.000	1.043	2375	0.004	1.042	2452	0.120	1.031
	707.5	0.000	1.042	707.5	0.000	1.042	707.6	0.000	1.042	721.4	0.071	1.049	778.6	0.358	1.066
	140.0	0.000	0.890	140.6	0.014	0.903	143.3	0.085	0.952	154.4	0.365	1.146	166.0	0.649	1.341
	51.9	0.083	0.319	52.9	0.152	0.504	54.8	0.283	0.810	58.8	0.562	1.461	62.0	0.771	1.822
	38.0	0.287	-0.060	38.2	0.314	0.270	39.2	0.409	0.767	41.5	0.640	1.667	43.3	0.813	2.048
400	6425	0.000	1.036	6425	0.000	1.036	6425	0.000	1.036	6426	0.000	1.036	6486	0.034	1.029
	2373	0.000	1.036	2373	0.000	1.036	2373	0.000	1.036	2375	0.004	1.036	2388	0.023	1.036
	707.5	0.000	1.015	707.5	0.000	1.015	707.6	0.000	1.015	719.3	0.060	1.030	772.8	0.329	1.089
	144.4	0.000	0.731	144.8	0.009	0.750	146.8	0.061	0.825	156.8	0.306	1.136	169.0	0.599	1.558
	65.3	0.049	0.037	66.0	0.085	0.260	67.6	0.178	0.619	72.6	0.449	1.454	77.3	0.699	2.202

Table 62. (Continued)

		r = 0.0				r = 0.2				r = 0.3				r = 0.4				r = 0.45					
Fc	Pe _L /z [*]	T		u		Pe _L /z [*]		T		u		Pe _L /z [*]		T		u		Pe _L /z [*]		T		u	
		Pe _L /z [*]	T	u	Pe _L /z [*]	T	u	Pe _L /z [*]	T	u	Pe _L /z [*]	T	u	Pe _L /z [*]	T	u	Pe _L /z [*]	T	u	Pe _L /z [*]	T	u	
800	6631	0.000	1.363	6631	0.000	1.363	6631	0.000	1.349	6586	0.031	1.001	6218	0.294	0.454								
	2104	0.000	1.525	2104	0.000	1.511	2104	0.000	1.383	2059	0.099	0.848	1902	0.458	0.389								
	829.8	0.000	1.682	829.8	0.000	1.579	828.8	0.005	1.330	792.1	0.214	0.807	729.6	0.579	0.380								
	258.4	0.000	1.609	258.3	0.002	1.473	255.4	0.053	1.328	236.3	0.406	0.858	220.7	0.705	0.409								
	103.9	0.001	1.085	103.2	0.034	1.349	99.9	0.184	1.449	91.8	0.562	0.910	87.1	0.788	0.837								
-200	6924	0.000	1.465	6924	0.000	1.464	6923	0.000	1.440	6821	0.069	0.904	6326	0.410	0.291								
	2039	0.000	1.831	2039	0.000	1.799	2036	0.006	1.514	1929	0.253	0.566	1777	0.617	0.162								
	877.8	0.000	2.277	877.7	0.000	2.061	869.9	0.042	1.407	800.1	0.421	0.400	747.1	0.719	0.116								
	252.0	0.000	3.189	250.7	0.024	2.279	240.4	0.216	1.134	219.7	0.617	0.282	209.6	0.818	0.088								
	88.0	0.003	3.686	85.6	0.128	2.219	80.7	0.397	1.018	74.9	0.721	0.285	72.4	0.868	0.101								

Table 63. Variable Property Velocity and Temperature
Profile Calculations for Liquids
Entrance Profile: Uniform
Viscosity Ratio: 0.5
Prandtl Number: 10

	r = 0.0				r = 0.2				r = 0.3				r = 0.4				r = 0.45			
Fc	Pe _L /z*	T	u	Pe _L /z*	T	u	Pe _L /z*	T	u	Pe _L /z*	T	u	Pe _L /z*	T	u	Pe _L /z*	T	u		
±0.1	4027	0.000	1.386	4027	0.000	1.385	4027	0.000	1.352	4015	0.033	0.955	3913	0.329	0.473					
	1142	0.000	1.688	1142	0.000	1.624	1142	0.002	1.376	1123	0.190	0.750	1087	0.557	0.355					
	478.0	0.000	1.986	478.0	0.000	1.748	476.7	0.032	1.324	463.2	0.360	0.660	450.3	0.677	0.314					
	94.2	0.002	2.265	93.6	0.071	1.793	91.9	0.281	1.249	89.0	0.639	0.620	87.5	0.826	0.306					
200	4027	0.000	1.353	4027	0.000	1.353	4027	0.000	1.324	4018	0.024	0.975	3925	0.292	0.528					
	1239	0.000	1.563	1239	0.000	1.519	1239	0.001	1.333	1225	0.130	0.834	1186	0.493	0.456					
	427.4	0.000	1.759	427.4	0.000	1.567	426.6	0.022	1.275	415.9	0.309	0.802	403.9	0.641	0.452					
	94.1	0.002	1.520	93.7	0.051	1.449	92.4	0.221	1.299	89.4	0.583	0.875	87.7	0.797	0.497					
400	4653	0.000	1.310	4653	0.000	1.309	4653	0.000	1.292	4646	0.015	1.007	4556	0.240	0.586					
	1111	0.000	1.500	1111	0.000	1.452	1111	0.000	1.285	1100	0.114	0.886	1066	0.471	0.541					
	411.1	0.000	1.549	411.1	0.000	1.410	410.6	0.014	1.229	401.7	0.264	0.926	389.6	0.608	0.582					
	93.3	0.003	0.888	93.0	0.039	1.132	91.9	0.177	1.322	89.0	0.536	1.112	87.2	0.772	0.684					
800	6359	0.000	1.246	6359	0.000	1.246	6359	0.000	1.241	6356	0.005	1.055	6272	0.157	0.677					
	1016	0.000	1.370	1016	0.000	1.327	1016	0.000	1.208	1009	0.082	0.975	979.4	0.423	0.698					
	481.1	0.000	1.282	481.1	0.000	1.212	480.9	0.003	1.150	473.9	0.171	1.078	459.2	0.528	0.784					
	99.8	0.007	-0.003	99.6	0.022	0.611	98.9	0.106	1.292	96.0	0.445	1.515	93.7	0.720	1.028					

Table 64. (Continued)

		r = 0.0				r = 0.2				r = 0.3				r = 0.4				r = 0.45			
Fc	Pe _L /z*	T		u		Pe _L /z*		T		u		Pe _L /z*		T		u		Pe _L /z*		T	
		T		u		Pe _L /z*		T		u		Pe _L /z*		T		u		Pe _L /z*		T	
800	10309	0.000	0.000	1.170	10309	0.000	1.170	10309	0.000	1.170	10310	0.000	1.170	10310	0.000	1.098	10381	0.066	0.809		
	2316	0.000	0.000	1.252	2316	0.000	1.243	2316	0.000	1.207	2319	0.014	0.997	2373	0.014	0.997	2373	0.233	0.771		
	709.0	0.000	0.000	1.216	709.0	0.000	1.172	709.1	0.000	1.111	715.2	0.083	1.071	739.8	0.083	1.071	739.8	0.410	0.914		
	204.2	0.000	0.000	0.457	204.2	0.000	0.705	204.6	0.018	1.068	209.6	0.247	1.460	216.9	0.247	1.460	216.9	0.583	1.223		
	145.6	0.000	0.000	0.060	145.7	0.003	0.520	146.2	0.038	1.097	150.3	0.307	1.609	155.3	0.307	1.609	155.3	0.627	1.319		
-200	9874	0.000	0.000	1.220	9874	0.000	1.220	9874	0.000	1.219	9877	0.002	1.104	10000	0.002	1.104	10000	0.121	0.709		
	2475	0.000	0.000	1.429	2475	0.000	1.423	2475	0.000	1.350	2490	0.057	0.919	2576	0.057	0.919	2576	0.388	0.486		
	907.9	0.000	0.000	1.716	907.9	0.000	1.629	908.4	0.005	1.366	929.4	0.224	0.763	964.1	0.224	0.763	964.1	0.583	0.365		
	294.0	0.000	0.000	2.167	294.2	0.004	1.828	296.8	0.089	1.324	308.7	0.469	0.616	317.2	0.469	0.616	317.2	0.739	0.269		
	102.4	0.001	2.488		103.1	0.070	1.932	105.5	0.285	1.276	109.4	0.644	0.544	111.4	0.644	0.544	111.4	0.829	0.232		

Table 65. Variable Property Velocity and Temperature
Profile Calculations for Liquids
Entrance Profile: Uniform
Viscosity Ratio: 5
Prandtl Number: 10

$r = 0.0$			$r = 0.2$			$r = 0.3$			$r = 0.4$			$r = 0.45$
F_c	Pe_L/z^*	T	u	Pe_L/z^*	T	u	Pe_L/z^*	T	u	Pe_L/z^*	T	u
±0.1	17328	0.000	1.091	17328	0.000	1.091	17328	0.000	1.091	17328	0.014	0.960
	7933	0.000	1.129	7933	0.000	1.129	7933	0.000	1.129	7933	0.052	0.893
	2332	0.000	1.227	2332	0.000	1.225	2332	0.000	1.196	2336	0.250	0.791
	789.4	0.000	1.370	789.4	0.000	1.325	789.5	0.001	1.218	800.6	0.485	0.698
	227.9	0.000	1.509	228.0	0.004	1.399	229.6	0.069	1.253	237.7	0.696	0.599
200	100.7	0.002	1.551	101.2	0.054	1.448	103.0	0.222	1.288	106.8	0.792	0.546
	17328	0.000	1.086	17328	0.000	1.086	17328	0.000	1.086	17328	0.012	0.964
	7933	0.000	1.117	7933	0.000	1.117	7933	0.000	1.116	7933	0.042	0.909
	2035	0.000	1.182	2035	0.000	1.179	2035	0.000	1.150	2038	0.222	0.870
	722.9	0.000	1.195	722.9	0.000	1.163	722.9	0.000	1.109	729.5	0.408	0.929
400	230.4	0.000	0.911	230.4	0.001	0.963	231.0	0.025	1.058	236.9	0.592	1.112
	87.2	0.010	0.366	86.5	0.043	0.669	88.4	0.147	1.048	91.4	0.723	1.307
	17328	0.000	1.082	17328	0.000	1.082	17328	0.000	1.082	17328	0.011	0.968
	8211	0.000	1.105	8211	0.000	1.105	8211	0.000	1.104	8211	0.033	0.923
	2190	0.000	1.137	2190	0.000	1.135	2190	0.000	1.115	2191	0.172	0.930
	824.1	0.000	1.084	824.1	0.000	1.067	824.1	0.000	1.045	828.2	0.329	1.061
	270.6	0.000	0.615	270.6	0.000	0.739	270.8	0.008	0.941	275.5	0.505	1.402
	132.4	0.001	-0.016	132.4	0.007	0.378	133.0	0.044	0.884	136.4	0.608	1.712
										93.8	0.723	1.307
										17349	0.011	0.968
										8240	0.033	0.923
										2230	0.172	0.930
										852.8	0.329	1.061
										285.1	0.505	1.402
										140.9	0.608	1.712

Table 65. (Continued)

		r = 0.0				r = 0.2				r = 0.3				r = 0.4				r = 0.45			
Fc	Pe_L/z^*	T	u	Pe_L/z^*	T	u	Pe_L/z^*	T	u	Pe_L/z^*	T	u	Pe_L/z^*	T	u	Pe_L/z^*	T	u	Pe_L/z^*	T	u
800	17328	0.000	1.073	17328	0.000	1.073	17328	0.000	1.073	17328	0.000	1.073	17328	0.000	1.066	17345	0.008	0.974			
	8211	0.000	1.087	8211	0.000	1.087	8211	0.000	1.087	8211	0.000	1.087	8211	0.000	1.055	8232	0.024	0.943			
	2261	0.000	1.075	2261	0.000	1.074	2261	0.000	1.062	2262	0.000	1.062	2262	0.002	1.018	2290	0.122	1.012			
	873.4	0.000	0.932	873.4	0.000	0.929	873.4	0.000	0.948	875.3	0.000	0.948	875.3	0.021	1.090	896.5	0.250	1.245			
	246.7	0.000	-0.076	246.7	0.000	0.275	246.8	0.002	0.754	249.7	0.113	1.530	258.1	0.435	1.934						
-100	17328	0.000	1.094	17328	0.000	1.094	17328	0.000	1.094	17328	0.000	1.094	17328	0.000	1.083	17356	0.015	0.957			
	7549	0.000	1.140	7549	0.000	1.140	7549	0.000	1.140	7549	0.000	1.140	7549	0.000	1.079	7600	0.064	0.878			
	2224	0.000	1.269	2224	0.000	1.265	2224	0.000	1.229	2230	0.000	1.229	2230	0.026	1.018	2295	0.302	0.729			
	847.8	0.000	1.478	847.8	0.000	1.428	848.1	0.002	1.291	863.9	0.179	0.939	897.0	0.547	0.540						
	203.2	0.000	2.064	203.6	0.018	1.813	206.8	0.162	1.420	215.6	0.575	0.633	220.6	0.800	0.178						

Table 66. Variable Property Velocity and Temperature
 Profile Calculations for Liquids
 Entrance Profile: Uniform
 Viscosity Ratio: 10
 Prandtl Number: 10

r = 0.0																r = 0.2																r = 0.3																r = 0.4																r = 0.45																								
Fc		Pe _L /z*		T		u		Pe _L /z*		T		u		Pe _L /z*		T		u		Pe _L /z*		T		u		Pe _L /z*		T		u		Pe _L /z*		T		u		Pe _L /z*		T		u		Pe _L /z*		T		u																																								
±0.1		32064	0.000	1.052	32064	0.000	1.052	32064	0.000	1.052	32064	0.000	1.052	32064	0.000	1.052	32064	0.000	1.052	32064	0.000	1.052	32064	0.000	1.052	32064	0.000	1.052	32064	0.000	1.051	32081	0.002	1.012	11595	0.000	1.080	11595	0.000	1.080	11595	0.000	1.065	11626	0.015	0.968	6948	0.000	1.101	6948	0.000	1.100	6949	0.000	1.063	7000	0.041	0.943	570.7	0.000	1.306	570.7	0.000	1.263	571.1	0.004	1.187	588.6	0.174	1.027	624.9	0.521	0.774	98.8	0.003	1.442	99.8	0.057	1.386	102.6	0.221	1.284	109.0	0.571	0.972	113.0	0.788	0.607
200		30288	0.000	1.051	30288	0.000	1.051	22519	0.000	1.057	22517	0.000	1.054	22536	0.004	1.000	10611	0.000	1.075	10611	0.000	1.059	10639	0.014	0.969	6583	0.000	1.088	6583	0.000	1.053	6625	0.035	0.954	1776	0.000	1.119	1776	0.010	1.031	1841	0.203	0.965	953.0	0.000	1.107	953.0	0.000	1.046	1007	0.315	1.017	532.9	0.000	1.038	542.6	0.101	1.093	573.4	0.419	1.111	73.4	0.050	-0.030	78.7	0.457	1.673	82.2	0.714	1.756																		
400		30288	0.000	1.049	30288	0.000	1.049	30288	0.000	1.049	30288	0.000	1.058	30302	0.002	1.011	11114	0.000	1.067	11115	0.000	1.054	11137	0.011	0.975	7080	0.000	1.075	7080	0.000	1.047	7112	0.025	0.965	1077	0.000	1.026	108	0.020	1.046	1124	0.240	1.110	603.1	0.000	0.897	608.9	0.053	1.107	639.2	0.330	1.265	171.3	0.000	0.035	177.5	0.202	1.479	187.7	0.523	1.911																											

Table 66. (Continued)

Table 67. (Continued)

$r = 0.0$		$r = 0.2$		$r = 0.3$		$r = 0.4$		$r = 0.45$	
Fc	Pe_L/z^*	T	u	Pe_L/z^*	T	u	Pe_L/z^*	T	u
-100	41397	0.000	1.035	41397	0.000	1.035	41397	0.000	1.035
	11910	0.000	1.060	11910	0.000	1.060	11910	0.000	1.052
	5758	0.000	1.090	5758	0.000	1.089	5758	0.000	1.058
	1065	0.000	1.295	1065	0.000	1.234	1097	0.110	1.074
	626.6	0.000	1.484	626.6	0.000	1.444	628.8	0.012	1.352
							678.0	0.293	1.021
							744.7	0.660	0.423

Table 69. Variable Property Velocity and Temperature
Profile Calculations for Gases
Entrance Profile: Uniform
Viscosity Ratio: 0.75
Prandtl Number: 0.7

r = 0.0					r = 0.2					r = 0.3					r = 0.4					r = 0.45				
Fc	Pe_L/z^*	T	ρu	Pe_L/z^*	T	ρu	Pe_L/z^*	T	ρu	Pe_L/z^*	T	ρu	Pe_L/z^*	T	ρu	Pe_L/z^*	T	ρu	Pe_L/z^*	T	ρu			
±0.1	2726	0.000	1.175	2726	0.000	1.175	2726	0.000	1.157	2694	0.032	1.140	2442	0.318	0.801	2442	0.318	0.801	2442	0.318	0.801			
	1292	0.000	1.238	1292	0.000	1.238	1291	0.000	1.237	1239	0.114	1.112	1095	0.495	0.651	1095	0.495	0.651	1095	0.495	0.651			
	528.1	0.000	1.347	528.1	0.000	1.347	524.7	0.017	1.331	473.6	0.314	0.979	427.4	0.660	0.518	427.4	0.660	0.518	427.4	0.660	0.518			
	261.9	0.000	1.474	261.3	0.006	1.469	253.2	0.092	1.377	222.9	0.484	0.862	206.7	0.754	0.448	206.7	0.754	0.448	206.7	0.754	0.448			
	111.3	0.003	1.701	108.5	0.073	1.628	100.8	0.289	1.345	90.4	0.654	0.758	86.1	0.837	0.393	86.1	0.837	0.393	86.1	0.837	0.393			
	56.0	0.046	1.926	52.7	0.221	1.696	48.7	0.470	1.297	44.9	0.756	0.711	42.8	0.944	0.368	42.8	0.944	0.368	42.8	0.944	0.368			
	20.4	0.334	2.103	19.3	0.523	1.715	18.4	0.697	1.268	17.6	0.863	0.691	17.3	0.935	0.359	17.3	0.935	0.359	17.3	0.935	0.359			
	10.0	0.658	2.074	9.7	0.754	1.703	9.5	0.843	1.270	9.3	0.928	0.700	9.2	0.976	0.366	9.2	0.976	0.366	9.2	0.976	0.366			
	3.9	0.956	2.008	3.9	0.968	1.682	3.8	0.979	1.277	3.8	0.990	0.717	3.8	0.995	0.378	3.8	0.995	0.378	3.8	0.995	0.378			
200	2726	0.000	1.168	2726	0.000	1.168	2726	0.000	1.167	2696	0.029	1.137	2450	0.307	0.820	2450	0.307	0.820	2450	0.307	0.820			
	1292	0.000	1.221	1292	0.000	1.221	1291	0.000	1.220	1244	0.104	1.117	1101	0.479	0.689	1101	0.479	0.689	1101	0.479	0.689			
	528.1	0.000	1.302	528.1	0.000	1.302	525.3	0.014	1.293	477.4	0.289	1.019	429.5	0.642	0.582	429.5	0.642	0.582	429.5	0.642	0.582			
	226.6	0.000	1.395	225.9	0.008	1.392	218.5	0.100	1.332	192.7	0.485	0.930	178.8	0.753	0.524	178.8	0.753	0.524	178.8	0.753	0.524			
	99.0	0.005	1.473	96.4	0.079	1.458	89.8	0.286	1.333	80.6	0.646	0.882	76.7	0.833	0.495	76.7	0.833	0.495	76.7	0.833	0.495			
	50.4	0.066	1.492	47.6	0.231	1.494	44.2	0.466	1.334	40.8	0.750	0.858	39.4	0.882	0.477	39.4	0.882	0.477	39.4	0.882	0.477			
	18.5	0.411	1.666	17.7	0.565	1.575	17.0	0.717	1.316	16.3	0.870	0.800	16.0	0.938	0.436	16.0	0.938	0.436	16.0	0.938	0.436			
	9.4	0.716	1.863	9.2	0.792	1.634	9.1	0.865	1.292	8.9	0.938	0.754	8.8	0.970	0.404	8.8	0.970	0.404	8.8	0.970	0.404			
	4.0	0.959	1.984	4.0	0.970	1.673	4.0	0.980	1.280	4.0	0.990	0.723	4.0	0.995	0.383	4.0	0.995	0.383	4.0	0.995	0.383			
400	2728	0.000	1.161	2728	0.000	1.161	2728	0.000	1.161	2700	0.027	1.134	2460	0.297	0.838	2460	0.297	0.838	2460	0.297	0.838			
	1293	0.000	1.205	1293	0.000	1.205	1292	0.000	1.204	1248	0.095	1.121	1106	0.464	0.725	1106	0.464	0.725	1106	0.464	0.725			
	528.5	0.000	1.262	528.5	0.000	1.262	526.1	0.011	1.257	481.3	0.266	1.054	431.9	0.625	0.644	431.9	0.625	0.644	431.9	0.625	0.644			

Table 69. (Continued)

	r = 0.0			r = 0.2			r = 0.3			r = 0.4			r = 0.45		
Fc	Pe _L /z*	T	ρ u	Pe _L /z*	T	ρ u	Pe _L /z*	T	ρ u	Pe _L /z*	T	ρ u	Pe _L /z*	T	ρ u
400	226.7	0.000	1.295	226.2	0.006	1.296	219.9	0.084	1.282	194.6	0.456	1.013	179.7	0.737	0.614
	99.1	0.005	1.218	96.9	0.066	1.270	90.8	0.253	1.315	81.3	0.618	1.021	77.0	0.819	0.611
	21.0	0.398	1.228	20.2	0.534	1.424	19.3	0.687	1.363	18.5	0.854	0.916	18.1	0.931	0.518
	10.0	0.728	1.692	9.9	0.798	1.575	9.7	0.867	1.310	9.5	0.938	0.799	9.4	0.970	0.437
	3.9	0.969	1.970	3.8	0.977	1.668	3.8	0.985	1.281	3.8	0.993	0.727	3.8	0.996	0.386
800	2728	0.000	1.148	2728	0.000	1.148	2728	0.000	1.148	2703	0.024	1.128	2474	0.279	0.870
	1100	0.000	1.182	1100	0.000	1.182	1099	0.000	1.181	1060	0.100	1.199	940.7	0.468	0.781
	469.6	0.000	1.191	469.5	0.000	1.191	467.6	0.011	1.192	429.7	0.252	1.108	385.2	0.611	0.762
	205.1	0.000	1.108	204.6	0.006	1.148	199.7	0.072	1.176	177.7	0.424	1.172	163.4	0.718	0.799
	92.8	0.077	0.698	91.2	0.055	0.885	86.4	0.208	1.252	77.2	0.574	1.319	72.6	0.796	0.872
-100	49.4	0.129	0.023	48.0	0.188	0.727	45.7	0.360	1.411	41.2	0.675	1.421	39.9	0.845	0.903
	3.8	0.977	1.952	3.8	0.983	1.661	3.8	0.988	1.283	3.8	0.994	0.732	3.8	0.997	0.389
	2726	0.000	1.179	2726	0.000	1.179	2726	0.000	1.179	2693	0.033	1.141	2438	0.323	0.792
	1023	0.000	1.274	1023	0.000	1.274	1022	0.002	1.272	963.8	0.166	1.078	853.4	0.552	0.588
	511.6	0.000	1.377	511.6	0.000	1.377	507.5	0.021	1.355	455.6	0.336	0.949	412.4	0.674	0.482
	257.8	0.000	1.530	257.1	0.007	1.522	248.2	0.105	1.400	218.1	0.504	0.816	202.8	0.765	0.405
	106.9	0.004	1.841	103.7	0.086	1.723	95.9	0.317	1.341	86.3	0.674	0.691	82.4	0.847	0.341
	43.9	0.085	2.236	40.8	0.297	1.802	37.9	0.542	1.260	35.3	0.793	0.631	34.4	0.902	0.313
	3.6	0.964	2.016	3.6	0.973	1.685	3.6	0.983	1.277	3.5	0.992	0.714	3.5	0.996	0.376

Table 70. Variable Property Velocity and Temperature
Profile Calculations for Gases
Entrance Profile: Uniform
Viscosity Ratio: 1
Prandtl Number: 0.7

Fc	r = 0.0				r = 0.2				r = 0.3				r = 0.4				r = 0.45			
	Pe_L/z^*	T	ρu	Pe_L/z^*	T	ρu	Pe_L/z^*	T	ρu	Pe_L/z^*	T	ρu	Pe_L/z^*	T	ρu	Pe_L/z^*	T	ρu	Pe_L/z^*	T
±0.1	3399	0.000	1.236	3399	0.000	1.236	3397	0.000	1.235	3186	0.049	1.134	2288	0.396	0.633					
	1340	0.000	1.339	1340	0.000	1.339	1335	0.002	1.335	1064	0.200	0.982	787.5	0.605	0.500					
	667.2	0.000	1.453	667.0	0.000	1.453	649.3	0.020	1.409	454.0	0.382	0.843	370.1	0.712	0.442					
	281.0	0.000	1.664	277.5	0.009	1.641	236.0	0.146	1.359	167.6	0.579	0.745	149.0	0.807	0.398					
	121.6	0.002	1.969	107.7	0.100	1.728	83.7	0.371	1.255	67.5	0.718	0.708	63.0	0.870	0.379					
	62.7	0.039	2.192	49.4	0.265	1.687	40.5	0.535	1.239	35.2	0.795	0.707	33.6	0.905	0.377					
	25.3	0.259	2.119	21.1	0.500	1.666	18.8	0.694	1.262	17.4	0.865	0.719	16.9	0.937	0.382					
200	10.6	0.630	1.958	10.0	0.740	1.662	9.6	0.836	1.284	9.2	0.926	0.731	9.1	0.965	0.387					
	2.1	0.995	1.995	2.1	0.996	1.677	2.1	0.997	1.279	2.1	0.999	0.720	2.1	0.999	0.380					
	2299	0.000	1.321	2299	0.000	1.229	2297	0.000	1.228	2196	0.047	1.136	2302	0.388	0.648					
	1340	0.000	1.321	1340	0.000	1.321	1336	0.002	1.317	1077	0.188	1.000	792.4	0.595	0.527					
	469.6	0.000	1.475	469.1	0.007	1.473	443.2	0.044	1.390	304.4	0.449	0.838	256.3	0.745	0.463					
	135.8	0.001	1.742	124.5	0.069	1.621	97.4	0.317	1.280	76.5	0.688	0.785	70.6	0.856	0.436					
	53.0	0.067	1.868	42.0	0.298	1.587	35.0	0.554	1.280	30.7	0.803	0.783	29.3	0.908	0.429					
400	15.9	0.465	1.807	14.4	0.628	1.609	13.4	0.768	1.300	12.7	0.896	0.771	12.4	0.951	0.416					
	2.6	0.989	1.988	2.6	0.992	1.675	2.6	0.994	1.280	2.6	0.997	0.722	2.6	0.998	0.381					
	3396	0.000	1.136	3396	0.000	1.136	3396	0.000	1.136	3375	0.016	1.121	3132	0.228	0.905					
	1099	0.000	1.194	1099	0.000	1.194	1099	0.000	1.193	1099	0.000	1.113	936.7	0.480	0.756					
	469.3	0.000	1.237	469.2	0.000	1.237	466.7	0.014	1.232	425.9	0.277	1.066	382.9	0.630	0.695					
400	135.9	0.000	1.204	134.5	0.029	1.220	128.0	0.168	1.257	113.6	0.547	1.069	106.5	0.783	0.682					

Table 70. (Continued)

$r = 0.0$			$r = 0.2$			$r = 0.3$			$r = 0.4$			$r = 0.45$			
Fc	Pe_L/z^*	T	ρu	Pe_L/z^*	T	ρu	Pe_L/z^*	T	ρu	Pe_L/z^*	T	ρu	Pe_L/z^*	T	ρu
400	46.4	0.099	0.821	44.2	0.234	1.153	41.4	0.445	1.360	38.1	0.731	1.112	36.8	0.873	0.678
	14.4	0.598	1.320	14.0	0.692	1.438	13.6	0.793	1.347	13.2	0.903	0.903	13.1	0.954	0.512
	3.7	0.976	1.957	3.7	0.982	1.664	3.6	0.988	1.282	3.6	0.994	0.730	3.6	0.997	0.388
800	3396	0.000	1.126	3396	0.000	1.126	3396	0.000	1.126	3377	0.005	1.115	3147	0.215	0.927
	1099	0.000	1.161	1099	0.000	1.161	1099	0.000	1.161	1063	0.090	1.115	945.2	0.450	0.830
	469.3	0.000	1.159	469.2	0.000	1.159	467.5	0.010	1.161	431.7	0.236	1.117	386.5	0.597	0.829
-100	139.9	0.000	0.916	138.9	0.018	0.956	133.9	0.119	1.131	119.1	0.482	1.287	110.5	0.748	0.934
	62.6	0.056	0.060	61.3	0.116	0.610	57.9	0.281	1.279	52.3	0.621	1.527	49.6	0.819	1.055
	3399	0.000	1.239	3399	0.000	1.239	3397	0.000	1.239	3181	0.051	1.133	2281	0.400	0.625
	1053	0.000	1.387	1053	0.000	1.387	1045	0.005	1.239	784.9	0.279	1.133	603.1	0.652	0.625
	430.5	0.000	1.579	429.5	0.001	1.574	394.2	0.069	1.419	270.0	0.499	0.761	232.2	0.770	0.395
	121.6	0.002	2.070	107.0	0.106	1.780	83.0	0.383	1.244	67.3	0.725	0.672	62.9	0.873	0.353
	45.1	0.092	2.382	35.1	0.357	1.715	29.7	0.605	1.225	26.6	0.827	0.675	25.6	0.919	0.351
	14.5	0.478	2.101	13.1	0.645	1.690	12.3	0.781	1.266	11.6	0.902	0.706	11.4	0.954	0.371
	2.1	0.995	1.996	2.1	0.996	1.678	2.1	0.997	1.279	2.1	0.999	0.720	2.1	0.999	0.330

Table 71. (Continued)

r = 0.0			r = 0.2			r = 0.3			r = 0.4			r = 0.45			
Fc	Pe _L /z*	T	pu	Pe _L /z*	T	pu	Pe _L /z*	T	pu	Pe _L /z*	T	pu	Pe _L /z*	T	pu
400	180.4	0.000	0.973	180.7	0.005	0.979	183.2	0.049	1.019	198.4	0.289	1.157	222.4	0.578	1.121
	98.4	0.004	0.771	99.2	0.032	0.823	102.0	0.121	0.970	112.5	0.398	1.279	125.6	0.659	1.263
	47.5	0.104	0.073	48.2	0.152	0.434	50.1	0.264	0.941	55.5	0.531	1.585	61.2	0.745	1.536
800	6666	0.000	1.034	6666	0.000	1.034	6666	0.000	1.034	6668	0.000	1.035	6729	0.031	1.031
	2136	0.000	1.049	2136	0.000	1.049	2136	0.000	1.049	2140	0.006	1.050	2225	0.131	1.041
	756.2	0.000	1.036	756.2	0.000	1.036	756.3	0.000	1.037	768.9	0.054	1.059	835.8	0.304	1.071
	155.4	0.000	0.755	155.7	0.006	0.768	157.6	0.045	0.854	169.1	0.261	1.231	189.1	0.549	1.450
	90.6	0.007	0.342	91.1	0.028	0.455	93.1	0.096	0.742	101.2	0.343	1.462	113.1	0.615	1.758
	77.8	0.017	0.124	78.4	0.041	0.321	80.2	0.114	0.713	87.5	0.365	1.561	97.7	0.632	1.874
-100	6666	0.000	1.038	6666	0.000	1.038	6666	0.000	1.038	6668	0.000	1.038	6732	0.032	1.030
	2565	0.000	1.065	2565	0.000	1.065	2565	0.000	1.065	2570	0.005	1.065	2668	0.126	1.030
	863.4	0.000	1.116	863.4	0.000	1.116	863.6	0.000	1.116	882.8	0.072	1.106	974.1	0.360	0.933
	223.0	0.000	1.262	223.3	0.005	1.263	227.2	0.062	1.254	251.2	0.356	1.045	283.0	0.644	0.661
	109.7	0.002	1.433	111.2	0.048	1.425	116.6	0.194	1.338	132.2	0.528	0.919	146.6	0.754	0.492
	42.6	0.083	1.881	44.8	0.236	1.726	48.4	0.444	1.374	54.5	0.716	0.689	58.6	0.858	0.285
	12.8	0.517	2.650	13.5	0.639	2.027	14.3	0.760	1.283	15.3	0.886	0.459	15.8	0.945	0.145
	6.7	0.807	2.614	6.8	0.858	1.941	7.0	0.907	1.240	7.2	0.956	0.520	7.3	0.990	0.222

Table 72. Variable Property Velocity and Temperature
Profile Calculations for Gases
Entrance Profile: Uniform
Viscosity Ratio: 2
Prandtl Number: 0.7

r = 0.0				r = 0.2				r = 0.3				r = 0.4				r = 0.45			

Table 72. (Continued)

	r = 0.0			r = 0.2			r = 0.3			r = 0.4			r = 0.45		
Fc	Pe_L/z^*	T	pu	Pe_L/z^*	T	pu	Pe_L/z^*	T	pu	Pe_L/z^*	T	pu	Pe_L/z^*	T	pu
400	216.5	0.000	0.939	216.7	0.002	0.941	218.6	0.027	0.965	235.4	0.213	1.100	272.0	0.486	1.190
	99.6	0.003	0.688	100.4	0.026	0.732	103.1	0.100	0.863	114.9	0.339	1.227	134.2	0.593	1.438
	46.8	0.141	0.127	47.2	0.161	0.220	48.9	0.241	0.735	55.3	0.473	1.592	64.6	0.689	1.924
800	3470	0.000	1.026	3470	0.000	1.026	3470	0.000	1.026	3471	0.001	1.026	3530	0.048	1.034
	1078	0.000	1.016	1078	0.000	1.016	1085	0.020	1.016	1085	0.020	1.028	1162	0.194	1.070
	484.7	0.000	0.972	484.7	0.000	0.972	485.1	0.001	0.974	498.7	0.078	1.033	555.0	0.322	1.150
	228.0	0.000	0.843	228.1	0.001	0.845	229.4	0.017	0.870	243.1	0.168	1.078	277.3	0.433	1.350
	114.0	0.001	0.514	114.5	0.013	0.553	116.4	0.060	0.699	126.6	0.261	1.233	146.5	0.522	1.721
	68.3	0.049	0.147	68.6	0.060	0.981	70.1	0.115	0.534	77.2	0.329	1.515	89.8	0.580	2.203
-100	3374	0.000	1.033	3374	0.000	1.033	3374	0.000	1.033	3376	0.001	1.034	3443	0.056	1.035
	1848	0.000	1.045	1848	0.000	1.045	1848	0.000	1.045	1853	0.007	1.047	1945	0.136	1.042
	977.8	0.000	1.065	977.8	0.000	1.065	977.8	0.000	1.065	991.2	0.038	1.072	1088	0.265	1.022
	512.3	0.000	1.098	512.3	0.000	1.098	513.0	0.003	1.100	536.6	0.124	1.100	615.6	0.411	0.953
	256.2	0.000	1.163	256.4	0.002	1.164	259.5	0.036	1.170	286.4	0.273	1.096	338.1	0.561	0.820
	123.7	0.001	1.301	125.0	0.031	1.036	130.7	0.146	1.282	152.4	0.455	1.015	180.8	0.696	0.614
	57.9	0.037	1.619	60.5	0.150	1.579	66.1	0.339	1.398	79.5	0.633	0.821	92.5	0.807	0.336
	35.9	0.122	1.969	38.5	0.278	1.817	42.8	0.476	1.448	51.5	0.727	0.641	58.7	0.860	1.442

APPENDIX I

SAMPLE CALCULATIONS

Dimensionless variables were used extensively throughout this work due to their convenience in the theoretical calculations; however their generality makes their relationship to actual physical quantities somewhat esoteric. In order to give some of these dimensionless variables more physical meaning, the following sample calculations are provided.

Description of Calculation

Consider Oil A flowing upward in a vertical, heated tube such that its entrance profile is parabolic. Let the following conditions exist:

$$T_o^i = 550^\circ \text{ R}$$

$$T_w^i = 671^\circ \text{ R}$$

$$W^i = 2940 \text{ lb/hr}$$

$$D^i = 0.042 \text{ ft}$$

$$\text{Heated Length} = 15 \text{ ft}$$

Then the entering viscosity and the viscosity at the wall* are

$$\mu_o^i = 95.65 \text{ lb/ft-hr}$$

*Property values are taken from Appendix C.

$$\mu_w' = 9.543 \text{ lb/ft-hr}$$

Therefore

$$\mu_r = \frac{95.65}{9.543} = 10.0$$

The Reynolds number is

$$Re = \frac{W'}{\pi D' \mu_o'} = \frac{2940}{(3.14)(0.042)(95.65)} = 233$$

The densities at the entrance and at the wall are

$$\rho_o' = 55.46 \text{ lb/ft}^3$$

$$\rho_w' = 52.77 \text{ lb/ft}^3$$

The Froude number is

$$Fr = \frac{\bar{u}'^2}{g_z' D'}$$

$$\bar{u}' = \frac{W'}{\pi D'^2 \rho_o'} = \frac{2940}{(3.14)(0.042)^2(55.46)(3600)} = 2.658 \text{ ft/sec}$$

$$Fr = \frac{(2.658)^2}{(-32.17)(0.042)} = -5.23$$

Then the free convection parameter is

$$Fc = 2\left(\frac{233}{-5.23}\right)\left(\frac{52.77 - 55.46}{52.77 + 55.46}\right) = 2.21$$

Calculation of Mean Temperature

Since the entrance profile is parabolic, the appropriate source of values for T_M for this problem is Table 20 in Appendix G. Since

$Fc = 2.21$, free convection effects will be small and values for $Fc = \pm 0.1^*$ can be used with little error. The Prandtl number is

$$Pr = \frac{c_p' \mu_o'}{K_o'} = \frac{(0.450)(95.65)}{(0.074)} = 582$$

therefore

$$\frac{Pe}{z^*} = \frac{(582)(233)(0.042)}{15} = 380$$

This allows the selection of an approximate mean temperature,

$$T_M = 0.146$$

$$T_M' = 0.146(671 - 550) + 550 = 567.7 \text{ } ^\circ\text{R}$$

A second trial using this value of T_M gives

$$\frac{Pe_M}{z^*} = 388$$

and the original value of $T_M = 567.7$ in this case is close enough.

Calculation of Pressure Drop

The pressure drop due to frictional and kinetic energy changes may be estimated from Figures 65 and 66 in Appendix F as follows

$$\frac{Pe_w}{z^*} = \frac{\frac{(0.515)(95.65)}{0.0713} (237)(0.042)}{15} = 450$$

Then at $Pr = 100$

*These values are plotted in Figure 45 of Appendix E.

$$\frac{f_{APP}}{f_{APPW}} = 2.78$$

and at $Pr = 500$

$$\frac{f_{APP}}{f_{APPW}} = 3.01$$

Since in this region the values do not change rapidly with Pr , a simple linear extrapolation should be accurate. This gives at $Pr = 582$

$$\frac{f_{APP}}{f_{APPW}} = 3.05$$

Then since

$$\frac{\Delta p}{(\Delta p)_w} = \frac{f_{APP}}{f_{APPW}}$$

$$\Delta p = (\Delta p)_w \left(\frac{f_{APP}}{f_{APPW}} \right)$$

and

$$\Delta p_i = (\Delta p)_w (3.05) (\rho_o \bar{u}_i^2)$$

$$(\Delta p)_w = \frac{-32 \mu_w}{\rho_w} = \frac{(-32)(357)(0.1)}{(0.97)(233)}$$

Then

$$-\Delta p_i = \frac{(32)(357)(0.1)(3.05)(55.46)(2.658)^2}{(0.97)(233)} = 6150 \frac{\text{lb}}{\text{ft-sec}^2}$$

or

$$-\Delta p' = \frac{1}{32.17} \frac{\text{lb-force-sec}^2}{\text{lb-ft}} 6150 \frac{\text{lb}}{\text{ft-sec}^2} = 191 \frac{\text{lb-force}}{\text{ft}^2}$$

which is the pressure drop due to frictional and kinetic energy effects.

LITERATURE CITED

1. W. J. Lee, "A Theoretical Study of Nonisothermal Flow and Heat Transfer in Vertical Tubes for Fluids with Variable Physical Properties," Georgia Institute of Technology Ph. D. Thesis, 1962.
2. R. C. Martinelli, C. J. Southwell, G. Alves, H. L. Craig, E. B. Weinberg, N. F. Lansing, and L. M. K. Boelter, "Heat Transfer and Pressure Drop for a Fluid Flowing in the Viscous Region Through a Vertical Pipe," Transactions of the American Institute of Chemical Engineers, 38, 493 (1942).
3. K. Yamagata, "A Contribution to the Theory of Nonisothermal Laminar Flow of Fluids Inside a Straight Tube of Circular Cross Section," Memoirs of the Faculty of Engineering, Kyushu Imperial University, Fukuoka, Japan, 8, 365 (1940).
4. R. L. Pigford, "Nonisothermal Flow and Heat Transfer Inside Vertical Tubes," Chemical Engineering Progress Symposium Series, 51, 79 (1955).
5. L. B. Koppel and J. M. Smith, "Laminar Flow Heat Transfer for Variable Physical Properties," Transactions of the American Society of Mechanical Engineers, Series C, 84, 1957 (1962).
6. R. G. Deissler, "Analytical Investigation of Fully Developed Laminar Flow in Tubes with Heat Transfer with Fluid Properties Variable Along the Radius," National Advisory Committee for Aeronautics Technical Note 2410, 1951.
7. K. T. Yang, "Laminar Forced Convection of Liquids in Tubes with Variable Viscosity," American Society of Mechanical Engineers Paper No. 61-WA-166.
8. R. C. Martinelli and L. M. K. Boelter, "The Analytical Prediction of Superposed Free and Forced Viscous Convection in a Vertical Pipe," University of California Publications in Engineering, 5, 23 (1942).
9. E. M. Rosen and T. J. Hanratty, "Use of Boundary-Layer Theory to Predict the Effect of Heat Transfer on the Laminar Flow Field in a Vertical Tube with a Constant Temperature Wall," Journal of the American Institute of Chemical Engineers, 7, 112 (1961).
10. A. Lee, W. O. Nelson, V. H. Cherry, and L. M. K. Boelter, "Pressure Drop and Velocity Distribution for Incompressible Viscous Non-Isothermal Flow in the Steady State Through a Pipe," Proceedings of the Fifth International Congress of Applied Mechanics, John Wiley and Sons, Inc., New York, 1939.

11. W. M. Kays and W. B. Nicoll, "Laminar Flow Heat Transfer to a Gas with Large Temperature Differences," Journal of Heat Transfer, Transactions ASME, Series C, 85, 329 (1963).
12. M. E. Davenport and G. Leppert, "The Effect of Transverse Temperature Gradients on the Heat Transfer and Friction for Laminar Flow of Gases," ASME Paper No. 64 - HT-10, 1964.
13. H. E. Lemmon, "Fluid Flow and Heat Transfer in the Inlet Region of Tubes," University of Utah Ph. D. Thesis, 1963.
14. J. R. Bodoia, "The Finite Difference Analysis of Confined Viscous Flows," Carnegie Institute of Technology Ph. D. Thesis, 1959.
15. R. B. Bird, W. E. Stewart, and E. N. Lightfoot, Transport Phenomena, John Wiley and Sons, Inc., New York, 1960.
16. H. Schlichting, Boundary Layer Theory, Pergamon Press, New York, 1955.
17. W. D. Campbell and J. C. Slattery, "Flow in the Entrance of a Tube," Journal of Basic Engineering, Transactions ASME, Series D, 85, 41 (1963).
18. E. Reshotko, "Experimental Study of the Stability of Pipe Flow, I. Establishment of an Axially Symmetric Poiseuille Flow," Progress Report No. 20-364, Jet Propulsion Laboratory, California Institute of Technology, 1958.
19. L. Prandtl and O. G. Tietjens, Applied Hydro- and Aero-mechanics, McGraw-Hill Book Company, Inc., New York, 1934.
20. H. L. Langhaar, "Steady Flow in the Transition Length of a Straight Tube," Journal of Applied Mechanics, 9, Transactions ASME, 64, A-55 (1942).
21. M. Collins and W. R. Schowalter, "Behavior of Non-Newtonian Fluids in the Inlet Region of a Channel," American Institute of Chemical Engineers Journal, 9, 809 (1963).
22. D. C. Bogue, "Entrance Effects and Development of Turbulence in Non-Newtonian Flow," Industrial Engineering Chemistry, 51, 874 (1959).
23. S. Goldstein, Modern Developments in Fluid Dynamics, Vol. 1, Clarendon Press, Oxford, England, 1938.
24. L. Schiller, "Die Entwicklung der laminaren Geschwindigkeitsverteilung und ihre Bedeutung für Zähigkeitmessungen," Zeitschrift für Angewandte Mathematik und Mechanik, 2, 96 (1922).
25. Y. Tomita, "Analytical Treatment of Non-Newtonian Fluid Flow by Introducing the Conception of Boundary Layer," Bulletin of the Japan Society of Mechanical Engineers, 4, 77 (1961)

26. W. Rieman, "The Value of the Hagenbach Factor in the Determination of Viscosity by the Efflux Method," Journal of the American Chemical Society, 50, 46 (1928).
27. A. H. Shapiro, R. Siegel, and S. J. Kline, "Friction Factor in the Laminar Entry Region of a Smooth Tube," Proceedings of the Second U. S. National Congress of Applied Mechanics, ASME, 733 (1954).
28. F. Kreith and R. Eisenstadt, "Pressure Drop and Flow Characteristics of Short Capillary Tubes at Low Reynolds Numbers," Transactions ASME, 79, 1070 (1957).
29. L. Graetz, "Ueber die Wärmeleitungsfähigkeit von Flüssigkeiten," Annalen der Physik und Chemie, 25, 337 (1885).
30. M. A. L  v  que, "Les Lois de la Transmission de Chaleur par Convection," Annales de Mines, Series 12, 13, 201 (1928).
31. A. J. Businger, "W  rme  bergang in het aanloopgebied van een buis bij gedwongen laminaire stroming," Ingenieur ('s Gravenhage), 64, 17 (1952).
32. W. M. Kays, "Numerical Solutions for Laminar-Flow Heat Transfer in Circular Tubes," Transactions of the American Society of Mechanical Engineers, 77, 1265 (1955).
33. P. Goldberg, "A Digital Computer Solution for Laminar Flow Heat Transfer in Circular Tubes," Massachusetts Institute of Technology Masters Thesis, 1958.
34. K. Stephan, "Beitrag zur Berechnung des W  rme  berganges und Druckabfalles laminarer Einlaufstr  mungen," Ingenieur-Archiv, XXIX, 176 (1960).
35. W. M. Kays, "Basic Heat Transfer and Flow Friction Design Data for Gas Flow in Circular and Rectangular Cylindrical Tube Heat Exchangers," Technical Report No. 14, Navy Contract N6-onr-251 T. O. 6, Stanford University, California, 1951.
36. A. L. London, W. M. Kays, and D. W. Johnson, "Heat Transfer and Flow Friction Characteristics of Some Compact Heat-Exchanger Surfaces, Part 3 - Design Data for Five Surfaces," Transactions of the American Society of Mechanical Engineers, 74, 1167 (1952).
37. C. L. Kroll, "Heat Transfer and Pressure Drop for Air Flowing in Small Tubes," Massachusetts Institute of Technology Ph. D. Thesis, 1951.
38. A. Cholett, "Heat Transfer - Local and Average Coefficients for Air Flowing Inside Tubes," Chemical Engineering Progress, 44, 81 (1948).
39. R. L. Bosworth, "Mass Transfer in the Entrance Length of a Pipe-Laminar Flow," Georgia Institute of Technology Ph. D. Thesis, 1962.

40. D. L. Ulrichson and R. A. Schmitz, "Chemical Reaction in the Entrance Length of a Tubular Reactor--Laminar Flow," Industrial and Engineering Chemistry, 4, 2 (1965).
41. G. F. Scheele, E. M. Rosen, and T. J. Hanratty, "Effect of Natural Convection on Transition to Turbulence in Vertical Pipes," Canadian Journal of Chemical Engineering, 38, 67 (1960).
42. A. Watzinger, and D. H. Johnson, "Warmeübertragung von Wasser an Rohrwand bei senkrechten stromung in Übergangsgebiet zwischen laminarer und turbulenter Stromung," Forschung auf dem Begeite des Ingenieurwesens, 10, 182 (1939).
43. L. Lapidus, Digital Computation for Chemical Engineers, McGraw-Hill Book Company, Inc., 1962.
44. G. G. O'Brien, M. A. Hyman, and S. Kaplan, "A Study of the Numerical Solution of Partial Differential Equations," Journal of Mathematics and Physics, 29, 223 (1950).
45. F. B. Hildebrand, Methods of Applied Mathematics, Prentice-Hall Inc., Englewood, New Jersey, 1961.
46. P. D. Lax, "Difference Approximation to Solutions of Linear Differential Equations - An Operator Theoretical Approach," Lecture Series of the Symposium on Partial Differential Equations, University of Kansas Press, Lawrence, Kansas, 1960.
47. R. D. Richtmyer, Difference Methods for Initial Value Problems, Interscience Publishers, Inc., New York, 1964.
48. Extended Algol Reference Manual for the Burroughs B-5000, Burroughs Corporation Bulletin 5000-21012, Detroit, Michigan, 1963.
49. P. Naur, "Report on the Algorithmic Language ALGOL 60," Communications of the Association for Computing Machinery, 3, No. 5, 299 (1960).
50. D. D. McCracken, An Introduction to Algol Programming, John Wiley and Sons, New York, 1962.
51. Selected Values of Properties of Hydrocarbons and Related Compounds, American Petroleum Institute Research Project 44, edited by K. D. Rossini, Carnegie Institute of Technology, 1952.
52. W. H. McAdams, Heat Transmission, McGraw-Hill Book Company, Inc., New York, 1954. 3rd Edition.

VITA

Bert Wilkins, Jr. was born in Hattiesburg, Mississippi in October, 1934. He attended the public schools there, graduating from Hattiesburg High School in June, 1953. He entered the Georgia Institute of Technology to study on the co-operative plan in September of 1953 and received the degree of Bachelor of Chemical Engineering in June of 1958. He received the degree of Master of Science in Nuclear Engineering in 1961.

During the author's undergraduate career he worked as a co-operative plan student for the Hercules Powder Company in Hattiesburg, Mississippi. Since graduation he has worked as a Research Assistant at the Georgia Institute of Technology Engineering Experiment Station, Atlanta, Georgia, as a Research Assistant at Columbia University in New York, New York, and as a Senior Research Engineer at the Lockheed-Georgia Company, Marietta, Georgia. He also has been a part-time instructor in the Georgia Institute of Technology Engineering Evening School and in the School of Chemical Engineering.

The author was the recipient of Humble Oil Company graduate fellowship during his graduate studies. He is a member of Sigma Xi, Tau Beta Pi, Phi Kappa Phi, and Phi Eta Sigma honorary societies and is an associate member of the American Institute of Chemical Engineers. He has co-authored six published papers in the fields of analytical chemistry, nuclear chemical separations, coatings for refractory metals, and two-phase flow void-fraction measurements in addition to a number of company and project technical reports.

He is married to the former Anne Olson Gillespie of Hattiesburg, Mississippi, and they have two sons.